UNIVERSIDADE ESTADUAL PAULISTA
"JÚLIO DE MESQUITA FILHO"
INSTITUTO DE BIOCIÊNCIAS – RIO CLARO

PROGRAMA DE PÓS-GRADUAÇÃO EM CIÊNCIAS BIOLÓGICAS (ZOOLOGIA)

TAXONOMIA, FILOGENÔMICA E MORFOMETRIA DE ESPÉCIES NEOTROPICAIS DO GÊNERO *IDIOPS* PERTY, 1833 (MYGALOMORPHAE, IDIOPIDAE)

RAFAEL DA FONSECA FERREIRA

Rio Claro – SP
2023

UNIVERSIDADE ESTADUAL PAULISTA
"JÚLIO DE MESQUITA FILHO"
INSTITUTO DE BIOCIÊNCIAS – RIO CLARO

PROGRAMA DE PÓS-GRADUAÇÃO EM CIÊNCIAS
BIOLÓGICAS (ZOOLOGIA)

TAXONOMIA, FILOGENÔMICA E MORFOMETRIA DE ESPÉCIES NEOTROPICAIS DO GÊNERO *IDIOPS* PERTY, 1833 (MYGALOMORPHAE, IDIOPIDAE)

RAFAEL DA FONSECA FERREIRA

Tese apresentada ao Instituto de Biociências do Câmpus de Rio Claro, Universidade Estadual Paulista, como parte dos requisitos para obtenção do título de Doutor em Ciências Biológicas (Zoologia)
Orientador: Dr. José Paulo Leite Guadanucci
Coorientadora: Dra. Millke Jasmine Arminini Morales

Rio Claro – SP
2023

F383t

Ferreira, Rafael da Fonseca
Taxonomia, filogenômica e morfometria de espécies Neotropicais do gênero Idiops Perty, 1833 (Mygalomorphae, Idiopidae) / Rafael da Fonseca Ferreira. -- Rio Claro, 2023
150 p. : tabs., fotos, mapas

Tese (doutorado) - Universidade Estadual Paulista (Unesp), Instituto de Biociências, Rio Claro
Orientador: José Paulo Leite Guadanucci
Coorientadora: Millke Jasmine Arminini Morales

1. Aranhas de alçapão. 2. Idiopinae. 3. Domiothelina. 4. UCE's. I. Título.

Sistema de geração automática de fichas catalográficas da Unesp. Biblioteca do Instituto de Biociências, Rio Claro. Dados fornecidos pelo autor(a).

Essa ficha não pode ser modificada.

UNIVERSIDADE ESTADUAL PAULISTA

Câmpus de Rio Claro

CERTIFICADO DE APROVAÇÃO

TÍTULO DA TESE: TAXONOMIA, FILOGENÔMICA E MORFOMETRIA DE ESPÉCIES NEOTROPICAIS DO GÊNERO IDIOPS PERTY, 1833 (MYGALOMORPHAE, IDIOPIDAE)

AUTOR: RAFAEL DA FONSECA FERREIRA
ORIENTADOR: JOSE PAULO LEITE GUADANUCCI
COORIENTADORA: MILLKE JASMINE ARMININI MORALES

Aprovado como parte das exigências para obtenção do Título de Doutor em Ciências Biológicas (Zoologia), pela Comissão Examinadora:

Prof. Dr. JOSE PAULO LEITE GUADANUCCI (Participaçao Presencial)
Departamento de Biodiversidade / Unesp - IB Rio Claro

Prof. Dr. FACUNDO MARTÍN LABARQUE (Participaçao Presencial)
Departamento de Ecologia e Biologia Evolutiva / UFSCar

Prof. Dr. GUILHERME HENRIQUE FERNANDES DE AZEVEDO (Participaçao Virtual)
Departamento de Biologia / San Diego State University

Profa. Dra. LAURA MONTES DE OCA (Participaçao Virtual)
Departamento de Ecologia y Biologia Evolutiva / Instituto de Investigaciones Biologicas Clemente Estable

Prof. Dr. RAFAEL PREZZI INDICATTI (Participaçao Presencial)
Instituto Butantan

Rio Claro, 10 de fevereiro de 2023

Dedico esta tese aos meus pais...

...e a todos os pesquisadores de aranhas de alçapão

Agradecimentos

Inicialmente quero agradecer aos meus pais, Maria Helena e Geraldo Magela, que sempre foram meu alicerce e meu suporte para chegar aonde estou. Tenho um orgulho imensurável e sou eternamente grato a vocês. Agradeço também a toda minha incrível família por todo apoio, em especial aos meus irmãos: Dani, Alessandra, Fernanda, Ricardo, Tiago e Ernane! Acreditaram em mim mesmo quando não entendiam muito sobre as minhas pesquisas. Amo todos vocês!

Faço um agradecimento especial ao meu companheiro Felipe, que nos dois últimos anos foi mais do que um suporte e um porto seguro, e sim um incentivo para ir mais longe e não mais sozinho. Sua curiosidade, visão crítica e correções do inglês certamente agregaram qualidade a esse trabalho. Agradeço a Dona Cida, por me receber em Rio Preto e por ser uma inspiração acadêmica. Agradeço toda a turma de Rio Preto, pelos ótimos momentos, nessa etapa final.

Agradeço ao meu orientador e amigo, José Paulo Leite Guadanucci, que em quase quatorze anos de amizade sempre foi um exemplo para mim, tanto como pessoa quanto profissional. Anos dedicados ao ensino e a pesquisa que certamente me serviram de inspiração. Obrigado por todos os conselhos e ensinamentos. Você é um orientador incrível!

Agradeço a Millke J. A. Morales, que iniciou como parceira de campo e se tornou mais do que minha coorientadora, mas uma amiga especial. Obrigado por tudo, pelas incontáveis reuniões, discussões, campos e principalmente pela parceria, pela amizade e por sempre ter acreditado em mim!

Agradeço ao Instituto de Biociências de Rio Claro, em especial ao antigo departamento de Zoologia e ao Departamento de Biodiversidade por terem me acolhido nesses últimos anos. É fundamental ressaltar que só foi possível o desenvolvimento e a concretização dos resultados apresentados nesta tese devido o financiamento da FAPESP, a partir do processo n° 2018/02842-2, Fundação de Amparo à Pesquisa do Estado de São Paulo (FAPESP).

Agradeço a incrível turma do Laboratório de Aracnologia de Rio Claro (LARC) pelas ótimas discussões, pelos campos, pelos churrascos e por engrandecerem tanto meu projeto. Agradeço a Vivinha, Giulia, Juliana, Ton, Victor e a Júlia pelos

anos memoráveis no antigo prédio da Zoologia e pelas inúmeras gargalhadas. Agradeço ao Hector, Wolf e Helô, pelo companheirismo e por me ensinarem tanto durante minha estadia no Departamento de Biodiversidade. Agradeço especialmente ao meu amigo Arthur, que esteve envolvido em todos os processos deste doutorado, incluindo os campos incríveis, as discussões sobre metodologias e resultados e as inúmeras vezes que me salvou em relação as questões burocráticas da Pós-graduação. Agradeço ao Rafa Indicatti, por ter me ensinado tanto sobre taxonomia de migalomorfas, pelo aprendizado em campo e por ser um exemplo de aracnólogo.

Faço um agradecimento mais que especial aos grandes amigos que criei em Rio Claro, em especial os da República Caçamba, que me acolheram durante toda minha estadia por Rio Claro. Foram momentos incríveis, incluindo de apoio durante a pandemia, ao lado do Parra, Prozac (e Amanda), Saul, TLG, Vic, e nos anos finais agradeço a Dreg, Vika, Assininho, Leo (e Thalita), Fábio e ao Filhinho! Também tenho de agradecer a turma do EGRIC pelas cavernadas, companhia e amizade, principalmente a Thatá, Felipe, Higor, Larissa e em especial minha eterna companheira Liz. Por fim não poderia deixar de agradecer ao Juliano, incrível amigo que sempre esteve do meu lado, inclusive me ajudando com as dúvidas ecológicas.

Não posso deixar de agradecer a muitos amigos de longa data, como o Washington, Allan, Isabela, Edmundo e Cristiano. Preciso também agradecer aos muitos amigos que em sua maioria transitam entre as áreas da Espeleologia e da Aracnologia. Da aracno, em nome dos demais, agradeço ao Leo, Nancy, David, Pedro Martins e William, pela amizade e inúmeras discussões, que me ajudaram a esclarecer dúvidas e delinear melhor minhas análises e discussões. Também agradeço ao Gabriel e a Marília, que me receberam em São Paulo. Marília, faço um agradecimento duplo a você, que me apresentou o Shahan! Da espeleo, representando todos os demais, e são muitos, não posso deixar de agradecer a Normitta, Leo Silva, Parra, Liz, Biro, Robson, Elê, Tomzinho, Paty, Ed, Naná e toda a turma do QA! Vocês são incríveis e tornaram todo o processo de reclusão causado pela pandemia mais fácil!

Esse doutorado só foi possível graças a ajuda de várias pessoas, que me ajudaram durante meus campos de coleta pelo país afora: Zé, Arthur, Rafa,

Bárbara, Ton, Ian, Pedro, Millke, Victor, Jair, Márcio (Mbs), Welton, Nicolas, Carlos e Leo. Também agradeço a Leda, pela oportunidade de fazer campo no Pará. Agradeço a todos os gestores das Unidades de Conservação por terem autorizado a realização desses campos.

Agradeço também a todos os curadores que me receberam, disponibilizaram o acervo das suas coleções e possibilitarem o empréstimo do material zoológico: Antônio D. Brescovit (IBSP), Ricardo Pinto da Rocha (MZUSP), Ricardo Ott (MCN-RS), Renato Teixeira (MCTP PUC-RS), Leonardo S. Carvalho (UFPI), Márcio Bernardino da Silva (UFPB) e Adalberto J. Santos (UFMG).

Agradeço a todos os colegas colaboradores que tornaram esse projeto, por muitos considerado megalomaníaco possível: Antonio Brescovit (IBSP), Millke A. Morales (Unicamp), Milton Ribeiro (Unesp), Vera Opatova (Charles University, Tchéquia) e Robin Lyle (Agricultural Research Council, África do Sul). Em especial agradeço ao Shahan Derkarabetian (Harvard University), por ter me possibilizado ir mais longe do que eu imaginava nas análises filogenômicas, ao me dar todo o apoio necessário, mesmo sem ter conseguido ir para os Estados Unidos.

Agradeço a todos os pesquisadores que participaram de alguma banca de acompanhamento deste doutorado e contribuíram em diferentes etapas do desenvolvimento e aprimoramento das pesquisas deste doutorado: Vera N. Solferini, Guilherme H. Azevedo, Leonardo S. Carvalho, Facundo Labarque e Ana Lúcia Tourinho. Também agradeço aos membros da banca de defesa, Laura Montes de Oca, Rafael Prezzi Indicatti, Facundo Labarque e Guilherme H. Azevedo.

Por fim, agradeço a Deus, por de alguma forma contribuir para o desenrolar dos fatos, que levaram onde estou hoje.

Resumo

A família Idiopidae, composta exclusivamente por aranhas de alçapão, compreende a segunda família mais diversa entre as aranhas Mygalomorphae, grupo que se caracteriza pelo estilo de vida geralmente sedentário, dispersão normalmente limitada e aparente uniformidade morfológica. Entre os gêneros de Idiopidae, o mais especioso é o gênero *Idiops* Perty, 1833 (Idiopinae), alvo desta tese de doutorado. Focado nas espécies Neotropicais do gênero, este trabalho explora diferentes faces da sistemática morfológica e molecular do gênero *Idiops*, a partir de três capítulos: 1. Taxonomic revision of the Neotropical spiders of the genus *Idiops* Perty, 1833 (Araneae, Idiopidae), with description of four new species; 2. Análises filogenômicas dos gêneros de Idiopinae 1889 (Idiopidae), com ênfase nas espécies Neotropicais de *Idiops* Perty 1833, baseado em Elementos Ultraconservados (UCE); e 3. Geographic variation of a trapdoor spider (Araneae, Idiopidae) across different Brazilian biomes reveals morphometric differentiation of spiders from the Brazilian Caatinga biome. No Capítulo 1, são apresentados os resultados da revisão taxonômica das espécies Neotropicais, que entre outros resultados, apresenta uma nova diagnose para as espécies Neotropicais do gênero, baseada no padrão de dentição das quelíceras, além de mapas de distribuição atualizados para todas as espécies, que agora totalizam 24 táxons na América do Sul. No Capítulo 2, são expostos os resultados da primeira filogenia molecular focada em *Idiops* e Idiopinae, que objetivaram testar a monofilia do gênero *Idiops* e da subfamília Idiopinae, e investigar as relações evolutivas entre os gêneros da subfamília, a partir de análises filogenômicas dos Elementos Ultraconservados (UCEs) do DNA. Segundo os resultados, tanto a subfamília Idiopinae quanto o clado composto pelas espécies neotropicais de *Idiops* foram recuperados como monofiléticos. Apesar disso, devido a maior proximidade filogenética entre espécies africanas de *Idiops* com os demais gêneros africanos da subfamília, o gênero *Idiops* foi recuperado como parafilético. Segundo análises de Reconstrução de Caracteres Ancestrais realizados para diferentes caracteres morfológicos, padrões distintos de dentição das quelíceras encontrado em espécimes Neotropicas e Afrotropicais de *Idiops* dão suporte a hipótese de parafilia do gênero. As relações filogenéticas entre os gêneros de Idiopinae bem como da família Idiopidae

também são discutidas neste capítulo. No Capítulo 3, focado na espécie *Idiops pirassununguensis*, que possui uma distribuição continental e que abrange diferentes biomas brasileiros, foram realizadas uma série de análises morfométricas, baseadas em medidas de estruturas lineares e formas morfogeométricas de espécimes oriundos de diferentes localidades inseridas nos biomas da Amazônia, Caatinga e Cerrado. Visando investigar se há variação geográfica e estruturação morfológica em relação a biomas, são apresentando os resultados, que sugerem a presença de estruturação morfológica entre os espécimes originários da Caatinga, quando comparado com os demais biomas. Os principais fatores que podem estar envolvidos nos padrões de estruturação observados são discutidos. Baseado em diferentes níveis de abordagens e métodos de análises, os resultados apresentados nesta tese reforçam a importância de estudos que investiguem as aranhas migalomorfas, em especial aranhas de alçapão, sob diferentes perspectivas, como forma de solucionar diferentes questões, direcionar pesquisas futuras e ampliar o conhecimento sobre estes táxons.

Palavras-chave: Aranhas de alçapão. Idiopinae. Domiothelina. Elementos Ultraconservados (UCEs).

Abstract

The Idiopidae family, composed exclusively of trapdoor spiders, comprises the second most diverse family among Mygalomorphae spiders, a group characterized by a generally sedentary lifestyle, normally limited dispersal, and apparent morphological uniformity. Among the genera of Idiopidae, the most specious is the genus *Idiops* Perty, 1833 (Idiopinae), the subject of this doctoral thesis. Focused on the Neotropical species of the genus, this work explores different aspects of the morphological and molecular systematics of the genus *Idiops*, based on three chapters: 1. Taxonomic revision of Neotropical spiders of the genus *Idiops* Perty, 1833 (Araneae, Idiopidae), describing four new species; 2. Phylogenetic analysis of the genera of Idiopinae 1889 (Idiopidae), with emphasis on Neotropical species of *Idiops* Perty 1833, based on Ultraconserved Elements (UCE); and 3. Geographic variation of trapdoor spider (Araneae, Idiopidae) across different Brazilian biomes reveals morphometric differentiation of spiders from the Brazilian Caatinga biome. In Chapter 1, the results of the taxonomic revision of the Neotropical species are presented, which, among other results, presents new diagnosis for the Neotropical species of the genus, based on dentition pattern of the chelicerae, in addition to updated distribution maps for all species, which now total 24 taxa in South America. In Chapter 2, the results of the first molecular phylogeny focused on *Idiops* and Idiopinae are presented, which aimed to test the monophyly of *Idiops* genus and the subfamily Idiopinae, and to investigate the evolutionary relationships between the genera of the subfamily, based on phylogenomic analyzes of Ultraconserved Elements (UCEs) of DNA. According to the results, both the subfamily Idiopinae and the clade composed of neotropical species of *Idiops* were recovered as monophyletic. Despite this, due to the most closely phylogenetic proximity between the African species of *Idiops* with the other African genera of the subfamily, *Idiops* genus was retrieved as paraphyletic. According to Ancestral Character Reconstruction, analyses carried out for different morphological characters, and distinct patterns of chelicerae dentition found in Neotropical and Afrotropical specimens of *Idiops* support the hypothesis of paraphyly of the genus. The phylogenetic relationships between the genera of Idiopinae, as well as the family Idiopidae, are also discussed in this chapter. Chapter 3, focused on the species *Idiops*

pirassununguensis, which has continental distribution and covers different Brazilian biomes, a series of morphometric analyzes were carried out, based on measurements of linear structures and morphogeometric shapes of specimens from different locations within the Amazon, Caatinga, and Cerrado biomes. Aiming to investigate whether there is geographic variation and morphological structure in relation to biomes, the results are presented, which suggest the presence of morphological structuration among the specimens originating from the Caatinga when compared with other biomes. The main factors that may be involved in the observed structuring patterns are discussed. Based on different levels of approaches and analysis methods, the results presented in this thesis reinforce the importance of studies that investigate mygalomorph spiders, especially trapdoor spiders, from different perspectives, to solve different questions, direct future research, and expand the scope of research knowledge about these taxa.

Keywords: Trapdoor spiders. Idiopinae. Domiothelina. Ultraconserved Elements (UCE's).

SUMÁRIO

Histórico do projeto e apresentação dos capítulos

Prezados leitores, antes de apresentar os conteúdos e resultados gerados durante a realização deste doutorado, se faz necessário apresentar o histórico de como o projeto atual se difere do inicialmente proposto, alterado devido a uma série de diferentes questões.

O projeto inicialmente proposto, intitulado **Análise filogeográfica de três espécies do gênero *Idiops* Perty 1833 (Araneae, Idiopidae)** tinha como principal objetivo realizar análises filogeográficas para aranhas de alçapão das espécies *Idiops fuscus* Perty, 1833, *Idiops camelus* (Mello Leitão, 1937) *e Idiops pirassununguensis*, Fukami & Lucas 2005, além testar a efetividade de novos marcadores moleculares (MRPL45, RPF2, XPNPEP3 e HAT1) propostos para aranhas por Rix *et al*. (2017) e comparar com as informações obtidas a partir do marcador mitocondrial Citocromo Oxidase Sub-unidade I (COI) e do marcador nuclear ITS2. Também propunha realizar análises morfogeométricas, com o intuito de investigar se há variações morfológicas significativas entre as populações das três espécies.

Baseado na proposta inicial, e seguindo o cronograma inicial de atividades, três frentes principais de ações foram realizadas nos dois primeiros anos de doutorado (2018-2019): viagens de coleta biológica para diferentes localidades com registro de ocorrência de *Idiops*; visitas a coleções zoológicas, para examinar, fotografar e medir os espécimes pertencentes as espécies alvo do estudo e extração do DNA das espécies de *Idiops* coletadas. Neste período, foram realizadas dez expedições à campo, que abrangeram 19 Unidades de Conservação Federais (UCs) em quatorze estados e amostraram 40 localidades, além de visitas a sete coleções aracnológicas. Também foram iniciados os procedimentos genéticos, realizados no Laboratório de Diversidade Genética da Universidade Estadual de Campinas (Unicamp).

A partir dos resultados coletados em campo e do material examinado nas coleções aracnológicas, chegou-se as seguintes observações: (1) foram coletados espécimes de *Idiops* em apenas 45% das ocasiões (18 localidades), e geralmente com baixo número de indivíduos; (2) os espécimes inicialmente identificados como representantes das três espécies alvo, na verdade pertenciam a mais espécies, inclusive a táxons até então novos para a ciência,

o que pode comprometer o delineamento filogeográfico do estudo, que depende de informações taxonômicas e geográficas precisas; (3) a dificuldade de coleta e obtenção de material fresco, para extração de DNA, poderia ser um fator limitante para a realização das análises filogeográficas, que dependem de uma quantidade mínima de espécimes por população para realização dos estudos. Estas constatações motivaram a revisão das espécies Neotropicais de *Idiops*, táxon que apesar de ser de difícil coleta (Dippenaar-Schoeman 2002, Fonseca-Ferreira *et al*. 2021), possui um contingente considerável de espécimes depositado nas coleções zoológicas, possibilitando a primeira alteração do projeto inicial. Além de ter um importante valor para o conhecimento taxonômico e sistemático para o grupo, esta revisão daria as bases para realização das análises moleculares futuras.

Durante o segundo ano, dois fatores congruentes e inesperados mudaram os rumos deste projeto de doutorado. O primeiro tem motivo acadêmico: durante as revisões bibliográficas, foram lidos uma série de trabalhos recentes focados em análises filogenômicas, que possibilitavam, inclusive, a utilização de amostras antigas de museu (Wood *et al*. 2018, Hedin *et al*. 2018, Derkarabetian *et al*. 2019). Por coincidência, o autor principal de parte destes trabalhos, Dr. Shahan Derkarabetian, da Universidade de Harvard, ministrou uma palestra nas dependências da Universidade de São Paulo (USP). Graças a esta palestra foi possível uma reunião com este autor, que resultou na proposição de uma colaboração, que seria posteriormente concretizada a partir de uma Bolsa de Estágio a Pesquisa no Esterior (BEPE). Esta BEPE teria como objetivos principais realizar análises filogenômicas e filogeográficas focadas em espécimes Neotropicais de *Idiops,* a partir de amostras frescas e amostras de museu, o que solucionaria o problema da limitação de acesso a amostras até então restritas aos espécimes especificamente armazenados para extração de DNA e possibilitaria o uso de amostras antigas e preservadas em álcool 70% e em temperatura ambiente.

O segundo fator, que afetou a todos, tem motivo sanitário: a pandemia do Covid-19. Para o segundo ano do doutorado, estavam previstas atividades de extração, quantificação e amplificação do DNA das espécies de *Idiops*. As análises foram iniciadas em dezembro de 2019 e para o primeiro semestre de 2020, estavam previstas novas extrações e análises com foco nas amostras de

museu e nos tecidos frescos das espécies *Idiops pirassununguensis* e *Idiops camelus*. Devido a pandemia, todas as atividades externas da Unicamp foram paralisadas. Na esfera internacional, a BEPE (FAPESP 2020/01511-2), prevista para ser realizada em 2020 sob coorientação do Dr. Gonzalo Giribet e supervisão do Dr. Shahan Derkarabetian, no Museu de Zoologia Comparada (MCZ) da Universidade de Harvard, foi diretamente afetada. A proposta de BEPE já estava em fase avançada de análise (despacho concluído), iria incluir 50 amostras, tanto recentes quanto depositadas em museus há mais de 30 anos e objetivava reconstruir a história evolutiva das espécies Neotropicais de *Idiops* a partir dos Elementos Ultraconservados (UCEs). Devido a pandemia, todos os processos de análise para BEPE foram cancelados e o projeto interrompido.

Durante o período da quarentena do Covid-19, que perdurou por boa parte dos anos 2020 e 2021, e afetou o andamento dos trabalhos, um dos focos principais foi a finalização do manuscrito da revisão taxonômica das espécies Neotropicais de *Idiops*. A revisão taxonômica, realizada em colaboração com pesquisadores do Instituto Butantan, culminou na sua publicação na forma de monografia no *European Journal of Taxonomy*, sob o seguinte título: **Taxonomic revision of the Neotropical spiders of the genus *Idiops* Perty, 1833 (Araneae, Idiopidae), with description of four new species.** Os resultados, apresentados no **Capítulo 1**, incluem a redescrição para a maioria das espécies, descrição de quatro novas espécies, pranchas com imagens para todas as espécies, incluindo as primeiras fotomicrografias em MEV para o gênero, sinonimização e revalidação de espécies e mapas de distribuição das espécies atualizado, que agora conta com 24 espécies na América do Sul (Fonseca-Ferreira *et al*. 2021).

Ainda durante a pandemia, em meados de 2020, foram reiniciados os contatos da colaboração com o Dr. Shahan Derkarabetian. Devido a impossibilidade de realização da BEPE e ao aumento do preço para sequenciamento e preparação das bibliotecas de UCEs, que afetou o desenho amostral inicial, novos caminhos foram propostos. Ao invés de 50 amostras, foram sequenciadas 30 amostras, e as análises foram focadas em testar a monofilia de *Idiops* e investigar as relações entre os gêneros da subfamília Idiopinae Simon, 1889. Para a obtenção de amostras dos demais gêneros de Idiopinae e de grupos externos, foram iniciadas colaborações com as

pesquisadoras Dra. Vera Opatova (Charles University, Tchéquia) e Dra. Robin Lyle (Agricultural Research Council, África do Sul). O processo de execução das análises filogenômicas, incluindo concepção do desenho amostral, extração do DNA das amostras, análises bioinformáticas e discussão dos resultados gerados também contou com a colaboração dos pesquisadores Dr. Shahan Derkarabetian (Universidade de Harvard) e Dra. Millke Morales (Universidade Estadual de Campinas). Todos os procedimentos e resultados obtidos a partir destas análises, que incluem a validação da monofilia de Idiopinae e a comprovação da hipótese de parafilia de *Idiops* e Idiopidae, são apresentados no Capítulo 2, intitulado **Análises filogenômicas dos gêneros de Idiopinae 1889 (Idiopidae), com ênfase nas espécies Neotropicais de *Idiops* Perty 1833, baseado em Elementos Ultraconservados (UCE)**.

Por fim, no Capítulo 3, intitulado **Geographic variation of a trapdoor spider (Araneae, Idiopidae) across different Brazilian biomes reveal morphometric differentiation of spiders from the Brazilian Caatinga biome**, são apresentados os resultados da primeira investigação morfométrica para uma espécie de Idiopidae, focados em uma série de análises baseadas em medidas tradicionais e geométrica de mais de 60 espécimes de *Idiops pirassununguensia.* Durante a revisão, esta espécie teve sua área de ocorrência mais que duplicada, com novos registros de ocorrência para os biomas da Amazônia, Caatinga e Cerrado. Iniciados durante a pandemia e finalizado no último ano, os estudos morfométricos, gerados a partir de uma série de análises multivariadas das medidas lineares das pernas, da carapaça e do esterno e das formas morfogeométricas do esterno, da disposição ocular e do bulbo copulador, objetivaram investigar os padrões de variação geográfica ao longo dos biomas de ocorrência (Amazônia, Caatinga e Cerrado). Os resultados sugerem a presença de estruturação morfológica entre os espécimes originários da Caatinga em relação aos demais bimas. Os possíveis fatores que podem estar envolvidos nos padrões de estruturação observados foram discutidos em seguida.

Apesar das evidentes diferenças observadas entre o projeto inicial, focado na filogeografia de três espécies de *Idiops*, os resultados gerados ao longo deste doutorado agregam uma quantidade sem precedentes de informações sobre o

gênero *Idiops* e a subfamília Idiopinae, que envolveram revisão taxonômica, análises filogenômicas e morfométricas de representantes de Idiopidae.

REFERÊNCIAS BIBLIOGRÁFICAS

Derkarabetian, S., Benavides, L. R., & Giribet, G. (2019). Sequence capture phylogenomics of historical ethanol-preserved museum specimens: Unlocking the rest of the vault. *Molecular Ecology Resources*, *19*(6), 1531–1544. https://doi.org/10.1111/1755-0998.13072

Dippenaar-Schoeman, A. S. (2002). Baboon and trapdoor spiders of southern Africa: an identification manual. Pretoria: Agricultural Research Council.

Fonseca-Ferreira, R., Guadanucci, J. P. L., Yamamoto, F. U., & Brescovit, A. D. (2021). Taxonomic revision of the Neotropical spiders of the genus *Idiops* Perty, 1833 (Araneae, Idiopidae), with description of four new species. *European Journal of Taxonomy*, *780*, 1–71. https://doi.org/10.5852/ejt.2021.780.1581

Hedin, M., Derkarabetian, S., Ramírez, M. J., Vink, C., & Bond, J. E. (2018). Phylogenomic reclassification of the world's most venomous spiders (Mygalomorphae, Atracinae), with implications for venom evolution. *Scientific Reports*, *8*(1). https://doi.org/10.1038/s41598-018-19946-2

Rix, M. G., Cooper, S. J. B., Meusemann, K., Klopfstein, S., Harrison, S. E., Harvey, M. S., & Austin, A. D. (2017a). Post-Eocene climate change across continental Australia and the diversification of Australasian spiny trapdoor spiders (Idiopidae: Arbanitinae). *Molecular Phylogenetics and Evolution*, *109*, 302–320. https://doi.org/10.1016/j.ympev.2017.01.008

Wood, H. M., González, V. L., Lloyd, M., Coddington, J., & Scharff, N. (2018). Next- generation museum genomics: Phylogenetic relationships among palpimanoid spiders using sequence capture techniques (Araneae: Palpimanoidea). *Molecular Phylogenetics and Evolution*, *127*, 907–918. https://doi.org/10.1016/j.ympev.2018.06.038

Capítulo 1

European Journal of Taxonomy 780: 1–71
https://doi.org/10.5852/ejt.2021.780.1581
ISSN 2118-9773
www.europeanjournaloftaxonomy.eu
2021 · Fonseca-Ferreira R. *et al.*

Monograph

urn:lsid:zoobank.org:pub:932663A6-D83D-49E0-B1F7-87F7DA8DC086

Taxonomic revision of the Neotropical spiders of the genus *Idiops* Perty, 1833 (Araneae, Idiopidae), with description of four new species

Rafael FONSECA-FERREIRA [1,*], José Paulo Leite GUADANUCCI [2], Flávio Uemori YAMAMOTO [3] & Antonio Domingos BRESCOVIT [4]

[1] Pós-graduação em Ecologia, Evolução e Biodiversidade, Instituto de Biociências, Universidade Estadual Paulista, Avenida 24A 1515, 13506-900 Rio Claro-SP,Brazil.
[2] Departamento de Ecologia, Evolução e Biodiversidade, Instituto de Biociências, Universidade Estadual Paulista, Avenida 24A 1515, 13506-900 Rio Claro-SP,Brazil.
[3,4] Laboratório de Coleções Zoológicas, Instituto Butantan, Av. Vital Brasil, 1500, Butantã, São Paulo, São Paulo, CEP 05503-900, Brazil.

[*] Corresponding author: rafaelbioferreira@gmail.com
[2] Email: jose.guadanucci@unesp.br
[3] Email: flayamamoto@gmail.com
[4] Email: antonio.brescovit@butantan.gov.br

Abstract. Neotropical species of the genus *Idiops* Perty, 1833 are reviewed, and four new species are described from Brazil: *I. duocordibus* Fonseca-Ferreira, Guadanucci & Brescovit sp. nov., *I. guri* Fonseca-Ferreira, Guadanucci & Brescovit sp. nov., *I. mocambo* Fonseca-Ferreira, Guadanucci & Brescovit sp. nov. and *I. sertania* Fonseca-Ferreira, Guadanucci & Brescovit sp. nov. The majority of species are redescribed based on the examination of the types and extensive material. Males of *I. petiti* (Guérin, 1838), *I. rastratus* (Pickard-Cambrige, 1889), *I. rohdei* Karsch, 1886 and *I. nilopolensis* Mello-Leitão, 1923, and females of *I. fuscus* Perty, 1833 and *I. pirassununguensis* Fukami & Lucas, 2005, hitherto unknown, are described for the first time. *Idiops nilopolensis*, considered a nomen dubium, is revalidated. *Idiops fulvipes* Simon, 1889 is synonymized with *I. argus* Simon, 1889, and *I. santaremius* (Pickard-Cambrige, 1896) is synonymized with *I. petiti*. Neotypes are designated for *Idiops fuscus*, *I. nilopolensis* and *I. siolii* (Bücherl, 1953). *Idiops bonapartei* Hasselt, 1888 is considered species inquirendae, since the type is an immature female. Finally, an updated distribution map of Neotropical species is included. The genus now has 24 species in the Neotropical region.

Keywords. Mygalomorphae, Idiopinae, Domiothelina, Arachnida, trapdoor spiders.

Fonseca-Ferreira R., Guadanucci J.P.L., Yamamoto F.U. & Brescovit A.D. 2021. Taxonomic revision of the Neotropical spiders of the genus *Idiops* Perty, 1833 (Araneae, Idiopidae), with description of four new species. *European Journal of Taxonomy* 780: 1–71. https://doi.org/10.5852/ejt.2021.780.1581

Introduction

The family Idiopidae Simon, 1889 comprises species popularly known as spiny trapdoor spiders. The spiders build and live in silk-lined burrows in the soil, which are closed with a camouflaged operculum, which functions as a trapdoor (Raven 1985; Dippenaar-Schoeman 2002; Fig. 1A–L). Idiopidae was erected by Raven (1985), who raised the tribe Idiopiae Simon, 1889, until then included in Ctenizidae Thorell, 1887, to the family level. Sustained by three apparently apomorphic features of the male palp (Raven 1985), the family monophyly was never questioned, being well supported by both morphological (Goloboff 1993) and molecular data (Hedin & Bond 2006; Bond *et al.* 2012; Opatova *et al.* 2020). With an origin dating back to the Lower Cretaceous, about 133 million years ago (Opatova *et. al.* 2020), and Gondwanan distribution (World Spider Catalog 2021), the family Idiopidae is currently divided into three subfamilies: Arbanitinae Simon, 1903, with spiders restricted to Oceania, Genysinae Simon, 1903, occurring in India, Sri Lanka, Madagascar and South America, and Idiopinae Simon, 1889, from South America, Africa, the Middle East, and Southern and Southeast Asia (Raven 1985; World Spider Catalog 2021). The idiopids are currently the third most diverse mygalomorph family, comprising 434 species in 23 genera (World Spider Catalog 2021). Despite this potential, only genera belonging to the subfamily Arbanitinae have recently been systematically reviewed, which have also formed the basis of subsequent biogeographic studies (Rix *et al.* 2017a, 2017b; Wilson *et al.* 2018, 2020).

Representatives of the subfamily Idiopinae are characterized by having the anterior lateral eyes projected in front of the others, close to the anterior margin of the carapace, the cephalic area of the carapace arched, distal segments of the front legs with numerous lateral spines and the tibia of leg I of males with the tibial apophysis with one or two apical branches (Raven 1985). It currently has seven genera: *Ctenolophus* Purcell, 1904, *Galeosoma* Purcell, 1903, *Gorgyrela* Purcell, 1902, *Segregara* Tucker, 1917 and *Titanidiops* Simon, 1903, restricted to the African continent, *Heligmomerus* Simon, 1892 occurring in India, Sri Lanka and Africa, and *Idiops* Perty, 1833 occurring in South America, Africa, Syria, Israel, Yemen, India, Myanmar and Thailand (World Spider Catalog 2021).

Among the genera of Idiopidae, the most diverse is *Idiops* Perty, 1833 (Fig. 2A–F), which currently includes 99 valid species (World Spider Catalog 2021). Their body size ranges from 5 to 35 mm and species are mainly characterized by chelicera with two rows of teeth on the prolateral and retrolateral margins, a sternum with two pairs of sigilla (posterior pair absent) and the absence of tiny spines on the coxae (Raven 1985; Dippenaar-Schoeman 2002). In the cladistic analysis carried out by Raven (1985), *Idiops* is closely related to *Ctenolophus* and *Galeosoma*, grouped in a trichotomy and supported by the absence of the posterior pair of sigillae (Raven 1985). According to the molecular phylogeny proposed by Opatova *et al.* (2020), *Idiops* is recovered as the sister-group to four other genera of Idiopinae that were recovered as a monophyletic clade.

Four genera are considered junior synonyms of *Idiops*. *Acanthodon* Guérin, 1838, proposed based on the species *A. petiti* Guérin, 1838 from Brazil, was synonymized with *Idiops* by Pickard-Cambridge (1870). However, Simon (1892) revalidated *Acanthodon*, differentiating it from *Idiops* by its ocular formation and restricted the American species to the genera *Pseudidiops* Simon, 1889 and *Idiops*. Later, Simon (1903), when examining a female of *Idiops germaini* Simon, 1892, considered that the differences in the eyes between *Idiops* and *Acanthodon* would not be valid, since they are dependent on sex. Consequently, he synonymized these two genera again, but kept the *Idiops* genus only for American species. The problem of *Acanthodon* was only solved by Tucker (1917) and its consequent synonymy with *Idiops*. *Dendricon*

Fig. 1. Natural habitats and diversity of burrows and trapdoors of *Idiops* Perty, 1833 spp. **A–G**. Ravine habitats. **H–L**. Ground habitats. Images by Rafael P. Indicatti (A–B); by Arthur Anker and Pedro H. Martins (C–D); by Leonardo S. Carvalho (E–F); by Rafael Fonseca-Ferreira (G–L).

Fig. 2. Live habitus of *Idiops* Perty, 1833. **A**. *I. fuscus* Perty, 1833, ♀. **B**. *I. fuscus*, ♂. **C**. *I. camelus* (Mello-Leitão, 1937), ♀. **D**. *I. camelus*, ♂. **E**. *I. pirassununguensis* Fukami & Lucas, 2005, ♀. **F**. *I. pirassununguensis*, ♂. Images by: Leonardo S. Carvalho (A–B); Rafael P. Indicatti (C–D); Pedro H. Martins (E–F).

O. Pickard-Cambridge, 1889 was proposed based on *D. rastratum* O. Pickard-Cambridge, 1889, but was synonymized with *Pseudidiops* Simon, 1889 by Pocock (1895). *Pseudidiops* was proposed based on the species *P. opifex* Pocock 1899, from Colombia. This genus was synonymized by Raven (1985) who considered the characteristics presented by Simon insufficient to differentiate this genus. *Juambeltzia* Mello-Leitão, 1946 was proposed based on the species *J. clara* Mello-Leitão, 1946, from Argentina, and later synonymized by Schiapelli & Gerschman de Pikelin (1971). *Pachyidiops* Simon, 1903 was established based on the species *Idiops crassus* Simon, 1884, from Burma and was synonymized by Raven (1985).

So far, no comprehensive review of the genus *Idiops* has been carried out, only propositions of species (Fonseca-Ferreira *et al.* 2017; Siliwal *et al.* 2020) or reviews limited to countries (Fukami & Lucas 2005; Mirza *et al.* 2012; Ferretti *et al.* 2017). Here we present a taxonomic revision of the Neotropical species of *Idiops* and present an updated distribution map of Neotropical species, thus expanding the knowledge of the family Idiopidae.

Material and methods

Repositories

The examinedspecimens are depositedinthefollowingtaxonomiccollections (curators indicated between parentheses):

BMNH	=	The Natural History Museum, London, UK (J. Beccaloni)
CAD	=	Coleção Aracnológica Diamantina, UNESP, Rio Claro, Brazil (J.P. Guadanucci)
CHNUFPI	=	Coleção de História Natural, Universidade Federal do Piauí, Brazil (L.S. Carvalho)
FCE	=	Facultad de Ciencias, Universidad de la República, Montevideo, Uruguay (M. Simó)
IBNP	=	Inventario Biológico Nacional de Paraguay, Asunción, Paraguay (J.A. Kochalka)
IBSP	=	Instituto Butantan, São Paulo, Brazil (A.D. Brescovit)
INPA	=	Instituto Nacional de Pesquisas da Amazônia, Manaus, Brazil (M.L. Oliveira)
MCN	=	Museu de Ciências Naturais, Sema, Porto Alegre, Brazil (R. Ott)
MCTP	=	Museu de Ciências e Tecnologia, Pontifícia Universidade Católica, Porto Alegre, Brazil (R.A. Teixeira)
MHNM	=	Museo Nacional de História Natural, Montevideo, Uruguay (A. Laborda)
MNHN	=	Muséum national d'histoire naturelle, Paris, France (C. Rollard)
MNRJ	=	Museu Nacional, Universidade Federal do Rio de Janeiro, Rio de Janeiro, Brazil (A.B. Kury)
MPEG	=	Museu Paraense Emilio Goeldi, Belém, Brazil (A.B. Bonaldo)
MZSP	=	Museu de Zoologia, Universidade de São Paulo, São Paulo, Brazil (R. Pinto da Rocha)
UFMG	=	Coleção de Invertebrados, Universidade Federal de Minas Gerais, Belo Horizonte, Brazil (A.J. Santos)
UFMT	=	Coleçãode Arachnida, Universidade Federaldo Mato Grosso, Cuiabá, Brazil(A. Chagas Junior)
UFPB	=	Coleção de Arachnida, Universidade Federal da Paraíba, João Pessoa, Brazil (M.B. da Silva)
ZMB	=	Zoologisches Museum Berlin, Berlin, Germany (J. Dunlop)

Measurements

Measurements were taken with the aid of a Leica M205C stereo microscope equipped with a Leica DFC295 digital camera. The measurements of the carapace, abdomen and legs were taken in dorsal view. For the diameter of the eyes, the largest values were considered. Leg measurements are given in the following order: total length (femur, patella, tibia, metatarsus, tarsus). All measurements are in millimeters. The coding and position of the leg spines follow the methodology proposed by Petrunkevitch

(1925). Spermathecae were dissected and immersed in enzyme (Ultrazyme®) for 24 hours for soft tissue digestion to allow observation of the internal structures.

Illustrations

Photographs were taken with a Leica DFC295 digital camera, with focus stacking using Leica Application ver. 2.5.0. For scanning electron microscopy (SEM) micrographs, body parts were dehydrated in a series of graded ethanol washes (80% to 100%), dried by critical point, mounted on metal stubs using adhesive copper tape and nail polish for fixation and covered with gold. SEM micrographs were taken with an FEI Quanta 250 scanning electron microscope at the Laboratório de Biologia Celular of Instituto Butantan, São Paulo, Brazil. The drawings were made with the aid of a Leica MZ12.5 stereo microscope equipped with a camera lucida. The final art of the drawings was made with graphite, on 180g opaline paper. Illustrations were digitalized using the HP Scanjet G4050 scanner. All generated pictures were later edited in Photoshop CC 2018 software.

Geographical data

Each locality from museum databases was carefully checked (lat-long coordinates) to correct for imprecise georeferences in decimal degrees, based on the WGS 1984 datum. In the case of samples with inaccurate or incomplete distribution data, the specimens were georeferenced to the geographic center of the given locality. For species from Argentina, recently reviewed by Ferretti *et al.* 2017, the coordinates available in the material examined were included. Species distribution maps were made using the QGIS ver. 3.12.3 program. Subsequently, they were organized into plates using the Photoshop CC 2018 software.

Abbreviations

ALE	=	anterior lateral eyes
AME	=	anterior median eyes
CL	=	carapace length
CW	=	carapace width
d	=	dorsal
DET	=	distal embolar tooth
EL	=	embolar lamella
Fe	=	femur
K	=	keel
Mt	=	metatarsus
LL	=	labium length
LW	=	labium width
p	=	prolateral
Pa	=	patella
PLE	=	posterior lateral eyes
PME	=	posterior median eyes
PT	=	promarginal teeth
r	=	retrolateral
RT	=	retromarginal teeth
SL	=	sternum length
SW	=	sternum width
Ta	=	tarsus
TBL	=	total body length
Ti	=	tibia
v	=	ventral

Results

Taxonomy

Class Arachnida Cuvier, 1812
Order Araneae Clerck, 1757
Family Idiopidae Simon, 1889
Subfamily Idiopinae Simon, 1889

Genus ***Idiops*** Perty, 1833

Idiops Perty, 1833: 197 (type species by monotypy: *I. fuscus* Perty, 1833).
Acanthodon Guérin, 1838: 163 (type species by monotypy: *A. petitii* Guérin, 1838). Synonymized by O. Pickard-Cambridge 1870: 107.
Dendricon O. Pickard-Cambridge, 1889: 250 (type species by monotypy: *D. rastratum* O. Pickard-Cambridge, 1889). Synonymized by Pocock 1895: 223.
Pseudidiops Simon, 1889: 215 (type species by monotypy: *P. opifex* Simon, 1889). Synonymized by Raven 1985: 139.
Juambeltzia Mello-Leitão, 1946: 6 (typespecies by monotypy: *J. clara* Mello-Leitão, 1946). Synonymized by Schiapelli & Gerschman de Pikelin 1971: 58.

Idiops – O. Pickard-Cambridge 1870: 101. — Simon 1892: 89. — Roewer 1953: 5. — Raven 1985: 139. — Dippenaar-Schoeman 2002: 68.
Acanthodon – Walckenaer 1837: 434. — Simon 1892: 90; 1903: 350. — Pocock 1897: 731.

Type species

Idiops fuscus Perty, 1833

Composition

Idiops includes 102 species, of which 24 occur in the Neotropical region, including the four new species herein described: *I. fuscus* Perty, 1833, the type species, *I. argus* Simon, 1889, *I. bonapartei* Hasselt, 1888, *I. cambridgei* Ausserer, 1875, *I. camelus* (Mello Leitão, 1937), *I. carajas* Fonseca-Ferreira, Zampaulo & Guadanucci, 2017, *I. clarus* (Mello-Leitão, 1946), *I. duocordibus* sp. nov., *I. germaini* Simon, 1892, *I. guri* sp. nov., *I. harti* (Pocock, 1893), *I. hirsutipedis* Mello-Leitão, 1941, *I. minguito* Ferretti, 2017, *I. mocambo* sp. nov., *I. nilopolensis* Mello-Leitão, 1923, *I. opifex* (Simon, 1889), *I. petiti* (Guérin, 1838), *I. piluso* Ferretti, Nime & Mattoni, 2017, *I. pirassununguensis* Fukami & Lucas, 2005, *I. sertania* sp. nov., *I. siolii* (Bücherl, 1953), *I. rastratus* (O. Pickard-Cambridge, 1889), *I. rohdei* Karsch, 1886 and *I. tolengo* Ferretti, 2017.

Distribution

South America, Africa, Syria, Israel, Yemen, India, Myanmar and Thailand. Here we present the updated distribution of the Neotropical species of the genus (Figs 3–4).

Diagnosis

The species of *Idiops* differ from all other Idiopinae by having the coxae without spines and by the chelicerae with a row of large teeth along the retromargin and small teeth concentrated in the basal third of the promargin and arranged in a row or randomly (Fig. 5A–B; except *I. harti* (Pocock, 1893)). *Idiops harti* differs from all other species of the genus by having only one prolateral row of large teeth (Fig. 5C).

Description

Small to medium sized spiders, with Neotropical species with total length ranging between 5.4 mm and 19.1 mm. Brown color, with variation between yellowish brown and almost entirely black (Fig. 2A–F). Anterior lateral eyes close to clypeal edge (Fig. 6A). Chelicerae with a prolateral row of large teeth and a retrolateral row of smaller teeth (Fig. 6B), retrolateral teeth occupying basal third of chelicerae, arranged in a row (Fig. 5A) or randomly (Fig. 5B), except *I. harti*, with retrolateral teeth absent (Fig. 5C), and rastellum consisting of a distinct process with large spines (Fig. 6C). Legs with three tarsal claws, paired claws with teeth and third claw smooth (Fig. 6D). Adhesive scopula absent, pseudoscopula present in males (Fig. 6D). Sternum with two anterior pairs of small marginal sigillae. Abdomen oval, without

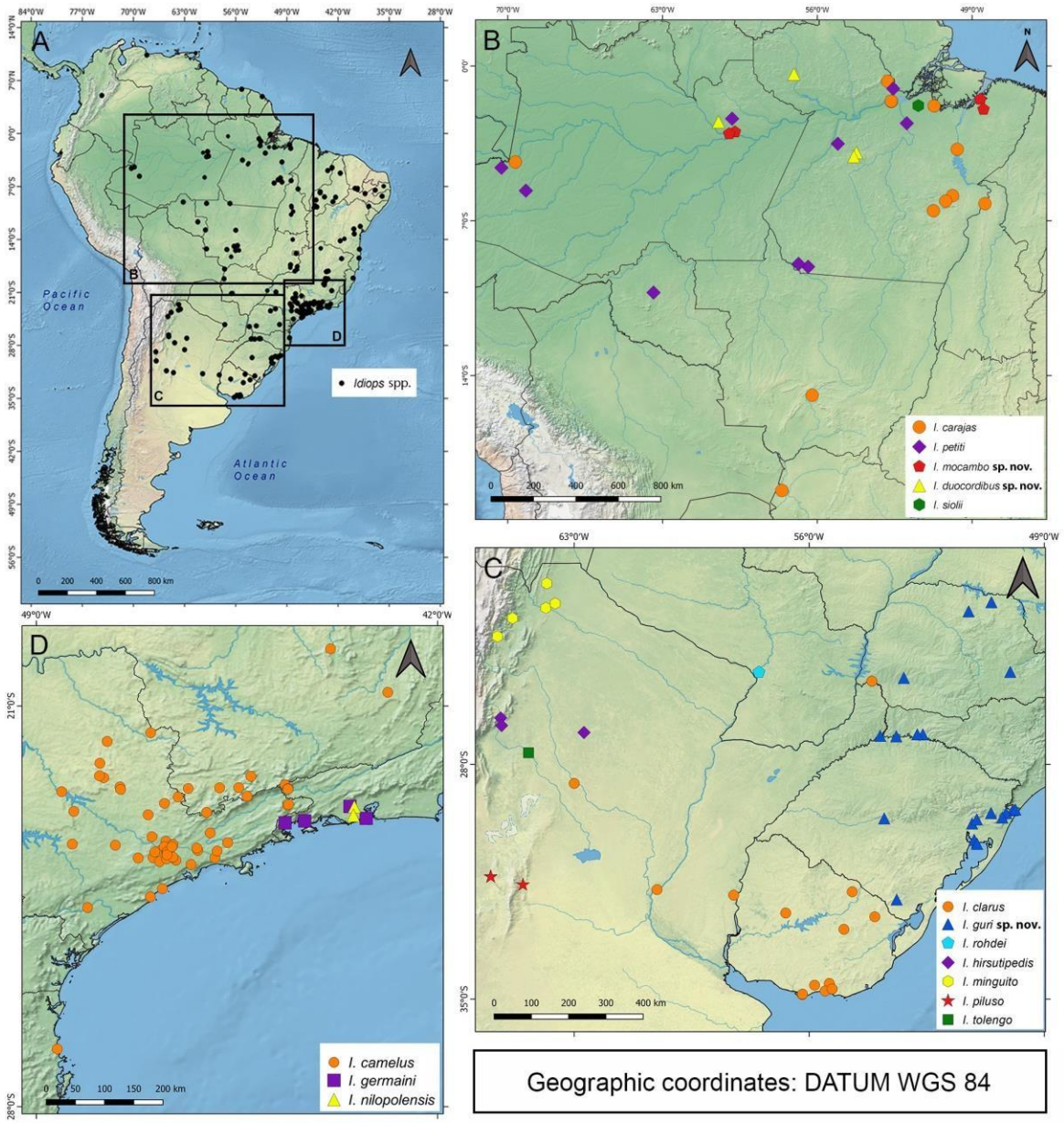

Fig. 24. Distribution of species of *Idiops* Perty, 1833 in the Neotropical region (part).

ornaments or sclerotic spots (Fig. 2A–F). Four spinnerets; posterior lateral spinnerets trisegmented and with a domed apical segment, posterior median spinnerets with one short segment. Males with enlarged palpal tibia, with retrolateral depression bordered by robust spines (Fig. 6E–F). Copulatory bulb presents an embolus withmedian curvature, subapical torsion, apical expansion, usuallyinflattenedshape(embolar lamella) (Fig. 7E–F) or pointed shape (distal embolar tooth) (Fig. 19E) (with the exception of *I. petiti*; Fig. 26E–F). Leg I with a double tibial apophysis, with apical branch wider than basal branch (Fig. 6G) (with the exception of *I. germaini*; Fig. 18H), with putative slit organ between the two branches (Fig. 6H–I). Metatarsus I smooth (with the exception of *I. duocordibus* sp. nov., *I. petiti* and *I. pirassununguensis*, which have a subapical prolateral projection (Figs 17I, 26I, 27I)). *Idiops* females have cuspules on labium and maxillae. In *I. duocordibus* sp. nov., *I. opifex* and *I. rastratus*, cuspules occupy entire ventral region of maxillae (Figs 17K, 29K). Tibia III presents dorsal depression in *I. fuscus*, *I. camelus*, *I. pirassununguensis* and *I. rohdei*. Spermathecae with sclerotized basal area, divided into two outward-sloping ducts, each one connected to rounded terminal receptacles (Fig. 7L) (with the exception of *I. duocordibus* sp. nov., *I. petiti* and *I. siolii*; Figs 17L, 26L, 34C) that have receptacles with lobular expansions.

Natural history

Spiders of the genus *Idiops* live in tubular silk-lined burrows, which are closed by a hinged lid (operculum), which functions as a trapdoor (Fig. 1A–F, H–L). The burrows, which can be found on ravines (Fig. 1G)

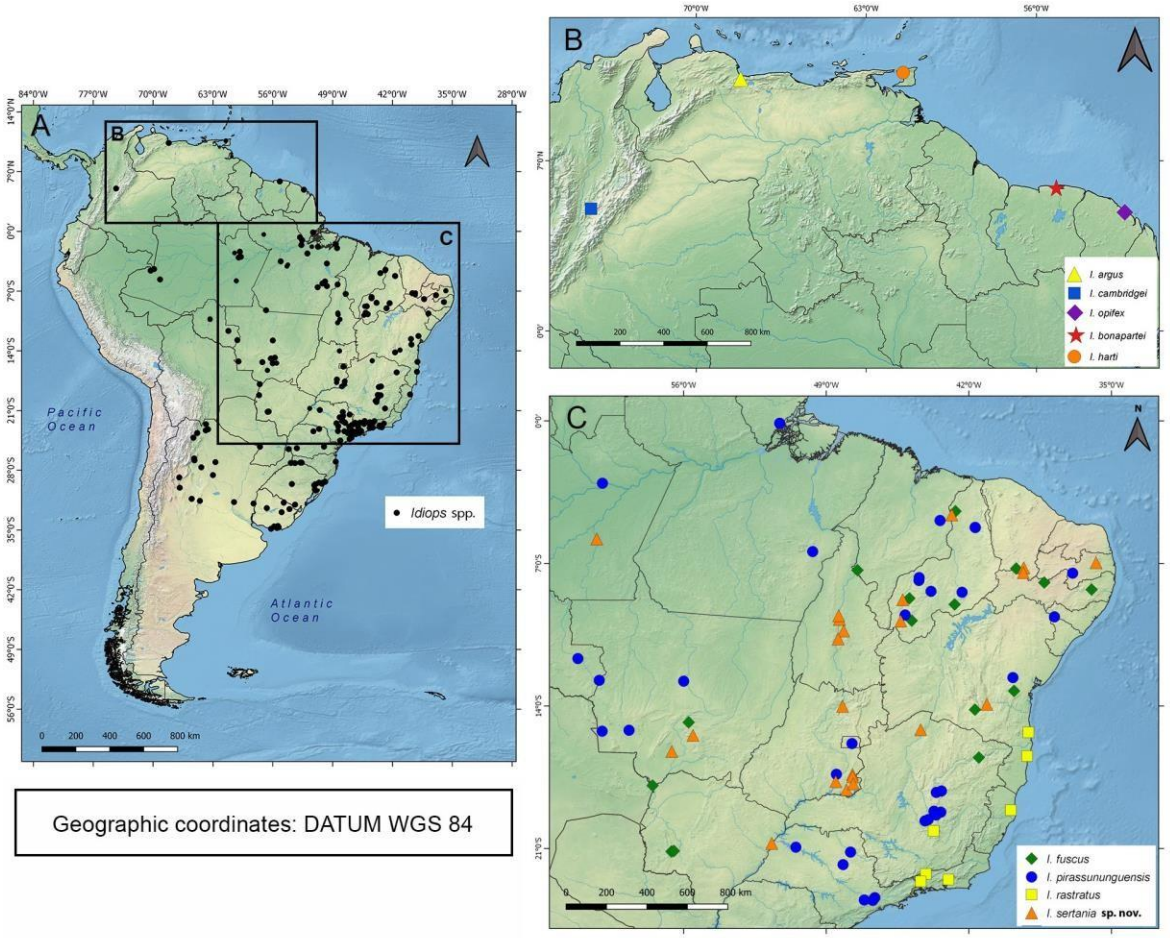

Fig. 4. Distribution of species of *Idiops* Perty, 1833 in the Neotropical region (part).

and on the ground (Fig. 1L), are dug with the help of the rastellum and first legs (Coyle *et al.* 1992). The opercula are usually camouflaged with mosses (Fig. 1A–D), grains of sand and clay (Fig. 6E–F), and small leaves and pieces of dry grass (Fig. 6H–K) (Coyle *et al.* 1992; Dippenaar-Schoeman 2002). These burrows provide a suitable microclimate that protects the spiders from predators, parasites and microbial infections, and behave as effective expansions for ambushing prey (Dippenaar-Schoeman 2002; Pérez-Miles & Perafán 2017). *Idiops* spiders live in a variety of habitats, ranging from dry environments with scattered vegetation and harder soils to more humid environments with dense vegetation and softer soils (Dippenaar-Schoeman 2002; Gupta *et al.* 2013; RFF pers. obs.). Some species can occasionally be found in termite mounds or in soil deposited near the base of trees (Gupta *et al.* 2015) and inside tree bark and rotten trunks (Pickard-Cambridge 1889: fig. 5; pers. obs.). Finally, some species can be found in degraded environments, often close to human dwelling and agricultural environments (Mirza & Sanap 2012; Gupta *et al.* 2013). In Brazil, specimens of *Idiops* were found in urban vegetation fragments, located even in large cities, such as São Paulo (*I. camelus*), Rio de Janeiro (*I. germaini*) and Brasília (*I. pirassununguensis*) (RFF pers. obs.).

Females and juveniles spend most of their lives in the burrows, leaving only during events of capturing prey and disposing of undigested parts. Males, after reaching adulthood, leave their burrows and wander in search for females to copulate (Dippenaar-Schoeman 2002; Pérez-Miles & Perafán 2017). Although less common, it is possible to find males living in individual burrows (Siliwal *et al.* 2020; RFF pers. obs.). It is common to find several nearby burrows, with spiders often belonging to the same population (Dippenaar-Schoeman 2002), with records reaching the density of 20 individuals per m² for *I. bombayensis* Siliwal, Molur & Biswas, 2005 (Mirza & Sanap 2012). At night, the spiders position themselves near the opening, with the trapdoor slightly ajar and wait for the prey that, upon approaching and being noticed, is captured and taken inside (Coyle *et al.* 1992). If disturbed, the spider closes the operculum firmly, holding the trapdoor with its anterior legs, and as a last resort, goes to the bottom of the burrow (Dippenaar-Schoeman 2002; Pérez-Miles & Perafán 2017; pers. obs.). In case there is an egg sac inside the burrow, the female positions itself on top of it to better protect its contents. The egg sac is usually oval and can contain up to 250 eggs held together by thick silk lining (as in *I. joida* Gupta, Das & Siliwal, 2013) (Gupta *et al.* 2013). In cases of adverse environmental events, these spiders can abandon their burrows, migrate to apparently more stable environments and build new burrows (Dippenaar-Schoeman 2002; Pérez-Miles & Perafán 2017).

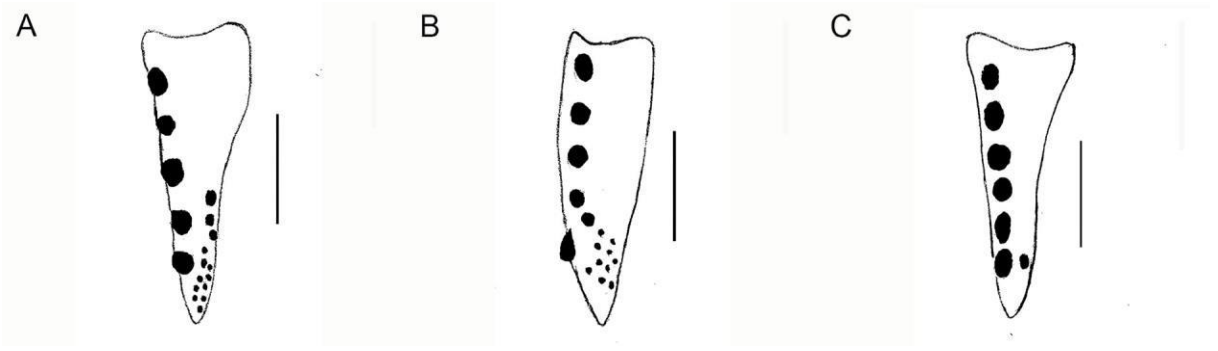

Fig. 5. Chelicera teeth arrangement. **A**. Smaller retrolateral teeth arranged in rows (*I. camelus* (Mello-Leitão, 1937)). **B**. Smaller retrolateral teeth arranged randomly (*I. germaini* Simon, 1892). **C**. Smaller retrolateral teeth absent (*I. harti* (Pocock, 1893)). Scale bars = 1 mm.

Idiops fuscus Perty, 1833
Figs 2A–B, 4C, 6A, 7–8

Idiops fusca Perty, 1833: 197, pl. 39 fig. 5 (♂).

Sphasus idiops – Walckenaer 1837: 379 (new name for *Idiops aculeatus* – lapsus). — Petrunkevitch 1911: 780.
Idiops aculeatus – Walckenaer 1837: 379 (lapsus). — Petrunkevitch 1911: 775.
Idiops fuscus – O. Pickard-Cambridge 1870: 103. — Simon 1892: 92, fig. 91.

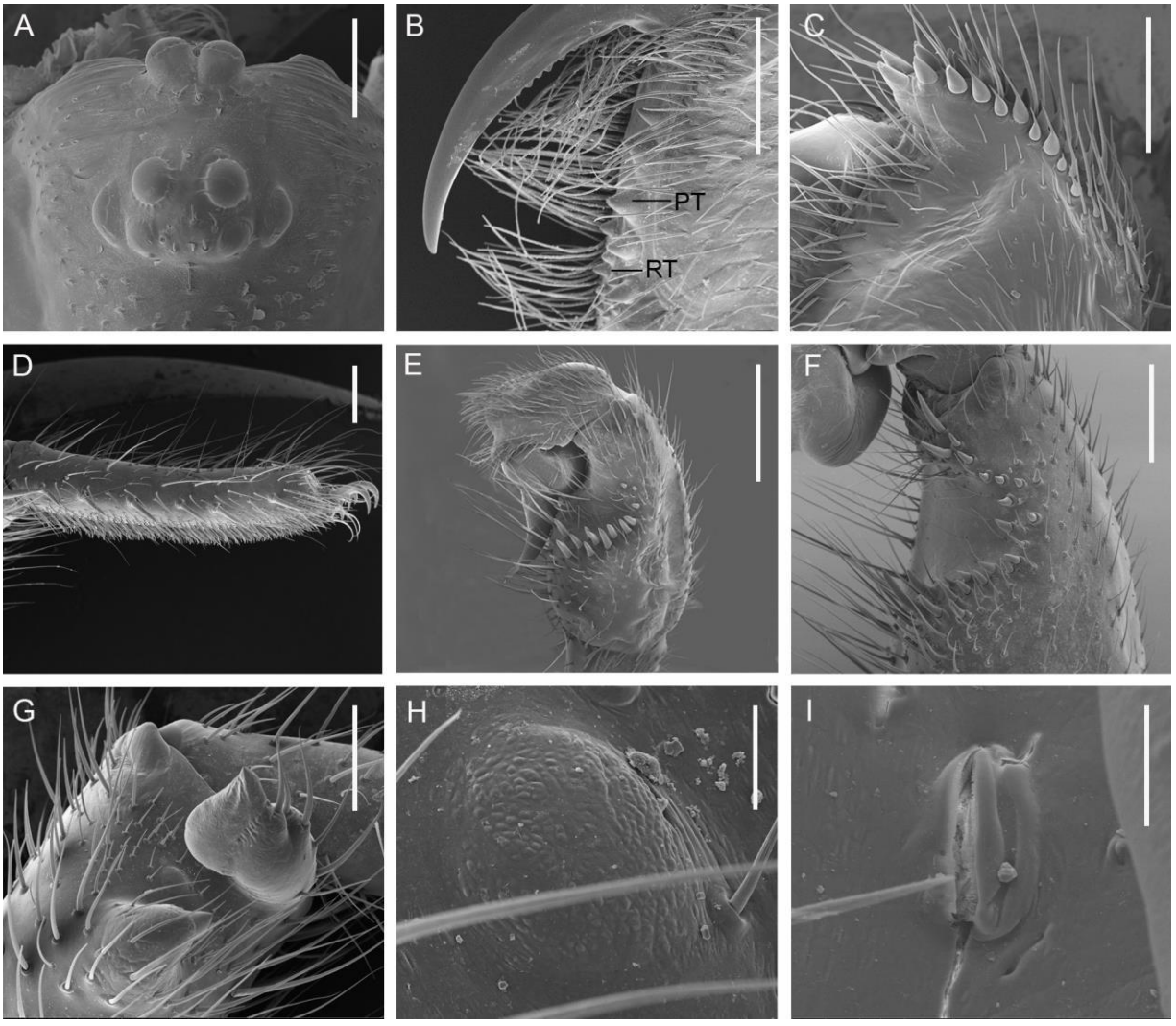

Fig. 6. Diagnostic characters of *Idiops* Perty, 1833 spp. **A**. Ocular disposition, with emphasis on the anterior lateral eyes apart from the others (*I. fuscus* Perty, 1833, CHNUFPI 0036). **B**. Rows of chelicera teeth (*I. clarus* (Mello-Leitão, 1946), FCE 0340). **C**. Rastellum (*I. carajas* Fonseca-Ferreira, Zampaulo & Guadanucci, 2017, MPEG 00109). **D**. Tarsus showing the pseudoscopula and tarsal claws (*I. camelus* (Mello-Leitão, 1937), MZSP 28832). **E**. Palpal bulb (*I. carajas*). **F**. Retrolateral depression of palpal bulb (*I. rastratus* (O. Pickard-Cambridge, 1889), MZSP 24215). **G**. Tibial apophysis (*I. pirassununguensis* Fukami & Lucas, 2005, MZSP 15651). **H–I**. Putative slit organ between the branches of the tibial apophysis (*I. camelus*). Abbreviations: PT = promarginal teeth; RT = retromarginal teeth. Scale bars: A–D, F– G = 0.5 mm; E = 1 mm; H–I = 0.05 mm.

Diagnosis

Males of *I. fuscus* (Figs 7A–I) differ from other Neotropical species of the genus, except *I. clarus* and *I. pirassununguensis*, by having palpal tibia with a prominent projection at the base of the retrolateral depression (Fig. 7C). Differs from *I. clarus* and *I. pirassununguensis* by the strong curvature of the median portion of the embolus in dorsal view (also present in *I. nilopolensis*). Differs from *I. nilopolensis* by the distal portion of the embolus having a pronounced embolar lamella with differentiated dorsal and ventral edges (also present in *I. rastratus*) (Figs 7D–F, 8E–F). The females differ from other Neotropical species by the aspect of the spermathecae, composed of two ducts slightly curved outward, with a soft and non-sclerotized basal portion and a median and apical portion strongly sclerotized and by the receptacula with a much larger diameter than the duct width (Fig. 7L).

Type material

Holotype

BRAZIL – **Piauí** • MNHN. Should be in the MNHN, lost.

Neotype (here designated)

BRAZIL – **Piauí** • ♂; Bom Jesus, Reserva Natural Serra do Teimoso; 8°52′52.6″ S, 44°58′12″ W; 12 Jul.–2 Aug. 2000; F. Curcioi and M. Pixo leg.; IBSP 11887.

Remark: Despite an intensive search, the type specimen of *Idiops fuscus* was not found in the MNHN, being considered lost. In accordance with the criteria of the ICZN Code (ICZN 1999), a neotype is designated here, because the type is lost and the original description is inadequate to stabilize the species. This neotype was based on a specimen collected near the type locality, in the state of Piauí,Brazil.

Other material examined

BRAZIL – **Maranhão** • 1 ♂; Carolina, Campus Hotel Rilton; 7°19′58″ S, 47°28′8″ W; 10 Dec. 2005; UFMT. – **Piauí** • 1 ♀; São Raimundo Nonato; 9°0′54″ S, 42°41′56″ W; 6 Dec. 1994; R. Bertani and D. Pinz leg.; IBSP 9574 • 3 ♂♂ (SEM); União, Campus OMVAPI Ltda; 4°35′9″ S, 42°51′50″ W; 2006; J. Queiroz *et al.* leg.; CHNUFPI 0036 • 2 ♂♂; same collection data as for preceding; CHNUFPI 0030, CHNUFPI 0038 • 1 ♂; Guaribas, Parque Nacional da Serra das Confusões; 9°12′55.5″ S, 43°29′.1″ W; 14 Dec. 2010; F.S. Silva leg.; CHNUFPI 4033 • 1 ♂; Guaribas, Parque Nacional da Serra das Confusões; 9°13′12.3″ S, 43°29′26.7″ W; 9–15 Dec. 2010; L.S. Carvalho leg.; CHNUFPI 4034 • 1 ♂; Guaribas, Parque Nacional da Serra das Confusões; 9°13′32.4″ S, 43°27′46.9″ W; 10 Dec. 2010; F.S. Silva leg.; CHNUFPI 4032. – **Ceará** • 1 ♂; Crato, Parque Estadual Sítio do Fundão; 7°13′3″ S, 39°20′21″ W; May 2016; IBSP 218297. – **Pernambuco** • 2 ♂♂; Caruaru, Brejo; 8°16′58″ S, 35°58′33″ W; Nov. 2010; H. Amorin leg.; IBSP 243978, IBSP 243980 • 1 ♂; Serra Talhada; 7°59′9″ S, 38°17′45″ W; Nov. 2010; H. Amorin leg.; IBSP 243979. – **Bahia** • 1 ♀; Santa Inês, BR420; 13°15′48.7″ S, 39°47′2.8″ W; 18 Jun. 2018; P.H. Martins and E.A. Araújo leg.; UFMG 24028 • 1 ♀; Brumado, Magnesita; 14°10′51.5″ S, 41°42′0.7″ W; 24 Feb. 2017; P. Martins leg.; UFMG 24029. – **Mato Grosso** • 1 ♂; Chapada dos Guimarães; 15°27′39″ S, 55°45′0″ W; 23 Mar. 2001; C. Strussmann leg.; MCTP 12212. – **Minas Gerais** • 1 ♂; Itaobim; 16º31′58.6″ S, 41º30′37.5″ W; 25 Nov. 2011; I.L.F. Magalhães *et al.* leg.; UFMG 10098. – **Mato Grosso do Sul** • 4 ♂♂; Corumbá, Serra do Amolar; 17°94′32″ S, 57°55′47″ W; 8–12 May 2001; C. Strussmann leg.; MCTP 12193 • 1 ♀; Bonito; 21°7′15″ S, 56°28′55″ W; Oct. 2002; C.A. Rheims leg.; IBSP 225943 • 1 ♂; Bonito, Abismo Anhumas; 21°08′60″ S, 56°36′00″ W; Oct. 2002; C.A. Rheims leg.; IBSP 243976 • 2 ♂♂; same collection data as for preceding; IBSP 243974 • 3 ♂♂; same collection data as for preceding; IBSP 243975.

Description

Male (neotype IBSP 11887)

HABITUS. See Fig. 7A.

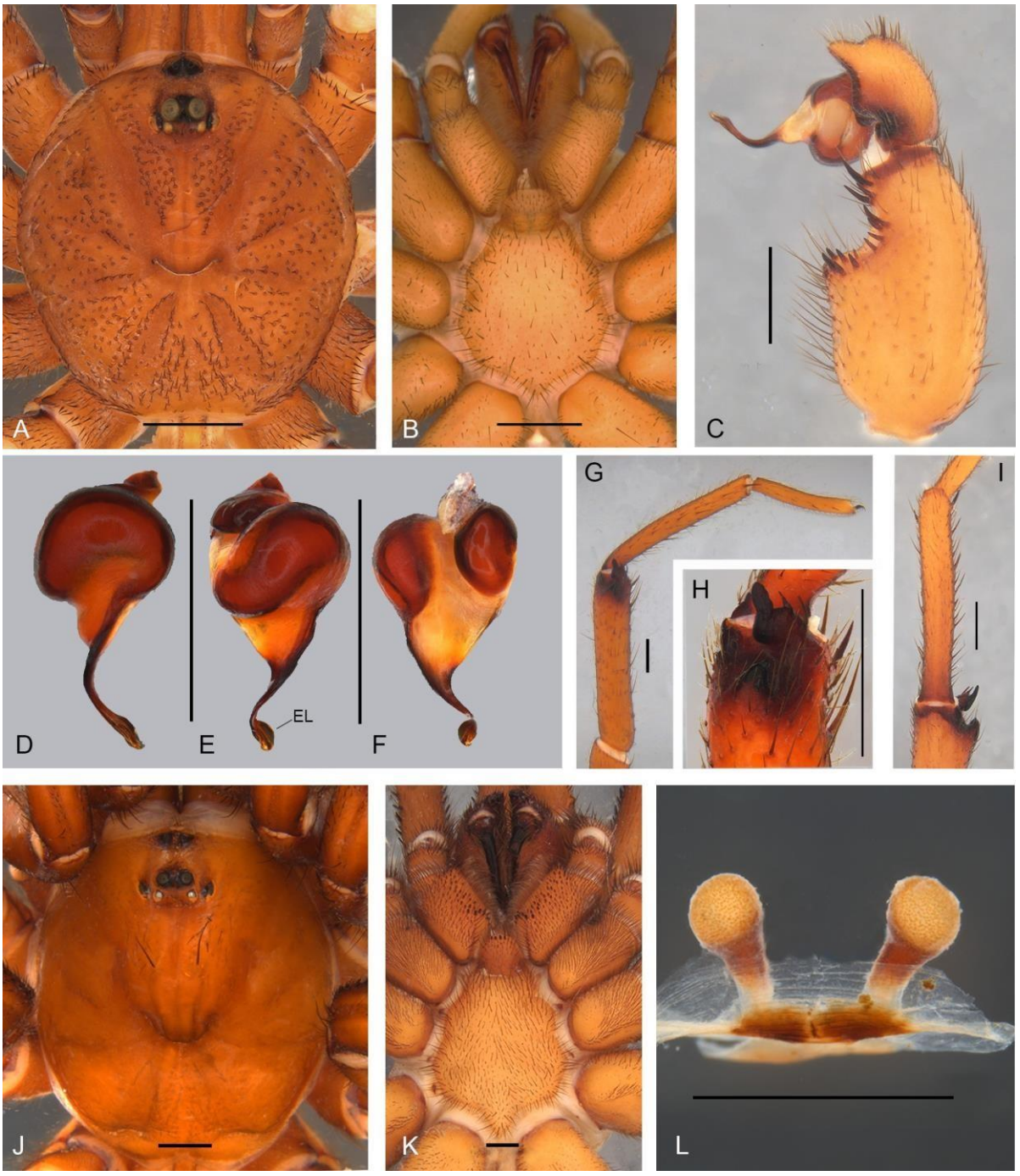

Fig. 7. *Idiops fuscus* Perty, 1833. **A–I**. ♂, neotype (IBSP 11887). **A**. Prosoma (dorsal view). **B**. Prosoma (ventral view). **C**. Part of palp (retrolateral view). **D–F**. Palpal bulb. **D**. Dorsal view. **E**. Retrolateral view. **F**. Prolateral view. **G**. Tibia, metatarsus and tarsus I (prolateral view). **H**. Tibial apophysis (prolateral view). **I**. Tibial apophysis and metatarsus I (dorsal view). **J–L**. ♀ (IBSP 9574). **J**. Prosoma (dorsal view). **K**. Prosoma (ventral view). **L**. Genitalia (dorsal view). Abbreviation: EL = embolar lamella. Scale bars = 1 mm.

MEASUREMENTS. TBL 11.2, CL 5.3, CW 5, LL 0.7, LW 1, SL 3, SW 2.7.

COLOR. Brown carapace and legs, light brown sternum and coxae (Fig. 7A–B), grayish brown abdomen.

PROSOMA. Carapace and ocular arrangement as shown in Fig. 7A. Eye distance AME-ALE 0.6. Eye diameters: AME 0.3, ALE 0.3, PME 0.2, PLE 0.3. Thoracic fovea procurved (Fig. 7A). Labium and sternum without cuspules (Fig. 7B). Basal segment of chelicerae with a prolateral row of 10 large teeth and a retrolateral row of 10 small teeth, grouped in basal half, rastellum with 10–12 spines, distal ones longer (Fig. 8A–B).

LEGS. Tibia, metatarsus and tarsus I as shown in Fig. 7G. Leg I with double tibial apophysis composed of a short, thickened basal branch with a small tapered spine and an apical branch composed of a base twice the size of the basal branch, a thickened apical spine followed by two smaller spines (Figs 7H–I, 8C). Pseudoscopula: tarsus I with apical half with weak coverage (Fig. 7G); tarsus II, III and IV fully covered.

PALP. Tibia with conspicuous retrolateral depression and spines distributed along margin (Fig. 7C); embolus with torsion in apical portion, followed by a pronounced lamella, with upper and lower edges with different sizes (Figs 7D–F, 8E–F).

PALP AND LEG MEASUREMENTS. Palp = 8.8 (3, 1.4, 3, 1.4), I = 22.1 (6.6, 3, 4.7, 5, 2.8), II = 18.9 (5.7, 2.5, 3.9, 4.4, 2.4), III = 16.6 (4.5, 2.3, 2.8, 4.6, 2.4), IV = 22.7 (5.9, 2.7, 5.2, 6, 2.9).

SPINATION. Palp: Ti r20, Ta d0-0-8. Leg I: Pa v0-0-4, Mt v0-12, Ta p0-1-1, r1-1-1. Leg II: Ti v0-1-1-2, Mt v1-2-1-3, Ta p1-1-2, r1-1-3. Leg III: Fe d1-2-2, Pa p3-2-4, r0 -0-4, Ti d0-1-0, v1-2-2, p1-1-4, r1-1-2, Mt v2-2-1-3, p1-1-1, r3-1-0, Ta p1-2-3, r0-1-1. Leg IV: Fe d1-1-2, Ti v1-1-3, Mt v1-1-1-3, Ta p1-1-4, r0-0-2.

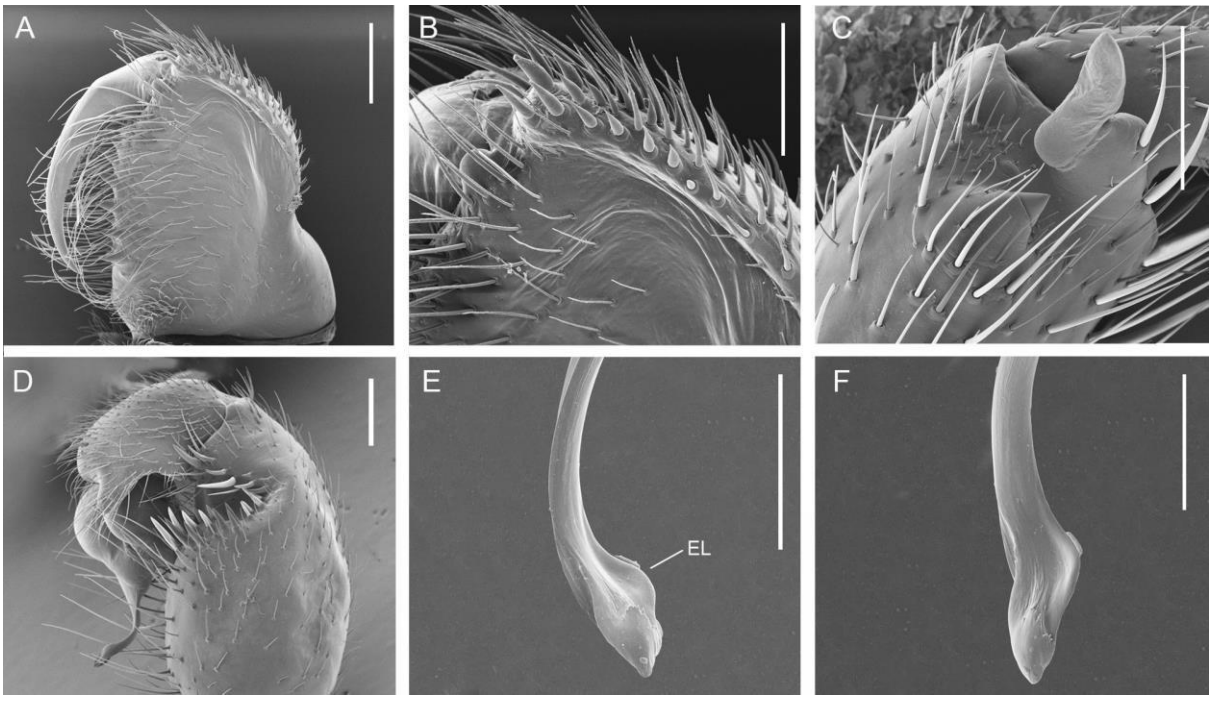

Fig. 8. Scanning electron micrographs of *Idiops fuscus* Perty, 1833, ♂ (CHNUFPI 0036). **A**. Chelicera (retrolateral view). **B**. Rastellum (retrolateral view). **C**. Tibial apophysis (dorsal view). **D**. Part of the palp, showing retrolateral depression. **E–F**. Detail of the distal portion of the embolus. **E**. Retrolateral view. **F**. Prolateral view. Abbreviation: EL = embolar lamella. Scale bars: A, C–D = 0.5 mm; B = 0.3 mm; E–F = 0.2 mm.

Female (IBSP 9574)

HABITUS. See Fig. 7J.

MEASUREMENTS. TBL 18.9, CL 8.2, CW 6.9, LL 1.2, LW 1.5, SL 4.7, SW 4.

COLOR. Brown carapace and legs, light brown sternum and coxae (Fig. 7J–K), grayish brown abdomen.

PROSOMA. Carapace and ocular arrangement as shown in Fig. 7J. Eye tubercle: 1.75 long, 1.83 wide. Distance AME-ALE 1. Eye diameters: AME 0.4, ALE 0.4, PME 0.3, PLE 0.5. Thoracic fovea procurved (Fig. 7J). Labium with 7 cuspules (Fig. 7K). Maxilla with 56 cuspules, distributed over anterior ventral half (Fig. 7K). Basal segment of chelicerae with a prolateral row of 10 large teeth and a retrolateral row of 10 small teeth, grouped in basal half. Robust rastellum, presenting 18–20 short and thick spines on a tubercle.

PALP AND LEG MEASUREMENTS. Palp = 12.3 (4.2, 2.7, 2.8, 2.6), I = 13.6 (4.6, 2.9, 2.9, 2.3, 0.9), II = 12.95 (4.3, 2.9, 2.5, 2.2, 1), III = 13.8 (3.7, 3.1, 2.3, 2.9, 1.85), IV = 19.4 (5.4, 3.8, 4.1, 4, 2.1).

SPINATION. Palp: Fe p0-0-2, Pa p0-0-1, Ti p3-6-7, r3-5-12, Ta v0-0-7, p7-7-7, r11-9-7. Leg I: Ti p3-4-8, r3-6-12, Mt p9-6-5, r8-7-5, Ta v0-0-5, p4-3-2, r4-2-2. Leg II: Ti p3-3-5, r1-1-1, Mt p9-7-7, r3-3-2, Ta v0-0-3, p4-5-2, r3-1-0. Leg III: Pa p3-5-10, r0-0-2, Ti v0-0-2, p1-3-3, r0-2-6, Mt v1r-1r-2, p7-1-1, r7-2-1, Ta v0-3-8. Leg IV: Pa p17-0-0, Ti v1-1-1, Mt v1-1-1-3, Ta v0-3-8.

SPERMATHECAE. Duct with apical half thicker than its basal half, oval receptacula (Fig. 7L).

Distribution

Brazil. Widely distributed, occurring in areas with phytophysiognomies in the Caatinga and Cerrado. Records for Central-West region (Mato Grosso, Mato Grosso do Sul), Northeast region (Bahia, Ceará, Maranhão, Paraíba, Pernambuco and Piauí) and the northern part of Minas Gerais (Fig. 4C).

Idiops argus Simon, 1889
Figs 4B, 9

Idiops argus Simon, 1889: 180, pl. 2 fig. 1.
Idiops fulvipes Simon, 1889: 181. **Syn**. **nov**.

Idiops argus – Dupérré & Tapia 2021: 272, fig. 14a–d.
Idiops fulvipes – Dupérré & Tapia 2021: 273, fig. 15a–d.

Diagnosis

Females of *Idiops argus* differ from the other Neotropical species by having the spermathecae with a unique morphology within the genus, with a long and spiral duct followed by an oval receptacle (Fig. 9).

Type material

Lectotype (here designated)

VENEZUELA – **Carabobo** • ♀; Puerto Cabello, San Esteban; 1889; E. Simon leg.; MNHN 4169.

Paralectotypes

VENEZUELA – **Carabobo** • 1 ♀, 2 juvs; same collection data as for lectotype; MNHN 4169a.

Holotype of *I. fulvipes* Simon, 1889

VENEZUELA– **Miranda** • juv.; La Silla de Caracas, Parque Nacional El Ávila; 10°32′0″ N, 66°52′0″ W; 1889; MNHN.

Remark: The type specimen of *Idiops fulvipes* was examined and recognized as a juvenile of *I. argus.* Although the spermathecae were presented by Dupérré & Tapia (2021: fig. 15c–d), we detected that it is a pre-adult female of *I. fulvipes*.

Description

Male

Unknown.

Female (MNHN 4169)

MEASUREMENTS. TBL 13.7, CL 6.7, CW 5.6, LL 0.9, LW 1.2, SL 3.9, SW 3.5.

COLOR. Carapace, sternum and legs brownish. Abdomen ventrally brownish and dorsally gray.

PROSOMA. Eye tubercle: 1.9 long; 1.7 wide. AME-ALE distance 1.2. Eye diameters: AME 0.3, ALE 0.5, PME 0.3, PLE 0.4. Thoracic fovea procurved. Labium with six cuspules. Maxilla with 54 cuspules, distributed over anterior ventral half. Basal segment of chelicerae with a prolateral row of 8 large teeth and 6 retrolateral small teeth, grouped in basal half.

PALP AND LEG MEASUREMENTS. Palp = 11.4 (3.9, 2.4, 2.4, 2.4), I = 12.48 (4.04, 2.80, 2.64, 2.04, 0.96), II = 11.1 (3.68, 2.52, 2.16, 1.84, 0.92), III = 11.2 (3.2, 2.6, 1.8, 2, 1.6), IV = 15.9 (4.3, 3.1, 3.5, 3.2, 1.8).

SPINATION. Palp: Fe p0-0-1, Pa p0-0-1, r0-0-1, Ti p8-7-13, r7-7-12, Ta v0-0-3, p13-12-9, r13-8-9. Leg I: Ti p6-8-10, r6-7-15, Mt p12-10-7, r11-9-8, Ta v0-1-6, p4-4-2, r5-4-2. Leg II: Ti p3-5-8, r1-1-1, Mtp13-11-6, r1-2-2, Ta v0-2-4, p5-4-3, r4-2-1. Leg III: Pa p6-7-12, r0-0-3, Ti v2-2-2, p2-3-6, r1-2-4, Mt v2-2-2, p5-3-2, r2-2-1, Ta v0-4-11. Leg IV: Pa p29-3-0, Ti v1-1-2, Ta v4-5-10.

SPERMATHECAE. Long spiral ducts and bean-shaped receptacula (Fig 9).

Distribution

Venezuela. Carobobo and Miranda (Fig. 4B).

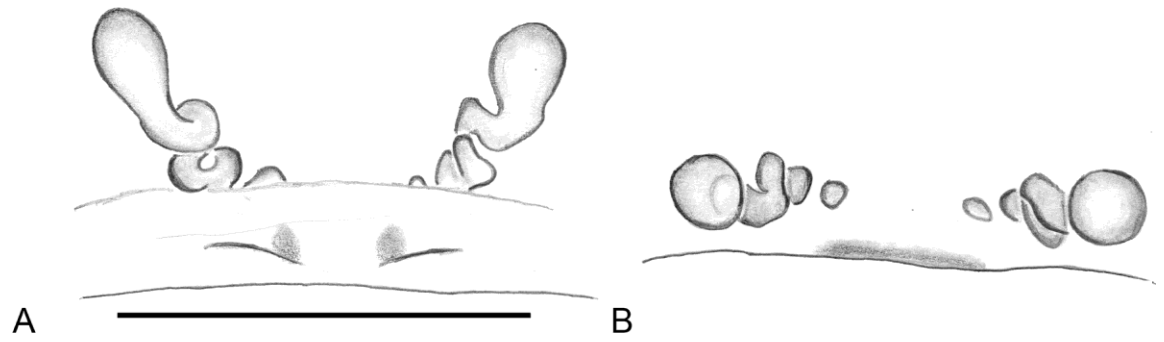

Fig. 9. *Idiops argus* Simon, 1889, ♀, genitalia, lectotype (MNHN 4169). **A**. Dorsal view. **B**. Frontal view. Scale bars = 1 mm.

Idiops cambridgei Ausserer, 1875
Figs 4B, 10

Idiops cambridgei Ausserer, 1875: 145.

Idiops cambridgei – Raven 1985: 158.
Pseudidiops cambridgei – Pocock 1895: 223.

Diagnosis

The female of *Idiops cambridgei* differs from that of the other Neotropical species by the spermathecae having ducts with strong outward curvature in the transition between duct and receptacle, and small receptacula, with diameter slightly larger than the width of the duct (Fig. 10).

Type material

Holotype
COLOMBIA • ♀; Bogotá; 1889; BMNH 1890.7.1.321.

Description

Male
Unknown.

Female (holotype BMNH 1890.7.1.321)
MEASUREMENTS. TBL 12.9, CL 7, CW 5.4, LL 0.9, LW 1.2, SL 3, SW 3.

COLOR. Carapace and legs brown. Sternum, coxae and abdomen brownish.

PROSOMA. Eye tubercle: 1.4 long; 1.3 wide. AME-ALE distance 0.5. Eye diameters: AME 0.3, ALE 0.3, PME 0.2, PLE 0.3. Thoracic fovea procurved. Labium with 16 cuspules. Maxilla with 114 cuspules, distributed throughout ventral area. Basal segment of chelicerae with a prolateral row of 6 large teeth and 3 retrolateral small teeth, grouped in basal half.

PALP AND LEG MEASUREMENTS. Palp = 8.3 (2.9, 1.8, 1.8, 1.8), I = 9.9 (3.4, 2.4, 1.9, 1.3, 0.9), II = 8.7 (2.9, 2, 1.7, 1.3, 0.8), III = 8.4 (2.4, 1.9, 1.5, 1.6, 1), IV = 11.2 (3.3, 2.3, 2.4, 2.1, 1.1).

SPINATION. Palp: Fe p0-0-3ap, r0-0-3ap, Pa p0-0-1, Ti p5-5-7, r2-4-7, Ta p7-6-6, r8-9-8. Leg I: Fe r0-0-3, Ti p5-5-5, r4-4-8, Mt p7-6-7, r3-3-2, Ta p3-2-1, r2-1-1. Leg II: Ti p2-4-3, r3-3-1, Mt p10-6-4, r4-3-1, Ta

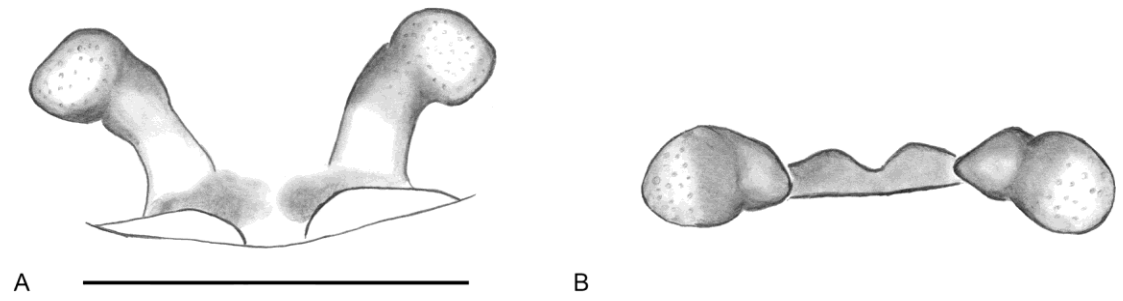

Fig. 10. *Idiops cambridgei* Ausserer, 1875, ♀, genitalia, holotype (BMNH 1890.7.1.321). **A.** Dorsal view. **B**. Frontal view. Scale bars = 1 mm.

p3-2-2, r2-0-0. Leg III: Pa p5-9-25, r0-1-1, Ti p5-13-19, r4-4-6, Mt v0-1-2, p8-5-5, r5-0-1, Ta v0-0-4. Leg IV: Pa p31-31-23, Ti v0-0-2, Mt v1-2-3ap, Ta v0-3-3.

SPERMATHECae. Spherical receptacula. Duct with basal translucent area and median area sclerotized (Fig. 10).

Distribution

Colombia. Known only from the type locality (Fig. 4B).

Idiops camelus (Mello-Leitão, 1937)
Figs 2C–D, 5A, 6D, H–I, 11–12

Pseudidiops camelus Mello-Leitão, 1937: 1, figs 1–2.
Idiops montealegrensis Soares, 1944: 156, figs 2–4. Synonymized by Fukami & Lucas 2005: 6, figs 6–7.

Idiops camelus – Raven 1985: 158. — Fukami & Lucas 2005: 6, figs 6–7.
Idiops montealegrensis – Bücherl 1957: 383, figs 2–2a.

Diagnosis

Males of *Idiops camelus* (Fig. 11A–I, 12) differ from other Neotropical species by having the apical half of the embolus tapering (Fig. 11D–F), with the presence of a distal embolar tooth (also present in *I. clarus* and *I. germaini*) close to the opening of the sperm duct (Fig. 12E–F). Differs from *I. clarus* and *I. germaini* by having the apical portion of the embolus more expanded (Fig. 12E–F). Females (Fig. 11J–L) have spermathecae with spherical receptacles slightly wider than the ducts, with a subtle constriction between duct and receptacle (Fig. 11L).

Type material

Holotype of *Pseudidiops camelus* Mello-Leitão, 1937
BRAZIL – **São Paulo** • ♀; Corumbataí; IBSP 3429.

Holotype of *Idiops montealegrensis* Soares, 1944
BRAZIL – **São Paulo** • ♂; Amparo, Monte Alegre, Fazenda Santa Maria; Nov. 1942; F. Lane leg.; MZSP 326.

Other material examined

BRAZIL – **Minas Gerais** • 1 ♀; Lima Duarte, Parque Estadual de Ibitipoca; 21°43′0″ S, 43°54′0″ W; 21 Oct. 1995; R. Baptista leg.; MNRJ • 1 ♀; Monte Verde, trail south of Monte Verde; 22°51′27″ S, 46°1′46″ W; V. Ghirotto leg.; CAD 827 • 8 ♂♂; Itajubá, Horto Florestal Anhumas; 22º25′36″ S, 45º28′10″ W; Mar. 2010; W.C.G.G. Castro leg.; UFMG 4274 • 7 ♂♂; same collection data as for preceding; UFMG 4270 • 7 ♂♂; same collection data as for preceding; UFMG 4272 • 7 ♂♂; same collection data as for preceding; UFMG 4275 • 8 ♂♂; same collection data as for preceding; UFMG 4273 • 8 ♂♂; same collection data as for preceding; UFMG 4271 • 2 ♂♂; Cristina, Parque Ecológico Municipal; 22º12′ S, 45º11′ W; Sep. 2009; C.G.G. Castro leg.; UFMG 4232 • 1 ♂; Nova Lima, RPPN Mata Samuel de Paula; 20º00′ S, 43º52′ W; 18 Oct. 2006; J.P.P.P. Barbosa *et al.* leg.; UFMG 2530 • 1 ♀; Bueno Brandão, 1.5 km from Socorro / Bueno Brandão; 22°26′27″ S, 46°21′3″ W; 22 Jul. 2010; R.P. Indicatti and B. Gambaré leg.; IBSP 210359 • 2 ♂♂; Delfim Moreira, Fazenda Boa Esperança; 22º34′33″ S, 45º19′19.7″ W; 3 Apr. 2014; A. Nogueira *et al.* leg.; IBSP 210175 • 1 ♀; Viçosa, Campus UFV, Recanto de Cigarras; 20°45′37″ S, 42°52′4″ W; 6 Mar. 2013; E.S. Barreto, A.A. Zaccaro and G.M. Diniz leg.; IBSP 221797. – **Rio de Janeiro** • 13 ♂♂, 1 ♀, 2 juvs; Itatiaia, Parque Nacional do Itatiaia; 22°22′31″ S, 44°39′44″ W; 20–30 May 2013;

R.P. Indicatti and F.U. Yamamoto leg.; IBSP 225155 • 1 ♀; Itatiaia, Parque Nacional do Itatiaia; 22°22′31″ S, 44°39′44″ W; 19–21 Mar. 2019; R.F. Ferreira, R. Indicatti, A.G. Lima and I. Meireles leg.; CAD 289 • 1 ♂; Itatiaia, Parque Nacional do Itatiaia, Cachoeira Poranga; 22º26′25.7″ S, 44º36′40″ W; 17 Apr. 2014; R. Pinto da Rocha, A. Benedeti, D. Chiviri and J. Cabra leg.; IBSP 210439 • 2 ♂♂; Itatiaia, Parque Nacional do Itatiaia, Casa Jardim Botânico; 22º27′07″ S, 44º36′35″ W; 17 Apr. 2014; R. Pinto da Rocha, A. Benedeti, D. Chiviri and J. Cabra leg.; IBSP 210440. – **Sao Paulo** • 2 ♀♀; São José do Barreiro, Parque Nacional da Serra da Bocaina, behind the accommodation; 23°2′30″ S, 44°39′42″ W; 24–26 Mar. 2019; R.F. Ferreira, A. Galleti, I. Meirelles and R. Indicatti leg.; CAD 830 • 1 ♂; São José do Barreiro, Parque Nacional da Serra da Bocaina; 22º43′ S, 44º36′ W; 28 Apr.–3 May 2002; Equipe Biota leg.; IBSP12372 • 1 ♂; Salesópolis, Estação Biológica de Boracéia; 23º39′ S, 45º53′ W; Jun. 2003; J.P.L. Guadanucci leg.; MZSP 27668 • 1 ♂; Salesópolis, Estação Biológica de Boracéia; MZSP 21159 • 2 ♂♂; Salesópolis, Estação Biológica de Boracéia; 11 May. 2003; J.P.L. Guadanucci leg.; MZSP 22005 • 8 ♂♂; Salesópolis, Estação Biológica de Boracéia; 7 Mar. 2003; J.P.L. Guadanucci leg.; MZSP 23714 • 1 ♀; Salesópolis, Estação Biológica de Boracéia; Dec. 1949; I. Travassos leg.; MZSP 11326 • 1 ♂; Salesópolis, Estação Biológica de Boracéia; Mar. 2006; M.U. Prado *et al*. leg.; IBSP 14547 • 1 ♀; Mogi-Salesópolis Road, Km 91; 25 Jun. 2002; R. Martins *et al*. leg.; IBSP 13111 • 1 ♂; Amparo, Fazenda Santa Maria; 22°42′3″ S, 46°45′50″ W; Nov. 1942; F. Lane leg.; MZSP 326 • 4 ♀♀; Iperó, Floresta Nacional de Ipanema; 23°25′49″ S, 47°37′22″ W; 10–14 Oct. 2019; J.P.L. Guadanucci, R.P. Indicatti and A. Galleti-Lima leg.; CAD 828 • 3 ♂♂; Santa Gertrudes, Fazenda Paraguaçu; 22°27′25″ S, 47°31′48″ W; J.H.B. Medeiros leg.; IBSP 243977 • 1 ♀; Barra Bonita; 22°29′42″ S, 48°33′28″ W; 6 Nov. 1979; O. Froelich leg.; MZSP 13876 • 2 ♂♂; Botucatu, Fazenda Edgardia, Mata do Bixiguento; 22°50′25.08″ S, 48°20′48.25″ W; Apr. 2014; R.C.B. Paradero leg.; IBSP 229983 • 4 ♂♂; Luis Antonio, Estação Ecológica de Jataí; 21°37′3″ S, 47°45′55″ W; 6–12 Dec. 2009; A.G. Cristovão leg.; IBSP 220958 • 3 ♂♂; same collection data as for preceding; IBSP 220944 • 1 ♂; same collection data as for preceding; IBSP 220949 • 3 ♂♂; Luis Antonio, Estação Ecológica de Jataí; 3–7 Oct. 2009; A.G. Cristovão leg.; IBSP 220948 • 5 ♂♂; same collection data as for preceding; IBSP 220961 to 220963, IBSP 220966 to 220967 • 8 ♂♂; Luis Antonio, Estação Ecológica de Jataí; Jan. 2010; A.G. Cristovão leg.; IBSP 243964, IBSP 243966 to 243972 • 2 ♂♂; same collection data as for preceding; IBSP 43965 • 2 ♂♂; Jacareí, Campos Vila Branca, UNIVAP; 23°13′ S, 45°58′ W; 2007; N.M.C. Velho *et al*. leg.; IBSP 141829 • 33 ♂♂; same collection data as for preceding; IBSP 141786, IBSP 141788 to 141791, IBSP 141796, IBSP 141798 to 141800, IBSP 141804 to 141810, IBSP 141818 to 141821, IBSP 141823 to 141828, IBSP 141831 to 141832, IBSP 141834 to 141835, IBSP 141837 to 141838, IBSP 143973 • 2 ♂♂; same collection data as for preceding; IBSP 141792 • 2 ♂♂; same collection data as for preceding; IBSP 141794 • 2 ♂♂; same collection data as for preceding; IBSP141802 • 2 ♂♂; same collection data as for preceding; IBSP 141822 • 2 ♂♂; same collection data as for preceding; IBSP 141830 • 1 ♀; Mococa; 21°28′4″ S, 47°0′18″ W; 6 Mar. 1991; J.A. Azevedo leg.; IBSP 11834 • 1 ♂; Itapecerica da Serra; 23°43′1″ S, 46°50′56″ W; IBSP 212207 • 1 ♂; Mairiporã, Parque Estadual da Serra da Cantareira; 23º25′ S, 46º37′ W; 24 Feb 2001; C.L. Firmo leg.; MCN 41851 • 2 ♂♂; Mairiporã, Parque Estadual da Serra da Cantareira, Pinheirinho; 23º25′ S, 46º37′ W; 17 Dec. 2000; MZSP 25748, MZSP 26029 • 3 ♂♂; Mairiporã, Parque Estadual da Serra da Cantareira, Pinheirinho; 24 Feb. 2001; MZSP 26030 to 26032 • 2 ♂♂; Mairiporã, Parque Estadual da Serra da Cantareira, Pinheirinho; 27 Apr. 2001; MZSP 26035 to 26036 • 1 ♂; Mairiporã, Parque Estadual da Serra da Cantareira, Pinheirinho; 1 Jul. 2001; MZSP 26033 • 1 ♂; Mairiporã, Parque Estadual da Serra da Cantareira, Pinheirinho; 27 May 2001; MZSP 26034 • 1 ♂; Paraibuna, Sitio Amici; 23°23′9″ S, 45°39′43″ W; 13 Jul. 2003; M.B. da Silva leg.; MZSP 21820 • 1 ♀; Jaú; 22°17′45″ S, 48°33′28″ W; 21 Dec. 2011; A.M. Giroti leg.; IBSP 210069 • 1 ♂; Paraibuna, Sitio Amici; 2008; A.M. Giroti leg.; IBSP 151641 • 1 ♀; Campinas, Condomínio Caminhos de San Conrado; 22°54′ S, 47°3′ W; 9 Jan. 2019; V. Ghirotto leg.; CAD 831 • 1 ♀; Campinas; 24 Aug. 1974; O. Froelich leg.; MZSP 13880 • 1 ♂; Jundiaí, Parque Estadual Serra do Japi; 23º17′ S, 46º59′ W; 13 Nov. 2007; J. Sobjac leg.; UFMG 6475 • 1 ♂; Itirapina; 22°15′10″ S, 47°49′22″ W; 19 Jul. 2000; G. Machado leg.; MZSP 20612 • 1 ♂; Estação Ecológica de Itirapina; 22°13′10″ S, 47°53′54″ W; 4–9 Oct. 2001; E.S. Cunha leg.; IBSP 13380 • 1 ♂; Santo André,

Reserva Biológica do Alto da Serra de Paranapiacaba; 23º46′ S, 46º18′ W; 20 Mar. 2007; M.U. Prado *et al.* leg.; IBSP 14566 • 1 ♀; Santo André, Reserva Biológica do Alto da Serra de Paranapiacaba; 17 Nov. 2006; M.U. Prado *et al.* leg.; IBSP 14567 • 1 ♀; São Carlos; 22°0′0″ S, 47°53′27″ W; 9 Jun. 1946; F. Salto leg.; MZSP E-3095 • 1 ♂; Itapevi, Condomínio Trensurb; 23°32′56″ S, 46°56′2″ W; 27 Oct. 2000; V. Onofrio and D.M.B.B. Batesti leg.; IBSP 123524 • 1 ♂; Itapevi, Condomínio Trensurb; 2000; V. Onofrio and D.M.B.B. Batesti leg.; IBSP 123525 • 1 ♀; Mogi das Cruzes; 23º31′26,27″ S, 46º11′0,685″ W; 30 Oct. 2009; R. Quadros leg.; UFMG 6265 • 9 ♂♂; Mogi das Cruzes, Parque Natural Municipal Serra do Itapety; 23º29′ S, 46º12′ W; 13 Nov.–19 Dec. 2003; Equipe Biota leg.; IBSP 13391, IBSP 13393, IBSP 13395 to 13396, IBSP 13398 to 13399, 13401 to 13403 • 1 ♂; same locality as for preceding; 5 Jun. 2003; IBSP 13392 • 2 ♂♂; Mogi das Cruzes, Parque Natural Municipal Serra do Itapety; May 2003; P. Goldoni *et al.* leg.; IBSP 10189 to 10190 • 1 ♂; Itapevi, Parque Natural Municipal Serra do Itapety; Feb.–Mar. 2004; P. Goldoni *et al.* leg.; IBSP 11781 • 2 ♂♂; Itapevi, Parque Natural Municipal Serra do Itapety; 2014–2015; C.C. Barbosa leg.; IBSP 258651 to 258652 • 1 ♂; São Bernardo do Campo; 23°41′38″ S, 46°33′54″ W; 17 Apr. 2009; Pref. Mun. SB Campo leg.; IBSP 151640 • 2 ♀♀; Socorro, Gruta do Anjo; 22°35′27″ S, 46°31′44″ W; 19–26 Dec. 2010; R.P. Indicatti and B. Gambaré leg.; IBSP 210350 to 210351 • 1 ♀; São Paulo; 23º25′ S, 46º37′ W; 5 Feb. 1996; L.A. Leme *et al.* leg.; IBSP 10569 • 1 ♂; São Paulo; 21 Oct. 2004; R.M. Nori leg.; IBSP 11040 • 1 ♂; São Paulo; 20 Oct. 2002; D.P.C. Souza leg.; IBSP 9961 • 1 ♂; São Paulo; Oct. 1971; A. Guarnieri leg.; IBSP 2113 • 1 ♂; São Paulo; 3 Oct. 1991; N. Cochrane leg.; IBSP 8256 • 1 ♀; São Paulo; 1937; A. Franci leg.; IBSP 3723 • 1 ♀; São Paulo, Serra da Cantareira; 27 Aug. 1999; F.L. da Silva leg.; IBSP 9579 • 1 ♂; São Paulo, Parque Estadual da Serra da Cantareira; 23º25′ S, 46º37′ W; 17 Dec. 2000; C.L. Firmo leg.; MCN 41849 • 1 ♂; São Paulo, Parque Estadual da Serra da Cantareira; 27 Apr. 2001; A.D. Brescovit leg.; MCN 41850 • 11 ♂♂; São Paulo, Parque Estadual da Serra da Cantareira; 3 Mar.–5 Jul. 2000; S. Favorito *et al.* leg.; MZSP 21316 • 2 ♂♂; same collection data as for preceding; MZSP 21324 • 2 ♂♂; same collection data as for preceding; MZSP 21325 • 2 ♂♂; same collection data as for preceding; MZSP 21314 • 3 ♂; same collection data as for preceding; MZSP 21322 • 6 ♂♂; same collection data as for preceding; MZSP 21323 • 2 ♂♂; same collection data as for preceding; MZSP 21313 • 4 ♂♂; same collection data as for preceding; MZSP 21326 • 2 ♂♂; same collection data as for preceding; MZSP • 2 ♂♂; same collection data as for preceding; MZSP 21309 • 6 ♂♂; same collection data as for preceding; MZSP 21306 • 7 ♂♂; same collection data as for preceding; MZSP 21305 • 8 ♂♂; same collection data as for preceding; MZSP 21304 • 5 ♂♂; same collection data as for preceding; MZSP 21320 • 18 ♂♂; same collection data as for preceding; MZSP 21307, MZSP 21315, MZSP 21329, MZSP 21333, MZSP 21335 to 21336, MZSP 21338 to 21342, MZSP 21345 to 21346, MZSP 21348 to 21352 • 2 ♀♀; same collection data as for preceding; MZSP 21311, MZSP 21330 • 2 ♂♂; same collection data as for preceding; IBSP 13088 • 6 ♂♂; same collection data as for preceding; IBSP 13082, IBSP 13084, IBSP 13087, IBSP 13089, IBSP 13094 to 13095, IBSP 13095 • 1 ♂; São Paulo, Parque Estadual da Serra da Cantareira; 29 Apr. 2001; R. Pinto da Rocha leg.; MCN 41848 • 1 ♀; São Paulo, Parque Estadual da Serra da Cantareira;18 Aug. 1999; F.L. da Silva leg.; IBSP 7913 • 1 ♂; São Paulo, Parque Estadual da Serra da Cantareira; 24 Jan. 2001; F.L. da Silva leg.; IBSP 130688 • 1 ♂; same locality as for preceding; 27 Apr. 2001; F.L. da Silva leg.; IBSP 130689 • 1 ♂; São Paulo, Parque Estadual da Serra da Cantareira; 1 Aug. 2001; F.L. da Silva leg.; IBSP 130690 • 1 ♂; same locality as for preceding; 1 Jul. 2001; IBSP 130687 • 1 ♂; same locality as for preceding; 27 May 2001; IBSP 130686 • 1 ♂; same collection data as for preceding; IBSP 130691 • 9 ♂♂; São Paulo, Parque Estadual da Serra da Cantareira; 17 Jul. 2000–1 Aug. 2001; C.L. Firmo leg.; MZSP 24046, MZSP 26027, MZSP 26037, MZSP 26039 to 26040, MZSP 26042, MZSP 26044 to 26046 • 2 ♂♂; same collection data as for preceding; MZSP 26041, MZSP 26038 • 5 ♂♂; São Paulo, Parque Estadual da Serra da Cantareira, Pedra Grande; 23º25′ S, 46º37′ W; 17 Dec. 2000–1 Jul. 2001; C.L. Firmo leg.; MZSP 26023 to 26026, MZSP 26028 • 1 ♂; São Paulo, Parque Estadual da Serra da Cantareira, Pedra Grande; 25 Aug.–3 Sep. 2000; C.C. Aires *et al.* leg.; MZSP 21328 • 1 ♀; São Paulo, Parque Estadual do Jaraguá; 23°27′34.3″ S, 46°46′2.8″ W; Apr. 2015; R.P. Indicatti and J.P.L. Guadanucci leg.; CAD 598 • 1 ♀; same locality as for preceding; Mar. 2015; R.P. Indicatti and J.P.L. Guadanucci leg.; CAD 605 • 1 ♀; São Paulo, Parque Estadual do Jaraguá;

18 Jul. 2010–31 Aug. 2012; R.P. Indicatti leg.; IBSP 171840 • 6 ♂♂; same collection data as for preceding; IBSP 171802, IBSP 171842 to 171843, IBSP 171845 to 171847 • 1 ♂; São Paulo, Jardim Botânico de São Paulo; 23°38′30.7″ S, 46°37′14.2″ W; 20 Oct. 1950; Kulmann leg.; MZSP 7800 • 1 ♀; São Paulo, Ipiranga; 23°35′07.8″ S, 46°35′56.4″ W; 5 Jan. 1998; MZSP 16060 • 1 ♀; São Paulo, Santo Amaro; 23º25′ S, 46º37′W; 16–17 Dec. 1966; P. de Biasi leg.; MZSP 5399 • 1 ♀; São Paulo, Campus USP; 23°33′34″ S, 46°43′26″ W; 10 Sep. 1975; O. Froelich leg.; MZSP 13886 • 1 ♂; São Paulo, Mata do Viveiro; 1980; MZSP 19530 • 1 ♂; São Paulo, Instituto de Pesquisas Energéticas e Nucleares; 12 Aug. 1991; P.I. Spencer leg.; IBSP 9576 • 2 ♂♂; São Paulo, Campus Instituto Butantan; 23º33′ S, 46º43′ W; 12–13 Nov. 2012; Equipe IBSP leg.; IBSP 210144 • 1 ♂; São Paulo, Campus Instituto Butantan; 30 Jul. 2009; F.P. Santos leg.; IBSP 210130 • 1 ♂; São Paulo, Campus Instituto Butantan; IBSP 9592 • 1 ♂; São Paulo, Campus Instituto Butantan; 20 Oct. 1988; A. Hoge leg.; IBSP 9563 • 1 ♂; São Paulo, Campus Instituto Butantan; 7 Aug. 2003; D. Candiani and C.S. Fukushima leg.; IBSP 9835 • 1 ♂; São Paulo, Campus Instituto Butantan; Sep. 1992; C. Bertin leg.; IBSP 9590 • 2 ♂♂; São Paulo, near the Instituto Butantan; 30 Oct. 2003; IBSP 12344 • 3 ♂♂; São Paulo, Parque da Previdência; 23º34′ S, 45º43′ W; May 2000–Feb. 2001; D. Candiani leg.; IBSP 14398, IBSP 14742 to 14743 • 2 ♀♀; São Paulo, Parque Ilha dos Eucaliptos, Represa Guarapiranga; 23°40′17″ S, 46°43′39″ W; 7–13 Apr. 2005; I. Cizauskas leg.; IBSP 13788, IBSP 13790 • 4 ♂♂; São Paulo, Parque do Estado; 23°38′24.6″ S, 46°37′3.1″ W; 26 Jul.–1 Aug. 2002; Valvassori leg.; IBSP 13340 to 13342, IBSP 13345 • 13 ♂♂; São Paulo, Parque dos Príncipes; 23º25′ S, 46º37′ W; 2005; IBSP 13234b • 1 ♂; São Paulo, Morumbi; 23°36′0″ S, 46°43′12″ W; Oct. 1968; O. Mamino leg.; IBSP 293 • 1 ♂; São Paulo, Parque Estadual Alberto Loefgren, Mandaqui; 23°27′33″ S, 46°38′2″ W; May 1973; IBSP 102438 • 1 ♀; highway Raposo Tavares, Km 21; 21 Jul. 1977; P. Alicke leg.; IBSP 104270 • 10 ♂♂; Cotia, Reserva do Morro Grande; 23°38′58.12″ S, 46°57′45.99″ W; Jul. 2006; C. Bragagnollo leg.; MZSP 28831 • 9 ♂♂ (SEM); same collection data as for preceding; MZSP 28832 • 3 ♂♂; same collection data as for preceding; MZSP 28823 • 2 ♀♀; Itapetininga, Estação Ecológica de Angatuba; 23°24′57″ S, 48°21′39″ W; 11–16 Nov. 2002; C. Firmo *et al*. leg.; IBSP 258658 to 258659 • 2 ♂♂; Itanhaém, Estação Ecológica São Camilo, Suarão; 24º10′60″ S, 46º46′60″ W; Dec. 2010; G. Aparecida and M. Pessoa leg.; IBSP 224494 to 224495 • 1 ♂; Peruíbe, Estação Ecológica da Juréia Itatins, Núcleo Arpoador; 24º23′13″ S, 47º1′3,3″ W; 21–26 Apr. 2012; G. Azevedo and J.P.P.P. Barbosa leg.; UFMG 11788. – **Santa Catarina** • 4 ♂♂; Balneário Camboriú; 26º59′27″ S, 48º38′38.6″ W; Jun. 2009–Jun. 2010; M. Zucatelli leg.; IBSP 245677 to 245680.

Description

Male (MZSP 26023)

HABITUS. See Fig. 11A.

MEASUREMENTS. TBL 12.8, CL 7, CW 5.9, LL 0.9, LW 1.2, SL 3.4, SW 4.

COLOR. Brownish carapace and legs, sternum and coxae yellow brown (Fig. 11A–B), abdomen brown.

PROSOMA. Carapace and ocular arrangement as shown in Fig. 11A. Eye tubercle: 1.6 long; 1.5 wide. Distance AME-ALE 0.9. Eye diameters: AME 0.4, ALE 0.4, PME 0.4, PLE 0.5. Thoracic fovea procurved (Fig. 11A). Labium and sternum without cuspules (Fig. 11B). Basal segment of chelicerae with a prolateral row of 9 teeth, 7 large and 2 small, and 6 small retrolateral teeth (Fig. 12A). Salient rastellum, presenting 12–13 spines of the same size (Fig. 12A–B).

LEGS. Tibia, metatarsus and tarsus I as shown in Fig. 11G. Leg I with double tibial apophysis, with wider apical branch, thickened base and conical distal area (Figs 11H–I, 12C). Pseudoscopula: tarsus I–III covered, IV absent.

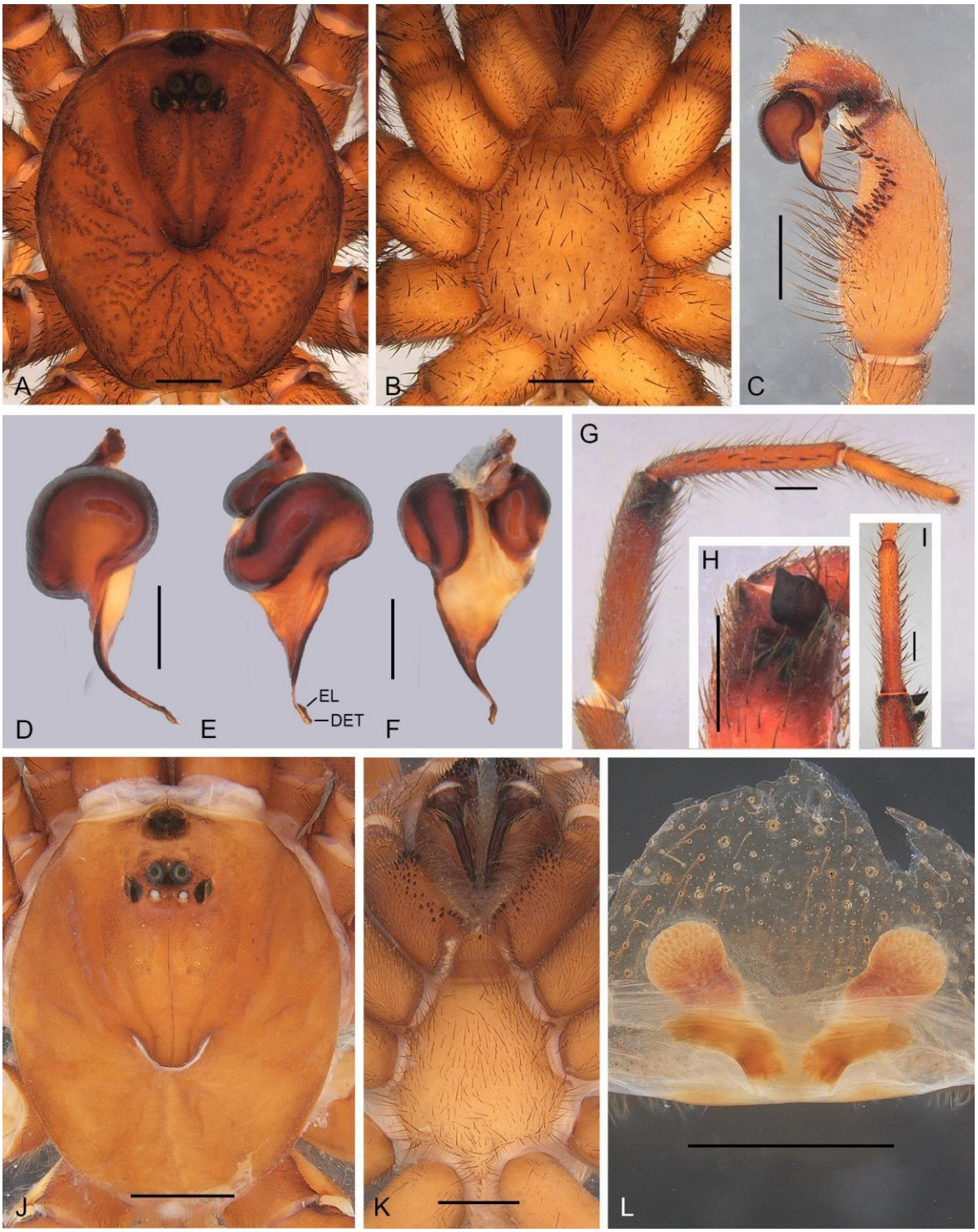

Fig. 11. *Idiopscamelus* (Mello-Leitão, 1937). **A–I**. ♂ (MZSP26023). **A**. Prosoma (dorsal view). **B**. Prosoma (ventral view). **C**. Part of palp (retrolateral view). **D–F**. Palpal bulb. **D**. Dorsal view. **E**. Retrolateral view. **F**. Prolateral view. **G**. Tibia, metatarsus and tarsus I (prolateral view). **H**. Tibial apophysis (prolateral view). **I**. Tibial apophysis and metatarsus I (dorsal view). **J–L**. ♀ (IBSP 9579). **J**. Prosoma (dorsal view). **K**. Prosoma (ventral view). **L**. Genitalia (dorsal view). Abbreviations: DET = distal embolar tooth; EL = embolar lamella. Scale bars: A–B, D–L = 1 mm; C = 2 mm.

PALP. Tibia with conspicuous retrolateral depression, bordered by short spines, with the exception of the spines of the basal and apical ends, which are twice the size of the others (Fig. 11C); embolus with subapical torsion and presence of a small lamella at spermatic duct opening (Figs 11D–F, 12E–F).

PALP AND LEG MEASUREMENTS. Palp = 10.6 (3.6, 2, 3.5, 1.5), I = 19.7 (5.9, 2.8, 4.4, 4.3, 2.3), II = 24 (6.3, 2.9, 5.4, 6.1, 3.3), III = 18.3 (4.6, 2.8, 3.1, 4.9, 2.9), IV = 24.9 (6.6, 3,3, 5.4, 6.3, 3.3).

SPINATION. Palp: Ti r3-3, Ta d-0-0-6. Leg I: Ti r0-1-2, Mt p5-3-2, r1-1-2, Ta p4-3-1, r3-2-2. Leg II: Ti v1-2-1-2, Mt p0-0-1, r1-1-3, Ta p0-1-2, r0-2-3. Leg III: Pa p4-5-7, r0-0- 3, Ti v0-2-0-4, p1-2-2, r0-1-3, Mt v2-3-2-3, p3-3-3, r3-1-3, Ta p1-2-5, r0-2-3. Leg IV: Pa p17-4-0, Ti v0-2-0-4, Mt v1-2-2-3, Ta v2-4-11.

Female (IBSP 9579)

HABITUS. See Fig. 11J.

MEASUREMENTS. TBL 18.4, CL 8.3, CW 8, LL 1.5, LW 1.8, SL 5.4, SW 4.9.

COLOR. Brownish carapace and legs, sternum and coxae yellow brown (Fig. 11J–K), abdomen brown.

PROSOMA. Carapace and ocular arrangement as shown in Fig. 11J. Eye tubercle: 2 long; 2 wide. Distance AME-ALE 1.3. Eye diameters: AME 0.4, ALE 0.6, PME 0.3, PLE 0.6. Thoracic fovea procurved (Fig. 11J). Labium with 2–5 cuspules (Fig. 11K). Maxilla with 48 cuspules, distributed over the anterior ventral half (Fig. 11K). Basal segment of chelicerae with a prolateral row of 6 large teeth and a retrolateral row with 4 small teeth.

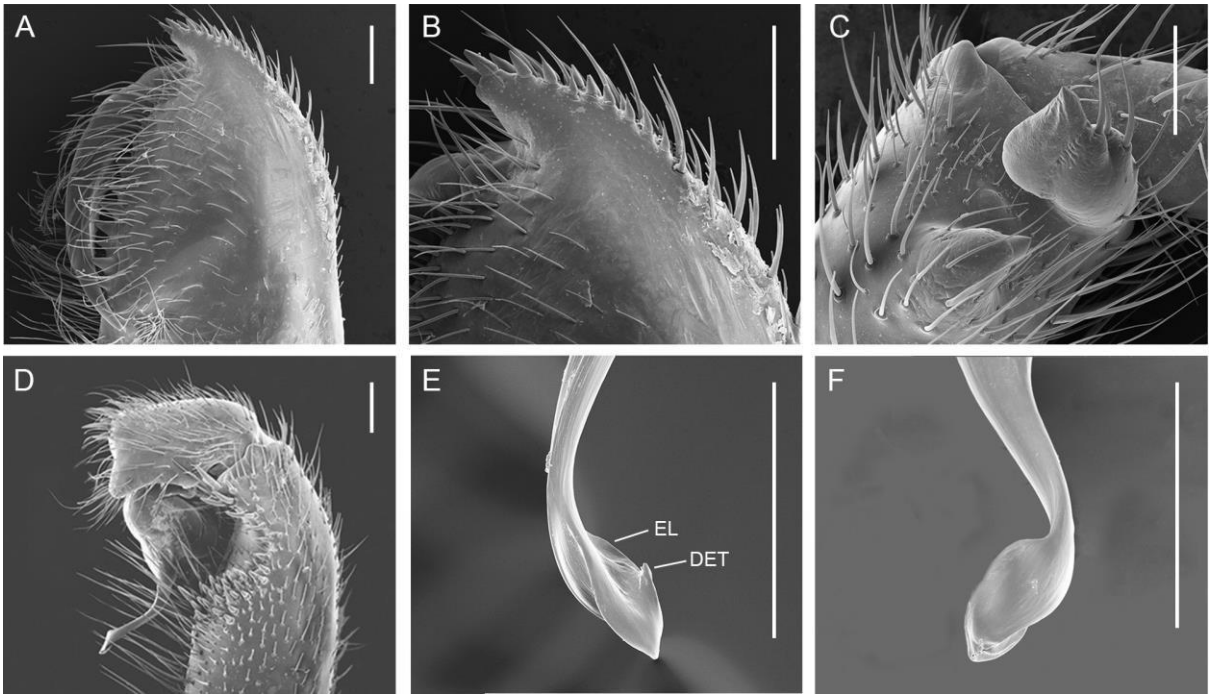

Fig. 12. Scanning electron micrographs of *Idiops camelus* (Mello Leitão, 1937), ♂ (MZSP 28832). **A**. Chelicera (retrolateral view). **B**. Rastellum (retrolateral view). **C**. Tibial apophysis (dorsal view). **D**. Part of the palp, showing retrolateral depression. **E–F**. Detail of the distal portion of the embolus. **E**. Retrolateral view. **F**. Prolateral view. Abbreviations: DET = distal embolar tooth; EL = embolar lamella. Scale bars = 0.5 mm.

PALP AND LEG MEASUREMENTS. Palp = 14.3 (4.8, 3.2, 3.1, 3.2), I = 16.7 (5.4, 3.7, 3.6, 2.8, 1.2), II = 14.9 (4.9, 3.4, 3, 2.3, 1.3), III = 15.6 (4.3, 3.7, 2.4, 3.1, 2.1), IV = 21.6 (6.1, 4.4, 4.5, 4.3, 2.3).

SPINATION. Palp: Fe p0-0-1, Pa p0-0-1, Ti p9-6-12, Ta p14-11-10. Leg I: Ti p7-7-10, r8-7-13, Mt p11-9-7, r12-8-13, Ta v0-0-5, p6-5-3, r6-4-3. Leg II: Ti p4-4-7, r2-1-7, Mt p8-4-2, r12-8-10, Ta v0-0-9, p6-1-2, r6-5-3. Leg III: Pa p5-5-17, r0-1-4, Ti v1-1-1, p4-5-12, r1-3-10, Mt v1-2-2, p11-3-3, r8-2-1, Ta v0-1-4, p0-1-3, r0-0-1. Leg IV: Pa p65-7-0, Ti v2-1-3, Mt 1-3-2, p0-1-0, Ta v1 -5-11.

SPERMATHECAE. Receptacula with evident granules. Duct with sclerotized apical portion (Fig. 11L).

Distribution.

Brazil. Mainly distributed in Atlantic Forest phytophysiognomies, with records for Southeast region (center-south of Minas Gerais, Rio de Janeiro and São Paulo) and northeast of Santa Catarina (Fig. 3D).

Idiops carajas Fonseca-Ferreira, Zampaulo & Guadanucci, 2017
Figs 3B, 6D–E, 13–14

Idiops carajas Fonseca-Ferreira, Zampaulo & Guadanucci, 2017: 191, figs 29–38.

Emended diagnosis

The male of *Idiops carajas* (Figs 13A–I, 14) differs from the other Neotropical species, except *I. petiti*, by the palpal tibia having spines concentrated on the basal half of the retrolateral depression (Figs 13C, 14D), apophysis with a narrow rectangular apical branch (Figs 13G–H, 14C) and by the presence of a lateral lamella that extends along the median portion of the embolus (Figs 13E–F). Differs from *I. petiti* by having the subapical portion of the embolus thickened in dorsal view (Fig. 13D) and the arrow-shaped apical end in retrolateral view (Figs 13E–F, 14E). Females (Fig. 13J–L) are distinguished from congeners, except *I. petiti*, by having the spermathecae with a sclerotized trapezoidal base. Differs from *I. petiti* by the ducts having a thickened basal half and shorter apical half and by the rounded receptacles, separated from the ducts by a strong constriction (Fig. 13L).

Type material

Holotype

BRAZIL – **Pará** • ♂; Parauapebas, FLONA Carajás Serra Norte, cave GEM-1758; 5°52′0.00″ S, 49°52′60.00″ W; 23 Nov. 2010; R.A. Zampaulo leg.; IBSP 166619.

Paratype

BRAZIL – **Pará** • 1 ♀; same collection data as for holotype; IBSP 166620.

Other material examined

BRAZIL – **Amazonas** • 1 ♂; Benjamin Constant; 4°22′58″ S, 70°1′51″ W; 2014; P.S. Pompeu *et al.* leg.; IBSP 243963. – **Pará** • 1 ♂ (SEM); Paraoapebas, Serra Norte, Serra de Carajás; 5°52′ S, 49°53′ W; 29 Mar.–6 Apr. 1989; N. Degallier leg.; MPEG 0109• 1 ♂; Flona Carajás, Cave N3-033; 6°6′34.92″ S, 50°11′40.11″ W ; 5–17 Mar. 2013; Equipe Carste leg.; IBSP 174029 • 1 ♂; Melgaço, Igarapé do Laranjal; 1°48′21.44″ S, 50°43′0″ W; 7 Apr. 1998; J.A.R. Bernardi and R.A.J. Rocha leg.; MPEG 0111 • 1 ♂; Almeirim, Rio Jari; 00°41′25.93″ S, 52°49′9.21″ W; 17–23 Aug. 2004; T. Gardner leg.; MPEG 7592 • 1 ♂; Almeirim, Rio Jari; 3 Apr. 2005; T. Gardner leg.; MPEG 7589 • 1 ♂; Almeirim, Rio Jari; 2004; T.C.S. Avila Pires leg.; MPEG 7591 • 2 ♂♂; Almeirim, Rio Jari; 22 Mar. 2005; T. Gardner & M.A. Ribeiro Junior leg.; MPEG 7587, MPEG 7590 • 1 ♂; Tucuruí, Base IV; 3°46′4″ S, 49°40′22″ W; 8–22 Feb. 1980; T. Gardner leg.; MPEG 0115. – **Mato Grosso** • 1 ♂; Chapada dos Guimarães; 15°27′39″ S, 55°45′0″ W;

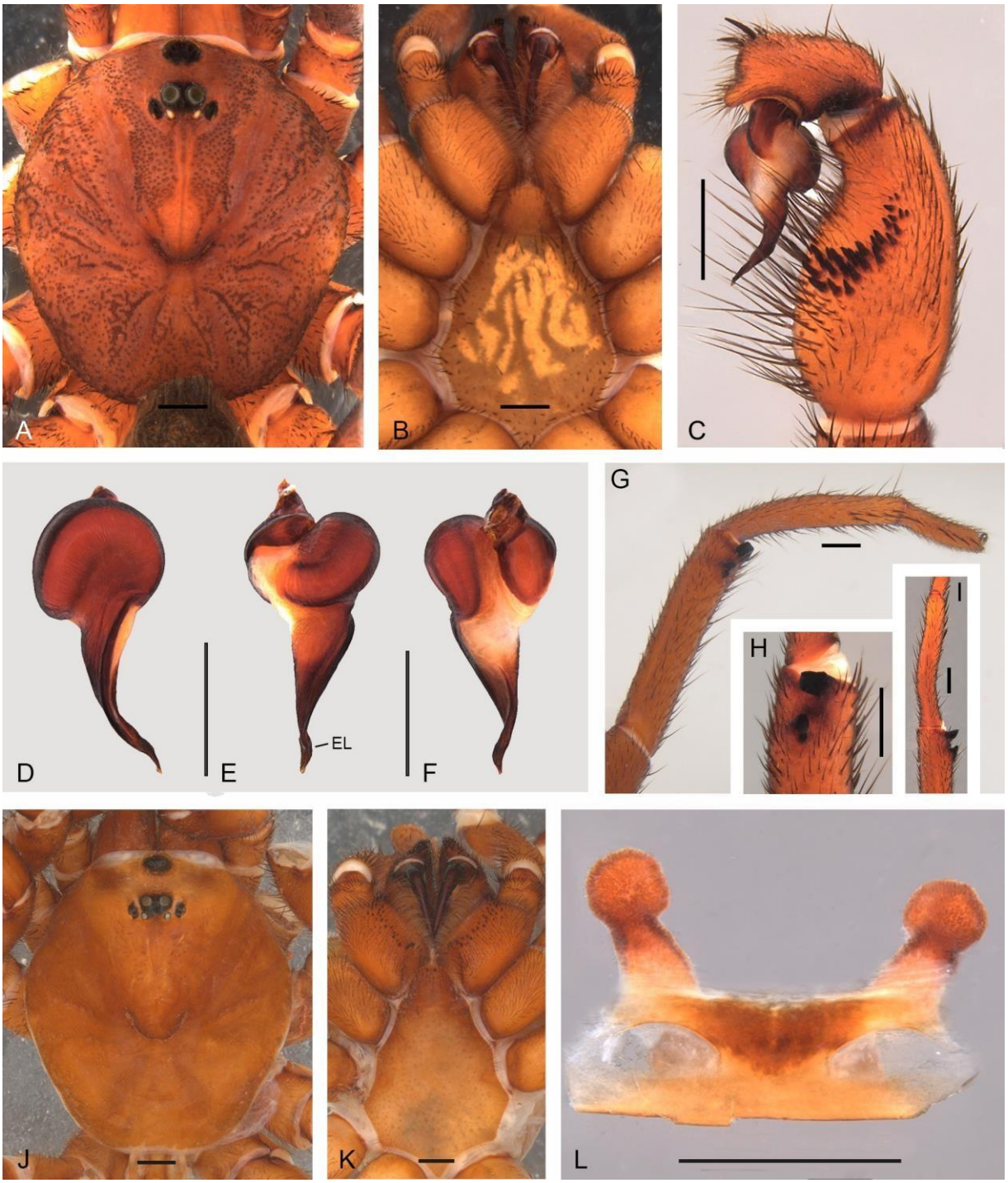

Fig. 13. *Idiops carajas* Fonseca-Ferreira, Zampaulo & Guadanucci, 2017. **A–I**. ♂, holotype (IBSP 166619). **A**. Prosoma (dorsal view). **B**. Prosoma (ventral view). **C**. Part of palp (retrolateral view). **D–F**. Palpal bulb. **D**. Dorsal view. **E**. Retrolateral view. **F**. Prolateral view. **G**. Tibia, metatarsus and tarsus I (prolateral view). **H**. Tibial apophysis (prolateral view). **I**. Tibial apophysis and metatarsus I (dorsal view). **J–L**. ♀, paratype (IBSP 166620). **J**. Prosoma (dorsal view). **K**. Prosoma (ventral view). **L**. Genitalia (dorsal view). Abbreviation: EL = embolar lamella. Scale bars = 1 mm.

18 Jun. 2000; C. Strussmann leg.; MCTP 11192 • 1 ♂; Porto Estrela; 15°19′26″S, 57°13′40″ W; 5 May 2019; J.R. Lema, D. Castro and M. Pessoa-Silva leg.; IBSP249141. – **Mato Grosso do Sul** • 1 ♂; Corumbá, Morro Santa Cruz; 19°12′07.6″ S, 57°36′09.9″ W; Jun. 2003; V.L. Ferreira leg.; MCTP 17591. – **Tocantins** • 1 ♂; Ananás; 6°13′34.70″ S, 48°25′2.39″ W; 21 Apr. 2009; W.U. Oliveira and M.D. Miranda leg.; UFMG 5749.

Emended description

Male and female recently described by Fonseca-Ferreira *et al.* (2017). New data on the male and female are included.

Male (holotype IBSP 166619)

PROSOMA. Basal segment of chelicerae with a prolateral row of 9 teeth, 6 large and 3 small, and 5 small retrolateral teeth (Fig. 14A); salient rastellum, presenting 12–13 short, thick spines with larger distal ends (Fig. 14B).

Female (paratype IBSP 166620)

PROSOMA. Basal segment of chelicerae with a prolateral row of 9 large teeth and 5 small retrolateral teeth; robust rastellum, presenting approximately 25 short and thick spines on a tubercle.

Distribution

Brazil. Distributed in the phytophysiognomies of Amazon and Cerrado, with records from the west of Central-west region (Mato Grosso, Mato Grosso do Sul) and from the North region (Amazonas, Pará and Tocantins) (Fig. 3B).

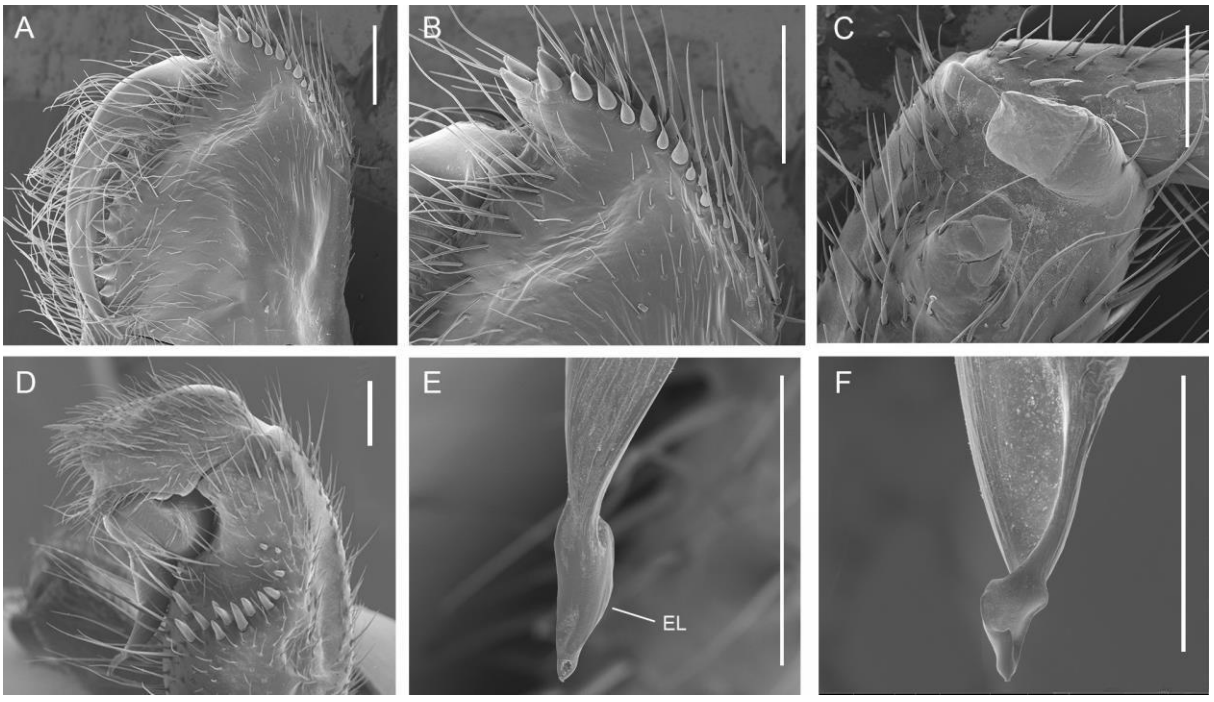

Fig. 14. Scanning electron micrographs of *Idiops carajas* Fonseca-Ferreira, Zampaulo & Guadanucci, 2017, ♂ (MPEG 0109). **A**. Chelicera (retrolateral view). **B**. Rastellum (retrolateral view). **C**. Tibial apophysis (dorsal view). **D**. Part of the palp, showing retrolateral depression. **E–F**. Detail of the final portion of the embolus. **E**. Retrolateral view. **F**. Prolateral view. Abbreviation: EL = embolar lamella. Scale bars = 0.5 mm.

Idiops clarus (Mello-Leitão, 1946)
Figs 3C, 6B, 15–16

Juambeltzia clara Mello-Leitão, 1946: 6, figs 6–9.

Juambeltzia clara – Bücherl 1957: 383, figs 3–3a.
Idiops clarus – Schiapelli & Gerschman de Pikelin 1971: 58, figs 1–7. — Ferretti *et al.* 2017: 977, figs 1a–f, 2a–c, 3d.

Emended diagnosis

Males (Fig. 15A–H) and females (Fig. 15I–K) of *Idiops clarus* differ from the other Neotropical species by having the posterior lateral eyes separated from the median eye group (Fig. 15A, I) and by the rounded sternum (Fig. 15B). Males also differ from others by having the palpal tibia short and thick, with a projection at the base of the retrolateral depression (also present in *I. fuscus* and *I. pirassunsunguensis*) (Fig. 15C) and by the presence of a distal embolar tooth close to the opening of the sperm duct (also present in *I. germaini*) (Fig. 16E). Females differ by the aspect of the spermathecae with the extensive basal area divided by a non-sclerotized portion and by ducts distant from each other and a sclerotized area in the transition between duct and receptacle (Fig. 15K).

Type material

Holotype
URUGUAY – **Florida** • ♂; San Gabriel; A. Juambeltz leg.; MHNM. The type specimen was not found in the MHNM, probably lost.

Other material examined

URUGUAY – **Rivera** • 1 ♂ (SEM); Rivera, Near Vichadero; 31°48′ S, 54°43′ W; 23 Nov. 1959; C.C., P.S.M. and A.M. leg.; FCE 0340. – **Cerro Largo** • 1 ♂; Arroyo Chui del Tacuarí; 32°32′42″ S, 54°2′45″ W; 15 Nov. 1972; A.S.P., C.C., L.Z.C. and N.E.L. leg.; MNHN 295. – **Río Negro** • 1 ♂; Tres Arboles; 32°26′ S, 56°42′ W; 1 Apr. 2009; Stora Enso/Trampa PC; FCE 1075 • 1 ♂; Tres Arboles; 1 Apr. 2009; Stora Enso/Trampa PB2; FCE 1085 • 2 ♂♂; Tres Arboles; 1 Mar. 2009; Stora Enso/Trampa PC; FCE 1115 • 1 ♂; Tres Arboles; 1 Feb. 2009; Stora Enso/Trampa PB4; FCE 1118 • 2 ♂♂; Tres Arboles; 1 Mar. 2009; Stora Enso/Trampa ECD; FCE 1152 • 1 ♂; Tres Arboles; 1 Mar. 2009; Stora Enso/Trampa PB; FCE 1161 • 4 ♂♂; 1 Jan. 2009; Stora Enso/Trampa MB and EC; FCE 1171. – **Treinta y Tres** • 1 ♂; Santa Clara de Olimar; 32°55′ S, 54°58′ W; 12 Jan. 1960; L.C. Zolessi and A. Spiritoso leg.; FCE 0337. – **Lavalleja** • 1 ♀, 1 juv.; Aguas Blancas; 34°32′ S, 55°24′ W; 9 Nov. 1958; FCE 0339. – **Canelones** • 1 ♂; Ruta 11 Km 144; 34°35′09″ S, 55°50′23″ W; 26 Jun. 2010; F. Costa and F. Pérez-Miles leg.; FCE 1015 • 1 ♂; Piedras de Afilar; 34°45′33″ S, 55°31′32″ W; 19–26 Apr. 2010; M. González leg.; trampa pitfall; FCE 1021. – **Maldonado** • 1 ♀; Sierra de las Animas; 34°42′ S, 55°19′ W; 23 Feb. 1969; L.C. Zolessi leg.; FCE 0335 • 1 juv.; Sierra de las Animas; 21 Mar. 1971; FCE 0336 • 1 ♀; Sierra de las Animas; 34º42′ S, 55º19′ W; 21 Mar 1971; FCE 0338 • 2 ♀♀, 2 juvs; Sierra de las Animas; 2 Nov. 1969; L.C. Zolessi leg.; FCE 0342 • 1 ♀; Sierra de las Animas; 11 Feb. 1970; L.C. de Zolessi leg.; MNHN 373 • 1 ♂; Sierra de las Animas; 21 Mar. 1971; S. Etcheverrigaray leg.; MNHN 718. – **Montevideo** • 1 ♂; Prado, Liceo Bauzá; 34°51′ S, 56°12′ W; 19 Apr. 2002; A. Mignone leg.; FCE 0341.

The specimens registered for Argentina and reviewed by Ferretti *et al.* 2017 were not examined here. Despite this, they were included in the species distribution map.

Description

Male (FCE 0341)
HABITUS. See Fig. 15A.

MEASUREMENTS. TBL 11, CL 5.7, CW 4.8, LL 0.6, LW 1.2, SL 3, SW 2.9.

COLOR. Carapace, legs and sternum light brown (Fig. 15A–B), abdomen gray.

PROSOMA. Carapace and ocular arrangement as shown in Fig. 15A. Eye tubercle: 1.4 long; 1.6 wide. Distance AME-ALE 0.8. Eye diameters: AME 0.3, ALE 0.4, PME 0.3, PLE 0.3. Thoracic fovea procurved. Labium and sternum without cuspules (Fig. 15B). Basal segment of chelicerae with a prolateral row of

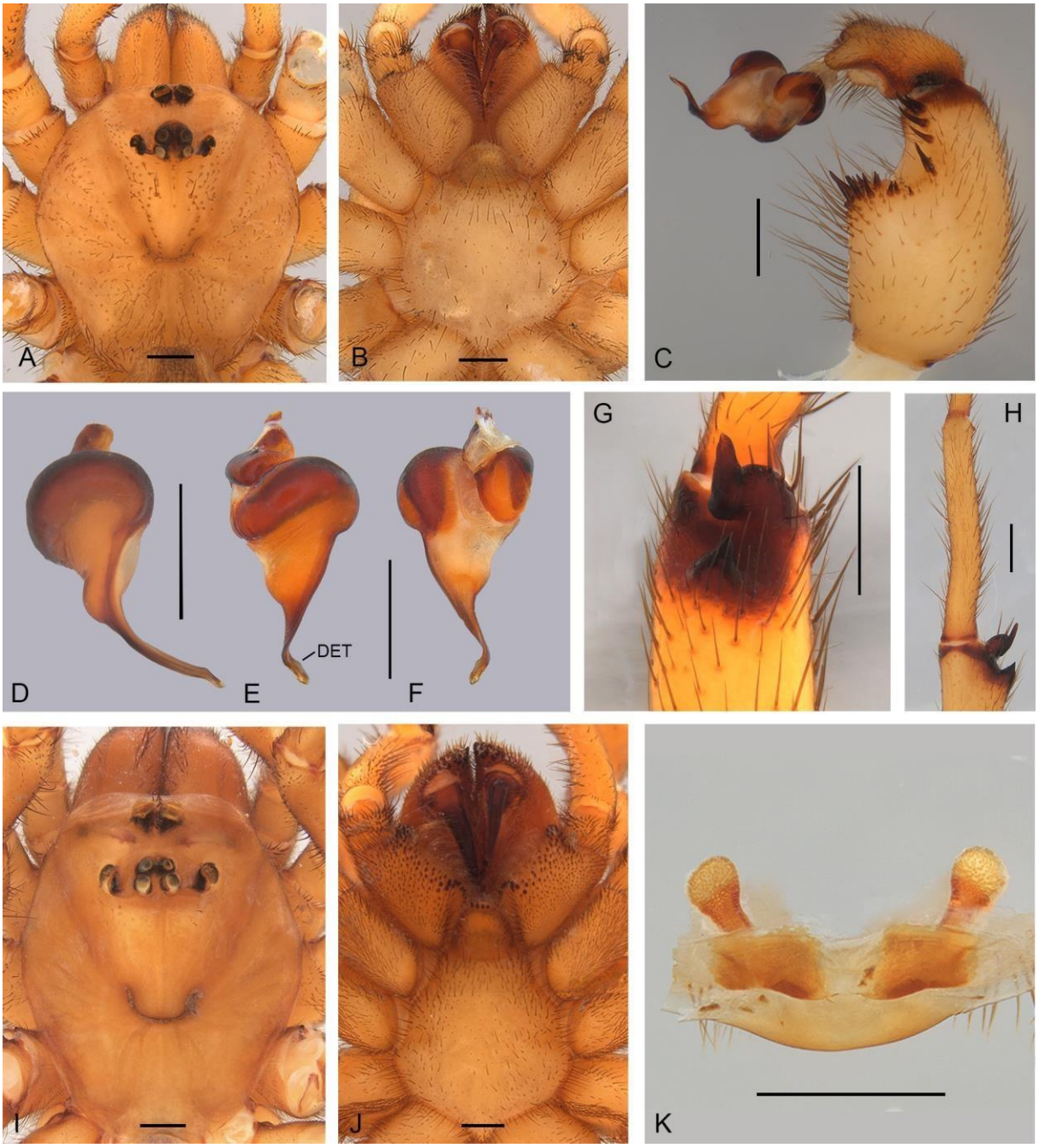

Fig. 15. *Idiops clarus* (Mello-Leitão, 1946). **A–H**. ♂ (FCE 0341). **A**. Prosoma (dorsal view). **B**. Prosoma (ventral view). **C**. Part of palp (retrolateral view). **D–F**. Palpal bulb. **D**. Dorsal view. **E**. Retrolateral view. **F**. Prolateral view. **G**. Tibial apophysis (prolateral view). **H**. Tibial apophysis and metatarsus I (dorsal view). **I–K**. ♀, (FCE 0338). **I**. Prosoma (dorsal view). **J**. Prosoma (ventral view). **K**. Genitalia (dorsal view). Abbreviation: DET = distal embolar tooth. Scale bars = 1 mm.

5 large teeth and retrolateral row with 9 small teeth (Fig 15A), rastellum with 8 spines, distal spines are longer (Fig. 16B).

LEGS. Tibia and metatarsus I as shown in Fig. 15H. Leg I with an apical branch of tibial apophysis with a short and triangular basal spine, and an apical branch with a conical spine twice the size of basal spine. Pseudoscopula: tarsus I divided into rows of thick hair; tarsus II–IV totally covered.

PALP. Tibia with conspicuous retrolateral depression, with projection on basal portion and larger spines concentrated on basal and apical portions (Figs 15G, 16C); embolus with subapical torsion and presence of a small embolar tooth close to spermatic duct opening (Figs 15D–F, 16E–F).

PALP AND LEG MEASUREMENTS. Palp = 9.3 (3, 1.6, 3.1, 1.6), I = 21.3 (5.9, 3.2, 4.3, 5, 2.9), II = 19.7 (5, 2.5, 3.4, 4.2, 2.6), III = 14. 9 (3.5, 2.3, 2.3, 4, 2.8), IV = 21.2 (5.4, 2.9, 4.5, 5.4, 3).

SPINATION. Palp: Ti r24, Ta d0-0-4. Leg I: Fe d1-1-2, Ti v1r-1r-2r, Mt 1r-2r-1ap, Ta r2-1-0. Leg II: Fe d1-1-2, Ti v0-2r-1r-1, Mt v1r-1r-1r-2, Ta p0-0-1, r2-2-0. Leg III: Fe d1-1-1, Pa d1-1-0, p3-5-8, r0-0-2, Ti v0-1r-0-2, p1-1-4, r1-1-2, Mt v3-4-0-4, p3- 2-2, r0-1-2, Ta p0-4-8, r0-4-8. Leg IV: Fe d1-1-2, Pa p16-3-0, Ti v1-2-2, Mt v1-2 -1-3, Ta p2-3-6, r0-0-2.

Female (FCE 0338)

HABITUS. See Fig. 15I.

MEASUREMENTS. TBL 17.3, CL 7.5, CW 6.3, LL 1.2, LW 1.6, SL 4.4, SW 4.3.

COLOR. Carapace, legs and sternum light brown (Fig. 15I–J), abdomen gray.

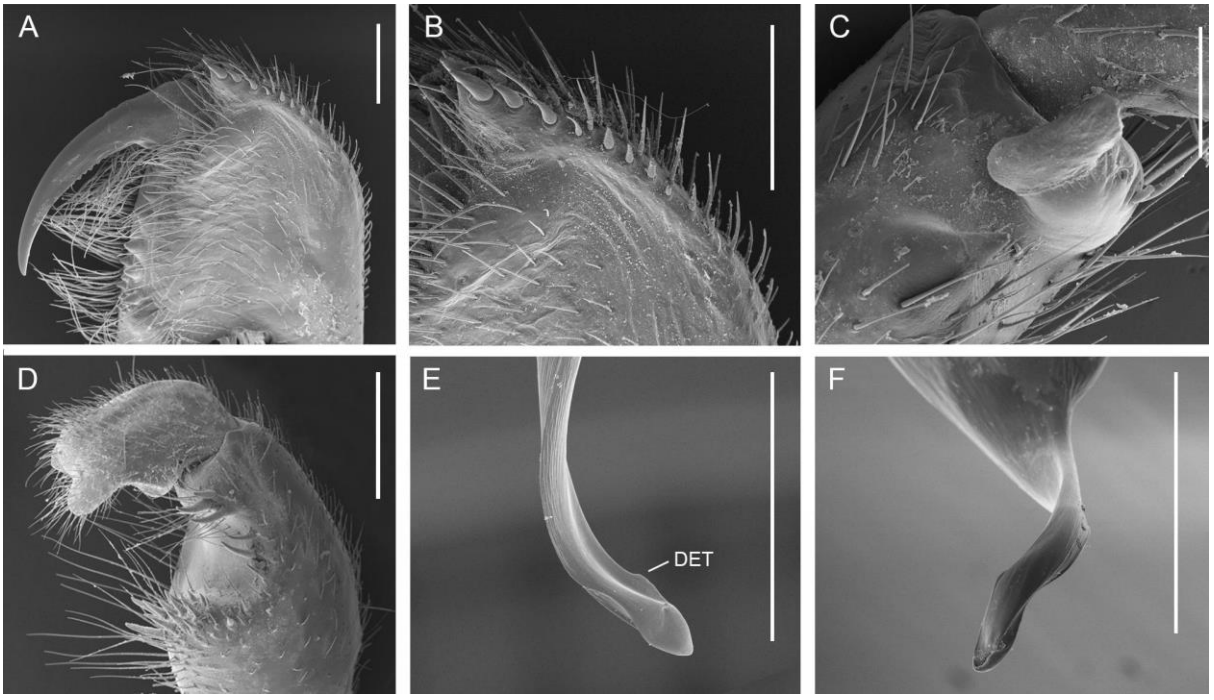

Fig. 16. Scanning electron micrographs of *Idiops clarus* (Mello-Leitão, 1946), ♂(FCE 0340). **A**. Chelicera (retrolateral view). **B**. Rastellum (retrolateral view). **C**. Tibial apophysis (dorsal view). **D**. Part of the palp, showing retrolateral depression. **E–F**. Detail of the final portion of the embolus. **E**. Retrolateral view. **F**. Prolateral view. Abbreviation: DET = distal embolar tooth. Scale bars = 0.5 mm.

PROSOMA. Carapace and ocular arrangement as shown in Fig. 15I. Eye tubercle: 2.2 long; 2.7 wide. Distance AME-ALE 1. Eye diameters: AME 0.4, ALE 0.6, PME 0.5, PLE 0.7. Thoracic fovea procurved. Labium with 4–6 cuspules (Fig. 15J). Maxilla with 83 cuspules, distributed over the anterior ventral half (Fig. 15J). Basal segment of chelicerae with a prolateral row of 5 large teeth and a retrolateral row with 7 small teeth, grouped at basal half.

PALP AND LEG MEASUREMENTS. Palp = 12.2 (4.1, 2.6, 2.7, 2.8), I = 13.3 (4.2, 3, 2.9, 2.2, 1), II = 11.1 (3.4, 2.7, 2.3, 2, 1), III = 12 (3.3, 2.6, 1.7, 2.4, 2), IV = 15.8 (4.1, 3.4, 3.3, 3.2, 1.8).

SPINATION. Palp: Fe p0-0-2, Pa p0-0-1, Ti p7-8-11, r3-10-13, Ta v0-0-6, p12-10-8, r12-10-12. Leg I: Ti p5-5-8, r6-8-12, Mt p11-8-10, r9-8-7, Ta v0-6-7, p4-5-2, r5-4-3. Leg II: Ti p2-7-6, r2-4-1, Mt p10-9-7, r4-5-3, Ta v0-1-7, p4-5-3, r4-2-1. Leg III: Pa p5-5-16, r0-0-2, Ti p5-7-10, r3-7-10, Mt v0-0-2, p12-7-6, r7-5-4, Ta v0-6-22. Leg IV: Pa p30-5-0, Ti v0-1-1-2, Mt v0-2-5-3, Ta v1-9-14.

SPERMATHECAE. Duct with basal portion shorter than apical portion and non-sclerotized spherical receptacles with evident granules (Fig. 15K).

Distribution

Uruguay and Argentina (Fig. 3C).

Idiops duocordibus Fonseca-Ferreira, Guadanucci & Brescovit sp. nov.
urn:lsid:zoobank.org:act:D3387D49-8B8B-42C0-ADB9-88D5A8A78B62
Figs 3B, 17A–L

Diagnosis

Males and females of *Idiops duocordibus* sp. nov. differ from the other Neotropical species by thelight brown coxae and trochanters, contrasting with the brown body (Fig. 17A–L). The male resembles that of *I. rohdei* by the short metatarsus I with prolateral curvature and with a slight prolateral projection on the apical half (Fig. 17I), but differs by the tibial apophysis with a triangular apical branch twice the size of the basal branch (Fig. 17G–H) and by the weakly curved embolus (Fig. 17D). The female (Fig. 17J–L) differs from those of the other species by having the spermathecae with bilobed receptacles in the shape of a heart (Fig. 17L).

Etymology

The specific epithet refers to the heart-shaped receptacles of the female genitalia.

Type material

Holotype

BRAZIL – **Pará** • ♂; Vitória do Xingu, Ilha Taboca; 3°23′12.7″ S, 51°57′26.2″ W; 3 Nov. 2000; F. Oliveira leg.; MPEG 0124.

Paratypes

BRAZIL – **Pará** • 1 ♂; Almeirim, Reserva de Itapeguara; 0°32′04.9″ S, 52°48′14.8″ W; Dec. 2001; MPEG 0122 • 1 ♀; Arapari, Rio Tocantins, left bank; 4°52′23.6″ S, 49°31′39.5″ W; 14 Mar. 1984; W.L. Overal leg.; MPEG 0123.

Other material examined

BRAZIL – **Amazonas** • 1 ♂; Manaus, Reserva Florestal Adolpho Ducke; 3°0′27″ S, 59°56′22.92″ W; 9 Sep. 1991; H. Höfer and T. Gasnier leg.; INPA 4592 • 1 ♂; Manaus, Reserva Florestal Adolpho Ducke;

14–24 Jul. 1991; A.D. Brescovit leg.; MCN 21485. – **Pará** • 2 ♂♂; Vitória do Xingu, Ilha Taboca; 3°23′12.7″ S, 51°57′26.2″ W; 23 Nov. 2000; F. Oliveira leg.; MPEG 0112, MPEG 0114.

Description

Male (holotype MPEG 0124)
HABITUS. See Fig. 17A.

MEASUREMENTS. TBL 10, CL 4.6, CW 4, LL 0.5, LW 0.7, SL 2.4, SW 2.2.

COLOR. Carapace brown, light brown coxae and trochanter (Fig. 17A–B). Abdomen dark gray.

PROSOMA. Carapace and ocular arrangement as shown in Fig. 17A. Eye tubercle: 0.68 long; 1.08 wide. AME-ALE distance 0.63. Eye diameters: AME 0.32, ALE 0.34, PME 0.13, PLE 0.22. Thoracic fovea procurved (Fig. 17A). Labium and sternum without cuspules (Fig. 17B). Basal segment of chelicerae with a prolateral row of 5 small teeth equally distributed, rastellum with 5 spines (Fig. 17B).

LEGS. Tibia, metatarsus and tarsus I as shown in Fig. 17G. Leg I with double tibial apophysis. Leg I tibial apophysis with apical branch twice the size of basal branch and with a conspicuous spine (Fig. 17G–I). Pseudoscopula: tarsus I weakly covered (Fig. 17G), tarsus II–IV totally covered.

PALP. Tibia with thickened median portion and with larger spines concentrated in basal portion of retrolateral depression (Fig. 17C), embolus elongated, tapered, and slightly curved, with torsion on apical portion (Fig. 17D–F), keel along embolus length extending to apical portion (Fig. 17D).

PALP AND LEG MEASUREMENTS. Palp = 6.9 (2.3, 1.3, 2.4, 0.9), I = 13.4 (4.3, 1.9, 3, 2.9, 1.3), II = 11.3 (3.5, 1.8, 2.5, 2.5, 1), III = 10 (2.7, 1.5, 1.9, 2.6, 1.3), IV = 13.6 (3.9, 1.9, 3.5, 3.1, 1.2).

SPINATION. Palp: Ti r39, Ta d0-0-3. Leg I: Pa v0-1-2, r1-2-3, Ti v1-2-3, r1-2-6, Mt v1-4-7, p0-0-2, p0-1-1, r4-4-5, Ta v0-1-0, p0-2-3, p1-2-3, r4-4-3. Leg II: Pa v0-0-3, d0-0-1, Ti v2-3-7, d3-4-8, Mt v4-6-8, d5-6-7, p1-2-4, r0-2-3, Ta p1-3-3, r2-2-3. Leg III: Pa v0-0-2, Ti v1-2-3 r0-1-0, Mt v3-6-7, d0-0-2, p2-2-3, r1-2-4, Ta p3-4-4, r1-3-3. Leg IV: Pa v0-0-3, Ti v1-2-2, Mt v1-4-8, p0-0-1, r0-2-3, Ta v2-4-5, p0-1-2, r2-3-2.

Female (paratype MPEG 0123)
HABITUS. See Fig. 17J.

MEASUREMENTS. TBL 9.9, CL 5.5, CW 4,8, LL 0.9, LW 1.2, SL 3.4, SW 2.9.

COLOR. Brown carapace and trochanter, remainder of leg light brown (Fig. 17J–L). Abdomen dark gray.

PROSOMA. Carapace and ocular arrangement as shown in Fig. 17J. Eye tubercle: 0.7 long; 1.1 wide. AME-ALE distance 0.9. Eye diameters: AME 0.3, ALE 0.3, PME 0.2, PLE 0.4. Thoracic fovea procurved (Fig. 17J). Labium with with 13 cuspules (Fig. 17K). Maxilla with 117 cuspules, distributed throughout the maxillae, with larger spines on anterior half (Fig. 17K). Basal segment of chelicerae with a prolateral row of 6 large teeth and 2 retrolateral small teeth, grouped in basal half, rastellum with 16–18 short and thick spines (Fig. 17K).

PALP AND LEG MEASUREMENTS. Palp = 6.4 (2.3, 1.2, 1.6, 1.3), I = 7.4 (2.5, 1.5, 1.6, 1, 0.8), II = 6.5 (2.3, 1.6, 1.2, 0.9, 0.5), III = 7 (1.9, 1.6, 1.3, 1.4, 0.8), IV = 9.5 (2.6, 1.7, 2.1, 2.2, 0.9).

SPINATION. Palp: Pa p0-0-1, Ti p4-7-7, r4-6-8, Ta p10-8-7, r10-7-9. Leg I: Ti p4-4-5, r3-5-8, Mt p8-7-8, r5-5-6, Ta p3-4-2, r5-4-0. Leg II: Ti v1-1-2, p3-3-4, r0-1-3, Mt v1-1-2, p6-7-9, r2-2-1, Ta p2-3-3, r2-1-0.

Leg III: Pa p4-5-10, Ti v0-0-2, p2-4-6, r4-4-6, Mt v1-1-2, d0-0-2, p3-3-3, r0-2-1. Leg IV: Ti v1-1-2, Mt v1-1-3, vp0-0-2, Ta v0-1-2, p1-1-2.

SPERMATHECAe. Single sclerotized base that is divided into two divergent ducts, receptacula strongly sclerotized (Fig. 17L).

Fig. 17. *Idiops duocordibus* Fonseca-Ferreira, Guadanucci & Brescovit sp. nov. **A–I**. ♂, holotype (MPEG 0124). **A**. Prosoma (dorsal view). **B**. Prosoma (ventral view). **C**. Part of palp (retrolateral view). **D–F**. Palpal bulb. **D**. Dorsal view. **E**. Retrolateral view. **F**. Prolateral view. **G**. Tibia, metatarsus and tarsus I (prolateral view). **H**. Tibial apophysis (prolateral view). **I**. Tibial apophysis and metatarsus I (dorsal view). **J–L**. ♀, paratype (MPEG 0123). **J**. Prosoma (dorsal view). **K**. Prosoma (ventral view). **L**. Genitalia (dorsal view). Abbreviation: K = keel. Scale bars = 1 mm.

Distribution

Brazil. Distributed in phytophysiognomies in the Amazon, with records for the North region (western Amazonas and northwestern Pará) (Fig. 3B)

Idiops germaini Simon, 1892
Figs 3D, 5B, 18–19

Idiops germaini Simon, 1892: 92.

Idiops germaini – Mello-Leitão 1923: 47. — Fukami & Lucas 2005: 6, figs 8–10.

Diagnosis

Males of *Idiops germaini* differ from those of other Neotropical species of *Idiops* by the long and slender palpal tibia, with the retrolateral depression restricted to the apical portion (Figs 18C, 19D), and by having the tibial apophysis reduced to two long spines inserted on a low tubercle (Figs 18G–I, 19C). Females with spermathecae composed of short ducts and fully sclerotized receptacles, almost twice the diameter of the duct (Fig. 18L).

Type material

Holotype
BRAZIL – **Rio de Janeiro** • ♂; Rio de Janeiro; P. Germain leg.; MNHN 417.

Paratype
BRAZIL – **Rio de Janeiro** • 1 ♀; same collection data as for holotype; MNHN 9977.

Other material examined

BRAZIL – **Rio de Janeiro** • 1 ♂ (SEM); Nova Iguaçu, Parque Municipal de Nova Iguaçu; 22°45′35″ S, 43°27′6″ W; 20 May 2004; R.L.C. Baptista leg.; MNRJ • 1 ♂; Nova Iguaçu, Parque Municipal de Nova Iguaçu; 20 Jun. 2004; R.L.C. Baptista leg.; MNRJ • 1 ♂; Nova Iguaçu, Parque Municipal de Nova Iguaçu; Jan. 2001; R.L.C. Baptista leg.; MNRJ • 1 ♀; Nova Iguaçu, Parque Municipal de Nova Iguaçu; 22 Jan. 2005; D.R. Pedroso leg.; MNRJ • 1 ♀; Paraty, Parque Nacional da Serra da Bocaina, Trilha da Cachoeira Sete Quedas; 23°2′30″ S, 44°39′42″ W; 24–26 Mar. 2019; R.F. Ferreira, A. Galleti, I. Meirelles and R. Indicatti leg.; CAD 832 • 1 ♀; Angra dos Reis, Distrito de Serra D'Agua; 23°0′25″ S, 44°19′4″ W; 25 Nov. 2010; C.A.S. Souza *et al*. leg.; CHNUFPI 0040 • 1 ♀; Mata da Tijuca; 13 Aug.1977; M. Júlio leg.; UFPB Ar418.

Description

Male (holotype MNHN 417)
HABITUS. See Fig. 18A.

MEASUREMENTS. TBL 12, CL 6.8, CW 6.1, LL 0.8, LW 1.1, SL 3.8, SW 3.3.

COLOR. Brown carapace and legs, brownish sternum and coxae (Fig. 18A–B), gray abdomen.

PROSOMA. Carapace and ocular arrangement as shown in Fig. 18A. Eye tubercle: 1.4 long; 1.4 wide. Distance AME-ALE 0.6. Eye diameters: AME 0.4, ALE 0.3, PME 0.2, PLE 0.4. Thoracic fovea procurved (Fig. 18A). Labium and sternum without cuspules (Fig. 18B). Basal segment of chelicerae with a prolateral row of 8 teeth, seven larger and one small, and a retrolateral row with 9 small teeth, grouped in basal half (Fig. 19A), with distal rastellum with 10 spines, with same size (Fig. 19B).

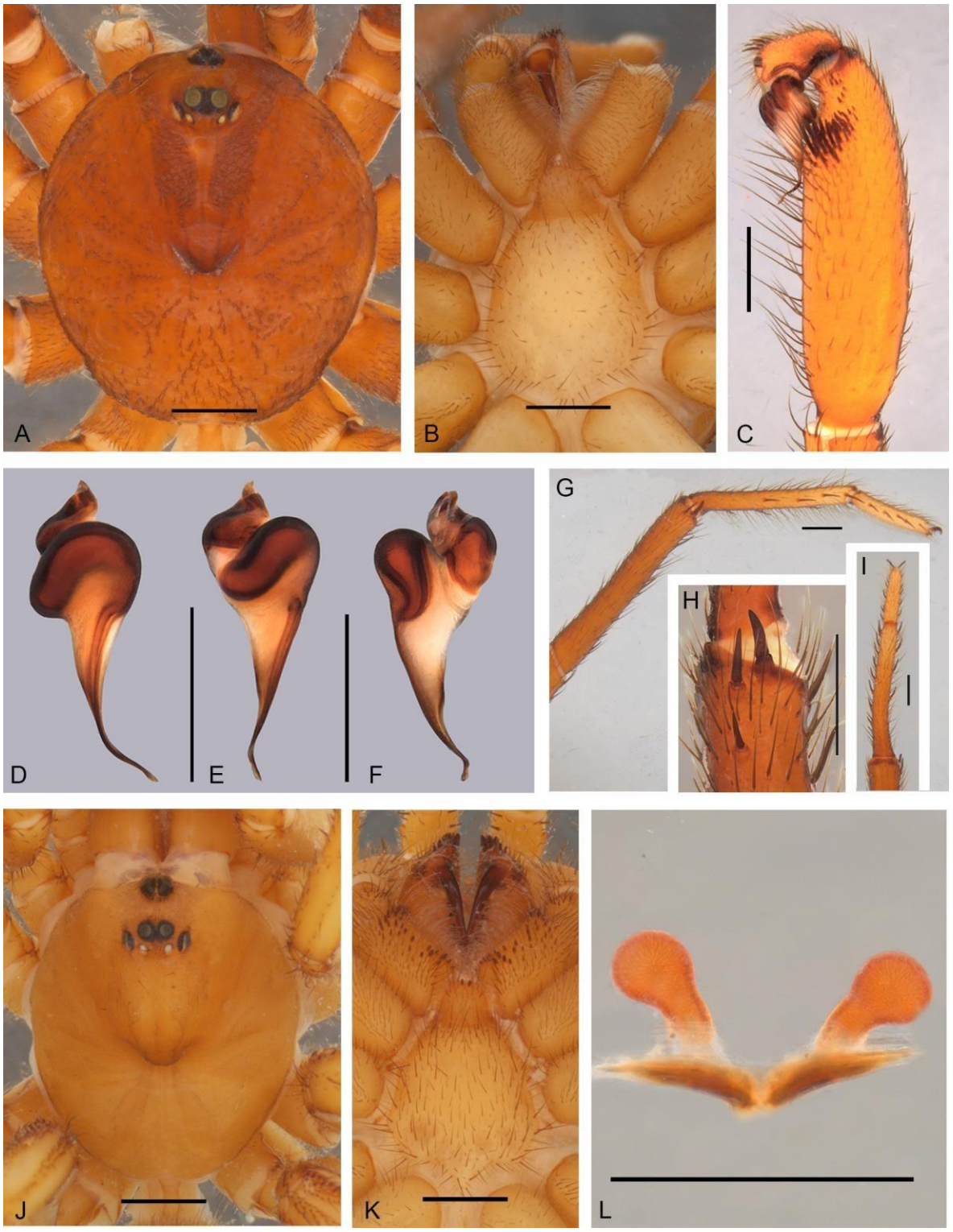

Fig. 18. *Idiops germaini* Simon, 1892. **A–I**. ♂ (MRNJ). **A**. Prosoma (dorsal view). **B**. Prosoma (ventral view). **C**. Part of palp (retrolateral view). **D–F**. Palpal bulb. **D**. Dorsal view. **E**. Retrolateral view. **F**. Prolateral view. **G**. Tibia, metatarsus and tarsus I (prolateral view). **H**. Tibial apophysis (prolateral view). **I**. Tibial apophysis and metatarsus I (dorsal view). **J–L**. ♀, (CAD 832). **J**. Prosoma (dorsal view). **K**. Prosoma (ventral view). **L**. Genitalia (dorsal view). Scale bars = 1 mm.

LEGS. Tibia, metatarsus and tarsus I as shown in Fig. 18G.

PALP. Tibia with a shallow retrolateral depression and spines concentrated at basal half of depression (Figs 18C, 19D); elongated embolus with median curvature (Fig. 18E–F) and a small distal embolar tooth close to sperm duct opening (Fig. 19E–F).

PALP AND LEG MEASUREMENTS. Palp = 12 (4.4, 2, 4.2, 1.4), I = 22.9 (7.2, 3.4, 5.4, 4.8, 2.1), II = 19.9 (6.4, 2.9, 4.4, 4.4, 1.8), III = 17.2 (4.6, 2.6, 3.3, 4.7, 2), IV = 24 (6.7, 3.4, 5.6, 5.9, 2.4).

SPINATION. Palp: Ti r3-4, Ta d0-0-4. Leg I: Fe d1-2-2, Ti p0-0-1, r0-2-2, Mt p0-0-2, r2-2-4, Ta p1-1-1, r2-1-2. Leg II: Fe d1-2-2, Ti v1-1-3ap, Mt p0-1-2, r2-2-2, Ta p0-1-1, r2-2-4. Leg III: Fe d1-1-1, Pa p2-5-6, r0-0-3, Ti v1-2-2, p1-2-4, r0-1-2, Mt vv2-1-4ap, p3-2-2, r2-1- 1, Ta p2-3-3, r1-2-3. Leg IV: Fe d1-1-2, Pa p13-3-0, Ti v1-1-3, Mt v1-1-1-3, Ta p2- 2-4, r0-0-2.

Female (paratype MNHN 9977)

HABITUS. See Fig. 18J.

MEASUREMENTS. TBL 16.6, CL 9.1, CW 6.7, LL 1.5, LW 1, SL 4.8, SW 4.

COLOR. Brown carapace and legs, brownish sternum and coxae (Fig. 18J–K), gray abdomen.

PROSOMA. Carapace and ocular arrangement as shown in Fig. 18J. Eye tubercle: 2.3 long; 2.8 wide. Distance AME-ALE 0.9. Eye diameters: AME 0.3, ALE 0.5, PME 0.3, PLE 0.5. Thoracic fovea procurved (Fig. 18J). Labium with 2 cuspules (Fig. 18K). Maxilla with 28 cuspules, with larger cuspules concentrated in anterior prolateral and retrolateral extremities (Fig. 18K). Basal segment of chelicerae with a prolateral

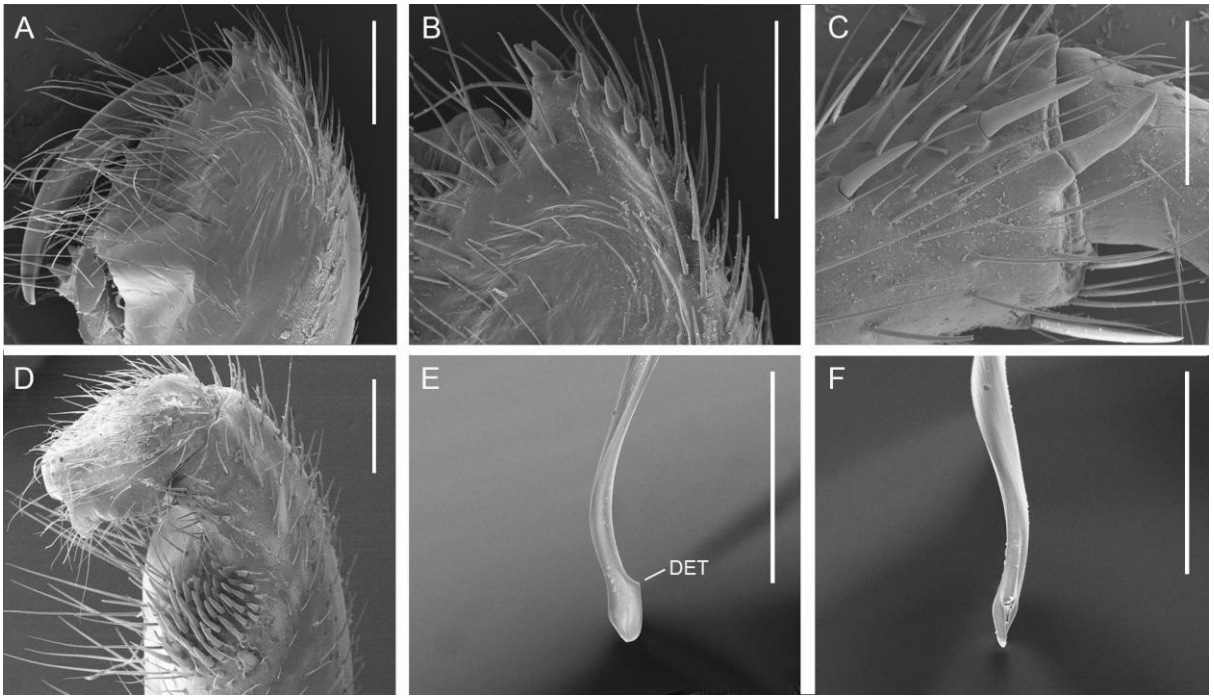

Fig. 19. Scanning electron micrographs of *Idiops germaini* Simon, 1892, ♂ (MNRJ). **A**. Chelicera (retrolateral view). **B**. Rastellum (retrolateral view). **C**. Tibial apophysis (dorsal view). **D**. Part of the palp, showing retrolateral depression. **E–F**. Detail of the final portion of the embolus. **E**. Retrolateral view. **F**. Prolateral view. Abbreviation: DET = distal embolar tooth. Scale bars = 0.5 mm.

row of 6 large teeth and a retrolateral row with 13 small teeth, grouped in basal half, rastellum with 14 spines, distal ones longer (Fig. 18K).

PALP AND LEG MEASUREMENTS. Palp = 11.9 (4, 2.6, 2.6, 2.7), I = 13.3 (4.5, 2.9, 2.7, 2.2, 1), II = 11.8 (3.8, 2.7, 2.2, 2, 1), III = 12.9 (3.5, 2.9, 1.9, 2.6, 2), IV = 17.6 (4.8, 3.5, 3.7, 3.5, 2.1).

SPINATION. Palp: Pa p0-0-1, Ti p4-9-11, r4-7-13, Ta v0-0-6, p14-9-8, r11-11-10. Leg I: Ti p3-8-11, r3-7-15, Mt p11-8-6, r11-7-9, Ta v0-0-6, p5-4-2, r6-5-0. Leg II: Ti p1-3-6, r0-1-1, Mt p10-10-10, r5-4-2, Ta v0-0-4, p5-5-4, r3-2-0. Leg III: Pa p3-5-7, r0-0-2, Ti p4-4-4, r0-3-4, Mt v1p-0-0-2, p5-0-3, r5-1-1, Ta v0-2 -7. Leg IV: Pa p30-5-0, Ti v0-1-2, Mt v1-1-1-3ap, Ta v0-2-6.

SPERMATHECAE. Ducts with translucent basal half and sclerotized apical half and spherical receptacula (Fig. 18L).

Distribution

Brazil. Found in Atlantic Forest phytophysiognomies, with records for the state of Rio de Janeiro (Fig. 3D).

Idiops guri Fonseca-Ferreira, Guadanucci & Brescovit sp. nov.
urn:lsid:zoobank.org:act:A7664A49-43C0-4157-BC48-B98BFB58252B
Figs 3C, 20–21

Diagnosis

The male of *Idiops guri* sp. nov. differs from those of other Neotropical species by having the palpal tibia with the retrolateral depression shallow and delimited by spines of decreasing lengths towards the apical portion (Figs 20C, 21D) and by the presence of a hook-shaped projection near the sperm duct opening in retroventral view (Fig. 21E–F). The female differs from the other species by the horseshoe-shaped spermathecae, with ducts curved inward and with sclerotization at the transition between the duct and the receptacle, and oval and weakly sclerotized receptacles (Fig. 20L).

Etymology

The specific epithet is a tribute to southern Brazil, the region where the species is distributed. The word 'guri' , which is of Tupi-Guarani origin, is commonly used in the region to refer to a child or a lad. It also alludes to the tiny size of the specimens.

Type material

Holotype

BRAZIL – **Rio Grande do Sul** • ♂; São Francisco de Paula, Cento de Pesquisas e Conservação da Natureza Pró Mata; 29°27′–29°35′ S, 50°08′–50°15′ W; 1 May 2001; R. Ott leg.; MCN 39594.

Paratypes

BRAZIL – **Paraná** • 1 ♂; Londrina, Parque dos Godoy; 23°26′ S, 51°15′ W; 5 Jan. 1999; J. Lopes and I.M. Madri leg.; MCTP 11840. – **Santa Catarina** • 1 ♂; Chapecó, Floresta Nacional de Chapecó; 27°06′10.5″ S, 52°46′48.8″ W; 10 Mar. 2004; M. Scartezini leg.; IBSP 126721. – **Rio Grande do Sul** • 1 ♂; Viamão, Parque Estadual de Itapuã; 30°22′6″ S, 50°59′52″ W; 28 May 2004; A.C.K. Ferreira *et al.* leg.; MCTP 16937.

Other material examined

BRAZIL– **Paraná** • 2 ♂♂ (SEM); Cornélio Procópio, Parque Estadual Mata São Francisco; 28°08′47.3″ S, 50°34′19.5″ W; 2009; J.L. Chavari leg.; IBSP 220523 • 1 ♂; Cornélio Procópio, Parque Estadual Mata

São Francisco; 8 May 2009; N.G. Cipola leg.; IBSP 150273 • 1 ♂; Londrina, Parque dos Godoy; 23°26′ S, 51°15′ W; 13 Apr. 1999; J. Lopes and I.M. Madri leg.; MCTP 11815 • 1 ♂; Londrina, Parque dos Godoy; 16 Mar. 1999; J. Lopes and I.M. Madri leg.; MCTP 11816 • 2 ♂♂; same collection data as for preceding; MCTP 11820 • 1 ♂; Londrina, Parque dos Godoy; 30 Mar. 1999; J. Lopes and I.M. Madri leg.; MCTP 11817 • 1 ♂; Ponta Grossa, Parque Estadual de Vila Velha; 25°14′17″ S, 50°0′39″ W; 22 Nov. 1986; Equipe Profaupar leg.; MCN 20668 • 2 ♂♂, 1 juv.; Três Barras do Paraná, Foz do Córrego Três Barras; 25°25′8″ S, 53°10′51″ W; 24 Feb.–24 Mar. 1993; A.B. Bonaldo leg.; MCN 23420. – **Santa Catarina** • 1 ♂; Chapecó, Floresta Nacional de Chapecó; 27°06′10.5″ S, 52°46′48.8″ W; 10 Mar. 2004; M. Scartezini leg.; IBSP 126735 • 2 ♂♂; same collection data as for preceding; IBSP 126732 • 2 ♂♂; same collection data as for preceding; IBSP 126729 • 8 ♂♂; same collection data as for preceding; IBSP 126723 to 126724, IBSP 126726 to 126728, IBSP 126730 to 126731, IBSP 126733. – **Rio Grande do Sul** • 2 ♀♀; São Francisco de Paula; Potreiro Velho; 29°26′52″ S, 50°35′2″ W; Feb. 2002; L. Bertocello; MCTP 17532, MCTP 23469 • 1 ♀; São Francisco de Paula, Centro de Pesquisas e Conservação da Natureza Pró-Mata; 29°27′–29°35′ S, 50°08′–50°15′ W; 18 May 2002; R. Ott leg.; MCTP 18549 • 2 ♂♂; Itaara; 29°36′36″ S, 53°45′54″ W; Apr. 2017; A.A. Lise leg; MCTP 20798 to MCTP 20799 • 1 ♂, 1 juv.; São Francisco de Paula, Centro de Pesquisas e Conservação da Natureza Pró-Mata; 1 May 2001, R. Ott leg.; MCN 39594a • 2 ♂♂, São Francisco de Paula, Centro de Pesquisas e Conservação da Natureza Pró-Mata; 3 Feb. 2001; R. Ott leg.; MCN 39593 • 1 ♂; Derrubadas, Parque Estadual do Turvo; 27°8′44″ S, 53°53′10″ W; 7 May 2004; R. Ott leg.; MCN 40380 • 3 ♂♂; Morrinhos do Sul, Tres Passos; 29°21′54″ S, 49°56′6″ W; 1 Nov. 2006; A. Gonçalves *et al.* leg.; MCN 52357 to 52358 • 1 ♂; Dom Pedro de Alcântara; 29°22′8″ S, 49°51′0″ W; 25 Apr. 2006; A. Gonçalves *et al.* leg.; MCN 52356 • 2 ♂♂; Viamão, Parque Estadual de Itapuã; 30°22′6″ S, 50°59′52″ W; 15 Apr. 2004; A.C.K. Ferreira *et al.* leg.; MCTP 16939, MCTP 16946 • 2 ♂♂; same collection data as for preceding; MCTP 16948 • 14 ♂♂; Viamão, Parque Estadual de Itapuã; 30 Apr. 2004; A.C.K. Ferreira *et al.* leg.; MCTP 16638 • 12 ♂♂; same collection data as for preceding; MCTP 16936 • 1 ♂; Viamão, Parque Estadual de Itapuã; 18 Apr.–8 May 2007; R. Moraes leg.; MCTP 29969 • 2 ♂♂; Porto Alegre, Reserva Biológica de Lami; 30°15′ S, 51°05′ W; 23 Mar.–2 Apr. 2006; MCN 46338 • 1 ♂; Porto Alegre, Reserva Biológica de Lami; 23 Mar.–12 Apr. 2006; R. Moraes leg.; MCN 56824 • 4 ♂♂; Porto Alegre, Jardim Botânico; 5 Mar.–5 Apr. 2013; G.O. Silva leg.; MCN 49909 to 49911; MCN 49913 • 1 ♂; Herval; 32°1′26″ S, 53°23′45″ W; 27–28 Apr. 2013; Equipe Sisbiota leg.; MCN 48527.

Description

Male (holotype MCN 39594)

HABITUS. See Fig. 20A.

MEASUREMENTS. TBL 5.3, CL 2.5, CW 2.4, LL 0.4, LW 0.6, SL 1.4, SW 1.3.

COLOR. Yellowish brown carapace and legs, gray abdomen (Fig. 20A–B).

PROSOMA. Carapace and ocular arrangement as shown in Fig. 20A. Eye tubercle: 0.4 long; 0.5 wide. AME-ALE distance 0.3. Eye diameters: AME 0.1, ALE 0.2, PME 0.1, PLE 0.12. Thoracic fovea procurved (Fig. 20A). Labium and sternum without cuspules (Fig. 20B). Basal segment of chelicerae with a prolateral row of 5 small teeth equally distributed, rastellum with 11–12 spines, distals largest (Fig. 21A–B).

LEGS. Tibia, metatarsus and tarsus I as shown in Fig. 20G. Tibial apophysis of leg I with short basal branch with small triangular spine and apical branch twice as large as basal branch (Fig. 20G–I), with elongated spine in digitiform shape (Fig. 21C). Pseudoscopula: tarsus I–IV totally covered.

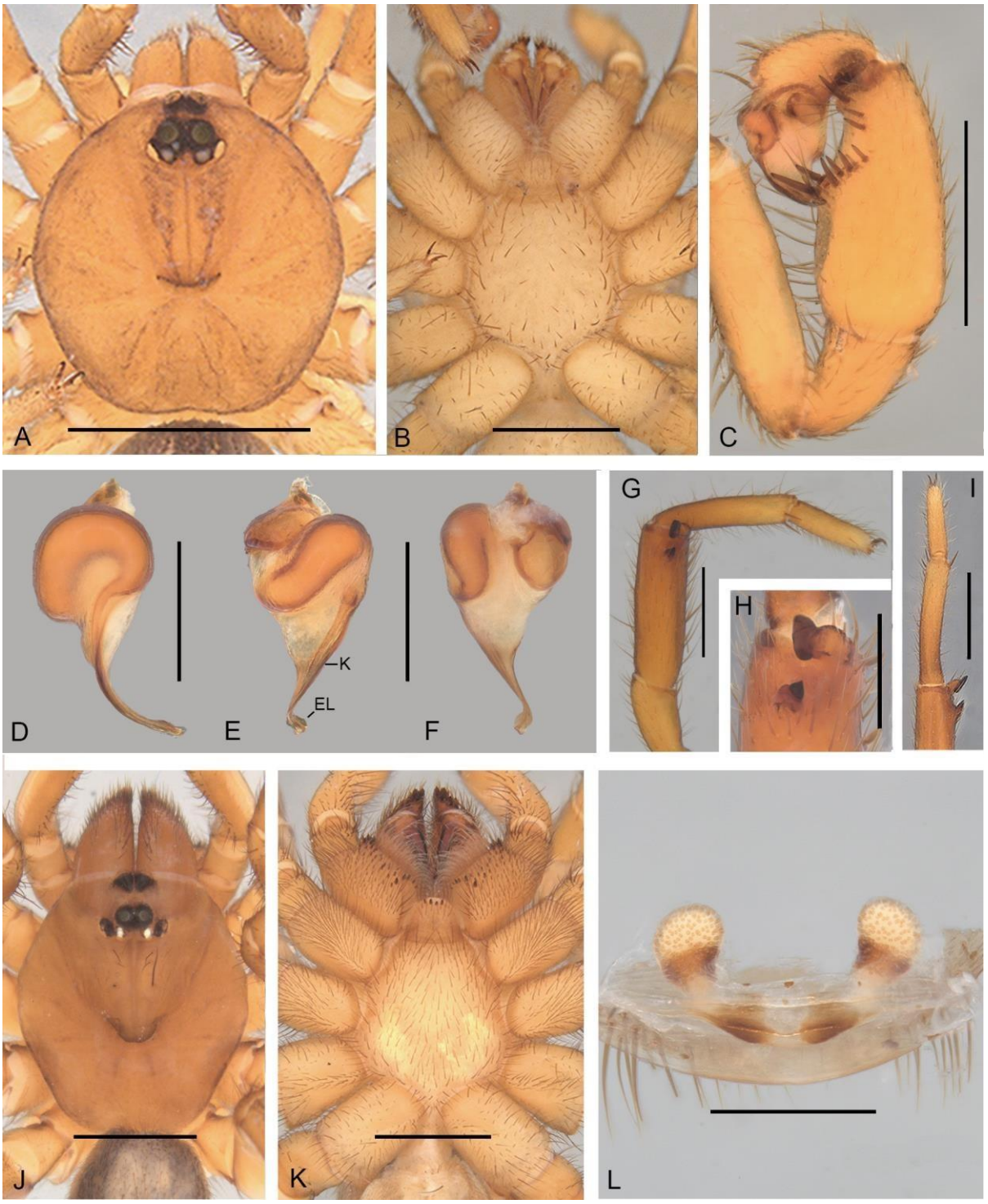

Fig. 20. *Idiops guri* Fonseca-Ferreira, Guadanucci & Brescovit sp. nov. **A–I**. ♂, holotype (MCN 39594). **A**. Prosoma (dorsal view). **B**. Prosoma (ventral view). **C**. Part of palp (retrolateral view). **D–F**. Palpal bulb. **D**. Dorsal view. **E**. Retrolateral view. **F**. Prolateral view. **G**. Tibia, metatarsus and tarsus I (prolateral view). **H**. Tibial apophysis (prolateral view). **I**. Tibial apophysis and metatarsus I (dorsal view). **J–L**. ♀ (MCTP 23469). **J**. Prosoma (dorsal view). **K**. Prosoma (ventral view). **L**. Genitalia (dorsal view). Abbreviations: EL = embolar lamella; K = keel. Scale bars: A–G, I–L = 1 mm; H = 0.5mm.

PALP. Tibia with larger spines arranged on basal half of retrolateral depression (Fig. 20C), embolus with keel in retrolateral view, embolus with subapical torsion, followed by lateral lamella close to opening of sperm duct (Figs 20D–F, 21E–F).

PALP AND LEG MEASUREMENTS. Palp = 3.8 (1.2, 0.6, 1.4, 0.6), I = 7.5 (2.2, 1.2, 1.7, 1.4, 1), II = 6.8 (2.2, 1, 1.4, 1.2, 1), III = 6.2 (1.7, 1, 1, 1.5, 1), IV = 8 (1.9, 1, 2, 1.9, 1.2).

SPINATION. Palp: Ti r13. Leg I: Pa v0-0-1, Ti r0-1-2 Mt v0-0-1, p0-0-1, r1-1-2, Ta p0-0-1 r0-1-0. Leg II: Pa v0-0-3, Ti v1-1-3, p0-0-2, Mt v1-1-3, p0-0-1, Ta p0-0-1. Leg III: Pa p1-2-2, Ti v0-0-2, p0-1-1, r0-0-1, Mt v0-1-2, p0-1-2, r0-1-2, d0-1-2. Leg IV: Pa 0-0-1, Ti v1-1-2, p0-0-1, r0-0-1, Mt v0-1-2, p0-0-1, r0-0-2, Ta p0-0-1, r0-0-1.

Female (MCTP 23469)

HABITUS. See Fig. 20J.

MEASUREMENTS. TBL 8.4, CL 4.2, CW 3.7, LL 0.7, LW 0.9, SL 2.5, SW 2.5.

COLOR. Brown carapace and legs, gray abdomen (Fig. 20J–K).

PROSOMA. Carapace and ocular arrangement as shown in Fig. 20J. Eye tubercle: 0.5 long; 0.9 wide. AME-ALE distance 0.7. Eye diameters: AME 0.2, ALE 0.3, PME 0.2, PLE 0.3. Thoracic fovea procurved (Fig. 20J). Labium with 4 cuspules (Fig. 20K). Maxilla with 29 cuspules, distributed over anterior ventral half, with 8 large cuspules at anterior ventral retrolateral end and 5 large cuspules at anterior ventral prolateral end (Fig. 20K). Basal segment of chelicerae with a prolateral row of 5 large teeth. Rastellum with 11–12 thick spines, distals largest.

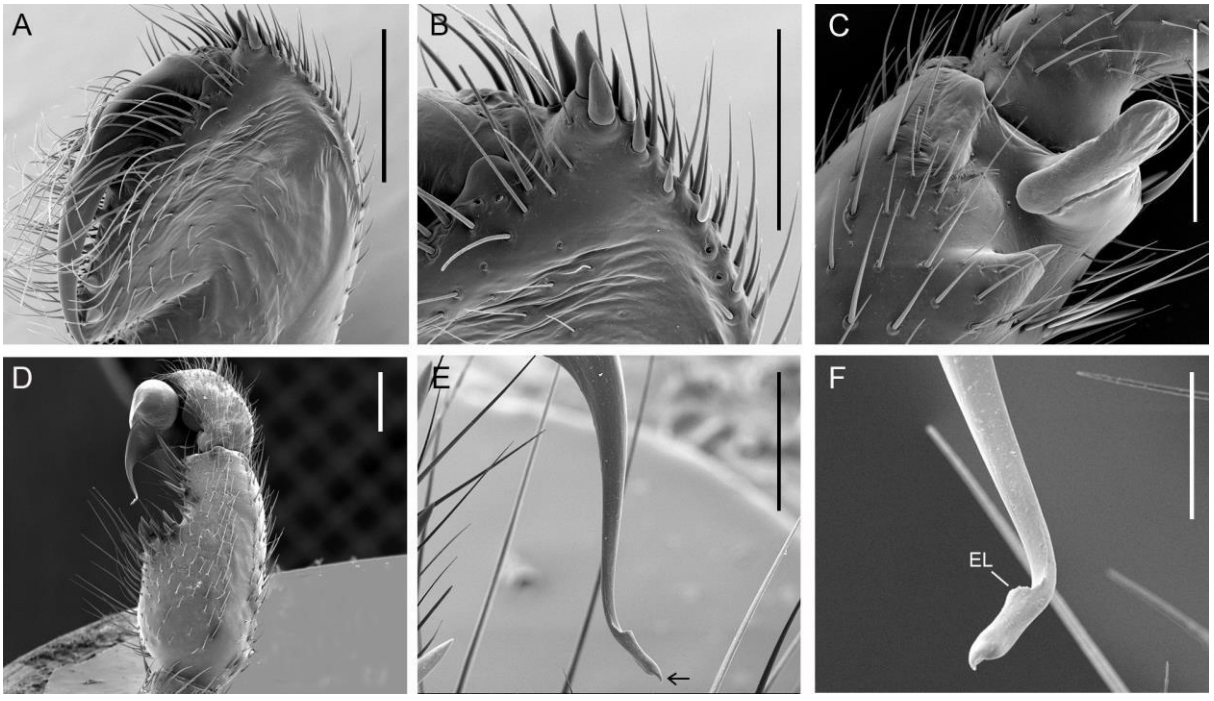

Fig. 21. Scanning electron micrographs of *Idiops guri* Fonseca-Ferreira, Guadanucci & Brescovit sp. nov., ♂ (IBSP 220523). **A**. Chelicera (retrolateral view). **B**. Rastellum (retrolateral view). **C**. Tibial apophysis (dorsal view). **D**. Part of the palp, showing retrolateral depression. **E–F**. Detail of the final portion of the embolus in prolateral view. Abbreviation: EL = embolar lamella. The arrow indicates the hook-shaped projection near the sperm duct. Scale bars: A = 0.4 mm; B, E–F = 0.2 mm; C = 0.3 mm; D = 1 mm.

PALP AND LEG MEASUREMENTS. Palp = 6.9 (2.5, 1.3, 1.5, 1.6), I = 7.7 (2.5, 1.6, 1.8, 1, 0.8), II = 6.6 (2.2, 1.4, 1.2, 1.1, 0.7), III = 7.3 (2, 1.6, 1.2, 1.5, 1), IV = 9.7 (2.6, 2, 1.8, 2, 1.3).

SPINATION. Palp: Ti r5-4-5, p2-4-6, Ta r4-6-6, p7-6-5. Leg I: Mt r3-4-5, p2-3-3, Ta v0-0-3, r5-4-6, p2-4-2. Leg II: Ti r2-3-3, p2-4-2, Mt r6-4-5, p5-5-5, Ta v0-0-3, r3-2-1, p2-4-2. Leg III: Pa p3-5-8, Ti p0-2-3, Mt d2-4-4, v1-2-2, p4-2-1, Ta v0-1-3, p0-2-0. Leg IV: Pa p12-0-0, Ti v1-1-1, Mt v1-2-2, p0-0-1, Ta v0-3-4.

SPERMATHECAE. Duct with translucent median portion and receptacle with evident granules and medial half slightly expanded (Fig. 20L).

Distribution

Brazil. Found mainly in Atlantic Forest phytophysiognomies, with records for the South region (Paraná, Santa Catarina and Rio Grande do Sul) (Fig. 3C).

Idiops harti (Pocock, 1893)
Figs 4B, 5C, 22

Pseudidiops harti Pocock, 1893: 407, pl. 19, figs 1–3.

Idiops harti – Raven 1985: 158.

Diagnosis

The female of *Idiops harti* differs from that of other species of the genus by having the spermathecae with short ducts (same length as the diameter of the receptacula) and a well-marked division between them, by having the receptacula shaped like a bean (Fig. 22) and by having only an internal row of large teeth on the chelicera (Fig. 5C).

Type material

Holotype

TRINIDAD AND TOBAGO • ♀; Trinidad; J.H. Hart leg.; BMNH 1893.3.25.1.

Description

Male

Unknown.

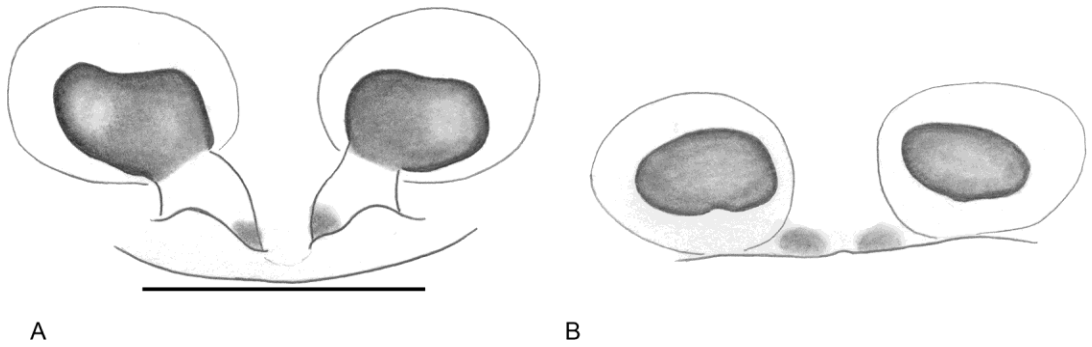

Fig. 22. *Idiops harti* (Pocock, 1893), ♀, genitalia, holotype (BMNH 1893.3.25.1). **A**. Dorsal view. **B**. Frontal view. Scale bar = 1 mm.

Female (holotype BMNH 1893.3.25.1)

MEASUREMENTS. TBL 18.8, CL 12.2, CW 9.8, LL 0.8, LW 1.3, SL 5.8, SW 5.6.

COLOR. Carapace and legs light brown. Abdomen brown.

PROSOMA. Eye tubercle: 1.7 long; 1.1 wide. AME-ALE distance 0.7. Eye diameters: AME 0.44, ALE 0.4, PME 0.3, PLE 0.4. Thoracic fovea procurved with 7 cuspules. Maxilla with 104 cuspules, distributed through ventral area. Basal segment of chelicerae with a prolateral row of 6 large teeth and one small retrolateral tooth (Fig. 4C).

PALP AND LEG MEASUREMENTS. Palp = 10.6 (3.6, 2.4, 2.3, 2.3), I = 12.8 (4.3, 2.8, 2.9, 1.9, 0.9), II = 11.5 (3.9, 2.5, 2.3, 1.8, 1), III = 8.6 (2.4, 1.9, 1.5, 1.8, 1), IV = 15.8 (4.5, 2.9, 3.5, 3.3, 1.6).

SPINATION. Palp: Fe p0-0-2, Pa p0-1-1, Ti p6-5-9, r3-6-8, Ta p8-6-9, r9-8-7. Leg I: Ti p3-3-8, r3-5-6, Mt p6-4-4, r5-5-3, Ta p3-1-1, r1-2-1. Leg II: Ti p3-4-6, r1-1-3, Mt p6-5-6, r2-2-4, Ta p2-3-1, r2-2-1. Leg III: Fe d0-0-1, Pa p3-5-9, r0-1-0, Ti v0-0-2, p2-4-7, Mt v0-0-2, p2-1-3, r1-2-1. Leg IV: Pa p0-0-1, Ti v1-1-2, r1-1-1, Mt v1-2-1-3.

SPERMATHECAE. Short ducts, receptacula wider than long (Fig. 22A).

Distribution

Trinidad and Tobago. Known only from the type locality (Fig. 3B).

Idiops mocambo Fonseca-Ferreira, Guadanucci & Brescovit sp. nov.

urn:lsid:zoobank.org:act:9A7CB56E-31BD-4122-81D0-D514069399D6

Figs 3B, 23A–I

Diagnosis

The male of *Idiops mocambo* sp. nov. differs from other Neotropical species by anterior region of the carapace in a pointed shape (Fig. 23A), sternum with distinct black edges (Fig. 23B) and by the apical branch of the tibial apophysis in rectangular shape (Fig. 23G–H).

Etymology

The specific epithet refers to the location where the holotype specimen was collected.

Type material

Holotype

BRAZIL – **Pará** • ♂; Belém, Mocambo; 1°27′21″ S, 48°30′14″ W; 4 Nov. 2002; A.B. Bonaldo leg.; MPEG 0110.

Paratype

BRAZIL – **Amazonas** • 1 ♂; Manaus, Reserva Florestal Adolpho Ducke; 3°0′27″ S, 59°56′22.92″ W; 9 Sep. 1991; H. Höfer and T. Gasnier leg.; INPA 4593.

Other material examined

BRAZIL – **Amazonas** • 1 ♂; Road Am-010, Km 54; 3°3′45″ S, 59°59′19″ W; 6–10 Nov. 1997; J. Vidal *et al.* leg.; INPA 4594. – **Pará** • 1 ♂; Barcarena; 1°30′21″ S, 48°37′33″ W; MPEG 1106.

Description

Male (holotype MPEG 0110)

HABITUS. See Fig. 23A.

MEASUREMENTS. TBL 7.9, CL 3.8, CW 3, LL 0.5, LW 0.7, SL 1.9, SW 1.7.

COLOR. Brown carapace and legs, except for coxae and trochanters, which are light brown (Fig. 23A–B).

PROSOMA. Carapace and ocular arrangement as shown in Fig. 23A. Eye tubercle: 0.5 long; 0.9 wide. AME-ALE distance 0.5. Eye diameters: AME 0.2, ALE 0.3, PME 0.2, PLE 0.2. Thoracic fovea procurved (Fig. 23A). Labium and sternum without cuspules (Fig. 23B). Basal segment of chelicerae with a prolateral row of 5 large teeth and 2 small retrolateral teeth, grouped on basal half, rastellum with 16–18 short and thick spines.

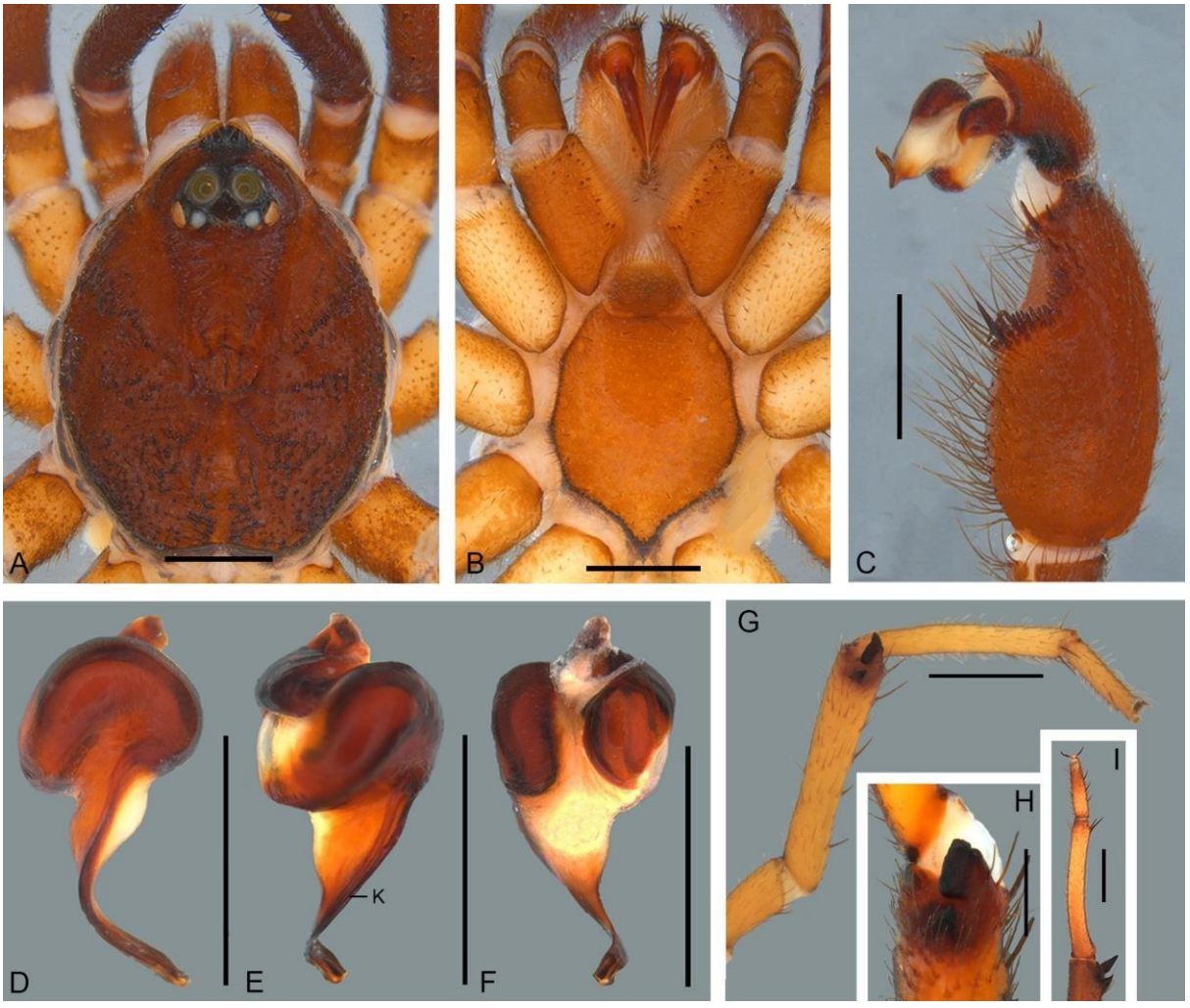

Fig. 23. *Idiops mocambo* Fonseca-Ferreira, Guadanucci & Brescovit sp. nov., ♂, holotype (MPEG 0110). **A**. Prosoma (dorsal view). **B**. Prosoma (ventral view). **C**. Part of palp (retrolateral view). **D–F**. Palpal bulb. **D**. Dorsal view. **E**. Retrolateral view. **F**. Prolateral view. **G**. Tibia, metatarsus and tarsus I (prolateral view). **H**. Tibial apophysis (prolateral view). **I**. Tibial apophysis and metatarsus I (dorsal view). Abbreviation: K = keel. Abbreviation: K = keel. Scale bars: A–G, I = 1 mm; H = 0.5 mm.

LEGS. Tibia, metatarsus and tarsus I as shown in Fig. 23G. Leg I with double tibial apophysis, apical branch twice the size of basal branch (Fig. 23G–I). Pseudoscopula: tarsus I–IV totally covered.

PALP. Tibia with spines distributed along margin of retrolateral depression, with large spines at apical and basal ends (Fig. 23C); embolus with lamelliform apical half, keel in retrolateral view and torsion close to sperm duct opening (Fig. 23D–F).

PALP AND LEG MEASUREMENTS. Palp = 7.1 (2.5, 1, 2.6, 1), I = 11.7 (3.4, 1.9, 2.6, 2.6, 1.2), II = 10.3 (2.8, 1.5, 2.3, 2.5, 1.2), III = 9.8 (2.6, 1.4, 1.9, 2.6, 1.3), IV = 12.6 (3.2, 1.8, 3, 3.2, 1.4).

SPINATION. Palp: Ti r25, Ta 0-0-1. Leg I: Pa v0-0-2, Ti v0-0-2, r1-2-3, Mt p0-0-1, r2-2-2, Ta p1-1-1, r1-1-1. Leg II: Ti v2-2-3, Mt v3-3-3, r1-1-2, Ta p0-2-0, r1-1-0. Leg III: Ti v0-2-3, Mt v1-2-4, p1-3-4, Ta p0-2-1. Leg IV: Ti v1-1-3, Mt v1-2-4, p1-3-6, Ta p1-1-1.

Distribution

Brazil. Distributed in phytophysiognomies in the Amazon, with records for the North region (eastern Amazonas and Pará) (Fig. 3B).

Idiops nilopolensis Mello-Leitão, 1923
Figs 3D, 24A–L

Idiops nilopolensis Mello-Leitão, 1923: 47.

Idiops nilopolensis – Bücherl *et al.* 1971: 121, figs 6–7. — Fukami & Lucas 2005: 7.

Diagnosis

Males of *Idiops nilopolensis* differ from those of other Neotropical species by the strong curvature of the median portion of the embolus in dorsal view (Fig. 24D–F; also present in *I. fuscus*). Differs from *I. fuscus* by having the embolus with a thickened basal half and by the small embolar lamella (smaller than in *I. fuscus*) close to spermatic duct opening (Fig. 24D–F). The female differs from those of other species by having the spermathecae with a translucent duct and without constriction between the duct and the sclerotized receptacles (Fig. 24L).

Type material

Holotype

BRAZIL – **Rio de Janeiro** • ♀; Rio de Janeiro; Nov. 1923; H. Blanc de Freitas leg.; MNRJ 10. Lost before the 2018 fire (Moreira *et al.* 2010: 34).

Neotype (here designated)

BRAZIL– **Rio de Janeiro** • ♂; Nova Iguaçu, Parque Municipal de Nova Iguaçu; 22°45′35″ S, 43°27′6″ W; 21 Jul. 2004; R. Baptista leg.; MNRJ.

Remark: The type specimen of *Idiops nilopolensis* was lost in the MNRJ long before the 2018 fire. In accordance with the criteria of the ICZN Code (ICZN 1999), a neotype is designated here, because the type is lost and the original description is inadequate to stabilise the species. This neotype is based ona specimen collected near the type locality, in the state of Rio de Janeiro, Brazil.

Other material examined

BRAZIL – **Rio de Janeiro** • 1 ♀; same locality as for neotype; 1 Nov. 2004; MNRJ.

Description

Male (neotype MNRJ)
HABITUS. See Fig. 24A.

MEASUREMENTS. TBL 16.9, CL 7.3, CW 6.4, LL 0.6, LW 1.2, SL 3.9, SW 3.5.

COLOR. Body uniformely light brown (Fig. 24A–B).

PROSOMA. Carapace and ocular arrangement as shown in Fig. 24A. Eye tubercle: 0.8 long; 1 wide. AME-ALE distance 0.9. Eye diameters: AME 0.4, ALE 0.4, PME 0.2, PLE 0.4. Thoracic fovea procurved (Fig. 24A). Labium and sternum without cuspules (Fig. 24B). Basal segment of chelicerae with a prolateral row of 7 large teeth and 3 small retrolateral teeth, grouped on basal half, rastellum with 16–18 spines, the distal ones longer.

LEGS. Tibia, metatarsus and tarsus I as shown in Fig. 20G. Leg I with double tibial apophysis. Apical branch twice the size of basal branch and with a conspicuous spine (Fig. 24H–I). Pseudoscopula: tarsus I–IV totally covered.

PALP. Tibia with retrolateral conspicuous depression and spines concentrated at basal and apical portions (Fig. 24C); embolus with basal torsion and opening of sperm duct in shape of a quill tip (Fig. 24D–E).

PALP AND LEG MEASUREMENTS. Palp = 11.8 (4.3, 2.2, 3.8, 1.5), I = 28.4 (8.5, 3.8, 6.6, 6.7, 2.8), II = 26.9 (7.8, 3.4, 6, 6.3, 3.1), III = 23.7 (6.1, 3.3, 4.3, 6.4, 3.6), IV = 32.6 (8.4, 3.7, 7.9, 8.6, 4).

SPINATION. Palp: Ti r20, Ta d0-0-1. Leg I: Mt p0-0-2, r2-2-4, Ta p2-2-2, r3-3-4. Leg II: Mt p0-0-2, r0-3-3, Ta p2-3-3, r3-4-5. Leg III: Fe d2-1-1, Pa p2-4-5, Ti d2-2-1, v1-2-2, p4-4-6, Mt d2-2-5, v3-4-5, p3-4-6, r2-2-4, Ta p3-4-2, r3-3-6. Leg IV: Ti v1-2-3, p0-0-1, Mt v2-4-6, p1-2-4, Ta p1-4-6.

Female (MNRJ)
HABITUS. See Fig. 24J.

MEASUREMENTS. TBL 15.7, CL 6.2, CW 5.7, LL 0.9, LW 1.3, SL 3.9, SW 3.4.

COLOR. Brown carapace and legs, brownish sternum and coxae (Fig. 24J–K), gray abdomen.

PROSOMA. Carapace and ocular arrangement as shown in Fig. 24J. Eye tubercle: 1.2 long; 0.8 wide. AME-ALE distance 1. Eye diameters: AME 0.2, ALE 0.3, PME 0.2, PLE 0.4. Thoracic fovea procurved (Fig. 24J). Labium with 2 cuspules (Fig. 24K). Maxilla with 48 cuspules, distributed over anterior ventral half, with 6 large cuspules at anterior ventral retrolateral end and 6 large cuspules at anterior ventral prolateral end (Fig. 24K). Basal segment of chelicerae with a prolateral row of 7 large teeth and 5 small retrolateral teeth, grouped on basal half, rastellum with 22 short and thick spines (Fig. 24K).

PALP AND LEG MEASUREMENTS. Palp = 11.4 (4, 2.4, 2.4, 2.6), I = 12.2 (3.7, 2.8, 2.6, 1.7, 1.4), II = 11.4 (3.6, 2.5, 2.3, 1.6, 1.4), III = 13.6 (4.1, 2.5, 2.2, 2.1, 2.7), IV = 15.7 (4.4, 3.1, 3.1, 3.2, 1.9).

SPINATION. Palp: Ti p4-10-12, r4-6-8, Ta p6-8-7, r10-13-9. Leg I: Ti v0-2-2, p4-5-6, r1-3-9, Mt v2-2-3, p6-6-9, r4-3-5, Ta v0-0-3, p2-3-3, r4-3-5. Leg II: Fe v0-0-2, Pa v0-0-1, Ti v1-1-2, p4-5-6, r0-0-1, Mt v1-2-1, p4-6-9, r1-2-1, Ta v0-1-3, p4-4-4, r4-4-2. Leg III: Pa d0-0-2, Ti p2-3-2, r0-0-3, Mt v0-0-1, r3-1-1, 4-4-3, Ta v0-4-3, p0-2-3. Leg IV: Fe d0-0-2, v0-0-3, Ti v1-1-3, Mt v3-4-6, p1-2-3, Ta v3-3-4, p1-2-3.

SPERMATHECAE. Short and narrow sclerotized base, ducts with same width as receptacles (Fig. 24L).

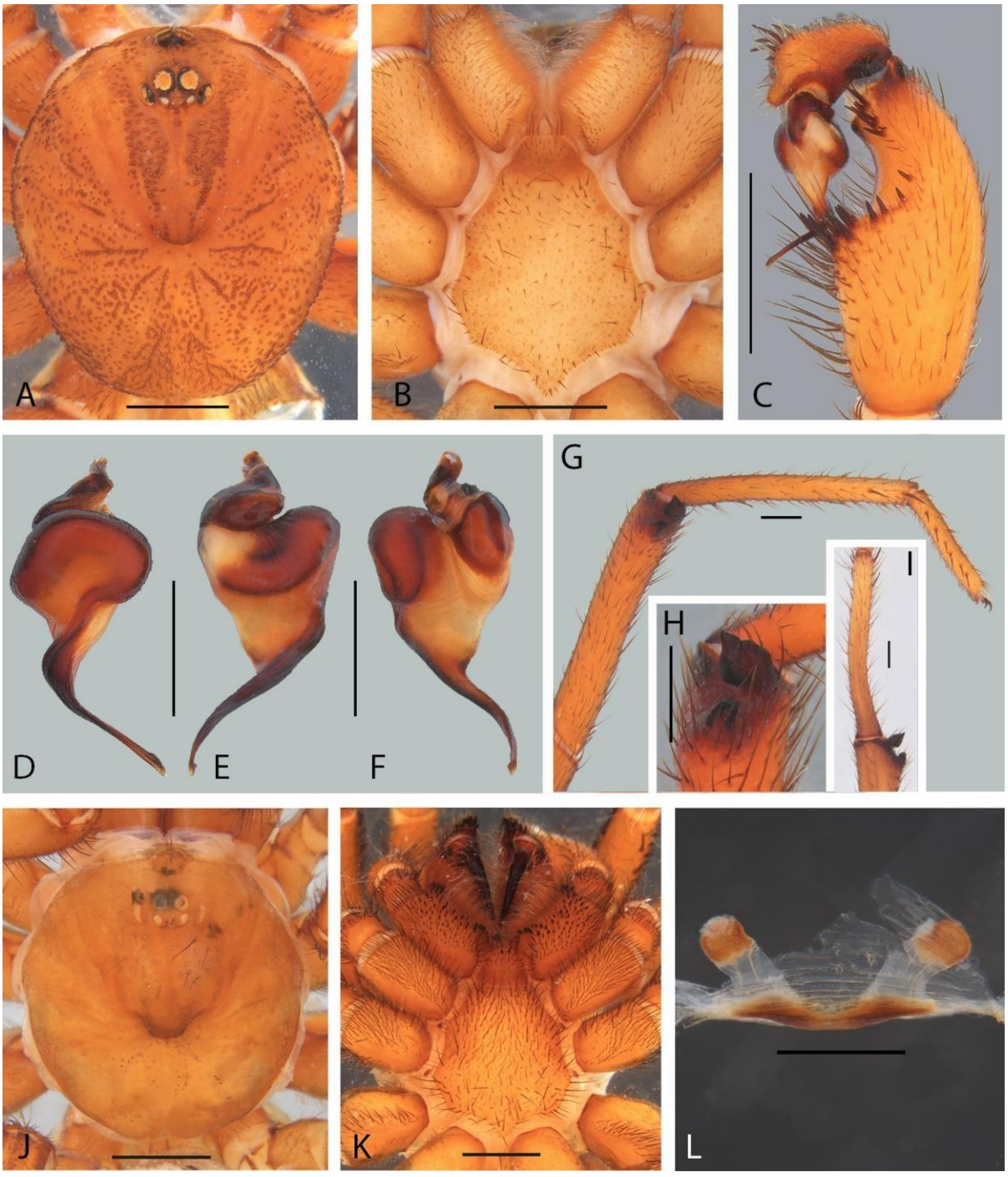

Fig. 24. *Idiops nilopolensis* Mello-Leitão, 1923. **A–I**. ♂, neotype (MRNJ). **A**. Prosoma (dorsal view). **B**. Prosoma (ventral view). **C**. Part of palp (retrolateral view). **D–F**. Palpal bulb. **D**. Dorsal view. **E**. Retrolateral view. **F**. Prolateral view. **G**. Tibia, metatarsus and tarsus I (prolateral view). **H**. Tibial apophysis (prolateral view). **I**. Tibial apophysis and metatarsus I (dorsal view). **J–L**. ♀, (MNRJ). **J**. Prosoma (dorsal view). **K**. Prosoma (ventral view). **L**. Genitalia (dorsal view). Scale bars: A–B, D–L = 1 mm; C = 2 mm.

Distribution

Brazil. Found in Atlantic Forest phytophysiognomie in the state of Rio de Janeiro (Fig. 3D).

Idiops opifex (Simon, 1889)
Figs 4B, 25

Pseudidiops opifex Simon, 1889: 215, pl. 1 fig. 3.

Idiops opifex – Raven 1985: 139. — Dupérré & Tapia 2021: 274, figs 16a–b, 17a–b.

Diagnosis

The female of *Idiops opifex* differs from that of all other Neotropical species of the genus, except *I. rastratus* and *I. duocordibus* sp. nov., by presenting cuspules on the entire maxillae ventral face. Differs from *I. rastratus* by the non-sclerotized spermathecae base (Fig. 25A) and from *I. duocordibus* sp. nov. by the spherical receptacula (Fig. 25).

Type material

Holotype

FRENCH GUIANA • ♀; Cayenne; MNHN 5340. The holotype is damaged, apparently smashed.

Description

Male

Unknown.

Female (holotype MNHN 5340)

Measurements. TBL 11, CL 5.4, CW 5.2, LL 0.9, LW 1.3, SL 2.9, SW 3.3.

COLOR. Carapace and legs brown. Abdomen dark gray.

PROSOMA. Eye tubercle: 1.7 long; 1.8 wide. AME-ALE distance 1. Eye diameters: AME 0.3, ALE 0.3, PME 0.2, PLE 0.4. Thoracic fovea procurved. Labium with 23 cuspules. Sternum destroyed. Maxilla with 160 cuspules, distributed through ventral area. Basal segment of chelicerae with a prolateral row of 5 large teeth and 4 small retrolateral basal teeth.

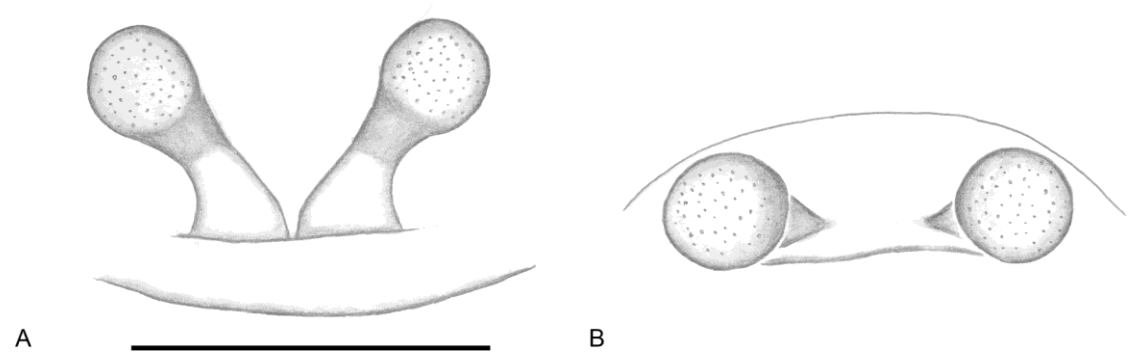

Fig. 25. *Idiops opifex* (Simon, 1889), ♀, genitalia, holotype (MNHN 5340). **A**. Dorsal view. **B**. Frontal view. Scale bar = 1 mm.

PALP AND LEG MEASUREMENTS. Palp = 10.6 (3.6, 2.3, 2.5, 2.2), I = 11.6 (3.8, 2.7, 2.6, 1.8, 0.7), II = 10 (3.4, 2.4, 2, 1.6, 0.6), III = 10.7 (3.3, 2.4, 1.8, 2, 1.2), IV = 14.1 (4.4, 2.8, 3, 3.7, 1.2).

SPINATION. Palp: Fe p0-0-3, Pa p0-1-0, Ti p7-9-9, Ta v0-0-2, p11-10-8, r12-9-7. Leg I: Ti p5-7-11, r4-4-5, Mt p9-7-6, r9-5-6, Ta v0-0-3, p5-2-1, r5-2-0. Leg II: Pa r0-0-1, Ti p3-5-5, r2-3-3, Mt p10-9-5, r5-4-3, Ta p3-3-1, r3-1-0. Leg III: Pa p2-3-9, r0-0-1, Ti v0-0-2, p4-4-10, r3-4-8, Mt v0-0-2, p4-4-6, r2-0-0, Ta v0-0-6. Leg IV: Pa p8-2-0, Mt v1-1-1-3, Ta v0-0-6.

SPERMATHECAE. Duct length similar to diameter of spherical receptacles, close to each other, with basal half thicker than apical half and with sclerotization at transition between duct and receptacle (Fig. 25).

Distribution

French Guyana. Know only from type locality (Fig. 4B).

Idiops petiti (Guérin, 1838)
Figs 3B, 26

Acanthodon petitii Guérin, 1838: 163, pl. 47 figs 1–8.
Acanthodon santaremia O. Pickard-Cambridge, 1896: 733, pl. 34 fig. 13. **Syn**. **Nov**.
Idiops crulsi Mello-Leitão, 1930: 55, fig. 2. Synonymized by Bücherl *et al.* 1971: 128.

Idiops petiti – O. Pickard-Cambridge 1870: 107; 1896: 732, pl. 34 figs 9–12. — Mello-Leitão 1923: 48. — Bücherl *et al.* 1971: 121, fig. 5.
Idiops santaremius – Petrunkevitch 1911: 73.

Diagnosis

The male of *Idiops petiti* differs from that of other Neotropical species, except *I. carajas*, by having the palpal tibia with spines concentrated in the basal half of the retrolateral depression (Fig. 26C), the tibial apophysis with a narrow apical branch and rectangular in shape (Fig. 26G–H) and by the presence of a lateral lamella that extends along the median portion of the embolus (Fig. 26E–F). Differs from *I. carajas* by having the subapical portion of the embolus thin and straight (Fig. 26E–F) and the metatarsus of the leg I slightly curved and with a small prolateral projection on the apical half (Figs 26I). Females are distinguished from congeners, except *I. carajas*, by having the spermathecae with a large sclerotized trapezoidal base and V-shapedducts (Fig. 26L). Differs from *I. carajas* by its largeoval-shaped receptacula (Fig. 26L).

Type material

Holotype of *Acanthodon petitii* Guérin, 1838
BRAZIL – **Pará** • ♀; Santarém; BMNH 1890.7.1.320.

Holotype of *Acanthodon santaremia* O. Pickard-Cambridge, 1896
BRAZIL – **Pará** • juv.; Santarém; Mar. 1896; O. P.-Cambridge leg.; BMNH 1896.12.13.66.

Holotype of *Idiops crulsi* Mello-Leitão, 1930
BRAZIL – **Pará** • ♀; Oriximná, Rio Cuminá; G. Cruls leg.; MNRJ 0007. Lost in the fire of 2018.

The type specimen of *Idiops petiti* was originally deposited in a dry collection and subsequently rehydrated and stored in alcohol. Although clearly an adult female, the specimen has lost many legs and the spermathecae, because the abdomen was stuffed with cotton. This prevented a more detailed description. The type specimen of *I. santaremius* was examined and recognized as a juvenile of *I. petiti*.

Other material examined

BRAZIL – **Amazonas** • 2 ♂♂; Manaus, Fazenda Esteio; 2°23′3.00″ S, 59°51′15.00″ W; 6 Nov.1985; B.C. Klein leg.; INPA4590 to 4591 • 1 ♂; Benjamin Constant; 4°22′58″ S, 70°1′51″ W; 2014; P.S. Pompeu leg.; IBSP 243961 • 1 ♂; Jutaí, near the Rio Jutaí; 5º38′21.7″ S, 69º10′58.8″ W; 14–19 Mar. 2006; M.S. Hoogmoed leg.; MPEG 2579. – **Pará** • 2 ♂♂; Belterra, Flona Tapajós, Km 83; 3°31′1″ S, 55°4′23″ W; 2010; J.L. Freitas leg.; IBSP 218829, IBSP 218868 • 1 ♂; Almeirim, Jari; 1°1′33.122″ S, 52°34′2.785″ W; MPEG 7588 • 1 ♂; Senador José Porfirio; Trilha do Censo, Margem Direita, Rio Xingu; 2°35′27″ S, 51°57′14″ W; 25 Feb. 2001; MPEG 0113 • 1 ♂; Senador José Porfirio; Trilha do Acampamento, Margem Direita, Rio Xingu; 25 Feb. 2001; MPEG 0116 • 1 ♂; Jacareacanga, UHN de São Manoel; 9°13′32″ S, 56°59′56″ W; 16 Feb. 2009; W.U. Prado leg.; UFMG 3205 • 1 ♂; Jacareacanga; 21 Feb. 2009; W.U. Prado leg.; UFMG 3206. – **Rondônia** • 1 ♀; Monte Negro, LC25, Km 10; 10°14′49″ S, 63°24′16.8″ W; 19 Dec. 2013; P.H. Martins leg.; UFMG 24031.

Description

Male (MPEG 0116)

HABITUS. See Fig. 26A.

MEASUREMENTS. TBL 17.2, CL 7.4, CW 6.7, LL 0.9, LW 1.4, SL 4, SW 3.6.

COLOR. Carapace and legs reddish brown, with yellowish coxae, brownish sternum; abdomen grey (Fig. 26A–B)

PROSOMA. Carapace and ocular arrangement as shown in Fig. 26A. Eye tubercle: 0.7 long; 1.3 wide. AME-ALE distance 0.9. Eye diameters: AME 0.4, ALE 0.4, PME 0.2, PLE 0.4. Thoracic fovea procurved (Fig. 26A). Labium and sternum without cuspules (Fig. 26B). Basal segment of chelicerae with a prolateral row of 8 large teeth and 4 small retrolateral teeth, grouped in basal half, rastellum presenting 12–13 spines of same size.

LEGS. Tibia, metatarsus and tarsus I as shown in Fig. 26G. Leg I with double tibial apophysis. Apical branch twice the size of basal branch and with a conspicuous spine (Fig. 26H–I). Pseudoscopula: tarsus I–IV totally covered.

PALP. Elongated palpal bulb with slightly curved embolus and without torsion of subapical portion (Fig. 26D–F).

PALP AND LEG MEASUREMENTS. Palp = 12 (3.8, 3.3, 3.21, 1.7), I = 22 (6.8, 3.5, 5.1, 4.8, 1.8), II = 18.9 (6, 3, 4.4, 3.8, 1.7), III = 17 (4.7, 2.9, 3, 4.3, 2.1), IV = 24.2 (6.9, 3.6, 5.9, 5.1, 2.7).

SPINATION. Palp: Ti r19, Ta d0-0-4. Leg I: Fe d1-2-1, Pa v0-1-5, Ti v10-15-16, p0-1-0, Mt v6-8-14, p0-0-5, r0-0-4, Ta p3-4-4, r5-6-6. Leg II: Fe d1-2-1, Pa p0-0-2, Ti v5-7-12, p2-2-9, r1-2-4, Mt v6-6-7, p3-5-10, r3-3-4, Ta p4-4-4, r6-6-7. Leg III: Fe d1-2-1, Ti p2-3-6, Mt r6-3-8, Ta p5-8-8, r2-4-7. Leg IV: Fe d1-2-1, Ti v1-2-3, r0-1-2, Mt v1-3-3, p1-2-5, r0-3-5, Ta p5-5-8, r5-5-8.

Female (UFMG 24031)

HABITUS. See Fig. 26J.

MEASUREMENTS. TBL 13, CL 5.8, CW 4.9, LL 0.8, LW 2, SL 3.5, SW 3.5.

COLOR. Carapace and legs brown, light brown sternum (Fig. 22J–K). Abdomen grey.

PROSOMA. Carapace and ocular arrangement as shown in Fig. 26J. Eye tubercle: 0.6 long; 1 wide. AME-ALE distance 0.8. Eye diameters: AME 0.2, ALE 0.3, PME 0.2, PLE 0.4. Thoracic fovea procurved (Fig. J). Labium with 3 cuspules (Fig. 26K). Maxilla with 30 cuspules, distributed throughout anterior ventral half (Fig. 26K). Basal segment of chelicerae with a prolateral row of 7 large teeth and 4 small

Fig. 26. *Idiops petiti* (Guérin, 1838). **A–I**. ♂ (MPEG 0116). **A**. Prosoma (dorsal view). **B**. Prosoma (ventral view). **C**. Part of palp (retrolateral view). **D–F**. Palpal bulb. **D**. Dorsal view. **E**. Retrolateral view. **F**. Prolateral view. **G**. Tibia, metatarsus and tarsus I (prolateral view). **H**. Tibial apophysis (prolateral view). **I**. Tibial apophysis and metatarsus I (dorsal view). **J–L**. ♀ (UFMG 24031). **J**. Prosoma (dorsal view). **K**. Prosoma (ventral view). **L**. Genitalia (dorsal view). Scale bars = 1 mm.

retrolateral teeth, grouped in basal half. Rastellum well developed, presenting 14–16 robust spines (Fig. 26K).

PALP AND LEG MEASUREMENTS. Palp = 9.6 (3, 2, 2.2, 2.4), I = 10.2 (2.8, 2.2, 2.3, 1.7, 1.2), II = 10.2 (3.3, 2.2, 2, 1.3, 1.4), III = 11.3 (3, 2.3, 2, 2.3, 1.7), IV = 15.2 (4, 3, 3.2, 2.9, 2.1).

SPINATION. Palp: Ti p5-6-9, r6-8-12, Ta p6-7-8, r8-8-9. Leg I: Pa v0-0-2, Ti v1-2-1, p4-6-9, r4-6-11, Mt v2-1-1, p8-6-8, r10-3-4, Ta v0-0-1, p3-4-4, r4-3-2. Leg II: Ti v1-1-1, p3-7-7, r0-1-2, Mt v1-1-1, p7-5-4, r1-2-2, Ta v0-1-1, p4-4-3, r2-2-1. Leg III: Fe d0-0-1, Pa d0-0-1, p4-5-8, r0-0-1, Ti v0-1-2, p3-4-5, r0-1-4, Mt v2-1-2, p2-3-2, r2-2-1, Ta v1-2-3, p0-0-3. Leg IV: Fe d0-0-1, Pa p12-4-2, Ti v1-1-2, Mt v2-3-5, p0-1-2, Ta v1-2-3, p0-3-6.

SPERMATHECAE. Ducts with weakly sclerotized basal half and thickened and sclerotized apical half; asymmetric receptacula, with expansion of medial half (Fig. 26L).

Distribution

Brazil. Widely distributed in the Amazon region, with records for the North region (Amazonas, Pará and Rondônia) (Fig. 3B).

Idiops pirassununguensis Fukami & Lucas, 2005
Figs 2E–F, 4C, 6G, 27–28

Idiops pirassununguensis Fukami & Lucas, 2005: 2, figs 1–5.

Diagnosis

Males of *Idiops pirassununguensis* differ from those of other Neotropical species by having the tibial apophysis with a robust apical branch and a prominent spine in prolateral view (Figs 27H–I, 28C), metatarsus I long with a prolateral projection on the apical half (Fig. 27I) and the embolus with a prominent lamella that expands along the apical half, with a constriction near the sperm duct opening (Figs 27D–F, 28E–F). Females differ by having the spermathecae with long vertical ducts, and strong sclerotization on the transition between duct and receptacula, with the same diameter as ducts (Fig. 27L).

Type material

Holotype

BRAZIL – **São Paulo** • ♂; Pirassununga; Nov. 1997; P. Valdujo leg.; IBSP 9565.

Other material examined

BRAZIL – **Amapá** • 7 ♂♂; Mazagão; 0°6′54″ S, 51°17′20″ W; 3 Dec. 2003; R.A. da Silva leg.; MCTP 16519. – **Amazonas** • 2 ♂♂; Manaus, PAE Lago Grande; 3°3′45″ S, 59°59′19″ W; 2–7 Jul. 2007; Projeto Geoma 2 leg.; INPA 6914, INPA 6916 • 1 ♀; Manaus, PAE Lago Grande; 5 May 2007; A.L. Tourinho and R. Saturnino leg.; INPA 6915. – **Pará** • 1 ♂; Parauapebas; 6°4′4″ S, 49°54′7″ W; Sep. 2008; C.A.R. Souza leg.; IBSP 225254. – **Rondônia** • 1 ♂; Pimenta Bueno; 11°40′21″ S, 61°11′37″W; Jul. 2000; L. Carvalho leg.; IBSP 13335 • 2 ♂♂; same collection data as for preceding; IBSP 13337 • 4 ♂♂; Vilhena; 12°44′26″ S, 60°8′45″ W; Sep. 1999; L. Carvalho leg.; IBSP 14400 • 2 ♂♂; same collection data as for preceding; IBSP 14401, IBSP 14403 • 2 ♂♂; same collection data as for preceding; IBSP 14402. – **Maranhão** • 1 ♂; Caxias, Área de Proteção Ambiental Municipal do Inhamum; 04°53′30″ S, 43°24′53″ W; 2–5 Oct. 2007; Lima-Lobato leg.; IBSP 130947 • 1 ♂; same collection data as for preceding; IBSP 129120. – **Goiás** • 2 ♂♂ (SEM); Caldas Novas, UHE Corumbá; 17°42′50″ S, 48°32′22″ W; 12–23 Aug. 1996; M.T.I. Rodrigues *et al*. leg.; MZSP 15651. – **Piauí** • 5 ♂♂; Alvorada do Gurguéia, Fazenda

Escola UFPI; 8°22′11.5″ S, 43°51′30.2″ W; 4–12 Sep. 2018; D.B.S. Barbosa *et al.* leg.; CHNUFPI 2715 • 5 ♂♂; same collection data as for preceding; CHNUFPI 2713 • 12 ♂♂; same collection data as for preceding; CHNUFPI 2714 • 15 ♂♂; same collection data as for preceding; CHNUFPI 2576 to 2590 • 2 ♂♂; Castelo do Piauí, Fazenda Bonito, ECB Rochas Ornamentais do Brasil LTDA; 5°13′59″ S, 41°41′14.5″ W; 11 Dec, 2005; F.M. Oliveira-Neto *et al.* leg.; MPEG 2336 • 2 ♂♂; same collection data as for preceding; MPEG 2339, MPEG 2401 • 1 ♂; Castelo do Piauí, Fazenda Bonito, ECB Rochas Ornamentais do Brasil LTDA; 5º13′47.7″ S, 41°41′36.6″ W; MPEG 2337 • 1 ♂; Castelo do Piauí, Fazenda Bonito, ECB Rochas Ornamentais do Brasil LTDA; 5º14′12.8″ S, 41°41′0.8″ W; MPEG 2338 • 2 ♂♂; Castelo do Piauí, Fazenda Bonito, ECB Rochas Ornamentais do Brasil LTDA; 5°19′19″ S, 41°33′10″; CHNUFPI CASTa0226 • 1 ♂; same collection data as for preceding; CHNUFPI CASTa0225 • 1 ♂; Castelo do Piauí, Fazenda Bonito, ECB Rochas Ornamentais do Brasil LTDA; 5°13′46.7″ S, 41°41′29.9″ W; 25 Oct. 2005; F.M. Oliveira-Neto *et al.* leg.; CHNUFPI 4024 • 2 ♂♂; Castelo do Piauí, Fazenda Bonito, ECB Rochas Ornamentais do Brasil LTDA; 5°13′59″ S, 41°41′14.5″ W; 8 May 2005; F.M. Oliveira-Neto *et al.* leg.; CHNUFPI 4028 • 2 ♂♂; same collection data as for preceding; CHNUFPI 2712 • 3 ♂♂; same collection data as for preceding; CHNUFPI 4025 to 4027 • 1 ♀; Guaribas, Parque Nacional da Serra das Confusões; 9°13′16″ S, 43°29′21″ W; Oct. 2006; P.R.R.Silva *et. al.* leg.; CHNUFPI 4029 • 1 ♂; same collection data as for preceding; CHNUFPI 4030 • 2 ♂♂; Gilbués, Olhos Dágua da Santa, PN Serra das Confusões; MZSP 19974 • 1 ♂; São Raimundo Nonato, Parque Nacional Serra da Capivara; 8°25′0″ S, 42°20′0″ W; 27 Oct.–9 Nov. 2012; R. Recoder and M. Teixeira Jr. leg.; IBSP 167608 • 1 ♂; Uruçuí, Vale do Rio Pratinha, 40 km from Uruçuí; 7°50′08″ S, 44°27′05″ W; M.P.D. Santos *et al.* leg.; CHNUFPI 2711 • 1 ♂; Uruçuí; Fazenda União, Topo da Chapada, 40 km from Uruçuí; 7°41′41″ S, 44°26′30″ W; 26 Oct. 2007; F.M. Oliveira-Neto leg.; CHNUFPI 2710. – **Paraíba** • 5 ♂♂; São José dos Cordeiros, RPPNAlmas; 7°28′45″ S, 36°54′18″ W; 2008–2009; A. Vasconcelos leg.; IBSP 228197, IBSP 228200 to 228201, IBSP 228205, IBSP 228207 • 2 ♂♂; same collection data as for preceding; IBSP 228202 • 2 ♂♂; same collection data as for preceding; IBSP 228199 • 3 ♂♂; same collection data as for preceding; IBSP 228193. – **Sergipe** • 1 ♂; Canindé do São Francisco, Fazenda São José-Olhos D'água, UHE de Xingó; 9°37′25″ S, 37°47′54″ W; 31 Oct. 2000; L. Ianuzzi leg.; IBSP 10183. – **Mato Grosso** • 2 ♂♂; Pontes e Lacerda; 15°19′10.38″ S, 59°17′33.70″ W; 5–10 Oct. 2013; R.A.K. Ribeiro leg.; UFMT • 2 ♂♂; Vila Bela da Santíssima Trindade, Córrego Areias; 14°50′29.9″ S, 69°39′01.2″ W; 2–4 Nov. 2013; R.A.K. Ribeiro leg.; UFMT • 1 ♂; Lucas do Rio Verde, PCH Canoa Quebrada; 12°47′ S, 56°00′ W; V.Azaias leg.; UFMT. – **Minas Gerais** • 1 ♂; Santana do Riacho, Parque Nacional Serra do Cipó; 19°22′1″ S, 43°32′17″ W; Oct. 2004; UFMG 1740 • 2 ♂♂; Santa Luzia; 19°46′12″ S, 43°51′3″ W; 9 Oct. 2004; UFMG 1730, UFMG 1732 • 1 ♂; Santa Luzia, 19º46′43.52″ S, 43º50′26.56″ W; 17 Sep. 2011; B.R.N. Leg keys; UFMG 8471 • 1 ♀; Morro do Pilar; 19º12′56″ S, 43º22′34″ W; 6 Aug. 2011; P.H. Martins leg.; UFMG 11296 • 1 ♀; Morro do Pilar; 19º12′56″ S, 43º22′34″ W; 29 Jul. 2011; P.H. Martins leg.; UFMG 11297 • 1 ♀; Santana do Riacho; 19º10′8″ S, 43º42′57″ W; 9 Jul. 2011; P.H. Martins leg.; UFMG 11264 • 2 ♂♂, 1 ♀; Santana do Riacho, Parque Nacional Serra do Cipó; 19°21′06.8″ S, 43°36′38.8″ W; 17–21 Oct. 2018; R.F. Ferreira, A. Galleti, P.H. Martins and V. Ghirotto leg.; CAD 833 • 1 ♀; Diamantina, Campus JK; 18°14′56″ S, 43°36′0″ W; 7 Mar. 2010; W.F. Silva leg.; CAD 27 • 1 ♂; São Gonçalo do Rio Preto, Parque Estadual do Rio Preto; 18°10′29.97″ S, 43°20′41.25″ W; 20–25 Oct. 2010; G. Monteiro, F. Sá, W.F. Silva and J.P.L. Guadanucci leg.; CAD 275 • 1 ♀; São Gonçalo do Rio Preto, Parque Estadual do Rio Preto; 14 Jan. 2010; J.P.L. Guadanucci, W.F. Silva, D. Moura, R. F. Ferreira and D. Weinmann leg.; CAD 14 • 1 ♂; Belo Horizonte, Campus UFMG; 19°52′19″ S, 43°57′58″ W; 27 Nov. 1999; E.S.S. Álvares leg.; UFMG 606 • 2 ♂♂; Belo Horizonte, Campus UFMG; 10–25 Sep. 2000; E.S.S. Álvares leg.; UFMG 607 • 1 ♂; Belo Horizonte, Campus UFMG; 30 Aug. 2000; E.S.S. Álvares leg.; UFMG 608 • 2 ♂♂; Belo Horizonte, Campus UFMG; 26 Sep. 2009; I.L.F. Magalhães leg.; UFMG 3211 • 1 ♂; Belo Horizonte, Reserva Biológica UFMG; IBSP 14488 • 1 ♂; Belo Horizonte, Campus UFMG, Centro Pedagógico UFMG; Jul. 2002; C. Torres leg.; IBSP 13659. – **São Paulo** • 1 ♂; Araraquara; 21°47′38″ S, 48°10′33″ W; 30 Sep. 1988; IBSP 9562 • 1 ♂; Ribeirão Preto; 21°10′40″ S, 47°48′36″ W; 24 Nov. 2004; IBSP 12337 •

1 ♂; Santo Antônio do Aracanguá; 20°56′13″ S, 50°29′45″ W; IBSP 14314 • 1 ♂; São Paulo, Parque dos Príncipes; 23°25′ S, 46°37′ W; IBSP 13324 • 1 ♂; Rio Pequeno; 23°33′ S, 46°43′ W; IBSP 3346 • 1 ♂; São Roque; 23°31′44″ S, 47°08′06″ W; 2 Aug. 2011; A.B. Canute leg.; IBSP 9133.

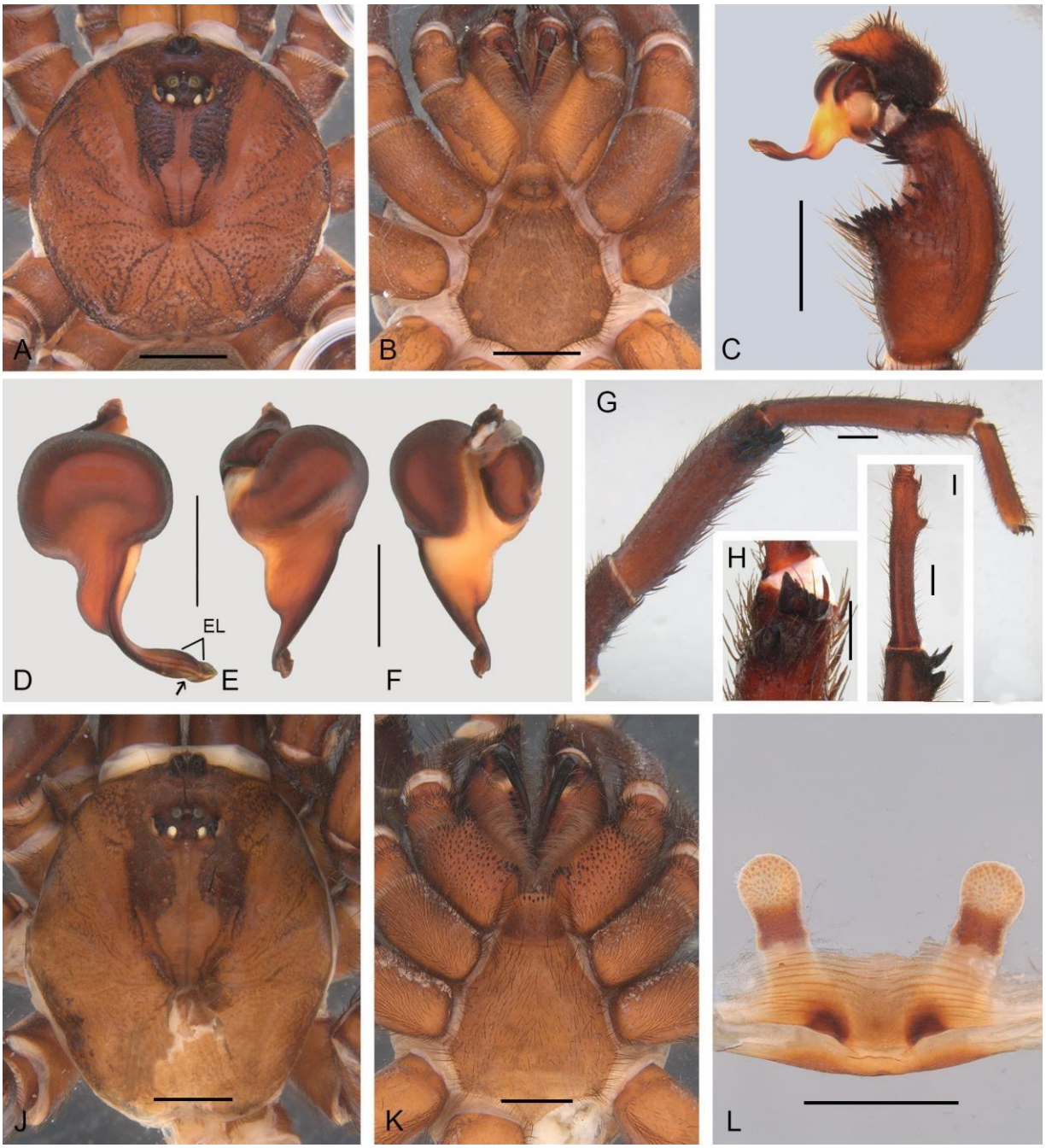

Fig. 27. *Idiops pirassununguensis* Fukami & Lucas, 2005. **A–I**. ♂ (UFMG 607). **A**. Prosoma (dorsal view). **B**. Prosoma (ventral view). **C**. Part of palp (retrolateral view). **D–F**. Palpal bulb. **D**. Dorsal view. **E**. Retrolateral view. **F**. Prolateral view. **G**. Tibia, metatarsus and tarsus I (prolateral view). **H**. Tibial apophysis (prolateral view). **I**. Tibial apophysis and metatarsus I (dorsal view). **J–L**. ♀ (UFMG 11264). **J**. Prosoma, dorsal view. **K**. Prosoma, ventral view. **L**. Genitalia (dorsal view). Abbreviation: EL = embolar lamella. The arrow indicates a constriction. Scale bars = 1 mm.

Emended description

Male and female recently described by Fukami & Lucas (2005). New data on the male and female are included here:

Male (UFMG 607)

HABITUS. See Fig. 27A.

COLOR. Carapace with dark brown spots on anterior half, mainly on cephalic area near eyes (Fig. 27A).

PROSOMA. Carapace and ocular arrangement as shown in Fig. 27A. Eye tubercle: 0.6 long; 1 wide. AME-ALE distance 0.8. Basal segment of chelicerae with a prolateral row of 6 large teeth and 4 small retrolateral teeth, grouped in basal half (Fig. 28A); rastellum presenting 12 spines of same size (Fig. 28B).

LEGS. Tibia, metatarsus and tarsus I as shown in Fig. 27G. Pseudoscopula: on tarsus I divided into rows of strong setae; tarsus II–IV totally covered.

PALP. Tibia with expansion of basal half of retrolateral depression (Figs 27C, 28D). Palpal bulb with short embolus with a strongly inclined basal portion and incomplete subapical torsion (Fig. 27D–F).

SPINATION. Palp: Ti r24, Ta d0-0-4. Leg I: Fe d1-1-2, Ti v1r-1r-2r, Mt 1r-2r-1, Ta r2-1-0. Leg II: Fe d1-1-2, Ti v0-2r-1r-1, Mt v1r-1r-1r-2, Ta p0-0-1, r2-2-0. Leg III: Fe d1-1-1, Pa d1-1-0, p3-5-8, r0-0-2, Ti v0-1r-0-2, p1-1-4, r1-1-2, Mt v3-4-0-4, p3- 2-2, r0-1-2, Ta p0-4-8, r0-4-8. Leg IV: Fe d1-1-2, Pa p16-3-0, Ti v1-2-2, Mt v1-2 -1-3, Ta p2-3-6, r0-0-2.

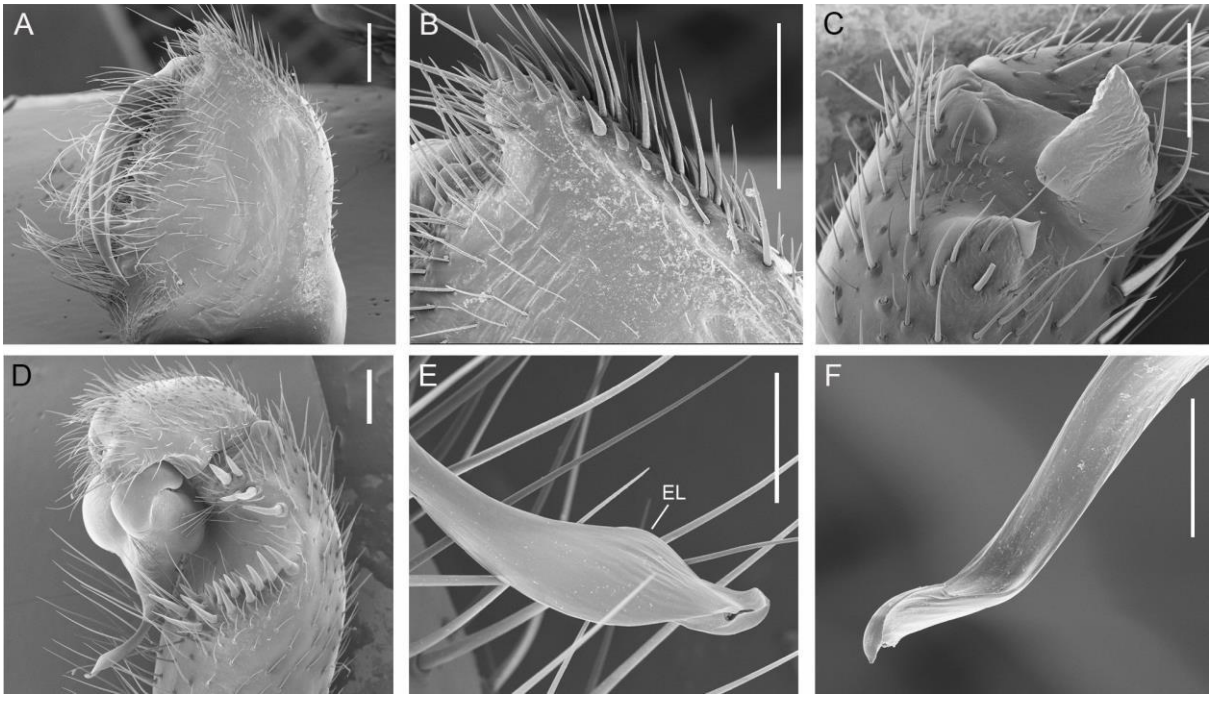

Fig. 28. Scanning electron micrographs of *Idiops pirassununguensis* Fukami & Lucas, 2005, ♂ (MZSP 15651). **A**. Chelicera (retrolateral view). **B**. Rastellum (retrolateral view). **C**. Tibial apophysis (dorsal view). **D**. Part of the palp, showing retrolateral depression. **E–F**. Detail of the final portion of the embolus. **E**. Dorsal view. **F**. Prolateral view. Abbreviation: EL = embolar lamella. Scale bars: A–D = 0.5 mm; E–F = 0.2 mm.

Female (UFMG 11264)
HABITUS. See Fig. 27J.

MEASUREMENTS. TBL 19.1, CL 9.8, CW 8.8, LL 1.5, LW 1.8, SL 5.4, SW 4.8.

COLOR. Similar to that of male, except sternum and coxae brownish and dark gray abdomen (Fig. 27J–K).

PROSOMA. Carapace and ocular arrangement as shown in Fig. 27J. Eye tubercle: 2.2 long; 1.9 wide. AME-ALE distance 1.4. Eye diameters: AME 0.4, ALE 0.5, PME 0.3, PLE 0.6. Thoracic fovea procurved (Fig. 27J). Labium with 6 cuspules (Fig. 27K). Maxilla with 92 cuspules, distributed over anterior ventral half, with 15 large cuspules at anterior prolateral end and 18 large cuspules at anterior retrolateral end (Fig. 27K). Basal segment of chelicerae with a prolateral row of 6 large teeth and a retrolateral row with 3 small teeth, grouped in basal third, rastellum presenting 22–24 spines of same size (Fig. 27K).

PALP AND LEG MEASUREMENTS. Palp = 14.4 (4.8, 3.1, 3.2, 3.3), I = 16.4 (5.3, 3.6, 3.6, 2.6, 1.3), II = 14.7 (4.8, 3.4, 2.9, 2.4, 1.2), III = 15.1 (4.1, 3.5, 2.4, 3.1, 2), IV = 20.3 (5.4, 4.1, 4.4, 4.2, 2.2).

SPINATION. Palp: Ti p5-12-13, r7-12-14, Ta v0-0-3, p12-10-8, r12-14-8. Leg I: Ti p5-7-8, r7-8-12, Mt p12-9-11, r11-10-9, Ta v0-0-6, p5-4-2, r5-4-2. Leg II: Ti p3-6-6, r1-3-3, Mt p12-9-12, r5-5-6, Ta v0-0-5, p7-4-3, r6-3-1. Leg III: Pa p3-4-8, r0-0-3, Ti v1-1-1, p2-3-6, r0-2-4, Mt v2-2-2, p6-2-2, r8-1-2, Ta v0-6-15. Leg IV: Pa p37-4-0, Ti v1-1-2, Mt v2-2-2, Ta v2-4-13.

SPERMATHECAE. Ducts with non-sclerotized basal region, thicker than apical portion; sclerotized apical portion; spherical and non-sclerotized receptacula, with evident granules (Fig. 27L).

Distribution

Brazil. Widely distributed, with areas in the phytophysiognomies of the Amazon, Caatinga and Cerrado. Records for Central-West region (Distrito Federal and Goiás), North region (Amazonas, Amapá, Pará and Rondônia), Northeast region (Bahia, Maranhão, Paraíba, Piauí and Sergipe) and Southeast region (Minas Gerais and São Paulo) (Fig. 4C).

Idiops rastratus (O. Pickard-Cambridge, 1889)
Figs 4C, 6F, 29–30

Dendricon rastratum O. Pickard-Cambridge, 1889: 250, figs 1–5. Synonymized by Pocock 1895: 223.

Dendricon rastratum – O. Pickard-Cambridge 1890: 623, pl. 53 fig. 2.
Pseudidiops rastratus – Pocock 1895: 223. — Petrunkevitch 1911: 87.
Idiops rastratus – Raven 1985: 139.

Diagnosis

The male of *Idiops rastratus* resembles that of *I. fuscus* by the shape of the palpal bulb, but differs by having the embolus curvature less accentuated (Fig. 29D–F) and the absence of a projection at the base of the retrolateral depression of the palpal tibia. The female differs from that of other species (except *Idiops opifex* and *I. duocordibus* sp. nov.) by the strong cuspules on the entire ventral face of the maxillae (Fig. 29K). Differs from *I. opifex* by the aspect of the spermathecae, with a shorter duct and a slightly larger receptacle compared to the diameter of the duct (Fig. 29L). Differs from *I. duocordibus* sp. nov. by the unmodified and rounded receptacle (Fig. 29L).

Type material

Syntypes
BRAZIL – **Rio de Janeiro** • 4 ♀♀; Serra dos Órgãos; W. Baker leg.; BMNH 1890.1.20.1 to 1890.1.20.4.

Other material examined

BRAZIL – **Bahia** • 2 ♂♂; Feira de Santana, Serra de São José; 12°16′1″S, 38°58′1″ W; 2009–2010; G. de Ferreira leg.; IBSP 258656 to 258657 • 1 ♀, 1 juv.; Porto Seguro, Arraial d'Ajuda; 16°27.643′ S,

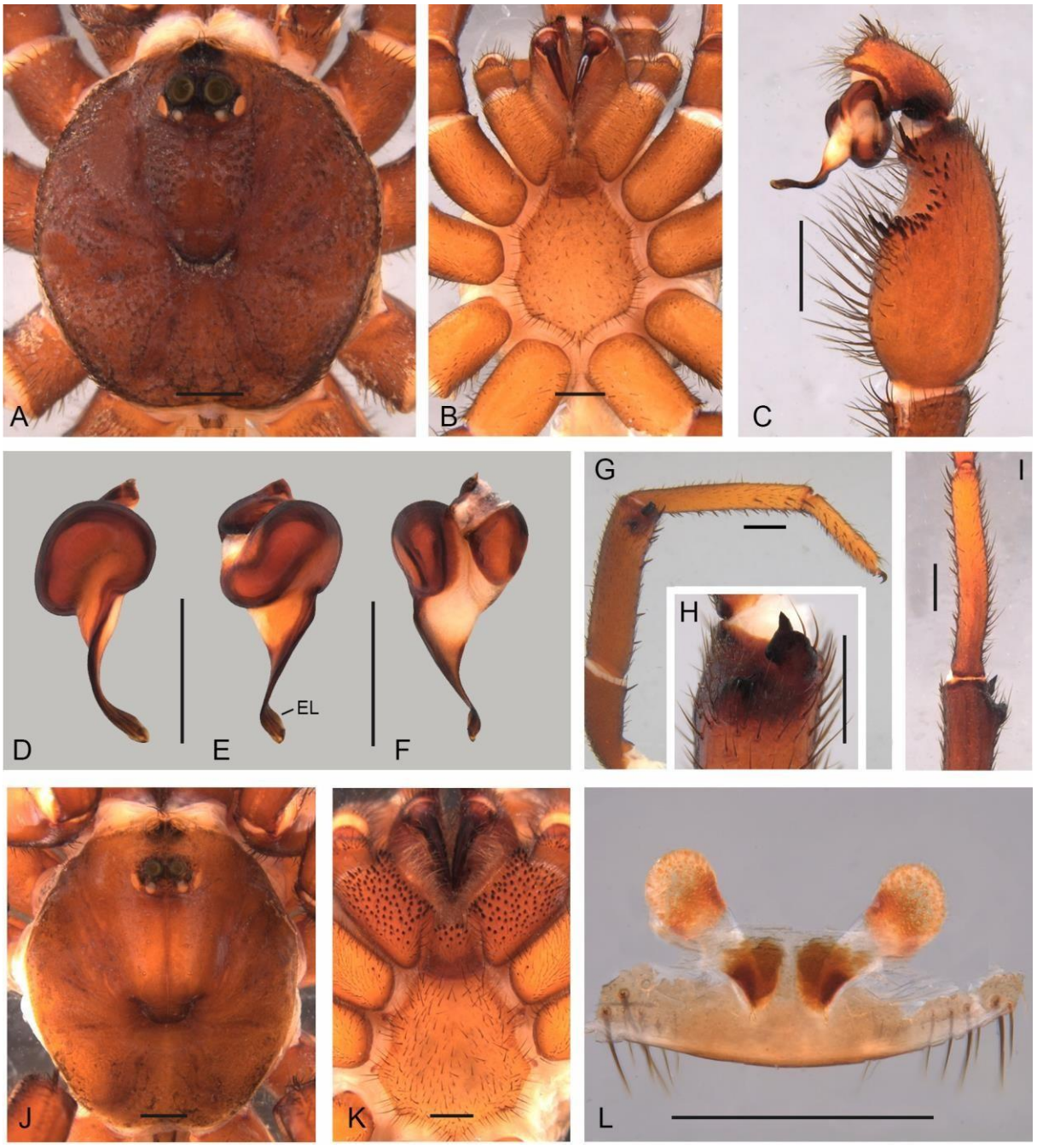

Fig. 29. *Idiops rastratus* (O. Pickard-Cambridge, 1889). **A–I**. ♂ (MZSP 24282). **A**. Prosoma (dorsal view). **B**. Prosoma (ventral view). **C**. Part of palp (retrolateral view). **D–F**. Palpal bulb. **D**. Dorsal view. **E**. Retrolateral view. **F**. Prolateral view. **G**. Tibia, metatarsus and tarsus I (prolateral view). **H**. Tibial apophysis (prolateral view). **I**. Tibial apophysis and metatarsus I (dorsal view). **J–L**. ♀ (MZSP 24282). **J**. Prosoma (dorsal view). **K**. Prosoma (ventral view). **L**. Genitalia (dorsal view). Abbreviation: EL = embolar lamella. Scale bars = 1 mm.

39°08.298′ W; 24–27 Feb. 2005; Expedição Arachné leg.; MNRJ • 18 ♂♂; Una; 15°17′34″ S, 39°4′30″ W; Dec. 1999; K. Kato leg.; MZSP 24233 • 11 ♂♂; same collection data as for preceding; MZSP 24218 • 15 ♂♂, 2 ♀♀; same collection data as for preceding; MZSP 24214 • 13 ♂♂; same collection data as for preceding; MZSP 24216 • 7 ♂♂; same collection data as for preceding; MZSP 24219 • 7 ♂♂; same collection data as for preceding; MZSP 24221 • 10 ♂♂; same collection data as for preceding; MZSP 24292 • 7 ♂♂; same collection data as for preceding; MZSP 24211 • 2 ♂♂, 1 ♀; same collection data as for preceding; MZSP 24282 • 2 ♂♂; same collection data as for preceding; MZSP 24212 • 5 ♂♂, 1 ♀; same collection data as for preceding; MZSP 24210 • 6 ♂♂; same collection data as for preceding; MZSP 24284 • 3 ♂♂ (SEM); same collection data as for preceding; MZSP 24215 • 6 ♂♂; same collection data as for preceding; MZSP 24675 • 5 ♂♂; same collection data as for preceding; MZSP 24220 • 3 ♂♂; same collection data as for preceding; MZSP 24213 • 5 ♂♂; same collection data as for preceding; MZSP 24217 • 4 ♂♂; same collection data as for preceding; MZSP 24288 • 3 ♂♂; same collection data as for preceding; MZSP 24273 • 2 ♂♂; same collection data as for preceding; MZSP 24222 • 4 ♂♂; same collection data as for preceding; MZSP 24275 • 3 ♂♂; same collection data as for preceding; MZSP 24276 • 6 ♂♂; same collection data as for preceding; MZSP 24287. – **Minas Gerais** • 1 ♂; Nova Lima, Serra da Moeda, Cave PBR_10_11; 20º09′20″ S, 43º58′24″ W; 15–20 Mar. 2010; R. Bessi leg.; IBSP 196034. – **Espírito Santo** • 2 ♂♂; Linhares, Reserva Natural Vale; 19°6′54″ S, 39°56′20″ W; 27–30 Apr. 2010; J.P.P.P. Barbosa *et al*. leg.; IBSP 234713. – **Rio de Janeiro** • 1 ♀; Teresópolis, Parque Nacional da Serra dos Órgãos; 23°27′33″ S, 46°38′2″ W; 10–22 Nov. 2010; R.P. Indicatti and F.U. Yamamoto leg.; IBSP 243973. – **São Paulo** • 36 ♂♂; Bananal, Estação Biológica de Bananal; 22°15′–22°37′ S, 44°07′–44°22′ W; 13–25 Apr. 2004; A.E. Monteiro leg.; MZSP 23781 • 39 ♂♂; same collection data as for preceding; MZSP 23732 • 1♀; Bananal, Estação Biológica de Bananal; 2010; J.M. Pereira leg.; IBSP 245408.

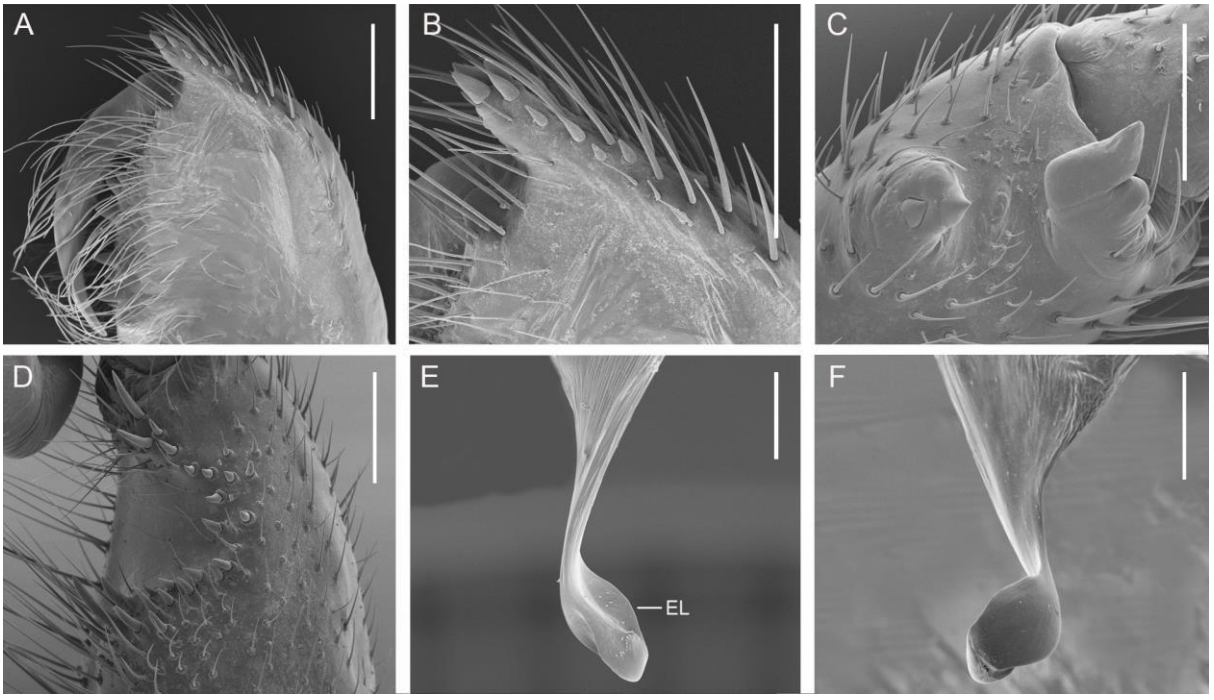

Fig. 30. Scanning electron micrographs of *Idiops rastratus* (O. Pickard-Cambridge, 1889), ♂ (MZSP 24215). **A**. Chelicera (retrolateral view). **B**. Rastellum (retrolateral view). **C**. Tibial apophysis (dorsal view). **D**. Part of the palp, showing retrolateral depression. **E–F**. Detail of the final portion of the embolus. **E**. Retrolateral view. **F**. Prolateral view. Abbreviation: EL = embolar lamella. Scale bars: A–D = 0.5 mm; E–F = 0.2 mm.

Description

Male (MZSP 24282)
HABITUS. See Fig. 29A.

MEASUREMENTS. TBL 11.2, CL 5.5, CW 5.2, LL 0.7, LW 1, SL 3, SW 2.6.

COLOR. Carapace and legs reddish brown, with yellowish coxae, brownish sternum (Fig. 29A–B), abdomen dorsally dark gray and ventrally brownish.

PROSOMA. Carapace and ocular arrangement as shown in Fig. 29A. Eye tubercle: 1.3 long; 1.4 wide. Distance AME-ALE 0.5. Eye diameters: AME 0.5, ALE 0.3, PME 0.2, PLE 0.4. Thoracic fovea procurved (Fig. 27A). Labium and sternum without cuspules (Fig. 29B). Basal segment of chelicerae with a prolateral row of 5 large teeth and 4–5 small retrolateral teeth in basal third (Fig. 30A), with proeminent rastellum, with 7–8 spines, with larger ones in distal region (Fig. 30B).

LEGS. Tibia, metatarsus and tarsus I as shown in Fig. 29G. Basal branch of tibial apophysis with additional tooth (Fig. 30C). Pseudoscopula: tarsus I smooth, II weakly covered, III–IV densely covered.

PALP. Tibia with conspicuous retrolateral depression and with larger spines concentrated on basal half (Figs 29C, 30D); embolus with apical lamella with a differentiated dorsal and ventral border (Figs 29D–F, 30E–F).

PALP AND LEG MEASUREMENTS. Palp = 9 (3.2, 1.6, 3, 1.2), I = 20.7 (6.4, 3, 4.9, 4.4, 2), II = 16,5 (5.3, 2, 3.6, 3.8, 1.8), III = 15.13 (4.1, 2.1, 3, 3.9, 1.9), IV = 21.7 (6, 2.7, 5.3, 5.3, 2.4).

SPINATION. Palp: Ti r36, Ta d-0-0-4. Leg I: Ti v1r-1r-2r-1ap, Mt v35-3, Ta v45, p2-3-3, r4-3-1. Leg II: Ti v1r-1r-3r-2, Mt v4-6-5-3ap, p0-1-1, Ta p3-4-2, r3-3-4. Leg III: Pa p1-2-7, r0- 1-2, Ti v1-2-2-1ap, p1-1-1, r1-1-1, Mt v2-4-3-4, p0-0-2, r1-1-1, Ta p2-3-2, r3-4-2. Leg IV: Pa p6-1-0, Ti v1-1-4, Mt v1-1r-1-3, Ta p2-1-3, r0-1-2.

Female (BMNH 1890.1.20.1)
HABITUS. See Fig. 29J.

MEASUREMENTS. TBL 13, CL 5.8, CW 4.9, LL 0.8, LW 2, SL 3.5, SW 3.5.

COLOR. Carapace and legs reddish brown, with yellowish coxae, brownish sternum (Fig. 29J–K), abdomen dorsally dark gray and ventrally brownish.

PROSOMA. Carapace and ocular arrangement as shown in Fig. 29J. Eye tubercle: 1.7 long; 1.5 wide. Distance AME-ALE 0.9. Eye diameters: AME 0.5, ALE 0.4, PME 0.3, PLE 0.4. Thoracic fovea procurved (Fig. 29J). Labium with 14 cuspules. Maxilla with 113 cuspules, distributed throughout ventral region (Fig. 29K). Basal segment of chelicerae with a prolateral row of 5 large teeth and a retrolateral row with 9 small teeth, grouped in basal third, rastellum with 12–14 spines, distal ones longer.

PALP AND LEG MEASUREMENTS. Palp = 11.4 (3.9, 2.4, 2.7, 2.4), I = 12.7 (4.4, 2.7, 2.7, 1.9, 1), II = 10.8 (3.3, 2.5, 2.2, 1.8, 1), III = 11.4 (3.4, 2.4, 1.9, 2.3, 1.4), IV = 16.2 (4.8, 2.9, 3.6, 3.1, 1.8).

SPINATION. Palp: Ti r36, Ta d-0-0-4. Leg I: Ti v1r-1r-2r-1ap, Mt v35-3, Ta v45, p2-3-3, r4-3-1. Leg II: Ti v1r-1r-3r-2ap, Mt v4-6-5-3, p0-1-1, Ta p3-4-2, r3-3-4. Leg III: Pa p1-2-7, r0-1-2, Ti v1-2-2, p1-1-1, r1-1-1, Mt v2-4-3-4, p0-0-2, r1-1-1, Ta p2-3-2, r3-4-2. Leg IV: Pa p6-1-0, Ti v1-1-4, Mt v1-1r-1-3, Ta p2-1-3, r0-1-2

SPERMATHECAE. Base divided by non-sclerotized area. Ducts short and slightly narrower than receptacles, which are spherical and with evident granules (Fig. 29L).

Distribution

Brazil. Mainly distributed in Atlantic Forest phytophysiognomies along the coastal zone, with records for the Southeast region (east of São Paulo, Espírito Santo and Rio de Janeiro) and Northeast region (center-south of Bahia). Only one record for the central region of Minas Gerais (Fig. 4C)

Idiops rohdei Karsch, 1886
Figs 3C, 31

Idiops rohdei Karsch, 1886: 93.

Diagnosis

The male of *Idiops rohdei* differs from that of other Neotropical species by the rectangular shape in dorsal view of the apical branch of the tibial apophysis (Fig. 31H) and by the short metatarsus I with a projection on the apical half (Fig. 31I). The female differs in having the spermathecae with ducts slightly curved outward in the median portion and elongated bean-shaped receptacles (Fig. 31J–K).

Type material

Holotype
PARAGUAY • ♀; R. Rohde leg.; ZMB 6230.

Other material examined

PARAGUAY• 1 ♂; Departamento Amambay, 33 km SW of Pedro Juan Caballero, Parque Nacional Cerro Corá, camping area; 22°38′04.6″ S, 56°01′33.8″ W; 22 Oct. 2019; A. Pérez-González, A. Ojanguren, D.J. Guerrero and J. Kochalka leg.; IBNP-2444.

Remark: The description of *Idiops rohdei* was based on a female specimen from Paraguay, without any further details about its locality. We had access to a male specimen from Parque Nacional Cerro Corá, mid-eastern Paraguay. The female holotype and the male specimen share the overall body coloration, especially close to the eye tubercle, which is dark brown. We decided to consider them as cospecifics, pending the availability of more specimens from Paraguay or nearby regions to support our decision.

Description

Male (IBNP-2444)
HABITUS. See Fig. 31A.

MEASUREMENTS. TBL 6.3, CL 3.3, CW 3.1, LL 0.5, LW 0.6, SL 1.8, SW 1.7.

COLOR. Carapace and legs reddish brown, with dark brown ocular tubercle, yellowish coxae, brownish sternum (Fig. 31A–B), abdomen dorsally dark gray and ventrally brownish.

PROSOMA. Carapace and ocular arrangement as shown in Fig. 31A. Eye tubercle: 0.6 long; 0.8 wide. Distance AME-ALE 0.5. Eye diameters: AME 0.3, ALE 0.3, PME 0.1, PLE 0.2. Thoracic fovea procurved (Fig. 31A). Labium and sternum without cuspules (Fig. 31B). Basal segment of chelicerae with a prolateral row of 4 larger teeth, and a small, retrolateral row with 2 small teeth, grouped in basal half, rastellum with 3 spines (Fig. 31B).

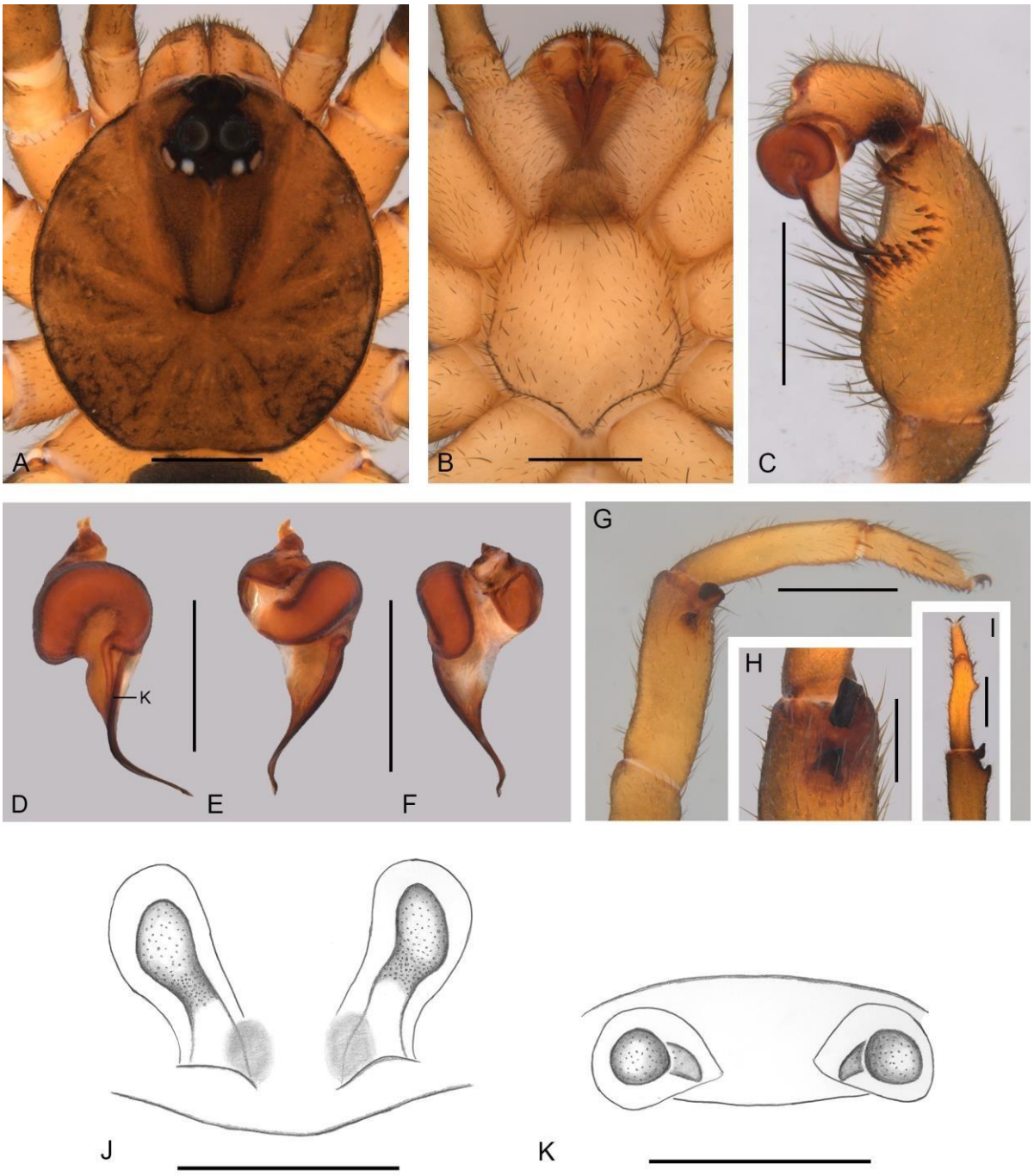

Fig. 31. *Idiops rohdei* Karsch, 1886. **A–I**. ♂ (IBNP-2444). **A**. Prosoma (dorsal view). **B**. Prosoma (ventral view). **C**. Part of palp (retrolateral view). **D–F**. Palpal bulb. **D**. Dorsal view. **E**. Retrolateral view. **F**. Prolateral view. **G**. Tibia, metatarsus and tarsus I (prolateral view). **H**. Tibial apophysis (prolateral view). **I**. Tibial apophysis and metatarsus I (dorsal view). **J–K**. ♀, genitalia, holotype (ZMB 6230). **J**. Dorsal view. **K**. Frontal view. Abbreviation: K = keel. Scale bars = 1 mm.

LEGS. Tibia, metatarsus and tarsus I as shown in Fig. 31G. Pseudoscopula: tarsus II–IV fully covered.

PALP. Tibia with spines distributed along margin of retrolateral depression, with larger spines on basal and apical portions (Fig. 31C), embolus with a keel in dorsal and retrolateral view, embolus strongly curved dorsally with abrupt reduction in thickness in its apical half, incomplete torsion at spermatic duct opening (Fig. 31D–F).

PALP AND LEG MEASUREMENTS. Palp = 2.8 (1, 0.5, 0.9, 0.4), I = 4.2 (1.4, 0.7, 1, 0.8, 0.3), II = 3.5 (1, 0.6, 1, 0.6, 0.3), III = 4.1 (1.5, 0.6, 0.7, 0.8, 0.5), IV = 4.4 (1, 0.7, 1.2, 1, 0.5).

SPINATION. Palp: Ti r25. Leg I: Fe d1-2-2, Pa v0-0-1, Ti v1-1-2, p0-0-1, r2-2-2, Mt v1-1-1, p0-0-1, r2-2-2, Ta v3-6-5, p0-1-1, r2-2-1. Leg II: Pa v0-0-2, Ti v2-1-3, r1-2-2, Mt v4-3-4, p0-0-3, r-2-2, Ta p0-1-1, r2-1-1. Leg III: Pa p0-0-3, Ti v0-2-2, Mt v0-1-3, p0-0-1, Ta r1-0-1. Leg IV: Pa p0-0-6, Ti p0-0-2, Mt v0-2-4, Ta p1-1-2.

Female (holotype ZMB 6230)

MEASUREMENTS. TBL 13.9, CL 6.8, CW 5.8, LL 1, LW 1.4, SL 4.2, SW 3.7.

COLOR. Carapace and legs red brown. Eye tubercle dark brown. Sternum brown.

PROSOMA. Eye tubercle: 1.7 long; 1.5 wide. AME-ALE distance 1. Eye diameters: AME 0.4, ALE 0.3, PME 0.3, PLE 0.4. Thoracic fovea procurved. Labium with 5 cuspules. Maxilla with 58 cuspules, distributed throughout anterior ventral half. Basal segment of chelicerae with a prolateral row of 6 large teeth and 11 small retrolateral teeth, grouped in median area.

PALP AND LEG MEASUREMENTS. Palp = 11.2 (3.7, 2.3, 2.6, 2.6), I = 13.1 (4.4, 2.9, 2.8, 2, 1), II = 11.7 (4, 2.7, 2.2, 1.8, 1), III = 12.6 (3.8, 2.7, 1.8, 2.6, 1.7), IV = 17.3 (4.9, 3.3, 3.7, 3.4, 2).

SPINATION. Palp: Fe p0-0-2, Pa p0-1-0, Ti p7-7-12, r6-11-12, Ta v6-11-12. Leg. I: Ti p6-5-8, r4-7-15, Mt p10-7-7, r11-8-7, Ta v0-0-7, p4-4-4, r4-4-0. Leg II: Ti p3-4-7, r1-2-4, Mt p13-7-9, r5-5-5, Ta v0-0-6, p5-5-3, r5-3-0. Leg III: Pa p6-5-12, r0-0-3, Ti v0-0-2, p0-4-8, r0-3-3, Mt v2-2-3, p10-4-3, r5-2-1, Ta v4-8-9. Leg IV: Pa p39-0-0, Ti v1-1-1, Mt v1-1-7, r0-0-1, Ta v4-6-11.

SPERMATHECae. Bean-shaped receptacula with conspicuous granules, long, translucent ducts (Fig. 31J–K).

Distribution

Paraguay. Departamento Amambay (Fig. 3C).

Idiops sertania Fonseca-Ferreira, Guadanucci & Brescovit sp.nov.
urn:lsid:zoobank.org:act:8C6CC368-27DF-45A0-9164-2CA32C4D0F39
Figs 4C, 32–33

Diagnosis

Males of *Idiops sertania* sp. nov. differ from those of other Neotropical species by having the robust embolus with a wide basal half, strongly curved dorsally, with torsion at the apical end and a conspicuous embolar lamella close to the opening of the sperm duct (Figs 32D–F, 33E–F) and by having the palpal tibia elongated (similar to *I. germaini*) (Fig. 32C). Differs from *I. germaini* by having large spines distributed along the margin of the retrolateral depression (Figs 32C, 33D) and by the robust tibial apophysis (Fig. 32H).

Etymology

The term 'sertania', referenced in the specific epithet, is a tribute to the 'sertão' of Brazil, a large region of the country where these spiders occur. The term sertão refers to culturally diverse regions, far from the coast and large cities, and generally associated with rural regions with little human occupation.

Type material

Holotype

BRAZIL – **Minas Gerais** • ♂; Januária, Parque Nacional Cavernas do Peruaçu; 15°10′0″ S, 44°22′0″ W; 3–25 Jan. 2008; M.T. Junior and R.S. Recoder leg.; IBSP 15348.

Paratypes

BRAZIL – **Amazonas** • 1 ♂; Nova Aripuanã, Santa Maria, Margem esquerda, Rio Arapuanã; 5°47′52″ S, 60°15′55″ W; May 2002; M. Trefaut leg.; MZUSP 21511. – **Piauí** • 1 ♂; Guaribas, Parque Nacional da Serra das Confusões; 9°13′16″ S, 43°29′21″ W; Oct. 2006; P.R.R.Silva *et al.* leg.; CHNUFPI 4031. –

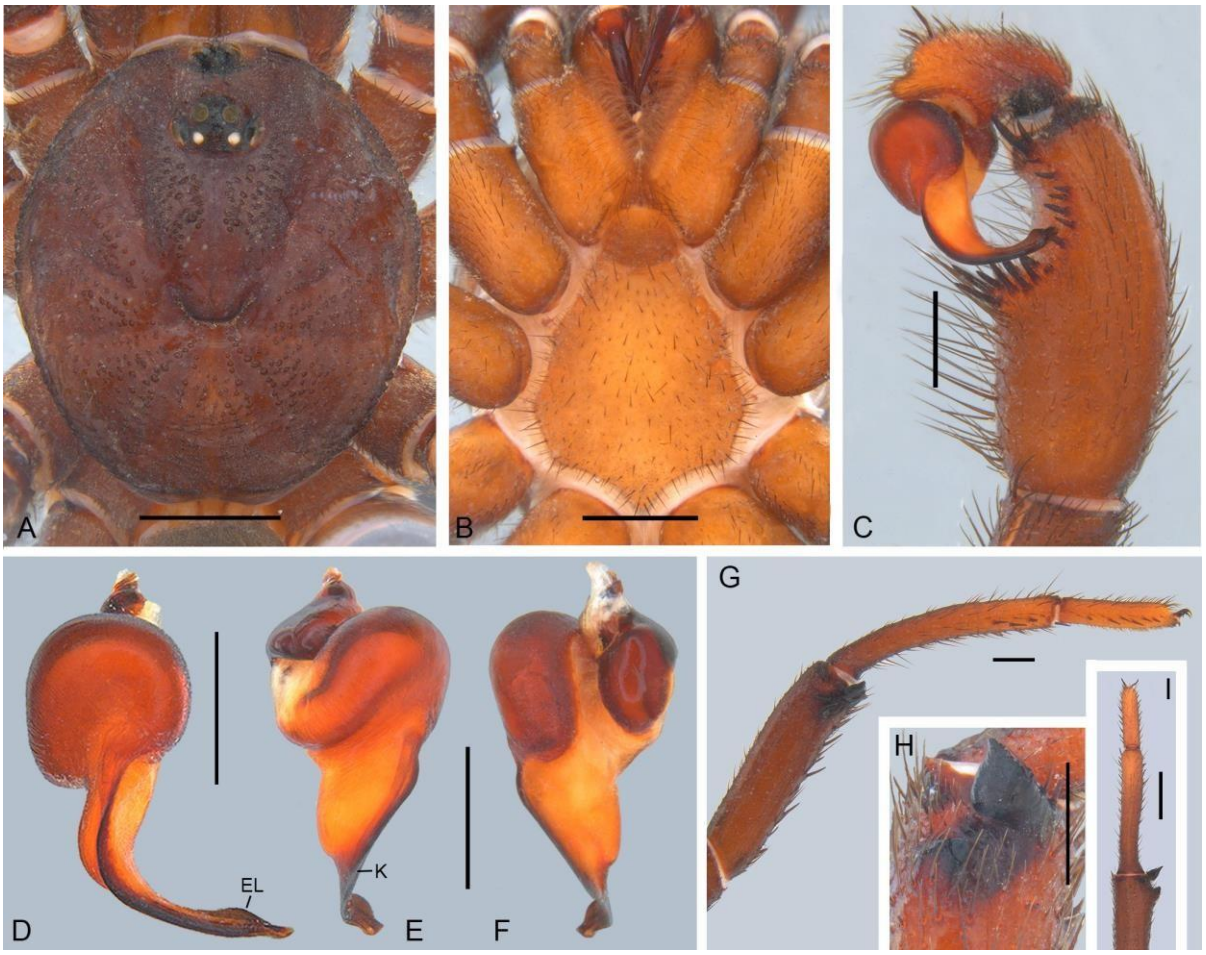

Fig. 32. *Idiops sertania* Fonseca-Ferreira, Guadanucci & Brescovit sp. nov., ♂, holotype (IBSP 15348). **A**. Prosoma (dorsal view). **B**. Prosoma (ventral view). **C**. Part of palp (retrolateral view). **D–F**. Palpal bulb. **D**. Dorsal view. **E**. Retrolateral view. **F**. Prolateral view. **G**. Tibia, metatarsus and tarsus I (prolateral view). **H**. Tibial apophysis (prolateral view). **I**. Tibial apophysis and metatarsus I (dorsal view). Abbreviations: EL = embolar lamella; K = keel. Scale bars = 1 mm.

Ceará • 1 ♂; Crato, Floresta Nacional do Araripe; 07°27′07.3″ S, 39°19′52.4″ W; 2018; R. Azevedo leg.; IBSP 227617. – **Minas Gerais** • 1 ♂; same collection data as for holotype; IBSP 15346.

Other material examined

BRAZIL – **Piauí** • 5 ♂♂ (SEM); Bom Jesus, Estação Ecológica de Uruçuí-Una; 08°52′5″ S, 44°57′ W; 19–29 Jan. 2001; G.G. Martinelle leg.; MZSP 21546 • 2 ♂♂; União, Campus COMVAPI Ltda; 4°35′9″ S, 42°51′50″ W; 2006; J. Queiroz *et al.* leg.; CHNUFPI 0032, CHNUFPI 0035 • 2 ♂♂; same collection data as for preceding; CHNUFPI 0037 • 3 ♂♂; same collection data as for preceding; CHNUFPI 0034 • 2 ♂♂ (SEM); same collection data as for preceding; CHNUFPI 0039 • 2 ♂♂; same collection data as for preceding; CHNUFPI 0033 • 1 ♂; same collection data as for preceding; 4°38′6″ S, 42°50′19″ W; CHNUFPI 4035 • 2 ♂♂; same collection data as for preceding; CHNUFPI 0031. – **Ceará** • 1 ♂; Crato, Parque Estadual Sítio do Fundão; 07°13′3″ S, 39°20′21″ W; 2018; R. Azevedo leg.; IBSP 218294 • 2 ♂♂; Crato, Floresta Nacional do Araripe; 07°27′07.3″ S, 39°19′52.4″ W; 2018; R. Azevedo leg.; IBSP 218307, IBSP 227583. – **Paraíba** • 1 ♂; Areia, Mata do Pau Ferro; 06°67′45.8″ S, 35°55′27″ W; 5 Aug. 2011; S.B.R. Alencar *et al.* leg.; CHNUFPI 0041. – **Bahia** • 1 ♂; Contendas do Sincorá, Floresta Nacional Contendas do Sincorá; 13°55′08,7″ S, 41°07′13,8″ W; 12–14 Jan. 2012; I.L.F. Magalhães *et al.* leg.; IBSP 271351 – **Tocantins** • 1 ♂; Palmas, Taquarussu; 10°19′ S, 48°9′ W; Equipe IBSP leg.; IBSP 10415 • 1 ♂; Porto Nacional, Área urbana, UHE Luiz Eduardo Magalhães; 10°42′28″ S, 48°25′1″ W; Equipe IBSP leg.; IBSP 10437. – **Goiás** • 6 ♂♂; Caldas Novas, UHE Corumbá; 17°42′50″ S, 48°32′12″ W; 12–23Aug. 1996; M.T.I. Rodrigues *et al.* leg.; MZSP 15656 • 2 ♂♂; Colinas do Sul, Serra da Mesa; 14°01′ S, 48°12′ W; 2–15 Dec. 1995; Silvestri, Dietz and Campaner leg.; MZSP 28851 • 1 ♂; Catalão, Barragem, Serra do Facão; 17°31′51.07″ S, 47°33′29.57″ W; Jul. 2013; R.B. Martines and R.M.C. Silveira leg.; UFMG 4442 • 4 ♂♂; Catalão, Barragem, Serra do Facão; 17°35′34″ S, 47°37′16″ W; Jul. 2011; R.B. Martines and

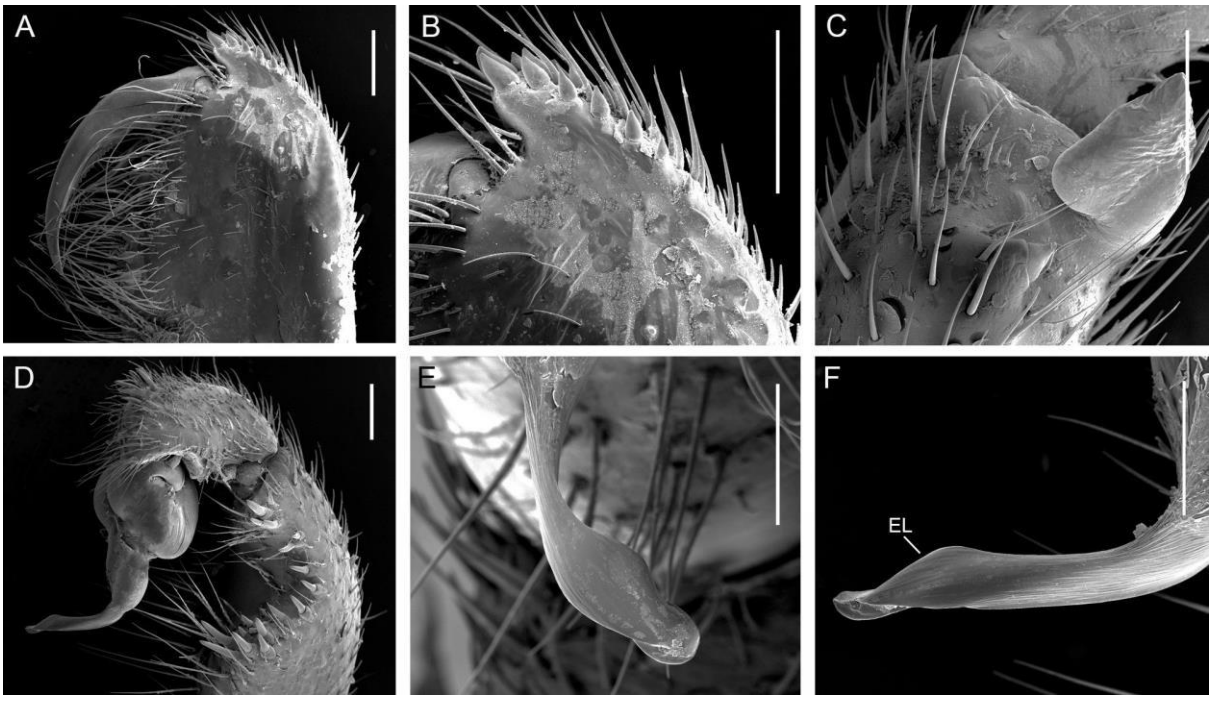

Fig. 33. Scanning electron micrographs of *Idiops sertania* Fonseca-Ferreira, Guadanucci & Brescovit sp. nov., ♂ (CHNUFPI 0039). **A**. Chelicera (retrolateral view). **B**. Rastellum (retrolateral view). **C**. Tibial apophysis (dorsal view). **D**. Part of the palp, showing retrolateral depression. **E–F**. Detail of the final portion of the embolus. **E**. Retrolateral view. **F**. Prolateral view. Abbreviation: EL = embolar lamella. Scale bars: A–D = 0.5 mm; E–F = 0.3 mm.

R.M.C. Silveira leg.; UFMG 4441 • 1 ♂; Catalão, Barragem, Serra do Facão; 17°51′40″ S, 47°37′38″ W; Jul. 2012; R.B. Martines and R.M.C. Silveira leg. UFMG 4440. – **Mato Grosso** • 1 ♂; Chapada dos Guimarães; 15°27′39″ S, 55°45′0″ W; 20–30 Sep. 2000; C. Strussmann leg.; MCTP 11557 • 2 ♂♂; Chapada dos Guimarães; 20–29 Sep. 2000; C. Strussmann leg.; MCTP 13614 • 2 ♂♂; Chapada dos Guimarães; 20–28 Sep. 2000; C. Strussmann; MCTP 13661; 2 ♂♂; Poconé; 16°15′25″S, 56°37′22″ W; 2010–2012; D. Batistella leg., Winkler extractor; IBSP 249196. – **Mato Grosso do Sul** • 1 ♂; Três Lagoas, Fazenda Canaã; 20°45′04″ S, 51°40′42″ W; Dec. 1967; F. Lane leg.; MZSP 7575. – **Minas Gerais** • 2 ♂♂; Januária, Parque Nacional Cavernas do Peruaçu; 15°10′0″ S, 44°22′0″ W; 3–25 Jan. 2008; M. Teixeira-Junior and R.S. Recoder leg.; IBSP 15345, IBSP 15347 • 2 ♂♂; same collection data as for preceding; IBSP 210881.

Description

Male (holotype IBSP 15348)

HABITUS. See Fig. 32A.

MEASUREMENTS. TBL 15.6, CL 7.7, CW 6.9, LL 1, LW 1.3, SL 4, SW 3.7.

COLOR. Dark brown carapace, reddish brown legs, light brown sternum, abdomen gray (Fig. 32A–B).

PROSOMA. Carapace and ocular arrangement as shown in Fig. 32A. Eye tubercle: 0.9 long; 1.2 wide. AME-ALE distance 1. Eye diameters: AME 0.2, ALE 0.4, PME 0.2, PLE 0.5. Thoracic fovea procurved (Fig. 32A). Labium and sternum without cuspules (Fig. 32B). Basal segment of chelicerae with a prolateral row of 6 large teeth and 6 small retrolateral teeth, grouped in the basal half, proeminent rastellum with 11–12 spines, distals largest (Fig. 33A–B).

LEGS. Tibia, metatarsus and tarsus I as shown in Fig. 32G. Leg I with tibial apophysis with apical branch twice the size of basal branch (Figs 32H–I, 33C). Pseudoscopula: tarsus I weakly covered, II–IV totally covered.

PALP. Tibia with conspicuous retrolateral depression and large spines distributed along its entire length (Figs 32C, 33D); embolus with keel in retrolateral view (Fig. 32E).

PALP AND LEG MEASUREMENTS. Palp = 10.2 (2.4, 2.2, 3.9, 1.7), I = 23.6 (7.2, 3.3. 4.9, 5.4, 2.8), II = 20.8 (6.4, 2.9, 4.4, 4.8, 2.3), III = 19.3 (5.3, 2.5, 3.6, 5, 2.9), IV = 27 (7.1, 3.4, 6, 7, 3.5).

SPINATION. Palp: Ti r20, Ta d0-0-2. Leg I: Pa v4, Ti v4-5-4, Mt r1-1-4, p0-0-4, Ta r3-4-3, p1-3-2. Leg II: Pa p0-0-4, r0-0-3, Ti v6-5-7, Mt p0-2-3, r2-3-4, Ta p2-2-3, r4-3-4. Leg III: Pa p1, Ti v1-2-2, p0-0-1, Mt v2-4-5, p2-2-2, Ta r4-4-5. Leg IV: Pa v0-0-2, Ti v1-1-3, Mt v9-9-11, d1-1-2, r0-0-3, p0-1-2, Ta p3-3-7, r0-0-2.

Distribution

Brazil. Widely distributed, with areas covering the phytophysiognomies of the Amazon, Caatinga and Cerrado. Records for Central-west region (Goiás, Mato Grosso and Mato Grosso do Sul), North region (Amazonas), Northeast region (Bahia, Ceará and Piauí) and Southeast region (northern part of Minas Gerais) (Fig. 4C).

Idiops siolii (Bücherl, 1953)
Figs 3B, 34

Pseudidiops siolli Bücherl, 1953: 126, figs 6–8.

Idiops siolii – Raven 1985: 158.

Diagnosis

The female of *Idiops siolii* differs from that of other Neotropical species by having the spermathecae with ducts with a thickened median portion and mushroom-shaped receptacles (Fig. 34C).

Type material

Holotype

BRAZIL – **Pará** • ♀; Belém, Campus do IAN - Embrapa Amazônia Oriental; IBSP 3123. Lost in the fire of 2010.

Neotype (here designated)

BRAZIL – **Pará** • ♀; Melgaço, Flona Caxiuanã, Estação Científica Ferreira Penna, Plote B; 1°47′32.3″ S, 51°26′2.5″ W; 6–11 Apr. 2002; MPEG 1012.

Remark: The type specimen of *Idiops siolii* was lost in the 2010 IBSP fire. In accordance with the criteria of the ICZN Code (ICZN 1999), a neotype is designated here, because the type is lost and the original description is inadequate to stabilise the species. The neotype is a specimen collected near the type locality, in the state of Pará, Brazil.

Description

Male

Unknown.

Female (neotype MPEG 1012)

HABITUS. See Fig. 34A.

MEASUREMENTS. TBL 13.8, CL 7.6, CW 6.6, LL 1.1, LW 1.5, SL 4.4, SW 3.7.

COLOR. Carapace and legs reddish brown, with yellowish coxae, reddish brown sternum (Fig. 34A–B). Abdomen gray.

PROSOMA. Carapace and ocular arrangement as shown in Fig. 34A. Eye tubercle: 0.7 long; 1.4 wide. AME-ALE distance 1. Eye diameters: AME 0.21, ALE 0.5, PME 0.2, PLE 0.4. Thoracic fovea procurved. Labium with 3 cuspules (Fig. 34B). Maxilla with 31 cuspules, distributed throughout anterior ventral

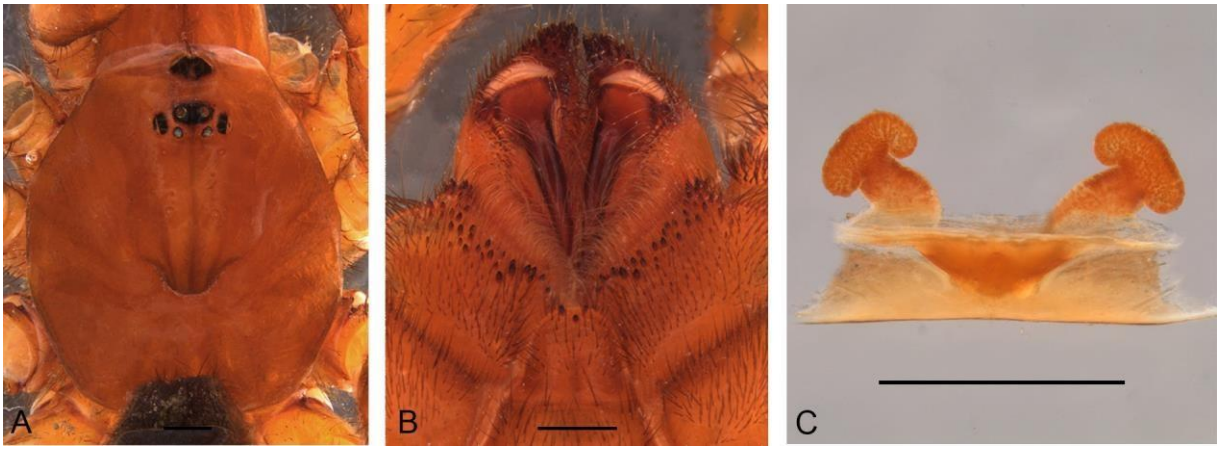

Fig. 34. *Idiops siolii* (Bücherl, 1953), ♀, neotype (MPEG 1012). **A**. Prosoma (dorsal view). **B**. Prosoma (ventral view). **C**. Genitalia (dorsal view). Scale bars = 1 mm.

half (Fig. 34B). Basal segment of chelicerae with a prolateral row of 8 large teeth and 4 small retrolateral teeth, grouped in basal half; rastellum with 20–22 short spines of same size (Fig. 34B).

PALP AND LEG MEASUREMENTS. Palp = 12.5 (4.2, 2.7, 2.7, 2.9), I = 13.8 (4.5, 2.8, 3, 2.1, 1.4), II = 13.2 (4.3, 3, 2.5, 2, 1.4), III = 12 (4.1, 2.3, 2.8, 2, 0.8), IV = 18.4 (4.4, 3.9, 4, 3.6, 2.5).

SPINATION. Palp: Ti p7-9-12, r6-10-10, Ta p12-10-11, r14-12-9. Leg I: Ti p3-7-10, r9-8-10, Mt p11-8-11, r3-9-8, Ta v0-0-3, p5-4-3, r5-5-4. Leg II: Pa p5-5-12, Ti v1-1-1, p2-4-6, r0-2-3, Mt v2-2-3, d2-2-2, p6-4-2, r2-3-1, Ta v2-4-5, p0-2-5, r0-1-1. Leg III: Ti v1-1-0, r0-1-1, p2-6-7, Mt v2-2-4, p9-7-9, r2-2-2, Ta v0-0-3, p5-5-2, r1-0-0. Leg IV: Ti v0-0-1, Mt v0-1-2, p1-2-3, r0-1-1, Ta v2-1-2, p1-5-5, r0-2-2.

SPERMATHECAE. V-shaped ducts with sclerotized portion between duct and receptacles. Bilobed ducts sclerotized, with evident granules (Fig. 34C).

Distribution

Brazil. Known only for the region of Belém and Melgaço (Pará), in the phytophysiognomies of the Amazonian region (Fig. 3B)

Species inquirenda

Idiops bonapartei Hasselt, 1888

Idiops bonapartei Hasselt, 1888: 166.

Remark

The female holotype from Suriname is deposited in National Museum of Natural History of Leiden. It was not possible to obtain the type specimen for loan. The examination of the type through photos revealed it to be an immature female specimen of Idiopinae. Moreover, the original description does not warrant species recognition, as it includes only generic level characteristics. Because of this, we consider *I. bonapartei* species inquirenda.

Distribution

Suriname. Known only from the type locality (Fig. 5B).

Discussion

Systematics and biogeography notes

Trapdoor spiders belonging to the infraorder Mygalomorphae Pocock, 1892, which include the family Idiopidae, are usually associated with a sedentary lifestyle, high longevity, limited dispersion skills and high environmental specificity (Dippenaar-Schoeman 2002; Bond & Stockman 2008; Pérez-Miles & Perafán 2017; Mason *et al.* 2018). These characteristics, together with the strong morphological homogeneity contrasted with the high genetic diversification, make these spiders great evolutionary and biogeographic models (Bond *et al.* 2001; Satler *et al.* 2013; Opatova & Arnedo 2014; Harrisson *et al.* 2017; Opatova *et al.* 2020).

The genus *Idiops* is the most diverse among idiopids, with 102 valid species hitherto, of which 24 occur in South America, corresponding to approximately a quarter of the known species (World Spider Catalog 2021). In this revision, an extensive number of specimens of *Idiops* was examined, revealing undescribed species (such as the widely distributed species *I. sertania* sp. nov.; Fig. 4C), indicating the existence of species with an apparently restricted distribution (such as *I. nilopolensis* and *I. germaini*)

(Fig. 3D), and expanding the geographic distribution of several species (such as *I. carajas*, *I. fuscus* and *I. pirassununguensis*; Figs 3B, 4C). The latter had their distributions expanded by more than a thousand kilometers after the revision of this material.

As the only genus of Idiopinae with species distributed in the Neotropical and Paleotropical regions, with the other six genera restricted to the Paleotropical region (World Spider Catalog 2021), this revision of the Neotropical species is essential for a better evolutionary and biogeographic understanding of the genus, both in the context of deep and recent evolution and diversification. In an ancient context, it is unknown whether the species of *Idiops* of the Old and New World comprise a monophyletic clade. Despite the type species, *Idiops fuscus*, being from Brazil, previous molecular analyses included only Old World species (Hedin & Bond 2006; Opatova *et al.* 2020). In an intraspecific context, we found morphologically similar widespread species, with disjunct distributions, which is poorly compatible with the sedentary habits of trapdoor spiders, suggesting the possible existence of a cryptic species complex.

The species *Idiops pirassununguensis* represents one of these cases: as a result of the present revision, the species had its distribution expanded to more than twice in size compared to the previous scenario, with records for phytophysiognomies in the Amazon, Caatinga and Cerrado. Presenting a conserved morphology and a continental distribution, uncommon in trapdoor spider (Buzzato *et al.* 2021), the current delimitation as a single species may actually be a complex of cryptic species. To solve this situation, an integrative approach is needed, involving molecular, morphometric, demographic and environmental data. Such an approach has already been taken to solve similar problems for species of the genera *Aptostichus* Simon, 1891 (Euctenizidae Raven, 1985) (Bond *et al.* 2001; Bond & Stockman 2008), *Aliatypus* Smith, 1908 (Antrodiaetidae Gertsch,1940) (Satler *et al.* 2013), *Ummidia* Thorell, 1878 (Halonoproctidae Pocock,1901) (Opatova *et al.* 2013, 2016), *Titanidiops* (Idiopidae) (Opatova & Arnedo 2014) and *Moggridgea* O. Pickard-Cambridge, 1875 (Migidae Simon,1889) (Harrisson *et al.* 2017).

An alternative hypothesis that may explain such a wide distribution that cannot be ruled out is ballooning, which is a behavioral mechanism of aerial dispersion with the use of silk, widely reported for silk-producing arthropods such as spiders, mites and moth larvae (Bell *et al.* 2005). Although not commonly witnessed in Mygalomorphae (Colye 1983; Bell *et al.* 2005; Buzzato *et al.* 2021), as in Araneomorphae Pocock, 1892, cases of ballooning dispersion have already been recorded for at least nine species from four families, all of trapdoor spiders (Atypidae Thorell, 1870, Actinopodidae Simon,1892, Halonoproctidae and recently Idiopidae) (Buzzato *et al.* 2021; Rossi *et al.* 2021). In this type of aerial dispersion, called suspended ballooning, spiderlings climb to elevated positions in the vegetation, exposing themselves to be carried passively by the wind, with the help of a drag line (Colye 1983; Bell *et al.* 2005; Buzzato *et al.* 2021). According to Opatova *et al.* (2013), ballooning possibly contributed to the dispersion of spiders of the genus *Ummidia* across the Mediterranean and between Europe and North America, when the continents were not too far apart. The ballooning, which has already been recorded for several species of *Ummidia*, could also explain the presence of the genus on Caribbean islands (Opatova *et al.* 2013; Godwin & Bond 2021).

For Idiopidae, ballooning was recently recorded for the species *Neocteniza toba* Goloboff, 1987 (Genysinae), a widely distributed trapdoor spider with records in Argentina, Brazil and Paraguay (Rossi *et al.* 2021). From laboratory experiments, the authors observed spiderlings being carried by gentle breezes reaching 20–30 cm from the dropping point, with some individuals reaching a distance ofthree meters from the initial point (Rossi *et al.* 2021). Although not directly registered, ballooningdispersion was inferred for species of the subfamily Arbanitinae with wide distribution, found in Australia (Buzzato *et al.* 2021). To explore the importance of ballooning in the distribution of Neotropical *Idiops*, such as *I. pirassununguensis*, we need studies that can infer, or even directly record, ballooning and investigate

populationgeneticstructuring, toestimatespiderlingdispersal skills fromtheirmaternal burrows(Buzzato *et al.* 2021).

Acknowledgements

We wish to give our thanks to all curators for the loan of specimens, to Beatriz Maurício, for her help with SEM images, to Abel Pérez Gonzáles and John Kochalka for sending the male of *I. rohdei*, to our arachnologist friends Arthur Galetti Lima, David Candiani, Felipe Garcia, Hector Gonzales Filho, Júlia Ayumi Ando, Leandro Malta Borges, Leonardo Souza Carvalho, Millke Jasmini Morales, Pedro Henrique Martins, Rafael Prezzi Indicatti, Willian Fabiano Silva and Wolf Moeller for their assistance and critical suggestions for this work, and to Leonardo Carvalho, Pedro Henrique Martins and Rafael Prezzi Indicatti for sending us photos. We also thank to the reviewers for their comments and suggestions that improved our manuscript. This study was financed by the Fundação de Amparo à Pesquisa do Estado de São Paulo (FAPESP 2018/02842-2 to RFF) (FAPESP 2017/11985-9 to JPLG) (FAPESP 2008/10147-0 to FUY) and CNPq (303903/2019-8 to ADB).

References

Ausserer A. 1875. Zweiter Beitrag zur Kenntniss der Arachniden-Familie der Territelariae Thorell (Mygalidae Autor). *Verhandlungen der Kaiserlich-Königlichen Zoologisch-Botanischen Gesellschaft in Wien* 25: 125–206.

Bell J.R., Bohan D.A., Shaw E.M. & Weyman G.S. 2005. Ballooning dispersal using silk: world fauna, phylogenies, genetics and models. *Bulletin of Entomological Research* 95 (2): 69–114. https://doi.org/10.1079/BER2004350

Bond J.E. & Stockman A.K. 2008. An integrative method for delimiting cohesion species: finding the population-speciesinterfaceinagroup of Californian trapdoorspiderswithextreme geneticdivergenceand geographicstructuring. *Systematic Biology* 57 (4): 628–646. https://doi.org/10.1080/10635150802302443

Bond J.E., Hedin M.C., Ramirez M.G. & Opell B.D. 2001. Deep molecular divergence in the absence of morphological and ecological change in the Californian coastal dune endemic trapdoor spider *Aptostichus simus*. *Molecular Ecology* 10 (4): 899–910. https://doi.org/10.1046/j.1365-294X.2001.01233.x

Bond J.E., Hendrixson B.E., Hamilton C.A. & Hedin M. 2012. A reconsideration of the classification of the spider infraorder Mygalomorphae (Arachnida: Araneae) based on three nuclear genes and morphology. *PloS One* 7 (6): e38753. https://doi.org/10.1371/journal.pone.0038753

Buzatto B.A., Haeusler L. & Tamang N. 2021. Trapped indoors? Long-distance dispersal in mygalomorph spiders and its effect on species ranges. *Journal of Comparative Physiology A* 207: 279–292. https://doi.org/10.1007/s00359-020-01459-x

Bücherl W. 1957. Sôbre a importância dos bulbos copuladores e das apófises tibiais dos machos na sistemática das aranhas caranguejeiras (Orthognatha). *Anais da Academia Brasileira de Ciências* 29: 377–416.

Bücherl W., Timotheo da Costa A. & Lucas S. 1971. Revisão de alguns tipos de aranhas caranguejeiras (Orthognatha) estabelecidos por Cândido de Mello-Leitão e depositados no Museu Nacional do Rio. *Memórias do Instituto Butantan* 35: 117–138.

Coyle F.A. 1983. Aerial dispersal by mygalomorph spiderlings (Araneae, Mygalomorphae). *Journal of Arachnology* 11 (2): 283–286.

Coyle F.A., Dellinger R.E. & Bennet R. 1992. Retreat architecture and construction behavior of an East African idiopine trapdoor spider (Araneae, Idiopidae). *Bulletin of the British Arachnological Society* 9: 99–104.

Dippenaar-Schoeman A.S. 2002. *Baboon and Trapdoor Spiders of Southern Africa: An Identification Manual*. Plant Protection Research Institute Handbook No. 13. Agricultural Research Council, Pretoria.

Dupérré N. & Tapia E. 2021. The endless search for type specimens; illustrations of eleven spider (Araneae, Mygalomorphae) species described by Eugène Simon. *Zootaxa* 4951 (2): 259–282. https://doi.org/10.11646/zootaxa.4951.2.3

Ferretti N., Nime M. & Mattoni C. 2017. Three new *Idiops* (Mygalomorphae: Idiopidae) from Argentina and redescription of the male of *I. hirsutipedis* Mello-Leitão, 1941. *Journal of Natural History* 51 (17–18): 975–994. https://doi.org/10.1080/00222933.2017.1319516

Fonseca-Ferreira R., de Almeida Zampaulo R. & Guadanucci J.P.L. 2017. Diversity of iron cave-dwelling mygalomorph spiders from Pará, Brazil, with description of three new species (Araneae). *Tropical Zoology* 30 (4): 178–199. https://doi.org/10.1080/03946975.2017.1367590

Fukami C.Y. & Lucas S.M. 2005. Notas sobre espécies de *Idiops* Perty, 1833 do sudeste Brasileiro com descrição de *I. pirassununguensis* sp. nov. (Mygalomorphae, Idiopidae, Idiopinae). *Biota Neotropica* 5 (18051a): 1–7. https://doi.org/10.1590/S1676-06032005000200016

Godwin R.L. & Bond J.E. 2021. Taxonomic revision of the New World members of the trapdoor spider genus *Ummidia* Thorell (Araneae, Mygalomorphae, Halonoproctidae). *ZooKeys* 1027: 1–165. https://doi.org/10.3897/zookeys.1027.54888

Goloboff P.A. 1993. Areanalysis of mygalomorph spider families (Araneae). *American Museum Novitates* 3056:1–32.

Guérin F.E. 1838. Arachnides. *In*: Eydoux J.F.T. & P. Gervais (eds) *Voyage autour du monde par les mers de l'Inde et de Chine exécuté sur la corvette de l'Etat La Favorite pendant les années 1830/1831 et 1832sous le commandement de M. Laplace capitaine de frégate*: 5, 161–167, pl. 47–48. Paris.

Gupta N., Ganeshkumar M., Das S.K. & Siliwal M. 2013. Three new species of *Idiops* Perty, 1833 (Araneae: Idiopidae) from India. *Zootaxa* 3635 (3): 237–250. https://doi.org/10.11646/zootaxa.3635.3.3

Gupta N., Das S.K. & Siliwal M. 2015. Natural history of the trapdoor spider *Idiops joida* Gupta *et al* 2013 (Araneae: Idiopidae) from the Western Ghats in India. *Journal of Asia-Pacific Biodiversity* 8 (1): 38–42. https://doi.org/10.1016/j.japb.2015.01.004

Harrison S.E., Harvey M.S., Cooper S.J., Austin A.D. & Rix M.G. 2017. Across the Indian Ocean: a remarkable example of trans-oceanic dispersal in an austral mygalomorph spider. *PloS One* 12 (8): e180139. https://doi.org/10.1371/journal.pone.0180139

Hasselt A.W.M. van. 1888. Araneae exoticae quas collegit, pro Museo Lugdunensi, Dr H. Ten Kate Jr. in Guyanâ Hollandicâ (Suriname). *Tijdschrift voor Entomologie* 31: 165–200.

Hedin M. & Bond J.E. 2006. Molecular phylogenetics of the spider infraorder Mygalomorphae using nuclear rRNA genes (18S and 28S): conflict and agreement with the current system of classification. *Molecular Phylogenetics and Evolution* 41 (2): 454–471. https://doi.org/10.1016/j.ympev.2006.05.017

ICZN. 1999. *International Code of Zoological Nomenclature. Fourth Edition.* International Trust for Zoological Nomenclature, London, UK. Available from https://www.iczn.org/the-code [accessed 28 Jul. 2021].

Karsch F. 1886. Araneologisches aus Südamerika. *Berliner Entomologische Zeitschrift* 30: 92–94.

Mason L.D., Wardell-Johnson G. & Main B.Y. 2018. The longest-lived spider: mygalomorphs dig deep, and persevere. *Pacific Conservation Biology* 24 (2): 203–206. https://doi.org/10.1071/PC18015.

Mello-Leitão C.F. 1923. Theraphosideas do Brasil. *Revista do Museu Paulista* 13: 1–438.

Mello-Leitão C.F. 1930. Aranhas do Cuminá. *Arquivos do Museu Nacional do Rio de Janeiro* 32: 51–75.

Mello-Leitão C.F. 1937. Aranhas novas ou raras. *Anais da Academia Brasileira de Ciências* 9:1–12.

Mello-Leitão C.F. 1946. Nuevos aracnidos sudamericanos de las colecciones del Museo de Historia Natural de Montevideo. *Comunicaciones Zoologicas del Museo de Historia Natural de Montevideo* 2 (35): 1–10.

Mirza Z.A. & Sanap R.V. 2012. A new species of the genus *Idiops* and notes on *Idiops bombayensis* Siliwal *et al*. 2005 (Araneae: Idiopidae) from Northern Western Ghats of Maharashtra, India. *The Journal of Arachnology* 40 (1): 85–95. https://doi.org/10.1636/A11-37.1

Mirza Z.A., Vaze V.V. & Sanap R.V. 2012. A new species of the trapdoor spiders genus *Idiops* Perty, 1833 (Araneae: Idiopidae) from theWestern Ghats, with a key to the *Idiops* of India. *Revista Ibérica de Aracnología* 21: 9–14.

Moreira T.D.S., Baptista R.L., Kury A.B., Giupponi A.P., Buckup E.H. & Brescovit A.D. 2010. Annotated check list of Arachnida type specimens deposited in the Museu Nacional, Rio de Janeiro. II — Araneae. *Zootaxa* 2588 (1): 1–91. https://doi.org/10.11646/zootaxa.2588.1.1

OpatovaV.&ArnedoM.A. 2014. Spidersonahotvolcanicroof:colonisationpathwaysandphylogeography of the Canary Islands endemic trap-door spider *Titanidiops canariensis* (Araneae, Idiopidae). *PLoS One* 9 (12): e115078. https://doi.org/10.1371/journal.pone.0115078

Opatova V., Bond J.E. & Arnedo M.A. 2013. Ancient origins of the Mediterranean trap-door spiders of the family Ctenizidae (Araneae, Mygalomorphae). *Molecular Phylogenetics and Evolution* 69 (3): 1135–1145. https://doi.org/10.1016/j.ympev.2013.08.002

Opatova V., Bond J.E. & Arnedo M.A. 2016. Uncovering the role of the Western Mediterranean tectonics in shaping the diversity and distribution of the trap-door spider genus *Ummidia* (Araneae, Ctenizidae). *Journal of Biogeography* 43 (10): 1955–1966. https://doi.org/10.1111/jbi.12838

Opatova V., Hamilton C.A., Hedin M., De Oca L.M., Král J. & Bond J.E. 2020. Phylogenetic systematics and evolution of the spider infraorder Mygalomorphae using genomic scale data. *Systematic Biology* 69 (4): 671–707. https://doi.org/10.1093/sysbio/syz064

Pérez-Miles F.& Perafán C. 2017. Behavior and biologyof Mygalomorphae. *In*: Viera C. & Gonzaga M.O. (eds) *Behaviour and Ecology of Spiders*. Springer International Publishing, Cham , Switzerland. https://doi.org/10.1007/978-3-319-65717-2

Perty M. 1833. Arachnides Brasilienses. *In*: de Spix J.B. & Martius F.P. (eds) *Delectus animalium articulatorum quae in itinere per Braziliam ann. 1817 et 1820 colligerunt*: 191–209, pls 38–39. Munich.

Petrunkevitch A. 1911. A synonymic index-catalogue of spiders of North, Central and South America with all adjacent islands, Greenland, Bermuda, West Indies, Terra del Fuego, Galapagos, etc. *Bulletin of the American Museum of Natural History* 29: 1–791. https://doi.org/10.5962/bhl.title.23819

Petrunkevitch A. 1925. Arachnida from Panama. *Transactions of the Connecticut Academy of Arts and Sciences* 27: 51–248.

Pickard-Cambridge O. 1870. Monograph of the genus *Idiops*, including descriptions of several species new to science. *Proceedings of the Zoological Society of London* 1870: 101–108. Available from https://www.biodiversitylibrary.org/part/67316 [accessed 2 Nov. 2021].

Pickard-Cambridge O. 1889. On a new tree trap-door spider from Brazil. *Proceedings of the Zoological Society of London* 1889: 250–252.

Pickard-Cambridge F.O. 1896. On the Theraphosidae of the lower Amazons: being an account of the new genera and species of this group of spiders discovered during the expedition of the steamship

"Faraday" up the river Amazons. *Proceedings of the Zoological Society of London* 64 (3): 716–766. https://doi.org/10.1111/j.1096-3642.1896.tb03076.x

Pocock R.I. 1837. On the spiders of the suborder Mygalomorphae from the Ethiopian Region, contained in the collection of the British Museum. *Proceedings of the Zoological Society of London* 65 (3): 724–774. https://doi.org/10.1111/j.1096-3642.1897.tb03116.x

Pocock R.I. 1893. Description of a new species of tree trap-door spider from Trinidad. *Annals and Magazine of Natural History* (6) 11: 407–409. https://doi.org/10.1080/00222939308677548

Pocock R.I. 1895. Notesontheidentityofsomeofthetypesof Mygalomorphaeinthecollectionofthe British Museum. *Journal of Natural History* 16 (93): 223–230. https://doi.org/10.1080/00222939508680262

Raven R.J. 1985. The spider infraorder Mygalomorphae (Araneae): cladistics and systematics. *Bulletin of the American Museum of Natural History* 182: 1–180.

Rix M.G., Cooper S.J., Meusemann K., Klopfstein S., Harrison S.E., Harvey M.S. & Austin A.D. 2017a. Post-Eocene climate change across continental Australia and the diversification of Australasian spiny trapdoor spiders (Idiopidae: Arbanitinae). *Molecular Phylogenetics and Evolution* 109: 302–320. https://doi.org/10.1016/j.ympev.2017.01.008

Rix M.G., Raven R.J., Main B.Y., Harrison S.E., Austin A.D., Cooper S.J. & Harvey M.S. 2017b. The Australasian spiny trapdoor spiders of the family Idiopidae (Mygalomorphae: Arbanitinae): a relimitation andrevisionatthegenericlevel. *Invertebrate Systematics* 31(5): 566–634. https://doi.org/10.1071/IS16065

Roewer C.F. 1953. Araneae-Orthognatha (Arachnoidae). *Exploration du Parc National de l'Upemba, Mission G. F. de Witte* 22: 1–80.

Rossi G.F., Ghirotto V.M., Galleti-Lima A., Indicatti R.P. & Guadanucci J.P.L. 2021. "Flying" or digging? The trapdoor spider genus *Neocteniza* Pocock, 1895: redescription of three species, new records from Brazil, notes on natural history and first record of ballooning for Idiopidae (Araneae, Mygalomorphae). *Zootaxa* 5023 (4): 451–485. https://doi.org/10.11646/zootaxa.5023.4.1

Satler J.D., Carstens B.C. & Hedin M. 2013. Multilocus species delimitation in a complex of morphologically conserved trapdoor spiders (Mygalomorphae, Antrodiaetidae, *Aliatypus*). *Systematic Biology* 62 (6): 805–823. https://doi.org/10.1093/sysbio/syt041

Schiapelli R.D. & Gerschman de Pikelin B.S. 1971. Estudio de algunas arañas descriptas por Mello-Leitão para el Uruguay. *Revista de la Sociedad Entomológica Argentina* 33 (1–4): 57–62.

Siliwal M., Hippargi R., Yadav A. & Kumar D. 2020. Five new species of trap-door spiders (Araneae: Mygalomorphae: Idiopidae) from India. *Journal of Threatened Taxa* 12 (13): 16775–16794. https://doi.org/10.11609/jott.5434.12.13.16775-16794

Simon E. 1889. Voyage de M. E. Simon au Venezuela (Décembre 1887–Avril 1888). 4e Mémoire. Arachnides. *Annales de la Société Entomologique de France* 9 (6): 169–220.

Simon E. 1892. *Histoire naturelle des Araignées. Deuxième édition, Tome premier, No 1.* Roret, Paris. https://doi.org/10.5962/bhl.title.51973

Simon E. 1903. *Histoire naturelle des Araignées. Deuxième édition, Tome second, No 4.* Roret, Paris. https://doi.org/10.5962/bhl.title.51973

Soares B.A.M. 1944. Aracnideos de Monte Alegre. *Papéis Avulsos do Departamento de Zoologia, Secretaria de Agricultura, Sao Paolo* 4: 151–168.

Tucker R.W.E. 1917. On some South African Aviculariidae (Arachnida). Families Migidae, Ctenizidae, Diplotheleae and Dipluridae. *Annals of the South African Museum* 17 (2): 79–138.

Walckenaer C.A. 1837. *Histoire naturelle des insectes. Aptères. Tome premier, No. 2.* Roret, Paris. https://doi.org/10.5962/bhl.title.61095

Wilson J.D., Hughes J.M., Raven R.J., Rix M.G.& Schmidt D.J. 2018. Spinytrapdoor spiders (*Euoplos*) of eastern Australia: broadly sympatric clades are differentiated by burrow architecture and male morphology. *Molecular Phylogenetics and Evolution* 122: 157–165. https://doi.org/10.1016/j.ympev.2018.01.022

Wilson J.D., Raven R.J., Schmidt D.J., Hughes J.M. & Rix M.G. 2020. Total-evidence analysis of an undescribed fauna: resolving the evolution and classification of Australia's golden trapdoor spiders (Idiopidae: Arbanitinae: Euoplini). *Cladistics* 36 (6): 543–568.https://doi.org/10.1111/cla.12415

World Spider Catalog. 2021. World Spider Catalog. Version 21.5. Natural History Museum Bern. https://doi.org/10.24436/2

Manuscript received: 28 April 2021
Manuscript accepted: 7 October 2021
Published on: 25 November 2021
Topic editor: Rudy C.A.M. Jocqué
Desk editor: Radka Rosenbaumová

Printed versions of all papers are also deposited in the libraries of the institutes that are members of the *EJT* consortium: Muséum national d'histoire naturelle, Paris, France; Meise Botanic Garden, Belgium; Royal Museum for Central Africa, Tervuren, Belgium; Royal Belgian Institute of Natural Sciences, Brussels, Belgium; Natural History Museum of Denmark, Copenhagen, Denmark; Naturalis Biodiversity Center, Leiden, the Netherlands; Museo Nacional de Ciencias Naturales-CSIC, Madrid, Spain; Real Jardín Botánico de Madrid CSIC, Spain; Zoological Research Museum Alexander Koenig, Bonn, Germany; National Museum, Prague, Czech Republic.

Capítulo 2

Análises filogenômicas dos gêneros de Idiopinae 1889 (Idiopidae), com ênfase nas espécies Neotropicais de *Idiops* Perty 1833, baseado em Elementos Ultraconservados (UCEs)

RESUMO

Entre as aranhas Mygalomorphae, Idiopidae é a segunda família mais diversa, composta exclusivamente por aranhas de alçapão, que são divididas em três subfamílias: Arbanitinae, Genysinae e Idiopinae. A subfamília Idiopinae, caracterizada principalmente por ter os olhos laterais anteriores projetados à frente dos demais, compreende atualmente 148 espécies, distribuídas em sete gêneros: o gênero-tipo *Idiops* Perty, 1833, composto por 96 espécies válidas, além dos gêneros *Ctenolophus* Purcell, 1904, *Galeosoma* Purcell, 1903, *Gorgyrela* Purcell, 1902, *Heligmomerus* Simon, 1892, *Segregara* Tucker, 1917 e *Titanidiops* Simon, 1903. Com base em um conjunto de dados composto por 29 táxons, composto por amostras recentes e de museu, são apresentados os resultados da primeira análise filogenômica baseada em Elementos Ultraconservados (UCEs) para a família, que incluiu espécies de *Idiops* tanto da América do Sul quanto da África, representantes de todos os gêneros de Idiopinae, exceto *Galeosoma*, além de *Neocteniza*, um enigmático gênero de Genysinae. Análises filogenéticas foram realizadas utilizando o método de Máxima Verossimilhança, que visaram avaliar a monofilia e as relações entre os gêneros de Idiopinae e a monofilia do gênero *Idiops*. Em seguida foram realizadas análises de Reconstrução de Caracteres Ancestrais (RCA) para os seguintes caracteres: disposição ocular, espínulos coxais, sigilas esternais e dentes das quelíceras. De acordo com a árvore filogenética gerada, baseada em uma matriz com 50% de cobertura taxonômica, composta por 832 *loci* de UCEs, Idiopinae forma um clado monofilético, suportado morfologicamente pelo padrão ocular distinto, e é dividido em dois clados geograficamente segregados: um composto pelas espécies africanas de Idiopinae e o outro pelas espécies Neotropicais. O clado composto pelas espécies africanas, dividido em dois grupos distintos, teve a relação entre os gêneros suportado por diferentes

combinações dos seguintes caracteres analisados na RCA: espínulos nas coxas, sigilas esternais e dentição da quelíceras. Segundo as análises realizadas, o gênero *Idiops* foi recuperado como parafilético, devido ao relacionamento mais próximo das espécies africanas do gênero com os demais gêneros africanos de Idiopinae do que com as espécies Neotropicais. Apesar disso, as espécies oriundas da América do Sul foram resgatadas em um táxon monofilético, suportado por um padrão de dentição distinto do encontrado nas espécies africanas, como o observado na RCA. Por fim, pela primeira vez a monofilia de Idiopidae é contestada, devido ao relacionamento filogeneticamente mais próximo de Idiopinae com *Cteniza* (Ctenizidae) do que com *Neocteniza* (Idiopidae), que pela primeira vez é incluída em uma filogenia molecular. Os resultados encontrados neste trabalho, baseados em um conjunto de dados gerado utilizando amostras recentes, devidamente armazenadas para análises moleculares e amostras antigas, conservadas em álcool 70% em temperatura ambiente, reforçam a importância da utilização de amostras de museu para ajudar a compreender as relações filogenéticas das aranhas migalomorfas, especificamente das aranhas de alçapão da família Idiopidae.

Palavras-chave: Mygalomorphae, aranhas de alçapão, Domiothelina, museômica, Máxima Verossimilhança,

INTRODUÇÃO

As aranhas inseridas na Infraordem Mygalomorphae, que inclui tarântulas, aranhas-alçapão e aranhas-funil, compreendem cerca de 7% da diversidade total de aranhas (> 3340 spp.) (World Spider Catalog, 2023), atualmente divididas em 32 famílias (Opatova *et al*. 2020, Montes de Oca *et al*. 2022, World Spider Catalog 2023). Sua origem antiga, estimada em mais de 300 milhões de anos (Ayoub *et al*. 2007, Opatova *et al*. 2020), associada ao estilo de vida geralmente sedentário, dispersão normalmente limitada e consequente estruturação genética (Stockman & Bond 2007, Pérez-Miles & Perafán 2017), fazem dessas aranhas bons modelos para estudos evolutivos e biogeográficos (Bond & Stockman 2008, Opatova & Arnedo 2014, Harrison *et al*. 2017, Foley *et al*. 2021, Rix *et al*. 2021).

Com uma origem datada no Cretáceo Inferior, há cerca de 133 milhões de anos (Opatova *et. al*. 2020), e uma distribuição predominantemente Gonduânica (Opatova *et. al*. 2020, World Spider Catalog 2023), a família Idiopidae Simon, 1889, é um desses grandes modelos para estudos filogenéticos. Sendo uma das poucas famílias resgatadas como monofilética em todas as filogenias até o momento (Raven 1985, Goloboff 1993, Hedin & Bond 2006, Bond *et al*. 2012, Wheeler *et al*. 2017, Opatova *et al*. 2020), Idiopidae atualmente é a segunda família mais diversa dentro de Mygalomorphae, compreendendo 440 espécies em 23 gêneros (World Spider Catalog 2023), divididos em três subfamílias: Idiopinae Simon, 1889, Arbanitinae Simon, 1903 e Genysinae Simon, 1903 (Raven 1985). Destas, apenas Arbanitinae, que se restringe à Austrália e Nova Zelândia, teve seus táxons revisados sistematicamente, que serviram de base para estudos filogenéticos e biogeográficos recentes (Rix *et. al*. 2017a, 2017b, Wilson *et. al*. 2018, 2020, 2021).

Os representantes da subfamília Idiopinae (Figura 1), grupo alvo deste trabalho, são caracterizados principalmente pela posição destacada dos Olhos Laterais Anteriores (OLA), que são projetados a frente dos demais, próximos à margem anterior da carapaça (Raven 1985), o que os torna um grupo marcadamente distinto das demais aranhas de alçapão. A subfamília atualmente compreende 152 espécies distribuídas em sete gêneros: *Ctenolophus* Purcell 1904, *Galeosoma* Purcell 1903, *Gorgyrela* Purcell 1902, *Segregara* Tucker 1917 e *Titanidiops* Simon 1903 restritos ao continente africano; *Heligmomerus* Simon 1892 com ocorrência na Índia, Siri Lanka e África; e, *Idiops* Perty 1833, com ocorrência nas Américas do Sul e Central, África e oeste asiático.

Dentre os gêneros de Idiopinae, o mais diverso é *Idiops* Perty 1833, que atualmente abrange 96 espécies válidas, distribuídas na América do Sul, África, Índia e Ásia Ocidental, das quais 24 ocorrem na América do Sul (Ferretti *et al*. 2017, Fonseca-Ferreira *et al*. 2021, World Spider Catalog, 2023), sendo doze endêmicas do Brasil (Fonseca-Ferreira *et al*. 2021). *Idiops* é o único gênero de Idiopinae com espécies distribuídas nas regiões Neotropical e Paleotropical, estando os outros seis gêneros restritos à região Paleotropical (World Spider Catalog, 2023). Apesar disso, apenas as espécies Neotropicais do gênero foram taxonomicamente revisadas (Fonseca-Ferreira *et al*. 2021), apresentando um padrão de dentição das quelíceras distinto do observado nas espécies

Paleotropicais (Dippenaar-Schoeman 2002, Mirza *et al*. 2012). Por apresentarem hábitos crípticos, baixa densidade populacional e distribuição comumente esparsa (Fonseca-Ferreira *et al*. 2021), os espécimes de *Idiops* geralmente são pouco coletados em campo (Dippenaar-Schoeman, 2002, Fonseca-Ferreira *et al*. 2021). Desta forma, este grupo tem como principal fonte de informação taxonômica as coleções zoológicas, o que até recentemente era um dos principais motivos limitantes para a realização de análises filogenéticas baseadas em dados moleculares.

Figura 1: Diversidade de aranhas da subfamília Idiopinae. **A**. *Idiops fuscus* Perty, 1833 ♂ (Brasil). **B**. *Idiops pirassununguensis* Fukami & Lucas, 2005 ♀ (Brasil). **C**. *Idiops camelus* (Mello Leitão, 1937) ♀ (Brasil). **D**. *Idiops castaneus* Hewitt, 1913 ♀ (África do Sul). **E**. *Idiops gunningi* Hewitt, 1913 ♀ (África do Sul). **F**. *Titanidiops* sp. ♀ (Marrocos). **G**. *Titanidiops* sp. ♂ (Marrocos). **H**. *Segregara* sp.

♂ (África do Sul). **I**. *Galeosoma planiscutatum* Hewitt, 1919 ♂ (África do Sul). **J**. *Galeosoma planiscutatum* Hewitt, 1919 ♀ (África do Sul). **K**. *Heligmomerus maximus* Sanap & Mirza, 2015 ♀ (Índia). **L**. *Ctenolophus oomi* Hewitt, 1913 ♀ (África do Sul). Créditos das imagens: Leonardo S. Carvalho (A), Pedro H. Martins (B), Rafael P. Indicatti (C), Peter Webb (D, E, I, J, L), Jan Korba (F, G), Zeeshan A. Mirza (K).

Com o advento do Sequenciamento de Nova-Geração, surgiram novas técnicas de extração e sequenciamento de DNA, além de métodos filogenômicos, que permitiram estudos em escala genômica (Faircloth *et. al*., 2012, Lemmon & Lemmon 2013, Anderman *et al*. 2020). Uma das técnicas mais promissoras de análise filogenômica é o método de captura de sequências de Elementos Ultraconservados (UCEs – *Ultraconserved Elements*), que consiste na captura e sequenciamento de regiões genômicas altamente conservadas que são compartilhadas entre táxons filogeneticamente distantes (Faircloth *et. al*, 2012, Zhang *et. al*, 2019). Os UCEs e suas regiões flanqueadoras, que aumentam a variabilidade genética ao se afastarem do núcleo dos UCEs, podem ser capturados seletivamente por conjuntos de sondas específicas e usados para reconstruir a história evolutiva de táxons em várias escalas de tempo, desde divergências filogenéticas profundas até recentes (Faircloth *et. al*, 2012, Smith *et al*. 2014, Starret *et. al*., 2017, Parada *et al*. 2021).

Em um estudo comparativo que utilizou formigas como modelo, Blaimer *et al*. (2015) demonstraram que as análises filogenômicas usando aproximadamente 1000 *loci* de UCEs permitiram uma resolução filogenética superior à encontrada em análises a partir de dez marcadores padrão sequenciados pelo método Sanger, com melhor aproveitamento em termos de custo, tempo e volume de dados. Tais vantagens têm possibilitado o desenvolvimento de estudos filogenômicos que têm gerado uma quantidade inédita de dados (Anderman *et al*. 2020), focados nas relações evolutivas de táxons não modelos, como por exemplo, anêmonas e corais (Quattrini *et al*. 2018), invertebrados bentônicos (Petersen *et al*. 2022), insetos aquáticos (Houston *et al*. 2022), cupins (Hellemans *et al*. 2022) e morcegos (Calderón-Acevedo *et al*. 2022).

Entre os aracnídeos, uma série de trabalhos têm sido publicados focados no desenvolvimento de conjuntos de sondas de UCEs, elaboradas

especificamente para aracnídeos (Starret *et al*. 2014), ácaros (Van Dam *et al*. 2018), aranhas (Kulkarni *et al*. 2019) ou mesmo para táxons mais específicos, como as aranhas da Infraordem Liphistiomorphae (Xu *et al*. 2021). Essas sondas de UCEs têm sido utilizadas para diferentes propósitos, como para resolução de problemas filogenéticos antigos (historicamente associados a clados parafiléticos ou mesmo polifiléticos), como os encontrados em aranhas migalomorfas (Hedin *et al*. 2018,a 2019), para esclarecer as relações internas e a posição filogenéticas de espécies de aranhas (Kulkarni *et al*. 2020, Ledford *et al*. 2021) e de opiliões (Derkarabetian *et al*. 2018, 2019), reconstruir a história evolutiva de opiliões amplamente distribuídos (Derkarabetian *et al*. 2021, Giribet *et al*. 2022) e no estudo de padrões de diversificação recente em aranhas (Hedin *et al*. 2018b, 2020, Ciaccio *et al*. 2022).

Um dos principais avanços no uso de Elementos Ultraconservados em análises filogenômicas, é a possibilidade de usar espécimes antigos depositadas em coleções históricas, e que em alguns casos possuem mais de 100 anos, para ajudar a reconstruir a história evolutiva de diferentes táxons (Yates *et. al*. 2016, Raxworthy & Smith 2021). Baseado em diferentes métodos de preservação zoológica, diferentes trabalhos utilizaram, por exemplo, DNA altamente degradado presente em peles de pássaros (Mccomarck *et. al.* 2016), em insetos alfinetados (Blaimer *et. al*. 2016) e em tecidos de aranhas (Wood *et. al.* 2018) e opiliões (Derkarabetian *et al*. 2019, 2021) armazenados em etanol 70% à temperatura ambiente. Devido aos novos métodos filogenômicos, englobados na recente área de estudo da Museômica (Guschanski *et al*. 2013, Raxworthy & Smith 2021), aproximadamente 3 bilhões de espécimes depositados em coleções biológicas estão disponíveis para contribuir com a reconstrução da história evolutiva das espécies (Yates *et. al*. 2016).

Considerando o amplo acervo de amostras recentes e antigas de Idiopinae, principalmente do gênero *Idiops,* depositadas em coleções zoológicas, as novas tecnologias de sequenciamento genético e os métodos disponíveis de análises filogenômicas a partir de sequências dos Elementos Ultraconservados, os principais objetivos deste trabalho foram testar a monofilia de Idiopinae e do gênero *Idiops* bem como reconstruir as relações filogenéticas entre os gêneros da subfamília.

MATERIAIS E MÉTODOS

Seleção das amostras

Para investigar as relações filogenéticas do grupo estudado, 30 táxons foram selecionados e tiveram regiões de DNA sequenciadas para esse estudo, dos quais 19 pertencem a espécies do gênero *Idiops*, sendo 15 provenientes de diferentes localidades da América do Sul e quatro da África (Tabela 1). Também foram incluídos representantes dos outros seis gêneros válidos de Idiopinae (*Ctenolophus, Galeosoma, Gorgyrella, Heligmomerus, Segregara* e *Titanidiops*), um de Arbanitinae (*Arbanitis* sp.) e um de Genysinae (*Neocteniza toba*), que pela primeira vez é incluído em uma filogenia molecular. Por fim, representantes de Ctenizidae (*Cteniza* sp.) e Migidae (*Moggridgea* sp.) foram sequenciados como grupos externos (Tabela 1). Entre os táxons sequenciados, 14 se referem a amostras recentes (2012-2021), preservadas em etanol > 95% e mantidas em freezer a -20 °C e 16 se referem a amostras históricas de museu (1915-2018), preservadas em etanol 70%-80% e conservadas em temperatura ambiente (Tabela 1).

Como grupos externos, também foram incluídos representantes das famílias Actinopodidae (*Actinopus* sp.), Atracidae (*Atrax* sp.), Halonoproctidae (*Cyclocosmia truncata*), Migidae (*Moggrigdea cf. crudeni*) e Euctenizidae (*Aptostichus stephencolberti* e *Promyrmekiaphila clathrate*), que tiveram o DNA sequenciado para trabalhos recentes (Bond *et al*. 2014, Hedin *et al*. 2018a). Os representantes de Ctenizidae, Halonoproctidae, Migidae e Euctenizidae foram escolhidos por também estarem incluídos no clado Domiothelina e serem proximamente relacionados a Idiopidae (Godwin *et al*. 2018, Bond *et al*. 2020, Opatova *et al*. 2020). Já os espécimes de Actinopodidae e Atracidae foram incluídos devido a presença de uma série de semelhanças morfológicas compartilhadas entre esses táxons e o gênero *Neocteniza* (Raven 1985), que apesar de pertencer a família Idiopidae, não possui seu posicionamento filogenético bem estabelecido e contém uma série de caracteres que os distinguem dos demais representantes da família Idiopidae (Raven 1985, Rossi *et al*. 2021). A árvore foi enraizada em *Cycloscomia truncata* (Halonoproctidae), família que geralmente é recuperado como uma linhagem mais antiga dentro do clado Domiothelina (Opatova *et al*. 2020).

Os espécimes aqui sequenciados pertencem as seguintes coleções zoológicas (sigla da coleção e curadores indicados entre parênteses): Coleção Aracnológica Diamantina, UNESP, Rio Claro, Brasil (**CAD**; J.P. Guadanucci), California Academy of Sciences, California, EUA (**CASENT**, L. Esposito), Coleção de História Natural, Universidade Federal do Piauí, Brasil (**CHNUFPI**, L.S. Carvalho), Facultad de Ciencias, Universidad de la República, Montevideo, Uruguai (**FCE**, M. Simó), Inventario Biológico Nacional de Paraguay, Asunción, Paraguai (**IBNP**, J.A. Kochalka), Instituto Butantan, São Paulo, Brasil (**IBSP**, A.D. Brescovit), Museu de Ciências e Tecnologia, Pontifícia Universidade Católica, Porto Alegre, Brasil (**MCTP**, R.A. Teixeira), Museum of Comparative Zoology, Harvard University, EUA (**MCZ**, G. Giribet), Museu Nacional, Universidade Federal do Rio de Janeiro, Rio de Janeiro, Brasil (**MNRJ**, A.B. Kury), Museu Paraense Emilio Goeldi, Belém, Brasil (**MPEG**, A.B. Bonaldo), Royal Museum for Central Africa – African Museum, Tervuren, Bélgica (**MRAC**, A. Henrard), Museu de Zoologia, Universidade de São Paulo, São Paulo, Brasil (**MZSP**, R. Pinto da Rocha) e National Collection of Arachnida (non-Acari), Pretoria, África do Sul (**NCA**, R. Lyle). O desenho amostral final contou com a participação e envio de amostras dos seguintes pesquisadores colaboradores: Millke Jasmine Arminini Morales (Universidade de Campinas), Robin Lyle (National Collection of Arachnida, África do Sul), Shahan Derkarabetian (Harvard University, EUA) e Vera Opatova (Charles University, Tchéquia).

Extração do DNA

O DNA de amostras frescas foi extraído usando o kit Qiagen DNeasy Blood and Tissue (Qiagen, Valencia, CA, EUA) seguindo o protocolo da fabricante, com um volume de eluição final de 150 µl. Já as amostras de museu, preservadas em etanol 70%-80%, foram extraídas seguindo o protocolo de Derkarabetian *et al*. (2019), adaptado de Tin *et al*. (2014), que segue uma abordagem que utiliza esferas magnéticas à base de sílica, projetadas especificamente para extração não destrutiva de DNA de amostras degradadas. Para cada amostra, o DNA foi extraído do tecido muscular presente nas pernas, que variaram de uma a três a depender do tamanho do espécime e da idade da amostra. Antes das extrações de DNA, o tecido foi colocado em H_2O destilada

durante a noite a 4°C para facilitar a remoção do etanol. As extrações das amostras de museu foram realizadas em capela de fluxo laminar, por maceração com pilões descartáveis estéreis, gerando um volume final de 50 µl de material extraído. Todas as extrações foram quantificadas e tiveram a integridade do material genômico avaliada usando um fluorômetro Qubit (Thermo Fisher Scientific). As extrações do DNA das amostras ocorreram nas dependências do Museu de Zoologia Comparada da Universidade de Harvard e foram realizadas pelo colaborador Dr. Shahan Derkarabetian.

Preparação e enriquecimento das bibliotecas de UCE e sequenciamento

As bibliotecas de captura de sequências de UCEs foram preparadas e enriquecidas seguindo o protocolo de trabalhos anteriormente publicados com aracnídeos, como Starrett *et al*. (2017), Derkarabetian *et al*. (2019), Hedin et al. (2018a, 2019) e Kulkarni *et al*. (2019). Em suma, esse processo consiste em sete etapas principais: 1) quantificação do DNA; 2) ligação dos adaptadores; 3) amplificação por Reação em Cadeia da Polimerase (PCR - *Polymerase Chain Reaction)* e agrupamento inicial de amostras; 4) enriquecimento híbrido; 5) amplificação das bibliotecas enriquecidas; 6) quantificação e montagem de um *pool* final de amostras; e 7) seleção do tamanho e quantificação final (Zhang *et al*. 2019, Anderman *et al*. 2020). Para a preparação das bibliotecas, até 500 ng de DNA extraído das amostras frescas ou que tinham < 20 anos foram sonicadas em em um volume final de 130 µl com o ultrasonicador modelo S220 (*Covaris*), usando as configurações padrão para um pico alvo de 500 pb (pares de bases). Os espécimes de museu com mais de 20 anos não passaram pelo processo de sonicação devido à fragmentação do material genômico inerente a este tipo de armazenamento de amostra. O enriquecimento do DNA foi realizado usando o conjunto de sondas de UCEs disponíveis no kit myBaits UCE Spider 2Kv1 (ver. 1, *Arbor Biosciences*; Kulkarni *et al*. 2019). A preparação e enriquecimento das bibliotecas *paired-end* e o sequenciamento do DNA, realizado em sequenciador automático HiSeq 2500 da plataforma Illumina (*Illumina, Inc.*) e que gerou fragmentos curtos de sequências de DNA com 125 pb, foi realizado pela empresa Rapid Genomic LLC, Flórida, EUA.

Tabela 1: Informações sobre as amostras sequenciadas, incluído identificação de vouchers, país, localidade, ano de coleta e idade das amostras. A linha tracejada separa as amostras frescas (acima da linha) das amostras de museu sequenciadas (abaixo da linha)

Espécie	Família	Voucher	País	Localidade	Ano de coleta	Idade (anos)
***Ctenolophus* sp.**	Idiopidae	MGL00092	África do Sul	KwaZulu-Natal, Pietermariezburg	2015	7
Gorgyrella namaquensis	Idiopidae	NCA 2017/1894	África do Sul	Eastern Cape, Willowmore	2017	5
***Heligmomerus* sp.**	Idiopidae	NCA 2021/1142	África do Sul	Limpopo, Soutpansberg District	2013	9
Idiops aff fryi	Idiopidae	NCA 2021/1143	África do Sul	Gauteng, Ezemvelo Nature Reserve	2012	10
Idiops camelus	Idiopidae	CAD 1274	Brasil	São Paulo, Santo André,	2018	4
Idiops fuscus	Idiopidae	CHNUFPI 3391	Brasil	Piauí, Coronel José Dias	2012	10
Idiops pirassununguensis	Idiopidae	CAD 833	Brasil	Minas Gerais, Santana do Riacho	2018	4
Idiops pretoriae	Idiopidae	NCA 2021/1140	África do Sul	Gauteng, Wonderboom District	2012	10
Idiops rohdei	Idiopidae	IBNP 2444	Paraguai	Amanbay, Pedro Juan Caballero	2019	3
Segregara cf. transvaalensis	Idiopidae	NCA 2021/1141	África do Sul	Gauteng, Ezemvelo Nature Reserve	2012	10
***Titanidiops* sp.**	Idiopidae	MGL00094	Marrocos	Foum Jemaa	2021	1
Neocteniza toba	Idiopidae	CAD 787	Brasil	São Paulo, Rio Claro	2018	3
***Cteniza* sp.**	Ctenizidae	MGL00053	Itália	Terranova di Sibari	2019	3
***Moggridgea* sp.**	Migidae	MGL00091	África do Sul	Amanzi, Free State	2015	7
***Galeosoma* sp.**	Idiopidae	MCZ70980	África do Sul	Gauteng, Mayville, Pretoria	1915	107
Idiops carajas	Idiopidae	MCTP 11192	Brasil	Mato Grosso, Chapada dos Guimarães	2000	22
Idiops clarus	Idiopidae	FCE 0341	Uruguai	Montevidéu, Parque del Padro	2002	20
Idiops curvicalcar	Idiopidae	MRAC 139.309	Rep. Dem. do Congo	Kanonga, Parc National de l'Upemba	1947	75
Idiops duocordibus	Idiopidae	CAS 9036910	Peru	Huánuco, Tingo María	1954	68
Idiops germaini	Idiopidae	MNRJ	Brasil	Rio de Janeiro, Nova Iguaçú	2004	18
Idiops guri	Idiopidae	MCTP 20798	Brasil	Rio Grande do Sul, Itaara	2007	15
Idiops kanoganus	Idiopidae	MRAC 139.283	Rep. Dem. do Congo	Kanonga, Parc National de l'Upemba	1947	75
Idiops nilopolensis	Idiopidae	MNRJ	Brasil	Rio de Janeiro, Nova Iguaçú	2004	18
Idiops petiti	Idiopidae	IBSP 218868	Brasil	Pará, Belterra	2010	12
Idiops rastratus	Idiopidae	MZSP 27675	Brasil	Bahia, Una	1999	23
Idiops sertania	Idiopidae	IBSP 227617	Brasil	Ceará, Crato	2018	4
***Idiops* sp.n.2**	Idiopidae	MPEG 2583	Brasil	Amazonas, Jutaí	2008	14
***Idiops* sp.n.3**	Idiopidae	CAS 9032481	Equador	Napo, Alinahui	1995	27
Titanidiops constructor	Idiopidae	CAS 9036909	Índia	Andhra Pradesh, Tirupatti	1962	60
Arbanitis sp.	Idiopidae	CAD	Austrália	Austrália, Mont Baw Baw Village	1976	46

Análises bioinformáticas e filogenômicas

A maior parte das análises de bioinformática, que vai da limpeza dos dados brutos até a montagem das matrizes finais, foi realizado através do pacote de softwares Phyluce 1.7.1 (Faircloth 2016), seguindo o tutorial disponível no site do desenvolvedor (https://phyluce.readthedocs.io) com adaptações sugeridas pelo colaborador Dr. Shahan Derkarabetian. Primeiro, através da ferramenta Illumiprocessor, foi realizada a remoção dos adaptadores e o controle inicial de qualidade dos fragmentos sequenciados (Faircloth 2013). Após esta etapa de limpeza, os fragmentos processados foram então montados (*assembly*) através dos softwares SPAdes 3.15.4 (Bankevich *et al*. 2012) e ABySS 2.1.5 (Simpson *et al*. 2009). Os *contigs* gerados em ambos os montadores utilizados foram combinados em um único arquivo por espécime, a fim de ampliar o número de UCEs recuperados (Derkarabetian *et al*. 2018, 2019, 2021, Hedin *et al*. 2018a). Para identificação dos *contigs* contendo os UCEs de interesse foi utilizada uma cobertura e identidade mínima de 65%.

Após a seleção dos *contigs*, as sequências foram alinhadas através do software MAFFT 7 (Katoh & Standley, 2013), usando as configurações padrão, e então os alinhamentos foram processados utilizando o gBlocks (Castresana, 2000, Talavera & Castresana, 2007), usando as seguintes configurações: -b1 0.5, -b2 0.5, -b3 6, -b4 6. Para filtrar e remover sequências divergentes não homólogas (< 70% de similaridade) e muito pequenas (< 50 pares de bases) para cada alinhamento, foi utilizado o software CIAling (Tumescheit *et al*. 2022). Todos os *loci* foram manualmente inspecionados no software Geneious Prime 2022 (https://www.geneious.com), e apenas os *loci* com pelo menos 50% de cobertura taxonômica foram retidos em uma matriz concatenada para as análises filogenéticas. Todas as análises de bioinformática foram realizado com recursos computacionais disponibilizados pelo Núcleo de Computação Científica (NCC/GridUNESP) da Universidade Estadual Paulista (UNESP).

A partir das matrizes de dados geradas, foram realizadas análises de Máxima Verossimilhança dos dados concatenados usando o software RAXML v. 8 (Stamatakis 2014; https://cme.h-its.org/exelixis/web/software/raxml/), com os dados particionados por *locus*, modelo de substituição GTR+GAMMA e suporte estimado por 200 pseudoréplicas de *bootstrap.* Análises não particionadas de Máxima

Verossimilhança adicionais também foram conduzidas no IQ-TREE (Nguyen *et al*. 2014, http://www.iqtree.org/), que permite a definição do melhor modelo evolutivo a partir do ModelFinder (Kalyaanamoorthy *et al*. 2017). Os valores de suporte foram inferidos via teste SH-aLRT (Anisimova *et al*. 2011) e via *Ultrafast Bootstrap* (Minh *et al*. 2013), ambos com 1000 pseudoréplicas. As árvores filogenéticas foram visualizadas no Software FigTree v. 1.4.3 e editadas no Photoshop CC2018.

Devido à natureza das amostras de museu, que geralmente resgatam menos *loci* de UCEs e que podem refletir em topologias de árvores filogenéticas com baixo suporte (Derkarabetian *et al*. 2019), foram gerados e analisados uma série de *datasets*, baseados em matrizes que continham entre 17 e 35 táxons e apresentaram diferentes proporções de amostras frescas e principalmente amostras de museu. Por fim, foi selecionada a hipótese filogenética que apresentou a topologia mais estável e que possuía os melhores valores de suporte de ramo, baseada em uma matriz de 29 táxons, dos quais 13 se referem a amostras frescas, 10 a amostras de museu e 6 a espécimes previamente sequenciados (Bond *et al*. 2014, Hedin *et al*. 2018a).

Análises de Reconstrução de Caracteres Ancestrais

Para realizar as análises de Reconstrução de Caracteres Ancestrais (RCA), primeiro foram selecionados os quatro principais caracteres morfológicos discretos usualmente utilizados para diagnosticar os espécimes da subfamília Idiopinae e distingui-los em diferentes gêneros: disposição ocular, padrão de dentição das quelíceras, presença de espínulos das coxas e quantidade de sigilas esternais (Raven 1985, Dippenaa-Schoeman 2002, Fonseca-Ferrera et al., 2021). Em seguida, foram examinados uma série de exemplares de Idiopinae, com foco nos táxons africanos, incluindo material-tipo de algumas espécies de *Idiops*, *Gorgyrella*, *Heligmomerus*, *Segregara* e *Titanidiops*, atualmente emprestados ao Instituto Butantan (IBSP). Os tipos e demais espécimes africanos examinados pertencem as seguintes coleções: The Natural History Museum, Londres, Reino Unido (**BMNH** J. Beccaloni), KwaZulu-Natal Museum, Pietermaritzburg, África do Sul (**NM**, J. Plisko), National Collection of Arachnida (non-Acari), Pretoria, África do Sul (**NCA**, R. Lyle), Royal Museum for Central Africa – African Museum, Bérgica (**MRAC**, A. Henrard) e Ditsong National

Museum of Natural History, Pretoria, África do Sul (**TM**, T. Bird). Também foram examinados alguns espécimes neotropicais, previamente revisados por Fonseca-Ferreira *et al.* (2021), incluindo um exemplar da espécie-tipo de *Idiops*, *I. fuscus*. Todas as aranhas examinadas foram fotografadas com o auxílio de um estereomicroscópio Leica M205C equipado com uma câmera digital Leica DFC295.

Para inferir a evolução dos traços morfológicos selecionados, os estados para cada um dos caracteres foram codificados em uma matriz no software Mesquite v. 3.51 (Maddison & Maddison 2021). A codificação dos caracteres para cada um dos táxons incluídos na filogenia foi baseada na análise dos espécimes examinados nesse estudo ou em dados disponíveis na literatura (Gertsch & Platnick 1975, Griswold 1987, Stockman & Bond 2008, Bond 2012, Decae *et al*. 2019, Miglio *et al*. 2020). As análises de Reconstrução dos Caracteres Ancestrais foram realizadas no software Mesquite v. 3.51 a partir de métodos de máxima verossimilhança, usando o modelo estruturado de Markov (Lewis 2001). Baseado na topologia gerada nas análises filogenômicas e nos dados morfológicos codificados, este método encontra para cada nó ancestral, o estado que maximiza a probabilidade de chegar aos estados observados nos táxons terminais (Maddison & Maddison 2021, https://mesquiteproject.org/). Como resultado, foram apresentadas árvores ultramétricas, que possuem em cada nó um diagrama de pizza com as probabilidades relativas de cada um dos estados definidos.

RESULTADOS

Estatísticas associadas aos UCEs

Das 30 amostras selecionadas, 29 tiveram o DNA sequenciado com sucesso. Apenas o espécime *I. nilopolensis*, que teve 608 ng de DNA extraído (152 ng/mL), falhou em alguma etapa do sequenciamento. Informações sobre a concentração inicial e input de DNA, número de fragmentos (*reads*) gerados, total de pares de bases, número e comprimento médio de *contigs* e quantidade de UCEs recuperados na matriz inicial e final são apresentados para cada uma das amostras incluídas na matriz, composta por 29 táxons (tabela 2).

Tabela 2: Tabela resumo com os dados gerados na extração do DNA e nas análises bioinformáticas. A linha tracejada separa as amostras frescas (acima da linha) das amostras de museu (abaixo da linha). A linha sólida separa as amostras sequenciadas para esse estudo das amostras sequenciadas em trabalhos anteriores.

Espécie	DNA (ng/uL)	Input DNA (ng)	Nº de reads (QC)	Pares de bases (pb)	Nº de contigs	Comp. médio (pb)	UCE loci (inicial)	UCE loci (final)
***Ctenolophus* sp.**	43.4	5991.7	7544344	1529490120	209125	149.038	1717	705
Gorgyrella namaquensis	17,5	2417.3	3719022	601446752	167568	92.925	1682	670
***Heligmomerus* sp.**	32.15	4437.5	3210658	496727773	129785	94.251	1663	674
Idiops aff fryi	17.88	2467.5	1266721	193939739	58017	99.759	1583	749
Idiops camelus	16.12	612.7	187336	26127665	690	93.123	28	24
Idiops fuscus	13.52	514.1	10108	1627867	72	131.305	13	8
Idiops pirassununguensis	16.9	611.7	4703998	853719616	52236	108.445	1406	714
Idiops pretoriae	14.51	2003.4	118773	16871710	6464	108.187	1132	679
Idiops rohdei	6.67	253.5	5845888	891027342	39922	105.031	1388	706
Segregara cf. transvaalensis	6.02	831.4	2318148	363169914	89943	95.036	1633	702
***Titanidiops* sp.**	34.4	4747.7	3571184	673594691	127256	128.741	1638	743
Neocteniza toba	11.21	426	10327489	1829924452	25402	150.902	749	319
***Cteniza* sp.**	48.66	6854.4	3367153	675643421	71041	163.871	1719	778
Idiops carajas	4.98	189.4	3107036	380661100	21097	91.044	907	556
Idiops clarus	6.13	233.3	2709077	289714202	13512	85.622	765	481
Idiops germaini	3.16	120.4	400924	53280380	2280	98.57	528	360
Idiops guri	3.84	146	2254282	267146650	12478	97.905	865	532
Idiops kanoganus	7.39	280.9	1320897	157463842	8421	90.156	778	507
Idiops petiti	31.18	1184.9	4095172	616107629	45585	93.054	1527	722
Idiops rastratus	5.41	205.9	10211540	1277196664	67061	75.18	648	419
Idiops sertania	3.18	121.1	634226	70575855	1832	81.224	53	36
***Idiops* sp.n.2**	20.24	769.5	4548113	729860766	51324	97.346	1385	689
***Idiops* sp.n.3**	4.22	160.6	3351172	455310062	24095	80.658	804	513
***Actinopus* sp.**	Hedin *et al* . (2018)						112	76
Aptostichus stephencolberti	Bond *et al.* (2014)						656	283
***Atrax* sp.**	Hedin *et al* . (2018)						95	75
Cyclocosmia truncata	Bond et al. (2014)						1051	475
Moggridgea cf. crudeni	Hedin *et al* . (2018)						212	114
Promyrmekiaphila clathrate	Bond *et al* . (2014)						899	403

A matriz inicial (não filtrada e não inspecionada) foi composta por 1907 *loci* de UCEs, que juntos totalizaram 358.190 pares de bases (comprimento médio de 186 pb), dos quais 51.713 se referem a sítios parcimoniosamente informativos. Cada *locus* de UCE foi alinhado em uma média de 12,64 táxons. Quando consideradas todas as 29 amostras, houve uma correspondência de cerca de 952 UCEs brutos por amostra. Quando analisadas separadamente, as amostras frescas sequenciadas (n = 13) recuperaram em média 1.257 UCEs, enquanto as amostras de museu (n = 10) recuperaram uma média de 826 UCEs.

Já a matriz final, baseada em uma cobertura de táxon de 50% (≥ 14 táxons alinhados por *locus*) e utilizada para as análises filogenéticas subsequentes, incluiu 832 *loci* de UCEs, que totalizaram 124.016 pb, com comprimento médio de 124 pb e 23.809 sítios parcimoniosamente informativos. Cada *locus* de UCE foi alinhado em uma média de 16,09 táxons. Uma média de 575 UCEs foram recuperados para as amostras recentes (n = 13), contra 471 UCEs para as amostras de museu (n = 10) na matriz final utilizada. Apesar da maioria das amostras sequenciadas terem resultado em milhares de *contigs*, algumas amostras incluídas no *dataset* final, como *I. fuscus*, *I. camelus* e *I. sertania*, tiveram um baixo número de fragmentos sequenciados, o que refletiu em um baixo número de *contigs* montados e com UCEs recuperados.

Na tabela 3 são apresentados os dados obtidos para as seis amostras inicialmente sequenciadas e processadas nas análises bioinformáticas, mas que não foram incluídas no *dataset* final, devido ao baixo número de UCEs. Entre estas amostras não incluídas na matriz final, destaque especial é dado ao gênero *Arbanitis*, representante da subfamília Arbanitinae, que apesar de ter seu posicionamento bem estabelecido em filogenias anteriores (Rix *et al*. 2017b, Opatova *et al*. 2020), foi recuperado incorretamente dentro de Idiopinae em algumas análises preliminares realizadas, sendo assim removido das análises.

Tabela 3: Tabela resumo com os principais dados gerados na extração do DNA e no processamento dos dados filogenômicos das seis amostras sequenciadas, mas não incluídas na filogenia final.

Espécie	DNA (ng/ml)	Input DNA (ng)	Nº de reads (QC)	Nº de contigs	Comp. médio (pb)	UCE loci (inicial)
***Arbanitis* sp.**	12.77	485.3	990647	3023	72.266	**11**
***Galeosoma* sp.**	30.7	1167	2793889	9570	78.555	**221**
Idiops curvicalcar	1.39	53	4990038	8234	95.321	**95**
Idiops duocordibus	0.87	33.3	1301586	6537	74.878	**12**
***Moggridgea* sp.**	71.44	9859.5	680	88	130.25	**21**
Titanidiops constructor	1.7	74.24	1628098	4747	80.56	**38**

Filogenômica e Reconstrução de Caracteres Ancestrais

As análises de Máxima Verossimilhança geradas no RAXML e no IQ-TREE, baseadas em uma matriz concatenada composta por 832 sequências de UCEs recuperados para 29 táxons, apresentaram uma mesma topologia final, mas com diferentes valores de suportes para alguns nós da árvore (Figura 2). Segundo o ModelFinder (Kalyaanamoorthy *et al*. 2017), o modelo evolutivo de substituição de bases mais adequado nas análises no software IQ-TREE foi o GTR + F + I + G4 (LogL: - 600.315,02, AICc: 1.200.760,12).

Baseado nos altos valores de suporte de ramo recuperados, essas análises corroboram o monofiletismo de Idiopinae (suporte de ramo = 100) e das espécies Neotropicais de *Idiops* (suporte de ramo > 80). Pela primeira vez os resultados também sustentam que tanto o gênero *Idiops* (suporte de ramo > 80) quanto a família Idiopidae (suporte de ramo > 90) formam grupos parafiléticos. As análises de Reconstrução de Caracteres Ancestrais realizadas para todos os caracteres analisados, suportaram morfologicamente as relações resgatadas na hipótese filogenética gerada pelas análises filogenômicas, que são analisadas em detalhes na discussão (Figuras 3-6).

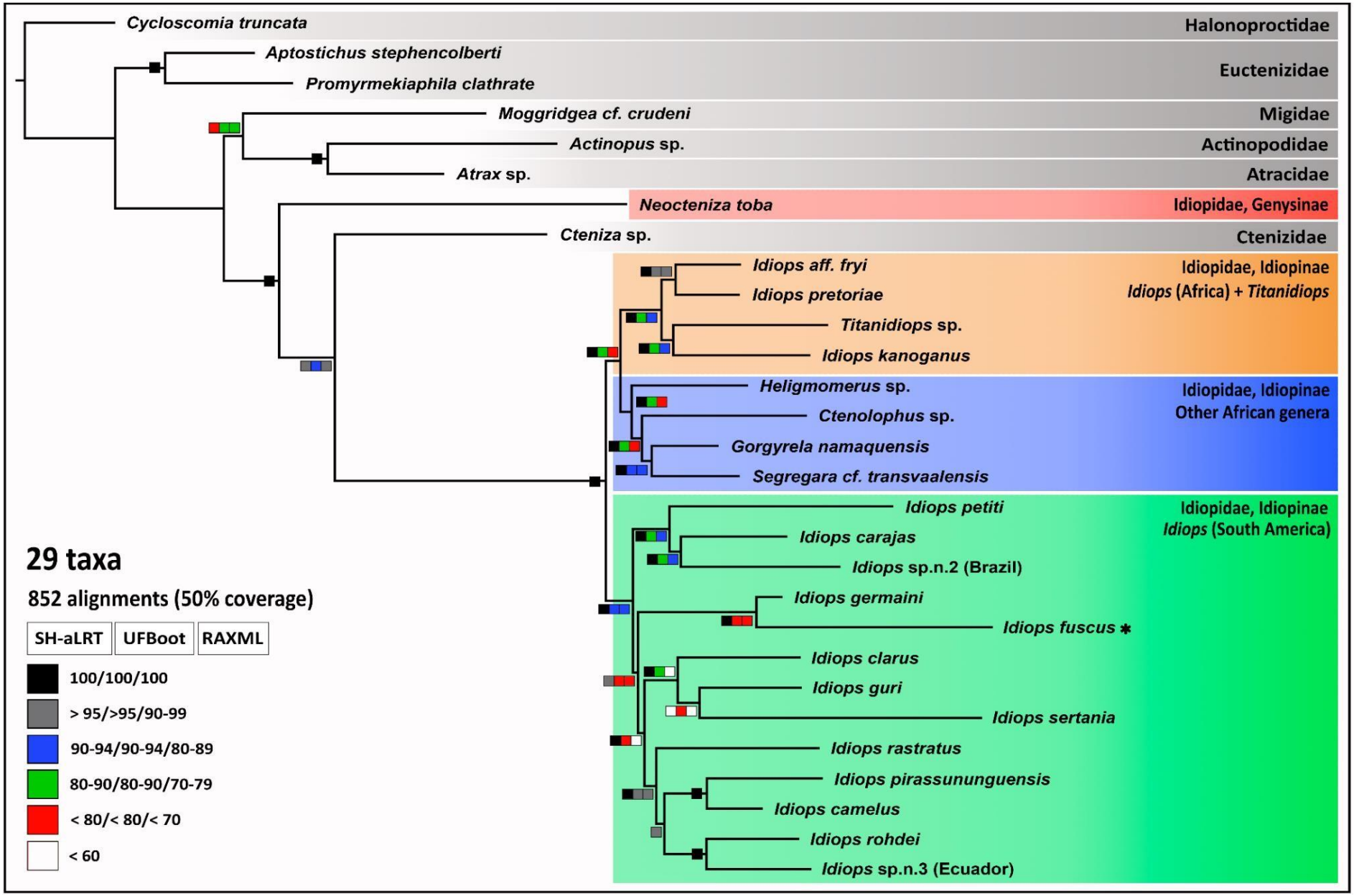

Figura 2: Filogenia gerada a partir de análises de Máxima Verossimilhança. O asterisco indica a espécie tipo de *Idiops*, *I. fuscus*. As caixas indicam os valores de suporte obtidos em cada abordagem (da esquerda para a direita): valores de suporte IQ-Tree SH-aLRT, IQ-Tree Ultrafast Bootstrap e RAXML. O código de cores das caixas corresponde a diferentes categorias de nível de suporte.

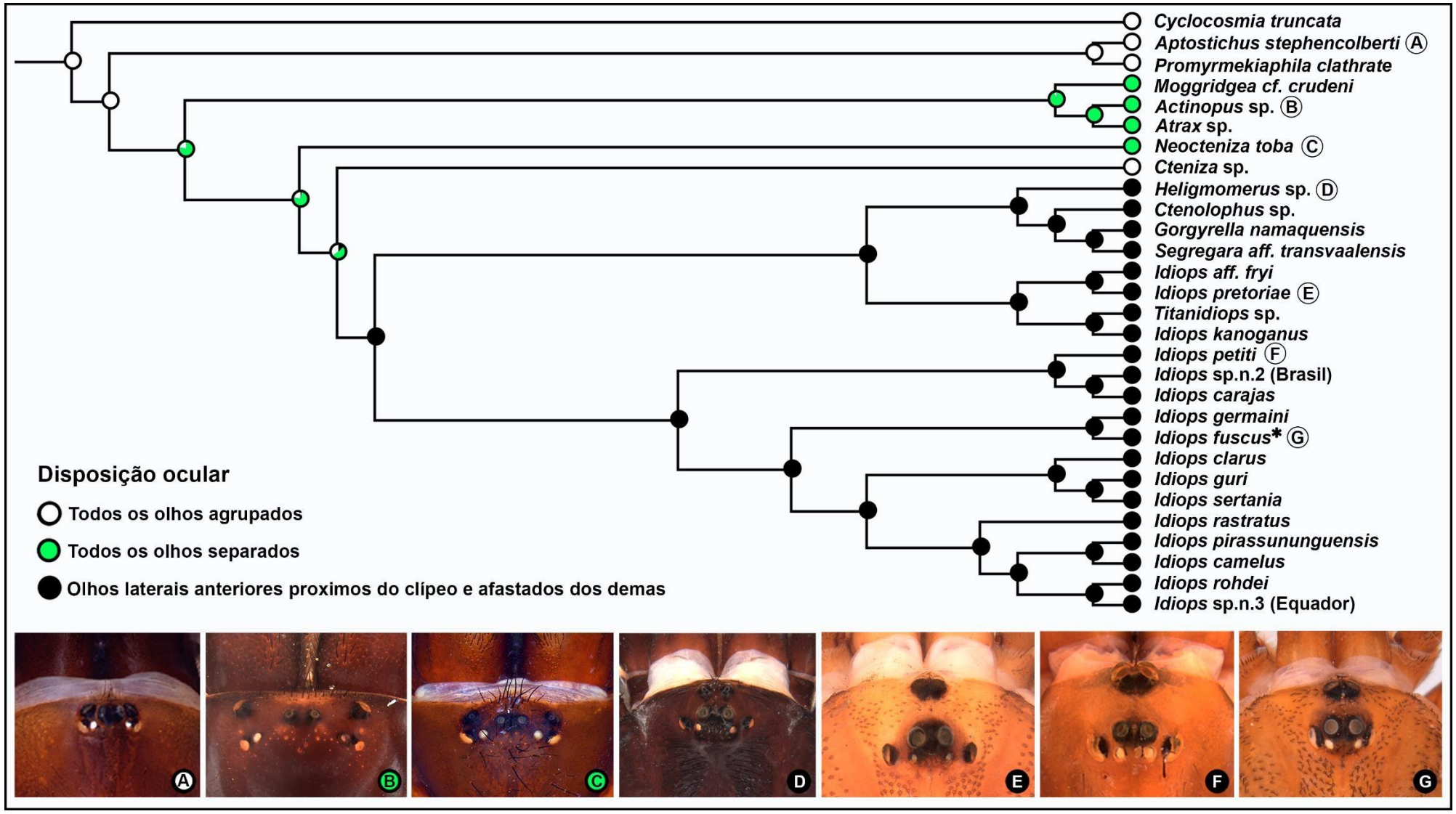

Figura 3: Reconstrução dos caracteres ancestrais para a disposição ocular.

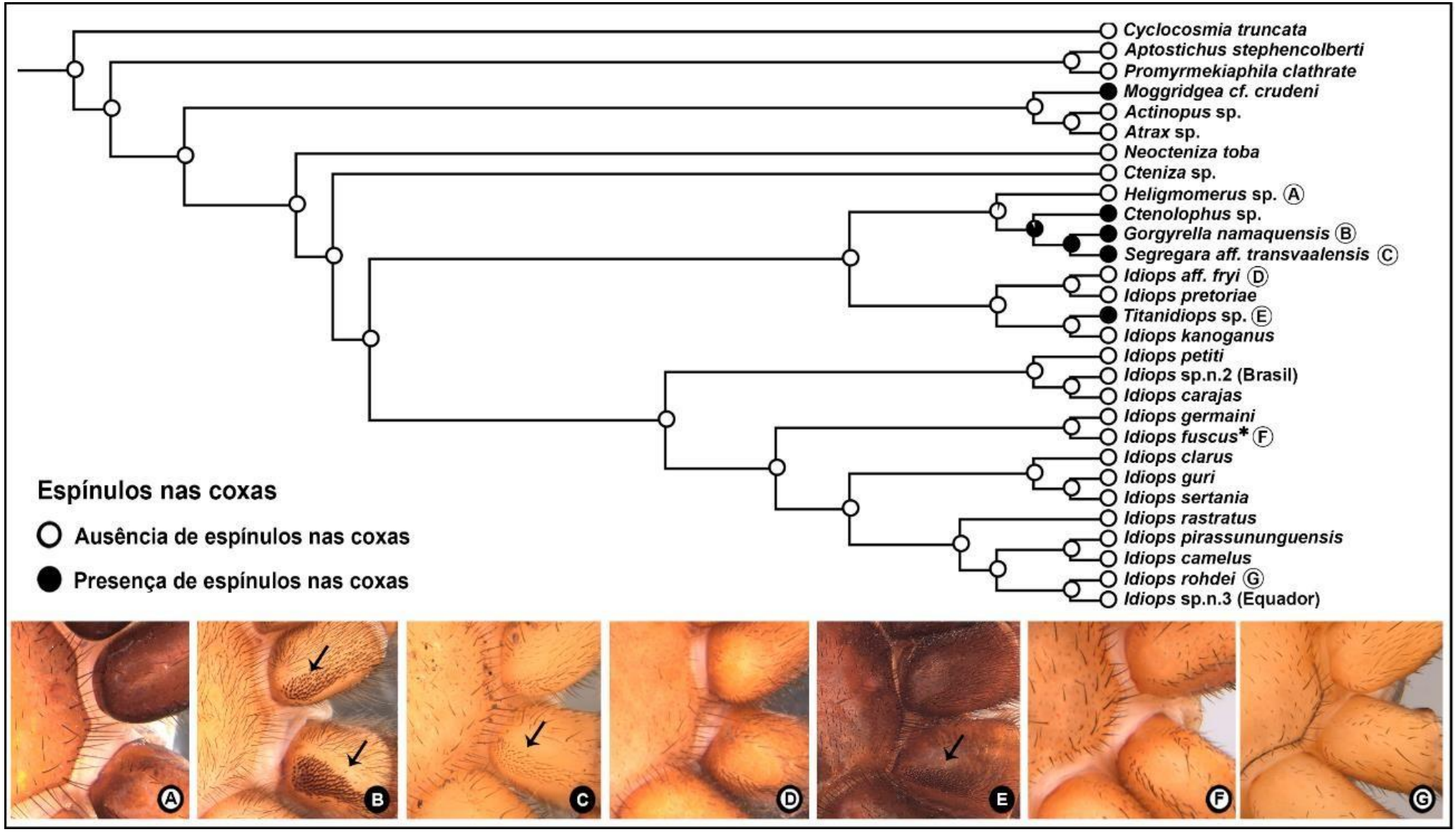

Figura 4: Reconstrução dos caracteres ancestrais para espínulos coxais.

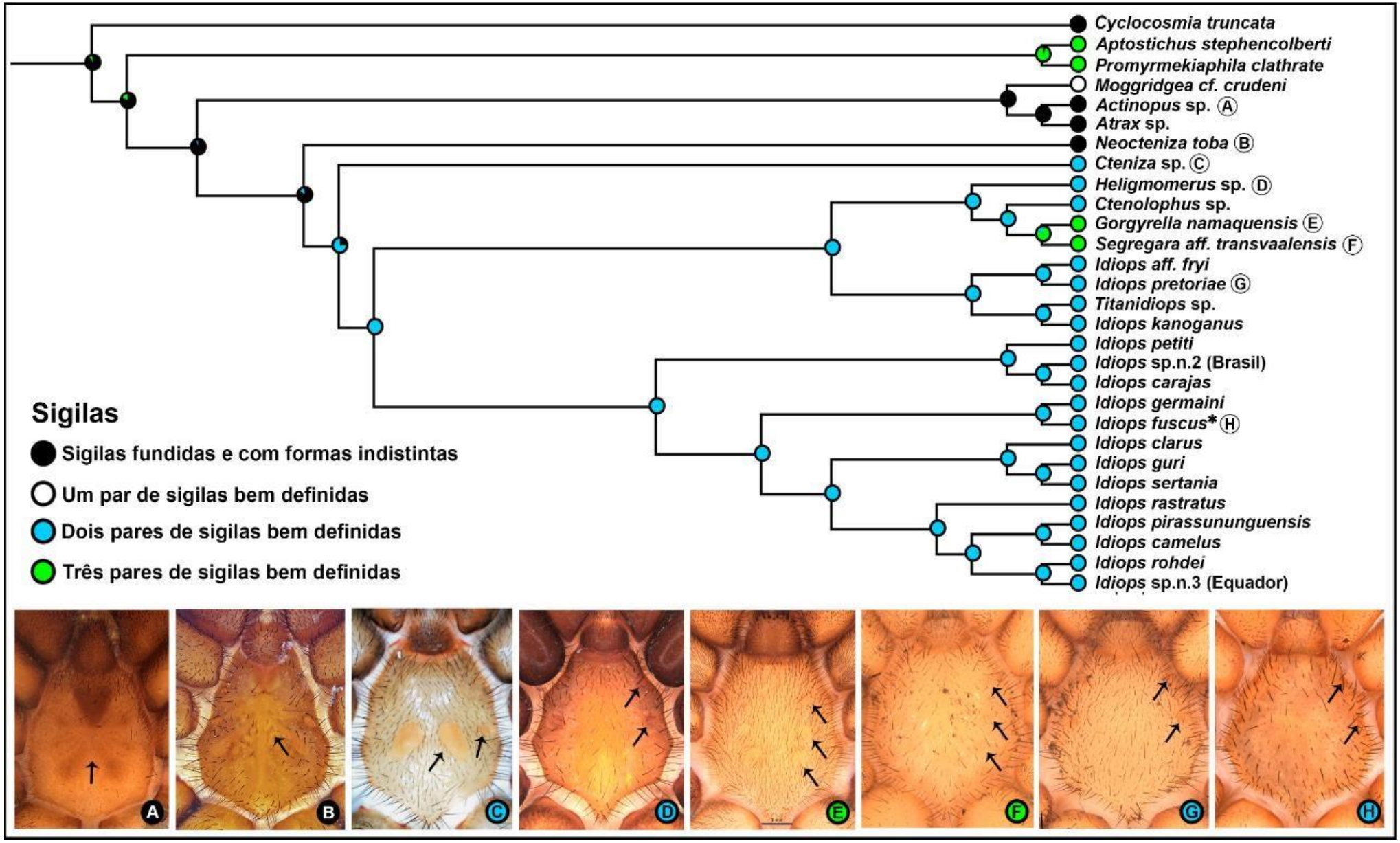

Figura 5: Reconstrução dos caracteres ancestrais para as sigilas esternais.

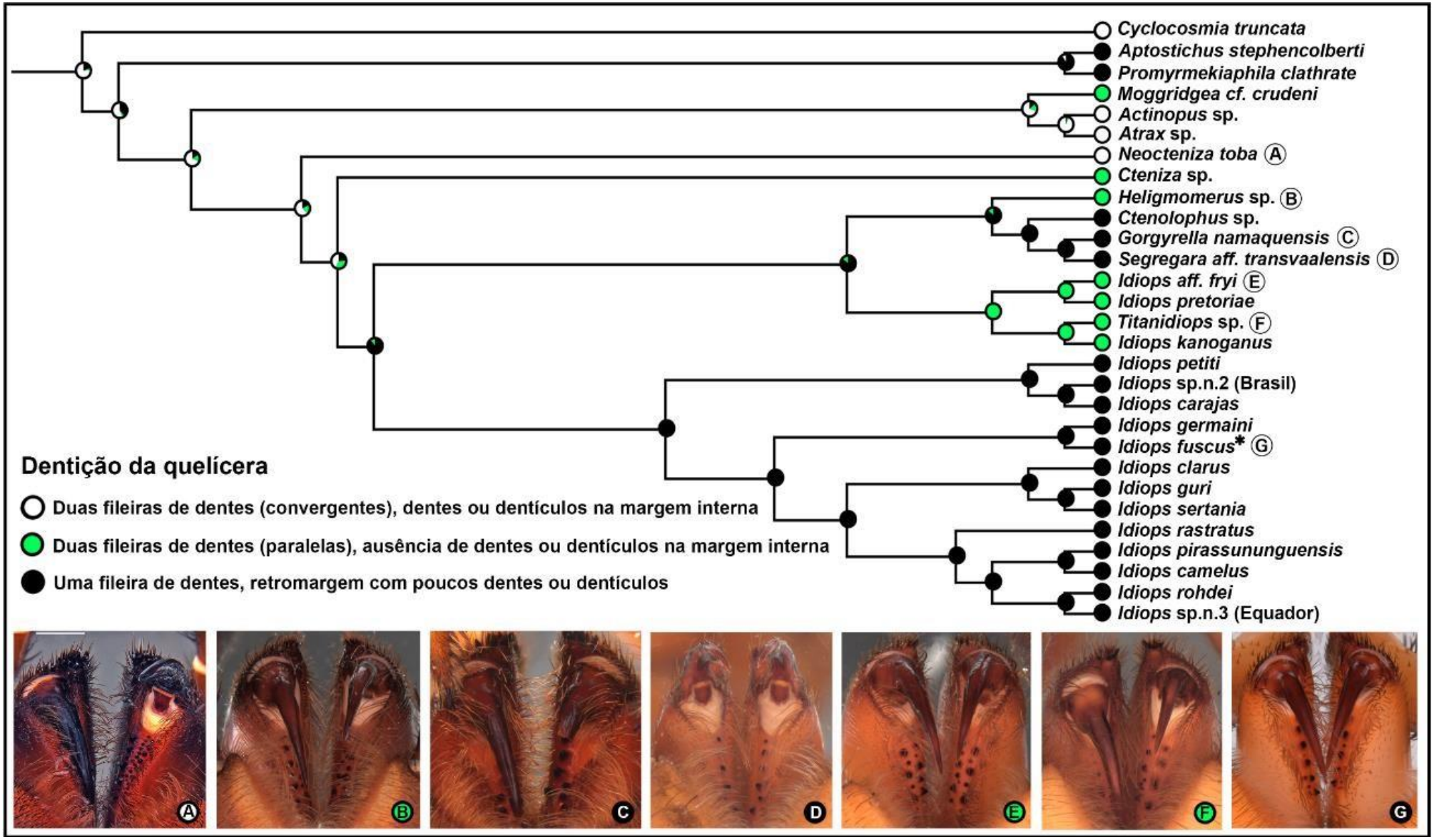

Figura 6: Reconstrução dos caracteres ancestrais para a dentição das quelíceras.

DISCUSSÃO

Os dados apresentados nesse trabalho são resultantes das primeiras análises filogenômicas focada na família Idiopidae, que contou com a mais abrangente amostragem focada na subfamília Idiopinae e no gênero *Idiops,* incluindo dez amostras de museu, com idades que variaram de 4 a 75 anos (Tabela 1). Além disso, este é o primeiro estudo filogenético a conter espécimes Neotropicais de *Idiops*, com foco nas espécies brasileiras, incluindo um representante da espécie-tipo do gênero (*I. fuscus*) (Tabela 1). Até a realização deste trabalho, todas as filogenias moleculares anteriores publicadas, que incluíram espécimes de *Idiops,* haviam contado apenas com representante africanos para o gênero (Hedin & Bond 2006, Hamilton *et al*. 2016 Godwin *et al*. 2018, Kulkarni *et al*. 2019, Bond *et al*. 2020, Opatova *et al*. 2020).

Devido à dificuldade em coletar espécimes de *Idiops* em campo, graças aos seus hábitos crípticos (Dippenaar-Schoeman 2002, Fonseca-Ferreira *et al*. 2021), e à escassez de tecidos para o gênero devidamente armazenados para análises moleculares em coleções zoológicas, a incorporação das amostras de museu foi fundamental para a realização das análises filogenômicas e para a reconstrução da história evolutiva do gênero. Assim como observado em trabalhos anteriores que incluíram amostras de museu (Blaimer *et al*. 2016, Wood *et al*. 2018, Derkarabetian *et al*. 2019), foi constatado que as amostras mais antigas incluídas, armazenadas em álcool 70% e em temperatura ambiente e consequentemente com material genômico mais fragmentado, em geral tiverem menos DNA sequenciado e recuperaram menos UCEs do que as amostras recentes armazenadas adequadamente para estudos moleculares (Tabelas 2 e 3). Apesar disso, a inclusão destas amostras nas análises filogenômicas, proporcionou a incorporação de espécimes com uma distribuição espaço-temporal que dificilmente poderiam ser utilizados em estudos focados em filogenias moleculares (Yeates *et al*. 2016, Young & Gillung 2020, Raxworthy & Smith 2021).

Entre os gêneros de Idiopinae, apenas o gênero *Galeosoma* não foi incluindo na filogenia final, que apesar de ter recuperado um número considerável de UCEs (221 *loci*), em geral apresentou sequências com alta proporção de *gaps*, possivelmente devido à natureza altamente degradada do

DNA da amostra, um exemplar tipo de 107 anos.

Relacionamento filogenético em Idiopinae e *Idiops*

A subfamília Idiopinae representa um grupo muito uniforme e distinto de aranhas de alçapão (Raven 1985), que sempre teve sua monofilia sustentada tanto em filogenias morfológicas (Raven 1985, Yamamoto 2013) quanto moleculares (Hedin & Bond 2006, Opatova *et al*. 2020). Devido a isso, era de se esperar que o clado fosse resgatado como monofilético nas análises baseadas em UCEs (Figura 2). Além dos resultados moleculares, o monofiletismo do clado também foi embasado pela RCA da disposição ocular, (Figura 3), que sustentou como caractere diagnóstico mais evidente da subfamília a posição dos Olhos Laterais Anteriores, que são afastados dos demais e posicionados próximo ao clípeo (Figura 3D-G, Raven 1985).

Segundo a topologia resultante, Idiopinae é dividida em dois clados principais geograficamente estruturados, um primeiro clado composto por todos os táxons africanos analisados, incluindo os espécimes africanos de *Idiops*, que a partir de agora serão referidos como "*Idiops*" e um segundo composto pelos espécimes Neotropicais de *Idiops* (Figura 2). De acordo com essa hipótese filogenética, os espécimes africanos estão divididos em dois grupos, um formado por *Heligmomerus* (*Ctenolophus* (*Gorgyrella* + *Segregara*) e o outro composto por "*Idiops*" + *Titanidiops*.

A relação entre os gêneros incluídos no clado composto por *Heligmomerus*, *Ctenolophus*, *Gorgyrella* e *Segregara*, que em geral apresentou altos valores de suporte de ramo (Figura 2), já havia sido proposto em trabalhos anteriores, a partir de topologias parcialmente distintas (Raven 1985, Dippenaar-Schoeman 2002, Hedin & Bond 2006, Opatova *et al*. 2020). Segunda a filogenia proposta por Raven (1985), *Gorgyrella* e *Heligmomerus* compartilham a presença de um processo estreito na porção distal das quelíceras (não analisado neste trabalho). Já segundo Dippenaar-Schoemann (2002), *Ctenolophus*, *Gorgyrella* e *Segregara* compartilham a presença de faixas de espínulos nas coxas e *Gorgyrella* e *Segregara* a presença de três pares de sigilas, diferente dos demais gêneros, que possuem dois pares. A relação entre esses dois últimos gêneros, também pode ser observada na filogenia molecular proposta por Hedin & Bond (2006). Tanto a presença de espínulos nas coxas (Figura 4), que foi

recuperado de forma independente em *Titanidiops,* quanto a presença de três pares de sigilas no esterno (Figura 5) também foram sustentadas nas análises de Reconstrução de Caracteres Ancestrais realizadas nesse trabalho. Como observado por Dippennaar-Schoeman (2002) e confirmado pela Figura 5, *Gorgyrella* e *Segregara* se diferenciam pelo tamanho e posição do terceiro par de sigilas, que são menores e localizadas próximas das margens do esterno em *Segregara* e maiores e mais centralizadas em *Gorgyrella*. Por fim, como observado na RCA do padrão de dentição da quelíceras (Figura 6), o clado composto por *Ctenolophus*, *Gorgyrella* e *Segregara*, compartilham o mesmo padrão de dentição, que se caracteriza pela presença uma fileira completa de dentes na retromargem e poucos dentes ou dentículos concentrados no terço basal da promargem.

Apesar de apenas três espécimes africanos de "*Idiops"* terem sido incluídos na hipótese filogenética final (*I. fryi*, *I. kanoganus* e *I. pretorieae*), eles foram suficientes para demonstrar a parafilia do gênero *Idiops*, ao serem recuperados como filogeneticamente mais relacionados com os demais gêneros africanos de Idiopinae, mais especificamente de *Titanidiops*, do que com os espécimes neotropicais de *Idiops* incluídos nas análises. Esta divisão de *Idiops* em dois clados também é suportada pelos padrões distintos de dentição das quelíceras, como observado na RCA desse caractere (Figura 6). Segundo a RCA, *Titanidiops* e "*Idiops*" compartilham a presença de duas fileiras de dentes nas quelíceras, que ocupam toda a retromargem e a promargem (Figura 4). Esses dois táxons também se assemelham por possuírem dois pares de sigilas, mas se diferenciam pela presença de espínulos nas coxas de *Titanidiops*.

Historicamente o gênero *Idiops* sempre teve como caracter diagnóstico a presença de duas fileiras de dentes nas quelíceras, que foi utilizado para descrever as espécies africanas de *Idiops,* descritas em sua maioria antes de 1940 (World Spider Catalog 2023), codificar caracteres para análises filogenéticas (Raven 1985), elaborar chaves taxonômicas (Raven 1985, Dippenaar-Schoeman 2002, Mirza *et al*. 2012) e descrever espécies recentes, principalmente na Índia (Siliwall *et al*. 2005, Mirza *et al*. 2012, Gupta *et al*. 2013, Siliwall *et al*. 2020). Apesar da espécie tipo do gênero *I. fuscus* possuir outro padrão de dentição (Figura 6G), caracterizado por ter apenas uma fileira completa de dentes na retromargem, e poucos dentes ou dentículos

concentrados no terço basal da promargem (Fonseca-Ferreira *et al*. 2021), certamente o holótipo não foi usado como referência para a descrição das novas espécies, assim como não foi utilizado nas análises filogenéticas propostas por Raven (1985). Dois motivos complementares suportam essa afirmação: a descrição original, realizada por Perty (1833), não apresenta informações sobre o padrão de dentição das quelíceras, e o material-tipo, originalmente depositado no Muséum National d'Histoire Naturelle, Paris, França (MNHN), encontra-se possivelmente perdido(Fonseca-Ferreira *et al*. 2021).

O padrão encontrado em *I. fuscus,* também é observado em todas as demais espécies Neotropicais (Fonseca-Ferreira *et al*. 2021), que foram recuperadas como um clado monofilético nas análises moleculares (Figura 2) e suportado pela RCA do padrão de dentição das quelíceras (Figura 6). Este clado também se caracteriza por possuir dois pares de sigilas esternais (Figura 5) e ausência de espínulos nas coxas (Figura 4), caractere que diferencia os espécimes do *Idiops* do gênero *Ctenolophus*.

Apesar das espécies Neotropicais formarem um clado monofilético, a ausência de pelo menos metade das espécies originárias da América do Sul nas análises filogenômicas, impossibilita uma análise mais apurada das relações evolutivas destes táxons. Uma exceção é o clado formado pelas espécies *I. carajas*, *I. petiti* e *I. sp.n.2*, que possuem distribuição amazônica e foram recuperadas em um clado distinto das demais espécies, com alto suporte de ramo (> 80). Estas espécies compartilham uma série de caracteres exclusivos associados principalmente ao formato do bulbo copulador masculino (Fonseca-Ferreira *et al*. 2017, 2021). É importante ressaltar que devido possivelmente ao número reduzido de UCEs recuperados, as espécies *I. fuscus* (n = 8) e *I. sertania* (n = 32) apresentaram ramos longos, que sabidamente provocam instabilidade na topologia apresentada (Blaimer *et al*. 2015, Derkarabetian *et al*. 2019). Apesar disso, elas foram mantidas na topologia final, por se referirem a espécie tipo do gênero (*I. fuscus*) e por compartilharem os caracteres morfológicos anteriormente apresentados.

Parafilia de Idiopidae e posição filogenética de *Neocteniza*

Em relação a família Idiopidae, a não monofilia da família é suportada pela relação filogeneticamente mais próxima entre os representantes de Idiopinae e

o gênero *Cteniza* (Ctenizidae) do que com o gênero *Neocteniza*, atualmente incluída na subfamília Genysinae (Figura 2), relação também resgatada em topologias preliminares. Apesar de trabalhos anteriores já indicarem uma relação próxima entre Idiopidae e Ctenizidae (e Euctenizidae) (Godwin *et al*. 2018, Bond *et al*. 2020, Opatova *et al*. 2020), não é possível discorrer com profundidade sobre essa relação, sem incluir mais representantes destas duas famílias. Também é necessário incluir espécimes que representem a diversidade de Arbanitinae, subfamília que apesar de ter tanto suas relações internas bem estabelecidas (Rix *et al*. 2017a, 2017b, Wilson et al. 2020, 2021), quanto sua relação com Idiopinae parcialmente exploradas (Raven 1985, Hedin & Bond 2006, Opatova *et al*. 2020), nunca teve vários representantes incluídos em uma análise filogenômica abrangente focada especificamente na família Idiopidae.

Em relação a *Neocteniza*, Raven (1985) discorre que o gênero representa um táxon enigmático e compreende uma linhagem única entre as aranhas migalomorfas, se diferindo morfologicamente inclusive dos demais gêneros de Genysinae, subfamília de Idiopidae no qual está atualmente alocado e que nunca teve os gêneros revisados. O relacionamento de *Neocteniza* com os demais táxons pertencentes a Idiopidae também foi mais bem discutido por Rossi *et al*. (2021), que discutem sobre a ausência dos caracteres considerados sinapomórficos para a família em espécimes do gênero, sobre uma série de características únicas encontradas nestas aranhas e pela primeira vez indicam a possibilidade de parafilia do gênero em relação a família.

Em diversos momentos, Raven (1985) apresenta informações que sugerem uma possível relação entre *Neocteniza* e o clado nomeado como Migoidea Raven, 1985, que incluía as famílias Actinopodidae e Migidae. Apesar desse clado não ter sido resgatado nas últimas filogenias moleculares, que suportam a relação entre Actinopodidae e Atracidae, conhecido como Venon Clade (Bond *et al*. 2012, Hedin *et al*. 2018a, Opatova *et al*. 2020), a presença de uma série de caracteres morfológicos compartilhados entre estas duas famílias e *Neocteniza* merece atenção. Entre os diversos caracteres morfológicos discutidos por Raven (1985) que sugeriu essa possível relação filogenética próxima, então a condição de olhos desagrupados, o formato das sigilas esternais e a dentição das quelíceras, que se diferencia pela presença de duas fileiras de dentes grandes na promargem e retromargem, além de dezenas de

dentículos na margem interna da quelíceras.

Apesar dos caracteres selecionados para a Reconstrução de Caracteres Ancestrais deste trabalho terem sido escolhidos baseado nas principais características morfológicas que diferem os gêneros de Idiopinae, os resultados encontrados na RCA para a disposição ocular (Figura 3), para as sigilas esternais (Figura 5) e para o padrão de dentição das quelíceras (Figura 6), também dão suporte a algumas relações propostas por Raven (1985). Estes resultados indicam que pode haver uma relação evolutiva mais próxima de *Neocteniza* com Actinopodidae e Atracidae do que com os demais representantes de Idiopidae. Apesar disso é necessário e fundamental realizar a revisão taxonômica das espécies de *Neocteniza*, bem como dos demais gêneros de Genysinae, bem como a inclusão de mais grupos externos em futuras filogenias, para compreender melhor o posicionamento do gênero dentro de Mygalomorphae.

CONSIDERAÇÕES FINAIS

Pela primeira vez foi reconstruída uma filogenia molecular focada na subfamília Idiopinae e no gênero *Idiops*, a partir de uma matriz com 50% de cobertura taxonômica composto por 832 *loci* de UCE. Segundo as análises filogenômicas, embasadas pelas análises de Reconstrução de Caracteres Ancestrais, os principais resultados obtidos são apresentados a seguir:

- A subfamília Idiopinae foi recuperada como um clado monofilético, e se caracteriza principalmente pela posição dos Olhos Laterais Anteriores, que são afastados dos demais e próximos ao clípeo, caractere observado em todos os gêneros da subfamília;
- A subfamília pode ser dividida em dois grupos principais geograficamente estruturados, um formado pelas espécies africanas e outro pelas espécies Neotropicais;
- Os gêneros africanos estão divididos em dois grupos que se diferenciam por possuírem diferente combinações dos seguintes caracteres: presença de espínulos nas coxas, números de pares de sigilas e padrão de dentição das quelíceras;

- O gênero *Idiops,* que atualmente conta com 96 espécies, das quais a maioria é originária da África*,* foi recuperado como parafilético nas análises filogenômicas, fato reforçado pela presença de diferentes padrões de dentição nas quelíceras. Apesar de apenas três espécies africanas terem representantes incluídos na filogenia, estes foram suficientes para contestar a filogenia do gênero;
- As espécies Neotropicais, incluído a espécie-tipo *I. fuscus*, se caracterizam por possuírem uma fileira de dentes completa na retromargem e alguns dentes ou dentículos restritos ao terço basal da promargem, enquanto as espécies africanas se distinguem por possuírem duas fileiras de dentes completas;
- Pela primeira vez a família Idiopidae foi resgatada como um clado parafilético. Esse resultado certamente tem relação com a inclusão de um representante do gênero *Neocteniza*, que nunca havia sido incluído em uma filogenia molecular. Este gênero enigmático, que pertencente a subfamília Genysinae, se difere morfologicamente dos demais representantes de Idiopidae e possui uma série de caracteres compartilhados com outras famílias, como Actinopodidae, Atracidae e Migidae.

Como próximas ações para uma melhor compreensão das relações evolutivas e biogeográficas de Idiopinae, se faz necessário a devida revisão taxonômica dos espécimes atualmente alocados no gênero *Idiops*, provenientes principalmente da África e da Índia. Devido à proximidade dos espécimes africanos de "*Idiops*" com os demais gêneros de Idiopinae, também é fundamental a revisão destes gêneros, que até então nunca foram revisados. Também é essencial a inclusão de mais representantes da família, incluindo mais amostras de museu, que abranjam mais espécimes de Idiopinae, além de Arbanitinae e Genysinae.

Os resultados gerados neste trabalho, a partir das análises filogenômicas dos Elementos Ultraconservados (UCEs), reforçam a importância da utilização de amostras de museu para compreender as relações filogenéticas das aranhas migalomorfas, e especificamente das aranhas de alçapão. Devido à marcante uniformidade morfológica, possivelmente uma consequência evolutiva de um

estilo de vida sedentário e dispersão limitada, além da natureza críptica destes táxons, a incorporação dessas amostras, que naturalmente possuem DNA degradado, em conjunto com amostras recentes, gera uma infinidade de novas possibilidades agora destravadas para reconstruir a histórias evolutiva de aranhas da família Idiopidae.

REFERÊNCIAS BIBLIOGRÁFICAS

Andermann, T., Torres Jiménez, M. F., Matos-Maraví, P., Batista, R., Blanco-Pastor, J. L., Gustafsson, A. L. S., Kistler, L., Liberal, I. M., Oxelman, B., Bacon, C. D., & Antonelli, A. (2020). A guide to carrying out a phylogenomic target sequence capture project. *Frontiers in Genetics*, *10*. https://doi.org/10.3389/fgene.2019.01407

Anisimova, M., Gil, M., Dufayard, J.-F., Dessimoz, C., & Gascuel, O. (2011). Survey of branch support methods demonstrates accuracy, power, and robustness of fast likelihood-based approximation schemes. *Systematic Biology*, *60*(5), 685–699. https://doi.org/10.1093/sysbio/syr041

Ayoub, N. A., Garb, J. E., Hedin, M., & Hayashi, C. Y. (2007). Utility of the nuclear protein-coding gene, elongation factor-1 gamma (EF-1γ), for spider systematics, emphasizing family level relationships of tarantulas and their kin (Araneae: Mygalomorphae). *Molecular Phylogenetics and Evolution*, 42(2), 394-409. https://doi.org/10.1016/j.ympev.2006.07.018

Bankevich, A., Nurk, S., Antipov, D., Gurevich, A. A., Dvorkin, M., Kulikov, A. S., Lesin, V. M., Nikolenko, S. I., Pham, S., Prjibelski, A. D., Pyshkin, A. V., Sirotkin, A. V., Vyahhi, N., Tesler, G., Alekseyev, M. A., & Pevzner, P. A. (2012). SPAdes: A new genome assembly algorithm and its applications to single-cell sequencing. *Journal of Computational Biology*, *19*(5), 455–477. https://doi.org/10.1089/cmb.2012.0021

Blaimer, B. B., Brady, S. G., Schultz, T. R., Lloyd, M. W., Fisher, B. L., & Ward, P. S. (2015). Phylogenomic methods outperform traditional multi-locus approaches in resolving deep evolutionary history: A case study of formicine ants. *BMC Evolutionary Biology*, *15*(1). https://doi.org/10.1186/s12862-015-0552-5

Blaimer, B. B., Lloyd, M. W., Guillory, W. X., & Brady, S. G. (2016). Sequence capture and phylogenetic utility of genomic ultraconserved elements obtained from pinned insect specimens. *Plos One*, *11*(8), Artigo e0161531. https://doi.org/10.1371/journal.pone.0161531

Bond, J. (2012). Phylogenetic treatment and taxonomic revision of the trapdoor spider genus *Aptostichus* Simon (Araneae, Mygalomorphae, Euctenizidae). *ZooKeys*, *252*, 1–209. https://doi.org/10.3897/zookeys.252.3588

Bond, J. E., Garrison, N. L., Hamilton, C. A., Godwin, R. L., Hedin, M., & Agnarsson, I. (2014). Phylogenomics resolves a spider backbone phylogeny and rejects a prevailing paradigm for orb web evolution. *Current Biology*, *24*(15), 1765–1771. https://doi.org/10.1016/j.cub.2014.06.034

Bond, J. E., Hamilton, C. A., Godwin, R. L., Ledford, J. M., & Starrett, J. (2020). Phylogeny, evolution, and biogeography of the north american trapdoor spider family Euctenizidae (Araneae: Mygalomorphae) and the discovery of a new 'endangered living fossil' along California's central coast. *Insect Systematics and Diversity*, *4*(5). https://doi.org/10.1093/isd/ixaa010

Bond, J. E., Hendrixson, B. E., Hamilton, C. A., & Hedin, M. (2012). A reconsideration of the classification of the spider Infraorder Mygalomorphae (Arachnida: Araneae) based on three nuclear genes and morphology. *PLoS ONE*, *7*(6), e38753. https://doi.org/10.1371/journal.pone.0038753

Bond J.E. & Stockman A.K. 2008. An integrative method for delimiting cohesion species: finding the population-species interface in a group of Californian trapdoor spiders with extreme genetic divergence and geographic structuring. *Systematic Biology* 57 (4): 628–646. https://doi.org/10.1080/10635150802302443

Calderón-Acevedo, C. A., Bagley, J. C., & Muchhala, N. (2022). Genome-wide ultraconserved elements resolve phylogenetic relationships and biogeographic history among Neotropical leaf-nosed bats in the genus *Anoura* (Phyllostomidae). *Molecular Phylogenetics and Evolution*, 167, 107356. https://doi.org/10.1016/j.ympev.2021.107356

Castresana, J. (2000). Selection of conserved blocks from multiple alignments for their use in phylogenetic analysis. *Molecular Biology and Evolution*, *17*(4), 540–552. https://doi.org/10.1093/oxfordjournals.molbev.a026334

Ciaccio, E., Debray, A., & Hedin, M. (2022). Phylogenomics of paleoendemic lampshade spiders (Araneae, Hypochilidae, *Hypochilus*), with the description of a new species from montane California. *ZooKeys*, 1086, 163. https://doi.org/10.3897/zookeys.1086.77190

Decae, A., Mammola, S., Rizzo, P., & Isaia, M. (2019). Systematics, ecology and distribution of the mygalomorph spider genus *Cteniza* Latreille, 1829 (Araneae, Mygalomorphae, Ctenizidae). *Zootaxa*, *4550*(4), 499. https://doi.org/10.11646/zootaxa.4550.4.2

Derkarabetian, S., Baker, C. M., & Giribet, G. (2021). Complex patterns of Gondwanan biogeography revealed in a dispersal-limited arachnid. *Journal of Biogeography*, *48*(6), 1336–1352. https://doi.org/10.1111/jbi.14080

Derkarabetian, S., Benavides, L. R., & Giribet, G. (2019). Sequence capture phylogenomics of historical ethanol-preserved museum specimens: Unlocking the rest of the vault. *Molecular Ecology Resources*, *19*(6), 1531–1544. https://doi.org/10.1111/1755-0998.13072

Derkarabetian, S., Starrett, J., Tsurusaki, N., Ubick, D., Castillo, S., & Hedin, M. (2018). A stable phylogenomic classification of Travunioidea (Arachnida, Opiliones, Laniatores) based on sequence capture of Ultraconserved Elements. *ZooKeys*, *760*, 1–36. https://doi.org/10.3897/zookeys.760.24937

Dippenaar-Schoeman, A. S. (2002). Baboon and trapdoor spiders of southern Africa: an identification manual. Pretoria: Agricultural Research Council.

Faircloth, BC. 2013. illumiprocessor: a trimmomatic wrapper for parallel adapter and quality trimming. http://dx.doi.org/10.6079/J9ILL.

Faircloth, B. C. (2016). PHYLUCE is a software package for the analysis of conserved genomic loci. *Bioinformatics*, *32*(5), 786–788. https://doi.org/10.1093/bioinformatics/btv646

Faircloth, B. C., McCormack, J. E., Crawford, N. G., Harvey, M. G., Brumfield, R. T., & Glenn, T. C. (2012). Ultraconserved elements anchor thousands of genetic markers spanning multiple evolutionary timescales. *Systematic Biology*, *61*(5), 717–726. https://doi.org/10.1093/sysbio/sys004

Ferretti, N., Nime, M., & Mattoni, C. (2017). Three new *Idiops* (Mygalomorphae: Idiopidae) from Argentina and redescription of the male of *I. hirsutipedis* Mello-Leitão, 1941. *Journal of Natural History*, *51*(17-18), 975–994. https://doi.org/10.1080/00222933.2017.1319516

Foley, S., Krehenwinkel, H., Cheng, D. Q., & Piel, W. H. (2021). Phylogenomic analyses reveal a Gondwanan origin and repeated out of India colonizations into Asia by tarantulas (Araneae: Theraphosidae). *PeerJ*, 9, e11162. https://doi.org/10.7717/peerj.11162

Fonseca-Ferreira, R., Guadanucci, J. P. L., Yamamoto, F. U., & Brescovit, A. D. (2021). Taxonomic revision of the Neotropical spiders of the genus *Idiops* Perty, 1833 (Araneae, Idiopidae), with description of four new species. *European Journal of Taxonomy*, *780*, 1–71. https://doi.org/10.5852/ejt.2021.780.1581

Fonseca-Ferreira, R., Zampaulo, R. d. A., & Guadanucci, J. P. L. (2017). Diversity of iron cave-dwelling mygalomorph spiders from Pará, Brazil, with description of three new species (Araneae). *Tropical Zoology*, *30*(4), 178–199. https://doi.org/10.1080/03946975.2017.1367590

Gertsch, W. J., & Platnick, N. I. (1975). A revision of the trapdoor spider genus *Cyclocosmia* (Araneae, Ctenizidae). *American Museum Novitates*; no. 2580.

Giribet, G., Shaw, M., Lord, A., & Derkarabetian, S. (2022). Closing a biogeographic gap: a new pettalid genus from South Australia (Arachnida: Opiliones: Cyphophthalmi: Pettalidae) with a UCE-based phylogeny of Cyphophthalmi. *Invertebrate Systematics*, *36* (11), 1002. https://doi.org/10.1071/is22043

Godwin, R. L., Opatova, V., Garrison, N. L., Hamilton, C. A., & Bond, J. E. (2018). Phylogeny of a cosmopolitan family of morphologically conserved trapdoor spiders (Mygalomorphae, Ctenizidae) using Anchored Hybrid Enrichment, with a description of the family, Halonoproctidae Pocock 1901. *Molecular Phylogenetics and Evolution*, 126, 303-313. https://doi.org/10.1016/j.ympev.2018.04.008

Griswold, C. E. (1987). The African members of the trap-door spider family Migidae (Araneae: Mygalomorphae) 1: the genus *Moggridgea* OP Cambridge, 1875. *Annals of the Natal Museum*, 28(1), 1-118.

Gupta, N., Ganeshkumar, M., Das, S. K., & Siliwal, M. (2013). Three new species of *Idiops* Perty, 1833 (Araneae: Idiopidae) from India. *Zootaxa*, *3635*(3), 237–250. https://doi.org/10.11646/zootaxa.3635.3.3

Guschanski, K., Krause, J., Sawyer, S., Valente, L. M., Bailey, S., Finstermeier, K., ... & Savolainen, V. (2013). Next-generation museomics disentangles one of the largest primate radiations. *Systematic Biology*, 62(4), 539-554. https://doi.org/10.1093/sysbio/syt018

Hamilton, C. A., Lemmon, A. R., Lemmon, E. M., & Bond, J. E. (2016). Expanding anchored hybrid enrichment to resolve both deep and shallow relationships within the spider tree of life. *BMC Evolutionary Biology*, *16*(1). https://doi.org/10.1186/s12862-016-0769-y

Harrison S.E., Harvey M.S., Cooper S.J., Austin A.D. & Rix M.G. 2017. Across the Indian Ocean: a remarkable example of trans-oceanic dispersal in an austral mygalomorph spider. *PloS One* 12 (8): e180139. https://doi.org/10.1371/journal.pone.0180139

Hedin, M., & Bond, J. E. (2006). Molecular phylogenetics of the spider infraorder Mygalomorphae using nuclear rRNA genes (18S and 28S): Conflict and

agreement with the current system of classification. *Molecular Phylogenetics and Evolution*, *41*(2), 454–471. https://doi.org/10.1016/j.ympev.2006.05.017

Hedin, M., Derkarabetian, S., Alfaro, A., Ramírez, M. J., & Bond, J. E. (2019). Phylogenomic analysis and revised classification of atypoid mygalomorph spiders (Araneae, Mygalomorphae), with notes on arachnid ultraconserved element loci. *PeerJ*, *7*, Artigo e6864. https://doi.org/10.7717/peerj.6864

Hedin, M., Derkarabetian, S., Ramírez, M. J., Vink, C., & Bond, J. E. (2018a). Phylogenomic reclassification of the world's most venomous spiders (Mygalomorphae, Atracinae), with implications for venom evolution. *Scientific Reports*, *8*(1). https://doi.org/10.1038/s41598-018-19946-2

Hedin, M., Derkarabetian, S., Blair, J., & Paquin, P. (2018b). Sequence capture phylogenomics of eyeless *Cicurina* spiders from Texas caves, with emphasis on US federally-endangered species from Bexar County (Araneae, Hahniidae). *ZooKeys*, (769), 49. https://doi.org/10.3897/zookeys.769.25814

Hedin, M., Foldi, S., & Rajah-Boyer, B. (2020). Evolutionary divergences mirror Pleistocene paleodrainages in a rapidly-evolving complex of oasis-dwelling jumping spiders (Salticidae, *Habronattus tarsalis*). *Molecular Phylogenetics and Evolution*, 144, 106696. https://doi.org/10.1016/j.ympev.2019.106696

Hellemans, S., Wang, M., Hasegawa, N., Šobotník, J., Scheffrahn, R. H., & Bourguignon, T. (2022). Using ultraconserved elements to reconstruct the termite tree of life. *Molecular Phylogenetics and Evolution*, 107520. https://doi.org/10.1016/j.ympev.2022.107520

Houston, D. D., Satler, J. D., Stack, T. K., Carroll, H. M., Bevan, A. M., Moya, A. L., & Alexander, K. D. (2022). A phylogenomic perspective on the evolutionary history of the stonefly genus *Suwallia* (Plecoptera: Chloroperlidae) revealed by ultraconserved genomic elements. *Molecular Phylogenetics and Evolution*, *166*, 107320. https://doi.org/10.1016/j.ympev.2021.107320

Kalyaanamoorthy, S., Minh, B. Q., Wong, T. K. F., von Haeseler, A., & Jermiin, L. S. (2017). ModelFinder: Fast model selection for accurate phylogenetic estimates. *Nature Methods*, *14*(6), 587–589. https://doi.org/10.1038/nmeth.4285

Katoh, K., & Standley, D. M. (2013). MAFFT: Iterative refinement and additional methods. In *Methods in molecular biology* (pp. 131–146). Humana Press. https://doi.org/10.1007/978-1-62703-646-7_8

Kulkarni, S., Kallal, R. J., Wood, H., Dimitrov, D., Giribet, G., & Hormiga, G. (2020). Interrogating genomic-scale data to resolve recalcitrant nodes in the

spider tree of life. *Molecular Biology and Evolution*, 38(3), 891-903. https://doi.org/10.1093/molbev/msaa251

Kulkarni, S., Wood, H., Lloyd, M., & Hormiga, G. (2019). Spider-specific probe set for ultraconserved elements offers new perspectives on the evolutionary history of spiders (Arachnida, Araneae). *Molecular Ecology Resources*, *20*(1), 185–203. https://doi.org/10.1111/1755-0998.13099

Ledford, J., Derkarabetian, S., Ribera, C., Starrett, J., Bond, J. E., Griswold, C., & Hedin, M. (2021). Phylogenomics and biogeography of leptonetid spiders (Araneae:Leptonetidae). *Invertebrate Systematics*. https://doi.org/10.1071/is20065

Lemmon, E. M., & Lemmon, A. R. (2013). High-Throughput genomic data in systematics and phylogenetics. *Annual Review of Ecology, Evolution, and Systematics*, *44*(1), 99–121. https://doi.org/10.1146/annurev-ecolsys-110512-135822

Lewis, P. O. (2001). A likelihood approach to estimating phylogeny from discrete morphological character data. *Systematic Biology*, *50*(6), 913–925. https://doi.org/10.1080/106351501753462876

Maddison, W. P. and D.R. Maddison. 2021. Mesquite: a modular system for evolutionary analysis. Version 3.70 http://www.mesquiteproject.org

McCormack, J. E., Tsai, W. L. E., & Faircloth, B. C. (2016). Sequence capture of ultraconserved elements from bird museum specimens. *Molecular Ecology Resources*, *16*(5), 1189–1203. https://doi.org/10.1111/1755-0998.12466

Miglio, L. T., Pérez-Miles, F., & Bonaldo, A. B. (2020). Taxonomic revision of the spider genus *Actinopus* Perty, 1833 (Araneae, Mygalomorphae, Actinopodidae). *Megataxa*, *2*(1). https://doi.org/10.11646/megataxa.2.1.1

Minh, B. Q., Nguyen, M. A. T., & von Haeseler, A. (2013). Ultrafast approximation for phylogenetic bootstrap. *Molecular Biology and Evolution*, *30*(5), 1188–1195. https://doi.org/10.1093/molbev/mst024

Montes de Oca, L., Indicatti, R. P., Opatova, V., Almeida, M., Pérez-Miles, F., & Bond, J. E. (2022). Phylogenomic analysis, reclassification, and evolution of South American nemesioid burrowing mygalomorph spiders. *Molecular Phylogenetics and Evolution*, 168, 107377. https://doi.org/10.1016/j.ympev.2021.107377

Nguyen, L.-T., Schmidt, H. A., von Haeseler, A., & Minh, B. Q. (2014). IQ-TREE: A fast and effective stochastic algorithm for estimating Maximum-Likelihood

phylogenies. *Molecular Biology and Evolution*, *32*(1), 268–274. https://doi.org/10.1093/molbev/msu300

Opatova, V., & Arnedo, M. A. (2014). Spiders on a hot volcanic roof: colonisation pathways and phylogeography of the Canary Islands endemic trap-door spider *Titanidiops canariensis* (Araneae, Idiopidae). *PLoS One*, 9(12), e115078. https://doi.org/10.1371/journal.pone.0115078

Opatova, V., Hamilton, C. A., Hedin, M., De Oca, L. M., Král, J., & Bond, J. E. (2020). Phylogenetic systematics and evolution of the spider infraorder mygalomorphae using genomic scale data. *Systematic Biology*, *69*(4), 671–707. https://doi.org/10.1093/sysbio/syz064

Parada, A., Hanson, J., & D'Eiía, G. (2021). Ultraconserved elements improve the resolution of difficult nodes within the rapid radiation of Neotropical sigmodontine rodents (Cricetidae: Sigmodontinae). *Systematic Biology*, 70(6), 1090-1100. https://doi.org/10.1093/sysbio/syab023

Pérez-Miles, F., & Perafán, C. (2017). Behavior and biology of Mygalomorphae. In *Behaviour and ecology of spiders* (pp. 29-54). Springer, Cham. https://doi.org/10.1007/978-3-319-65717-2

Perty M. 1833. Arachnides Brasilienses. In: de Spix J.B. & Martius F.P. (eds) *Delectus animalium articulatorum quae in itinere per Braziliam ann*. *1817 et 1820 colligerunt*: 191–209, pls 38–39. Munich.

Petersen, H. C., Knott, K. E., Banta, G. T., & Hansen, B. W. (2022). Ultra-conserved elements provide insights to the biogeographic patterns of three benthic macroinvertebrate species in the Baltic Sea. *Estuarine, Coastal and Shelf Science*, 107863. https://doi.org/10.1016/j.ecss.2022.107863

Quattrini, A. M., Faircloth, B. C., Dueñas, L. F., Bridge, T. C., Brugler, M. R., Calixto-Botía, I. F., ... & McFadden, C. S. (2018). Universal target-enrichment baits for anthozoan (Cnidaria) phylogenomics: New approaches to long-standing problems. *Molecular Ecology Resources*, 18(2), 281-295. https://doi.org/10.1111/1755-0998.12736

Raven, R. J. (1985). *The spider infraorder Mygalomorphae (Araneae): Cladistics and systematics*. American Museum of Natural History.

Raxworthy, C. J., & Smith, B. T. (2021). Mining museums for historical DNA: advances and challenges in museomics. *Trends in Ecology & Evolution*, 36(11), 1049-1060. https://doi.org/10.1016/j.tree.2021.07.009

Rix, M. G., Cooper, S. J. B., Meusemann, K., Klopfstein, S., Harrison, S. E., Harvey, M. S., & Austin, A. D. (2017a). Post-Eocene climate change across continental Australia and the diversification of Australasian spiny trapdoor spiders

(Idiopidae: Arbanitinae). *Molecular Phylogenetics and Evolution*, *109*, 302–320. https://doi.org/10.1016/j.ympev.2017.01.008

Rix, M. G., Raven, R. J., Main, B. Y., Harrison, S. E., Austin, A. D., Cooper, S. J. B., & Harvey, M. S. (2017b). The Australasian spiny trapdoor spiders of the family Idiopidae (Mygalomorphae: Arbanitinae): a relimitation and revision at the generic level. *Invertebrate Systematics*, *31*(5), 566. https://doi.org/10.1071/is16065

Rix, M. G., Wilson, J. D., Huey, J. A., Hillyer, M. J., Gruber, K., & Harvey, M. S. (2021). Diversification of the mygalomorph spider genus *Aname* (Araneae: Anamidae) across the Australian arid zone: Tracing the evolution and biogeography of a continent-wide radiation. *Molecular Phylogenetics and Evolution*, 160, 107127. https://doi.org/10.1016/j.ympev.2021.107127

Rossi, G. D. F., Ghirotto, V. M., Galleti-Lima, A., Indicatti, R. P., & Guadanucci, J. P. L. (2021). "Flying" or digging? The trapdoor spider genus *Neocteniza* Pocock, 1895: Redescription of three species, new records from Brazil, notes on natural history and first record of ballooning for Idiopidae (Araneae, Mygalomorphae). *Zootaxa*, *5023*(4), 451–485. https://doi.org/10.11646/zootaxa.5023.4.1

Siliwal, M., Molur, S., & Biswas, B. K. (2005). Indian spiders (Arachnida: Araneae): Updated checklist 2005. *Zoos' Print Journal*, *20*(10), 1999–2049. https://doi.org/10.11609/jott.zpj.1283.1999-2049

Siliwal, M., Rajshekhar Hippargi, Archana Yadav & Dolly Kumar. (2020). Five new species of trap-door spiders (Araneae: Mygalomorphae: Idiopidae) from India. *Journal of Threatened Taxa*, *12*(13), 16775–16794. https://doi.org/10.11609/jott.5434.12.13.16775-16794

Simpson, J. T., Wong, K., Jackman, S. D., Schein, J. E., Jones, S. J. M., & Birol, I. (2009). ABySS: A parallel assembler for short read sequence data. *Genome Research*, *19*(6), 1117–1123. https://doi.org/10.1101/gr.089532.108

Smith, B. T., Harvey, M. G., Faircloth, B. C., Glenn, T. C., & Brumfield, R. T. (2014). Target capture and massively parallel sequencing of Ultraconserved Elements for comparative studies at shallow evolutionary time scales. *Systematic Biology*, 63(1), 83-95. https://doi.org/10.1093/sysbio/syt061

Stamatakis, A. (2014). RAxML version 8: A tool for phylogenetic analysis and post-analysis of large phylogenies. *Bioinformatics*, *30*(9), 1312–1313. https://doi.org/10.1093/bioinformatics/btu033

Starrett, J., Derkarabetian, S., Hedin, M., Bryson, R. W., McCormack, J. E., & Faircloth, B. C. (2016). High phylogenetic utility of an ultraconserved element

probe set designed for Arachnida. *Molecular Ecology Resources*, *17*(4), 812–823. https://doi.org/10.1111/1755-0998.12621

Stockman, A. K., & Bond, J. E. (2007). Delimiting cohesion species: extreme population structuring and the role of ecological interchangeability. Molecular Ecology, 16(16), 3374-3392. https://doi.org/10.1111/j.1365-294X.2007.03389.x

Stockman, A., & Bond, J. E. (2008). A taxonomic review of the trapdoor spider genus *Promyrmekiaphila* Schenkel (Araneae, Mygalomorphae, Cyrtaucheniidae, Euctenizinae). *Zootaxa*, *1823*(1), 25. https://doi.org/10.11646/zootaxa.1823.1.2

Talavera, G., & Castresana, J. (2007). Improvement of phylogenies after removing divergent and ambiguously aligned blocks from protein sequence alignments. *Systematic Biology*, *56*(4), 564–577. https://doi.org/10.1080/10635150701472164

Tin, M. M.-Y., Economo, E. P., & Mikheyev, A. S. (2014). Sequencing degraded DNA from non-destructively sampled museum specimens for rad-tagging and low-coverage shotgun phylogenetics. *PLoS ONE*, *9*(5), Artigo e96793. https://doi.org/10.1371/journal.pone.0096793

Tumescheit, C., Firth, A. E., & Brown, K. (2022). CIAlign: A highly customisable command line tool to clean, interpret and visualise multiple sequence alignments. *PeerJ*, *10*, Artigo e12983. https://doi.org/10.7717/peerj.12983

Van Dam, M. H., Trautwein, M., Spicer, G. S., & Esposito, L. (2019). Advancing mite phylogenomics: designing ultraconserved elements for Acari phylogeny. Molecular Ecology Resources, 19(2), 465-475. https://doi.org/10.1111/1755-0998.12962

Wheeler, W. C., Coddington, J. A., Crowley, L. M., Dimitrov, D., Goloboff, P. A., Griswold, C. E., Hormiga, G., Prendini, L., Ramírez, M. J., Sierwald, P., Almeida-Silva, L., Alvarez-Padilla, F., Arnedo, M. A., Benavides Silva, L. R., Benjamin, S. P., Bond, J. E., Grismado, C. J., Hasan, E., Hedin, M., ... Zhang, J. (2016). The spider tree of life: Phylogeny of Araneae based on target-gene analyses from an extensive taxon sampling. *Cladistics*, *33*(6), 574–616. https://doi.org/10.1111/cla.12182

Wilson, J. D., Hughes, J. M., Raven, R. J., Rix, M. G., & Schmidt, D. J. (2018). Spiny trapdoor spiders (Euoplos) of eastern Australia: broadly sympatric clades are differentiated by burrow architecture and male morphology. *Molecular Phylogenetics and Evolution*, 122, 157-165. https://doi.org/10.1016/j.ympev.2018.01.022

Wilson, J. D., Raven, R. J., Schmidt, D. J., Hughes, J. M., & Rix, M. G. (2020). Total-evidence analysis of an undescribed fauna: Resolving the evolution and

classification of Australia's golden trapdoor spiders (Idiopidae: Arbanitinae: Euoplini). *Cladistics*, *36*(6), 543–568. https://doi.org/10.1111/cla.12415

Wilson, J. D., Rix, M. G., Schmidt, D. J., Hughes, J. M., & Raven, R. J. (2021). Systematics of the spiny trapdoor spider genus *Cryptoforis* (Mygalomorphae: Idiopidae: Euoplini): documenting an enigmatic lineage from the eastern Australian mesic zone. *The Journal of Arachnology*, 49(1), 28-90. https://doi.org/10.1636/JoA-S-18-100

Wood, H. M., González, V. L., Lloyd, M., Coddington, J., & Scharff, N. (2018). Next-generation museum genomics: Phylogenetic relationships among palpimanoid spiders using sequence capture techniques (Araneae: Palpimanoidea). *Molecular Phylogenetics and Evolution*, *127*, 907–918. https://doi.org/10.1016/j.ympev.2018.06.038

World Spider Catalog (2023). World Spider Catalog. Version 23.5. Natural History Museum Bern, online at http://wsc.nmbe.ch, accessed on January 9, 2023. https://doi.org/10.24436/2

Xu, X., Su, Y. C., Ho, S. Y., Kuntner, M., Ono, H., Liu, F., ... & Li, D. (2021). Phylogenomic analysis of ultraconserved elements resolves the evolutionary and biogeographic history of segmented trapdoor spiders. *Systematic Biology*, 70(6), 1110-1122. https://doi.org/10.1093/sysbio/syaa098

Yamamoto, F. U. (2013). Revisão taxonômica e análise filogenética do gênero Idiops Perty, 1833 (Araneae, Idiopidae) (Doctoral dissertation, Universidade de São Paulo).

Yeates, D. K., Zwick, A., & Mikheyev, A. S. (2016). Museums are biobanks: Unlocking the genetic potential of the three billion specimens in the world's biological collections. *Current Opinion in Insect Science*, *18*, 83–88. https://doi.org/10.1016/j.cois.2016.09.009

Young, A. D., & Gillung, J. P. (2019). Phylogenomics — principles, opportunities and pitfalls of big-data phylogenetics. *Systematic Entomology*, *45*(2), 225–247. https://doi.org/10.1111/syen.12406

Zhang, Y. M., Williams, J. L., & Lucky, A. (2019). Understanding UCEs: A Comprehensive Primer on Using Ultraconserved Elements for Arthropod Phylogenomics. *Insect Systematics and Diversity*, *3*(5). https://doi.org/10.1093/isd/ixz016

Capítulo 3

Geographic variation of a trapdoor spider (Araneae, Idiopidae) across different Brazilian biomes reveals morphometric differentiation of spiders from the Brazilian Caatinga biome

Manuscrito formatado segundo as normas do *Journal of Zoology*

ABSTRACT

The trapdoor spiders of the family Idiopidae are associated with a sedentary lifestyle and limited dispersion. After a recent revision of the Neotropical species of the genus *Idiops* Perty 1833, the species *Idiops pirassununguensis* Fukami & Lucas, 2008, had its distribution expanded, occurring in the Brazilian biomes of the Amazon, Caatinga, and Cerrado. Considering this unusually wide distribution, we investigated, through linear and geometric morphometric analysis, the patterns of geographic variation along these biomes. Our objectives were to answer whether: (A) There are morphometric differences between the specimens of *I. pirassununguensis* from the Amazon, Caatinga and Cerrado biomes (B) The Caatinga specimens are morphometrically different from their conspecifics from the Amazon and Cerrado biomes. To explore this variation, nine linear variables were selected, in addition to morphogeometric shapes of the copulatory bulb, sternum, and eye arrangement. The results of the linear and geometric morphometrics were congruent and complementary, indicating that the specimens from the Caatinga are morphologically distinct from their conspecifics from the Amazon and the Cerrado. According to our results, specimens from the Caatinga tend to be smaller when compared to specimens from the Amazon and Cerrado, in addition to having shorter legs and pedipalps, a narrower and elongated sternum, and Anterior Lateral Eyes (ALE) furthest from the eye tubercle. This differentiation may be associated with morphological and physiological adaptations related to thermoregulation and water balance of these spiders to the restrictions imposed by the semi-arid Caatinga. They may also be related to ecological limitations, associated with the lower availability of food and water resources, common in arid and open environments affected by drought, typical of this biome. These results involve possible adaptive processes

associated with the evolution of these spiders in arid environments, especially those associated with semi-arid Caatinga environments.

INTRODUCTION

The existence of morphological, ecological, and/or behavioral differences between geographically segregated and spatially distributed populations is known as geographic variation (Mayr, 1970; Gould & Johnston, 1972). The occurrence of variation in environmental and spatial gradients along the distribution of species and populations is one of the factors that affect the morphological variation of organisms (Endler, 1977). Therefore, individuals of the same species exposed to different environmental drivers may present variations in body size and shape, which are often a reflection of adaptations of these organisms to different environments (Gould & Johnston, 1972; Chown & Gaston, 2010). As a continental country, which encompasses a wide range of environmental conditions, Brazil has a diversity of biomes and phytophysiognomies, which are shaped by both abiotic conditions, such as temperature, precipitation, aridity, and relief and soil characteristics, and biotic, such as vegetation cover and availability of organic resources (Werneck et al., 2011; Rull & Carnaval, 2020). These different environmental variables reflect in heterogeneous environments for organisms, influencing geographic variation both at an intraspecific level, especially in the case of widely distributed species, and at an interspecific level (Mayr, 1970).

Biometric measurement of body size and shape is the core of morphometric analyzes (Reyment, 2010), which can be explored through two different types of analytical methods related to the nature of the analyzed structures. The first is traditional or linear morphometry, based on the analysis of linear measurements, such as length, width, and height of the body and other morphological traits (Zelditch et al., 2004). The second, more recent, is geometric morphometry, one of the most effective techniques to explore patterns of structuring and diversification among organisms, which aims to analyze and quantify the differences between complex morphological forms, through multivariate analyzes and visualization of variation in a morphospace (Zelditch et al., 2004, Klingenberg, 2010). Based on these morphometric tools, it is possible to explore several biological aspects, ranging from the recognition and

delimitation of possible cryptic or morphologically related species (Zúñiga-Reinoso & Benitez 2015; Struck et al., 2018; Wilson et al., 2021) to the exploration of patterns of ecogeographic variation (Recoder et al., 2013; Álvarez-Varas et al. 2019; Vilaseca et al. 2021).

Based on a combined perspective, which involves measurements of both linear and geometric structures, few studies have investigated the possible patterns of geographic variation between different environments using different morphometric methods (Nattero et al., 2017; Smith et al., 2019; Aglagane et al., 2022). In an intraspecific and regional morphometric approach, focused on the Brazilian fauna, most studies were based on morphogeometric analyses, which found diverse results, ranging from little morphological variation among bee populations in Northeast Brazil (Ferreira et al., 2011) to populations widely distributed across the country, but geographically structured, for species of grasshoppers (Silva et al., 2018), beetles (Regueira et al., 2020) and bats (Cordeiro-Estrela et al., 2006).

In spiders, morphometric studies, based mainly on morphogeometric analyzes and carried out mostly on Araneomorphae, Pocock, 1892, are generally focused on species delimitation and on the investigation of sexual dimorphism (Bond & Stockman, 2008; Costa-Schmidt & Araújo, 2010; Fernández-Montraveta & Marugán-Lobón, 2017; Valdéz-Mondragón et al., 2019). There are also some works focused on habitat preference and foraging ecology (Lapinski et al., 2015; Wolff et al., 2022), and investigation of morphological variation of specific structures, under a phylogenetic context (Bond & Beamer, 2006; Kallal et al. 2019). Only a few works have explored geographic variation along different environmental gradients from a morphometric point of view (Entling et al., 2010; Puzin et al., 2014; Krehenwinkel et al., 2016; Wilson et al., 2021).

Regarding the spiders of the Infraorder Mygalomorphae Pocock, 1892, which includes tarantulas and trapdoor spiders, few studies have explored the morphometric variation, based on different analytic tools. Among these works, we have as an example the study by Bond & Beamer (2006), who investigated the variation in carapace height in an interfamilial phylogenetic context, based on analyzes using contour shapes, the work by Ríos-Tamayo (2016), who analyzed the intraspecific morphological variation of species of *Actinopus* Perty, 1833 (Actinopodidae), based on linear and geometric measurements of the carapace,

sternum and copulatory bulb and the research by Wong et al. (2017), who investigated the phenotypic variation of the species *Atrax sutherlandi* Gray, 2010 (Atracidae) in a geographically continuous area, based on molecular analysis and linear morphometry.

Mygalomorph trapdoor spiders generally show marked morphological homogeneity and are typically associated with a sedentary lifestyle, limited dispersal, and high environmental specificity (Dippenaar-Schoeman, 2002; Pérez-Miles & Perafán, 2017; Mason et al., 2018). The reduced number of taxonomic characters, generally morphologically conservative, associated with a generally limited geographic distribution, make trapdoor spiders excellent models for morphometric studies (Bond & Stockman, 2008; Opatova & Arnedo, 2014; Harrison et al., 2017; Opatova et al., 2020). Here, we investigated, through a broad analysis based on linear and geometric morphometric methods, the patterns of geographic variation of trapdoor spiders of the species *Idiops pirassununguensis* Fukami & Lucas, 2008 (Idiopidae), along different biomes of Brazil, which include the tropical rainforest of the Amazon, the savannas of the Cerrado and the Seasonally Dry Tropical Forests of the Caatinga (Fonseca-Ferreira et al., 2021). Taking into account the species' continental distribution, which is unusual among trapdoor spiders, the presence of records of the species for the Amazon, Caatinga, and Cerrado biomes, and the apparent differentiation between specimens from the Caatinga in relation to specimens from the Amazon and the Cerrado, our objectives were to answer whether: (A) There are morphometric differences between the specimens of *I. pirassununguensis* from the Amazon, Caatinga and Cerrado (B) The Caatinga specimens are morphometrically different from their conspecifics from the Amazon and Cerrado.

MATERIALS AND METHODS

Selection and preparation of specimens

For morphometric analyses, we selected 64 specimens of *I. pirassununguensis*, previously identified during the review of Neotropical species of the genus *Idiops* (Fonseca-Ferreira et al., 2021). Only males were used in the analyses, as they represent more than 90% of the material available for examination. Specimens from 21 of the 26 localities with records for the species

from Brazil were included (Table S1), to cover the entire distribution area, which includes phytophysiognomies belonging to the Amazon (n: 20), Caatinga (n: 18) and Cerrado (n: 26) biomes (Figure 1). Males from the five remaining locations were excluded as they were partially damaged. The definition of the biomes of the localities with records for the species was based on the Biome Map of the Instituto Brasileiro de Geografia e Estatística (IBGE, 2019). To perform the morphometric analyses, the specimens were photographed and measured using a Leica M205C stereomicroscope equipped with a Leica DFC295 digital camera.

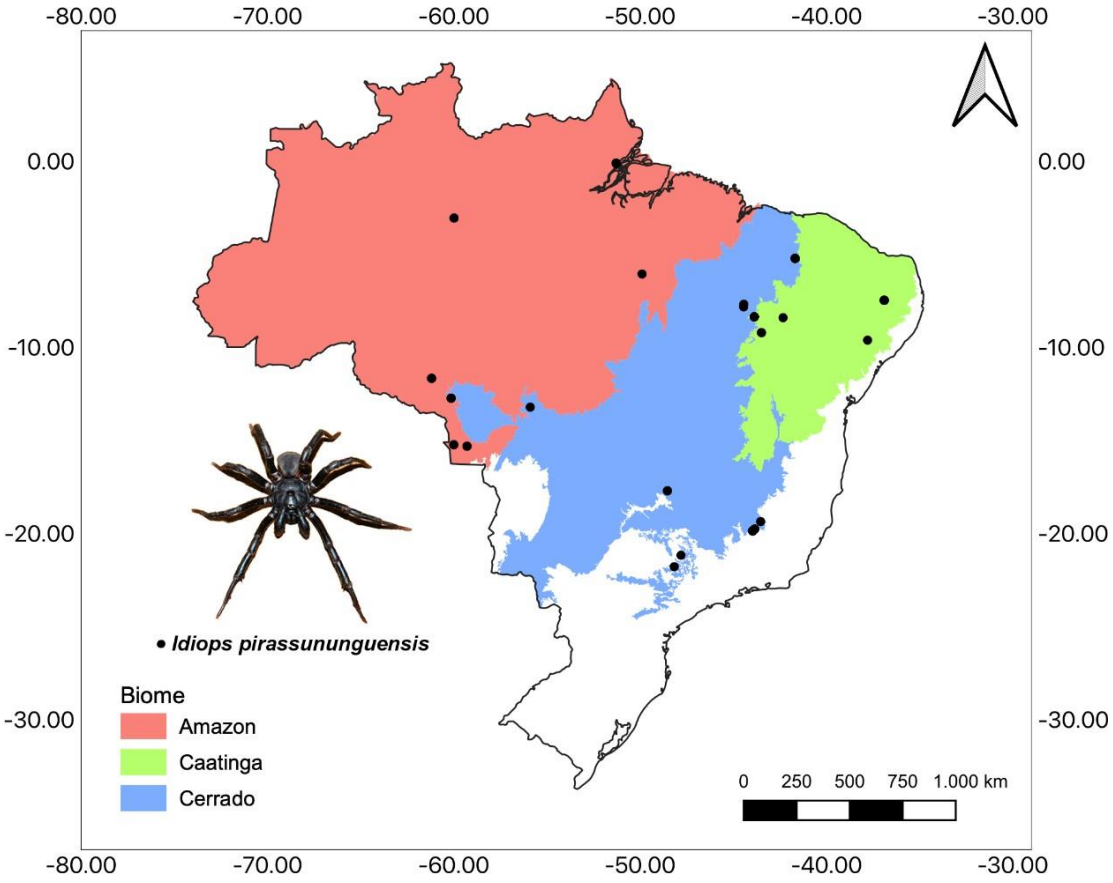

Figure 1. Distribution map of males of *I. pirassununguensis*, highlighted by biomes

The material examined is deposited in the following Brazilian zoological collections: Coleção Aracnológica Diamantina (CAD), Coleção de História Natural, Universidade Federal do Piauí (CHNUFPI), Instituto Butantan (IBSP), Instituto Nacional de Pesquisas da Amazônia (INPA), Museu de Ciências e Tecnologia, Pontifícia Universidade Católica (MCTP), Museu Paraense Emilio Goeldi (MPEG), Museu de Zoologia, Universidade de São Paulo (MZSP),

Coleção de Invertebrados, Universidade Federal de Minas Gerais (UFMG) and Coleção de Arachnida, Universidade Federal do Mato Grosso (UFMT).

Definition and measurement of morphometric variables

To explore the variation of linear structures in relation to the biome, nine variables, associated with measurements of the carapace, sternum, legs and pedipalps of spiders were selected. For each specimen, the following measurements were taken: Carapace Length (CL), Carapace Width (CW), Sternum Length (SL), Sternum Width (SW), Leg Length 1 (LL1), Leg Length 2 (LL2), Leg Length 3 (LL3), Leg Length 4 (LL4) and Pedipalp Length (PpL) (Figure 2A-C). The definition of the linear measurements used was based on structures that showed morphological variation between different groups of spiders in previous morphometric studies (Lapinski et al., 2015; Wong et al., 2017; Wolff et al., 2022).

In addition to linear morphometry, to detect geometrically significant variations of specimens in relation to biomes, geometric morphometric analyzes were performed based on images of the dorsal copulatory bulb (Figure 2D), sternum (Figure 2B) and eye arrangement (Figure 2E). These structures were analyzed according to their biological characteristics, so that information from the contours of the structure was used for the copulatory bulb, while for the sternum and eye arrangement information from previously defined landmarks was used.

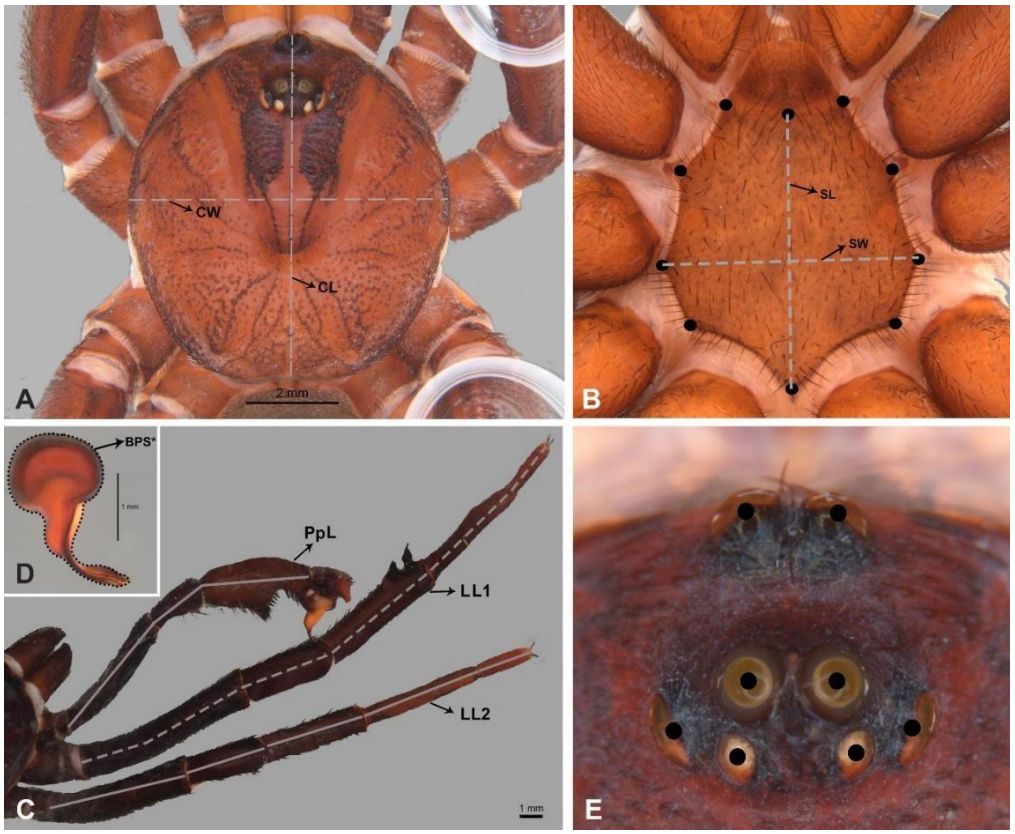

Figure 2. Morphometrics variables of *I. pirassununguensis*. **A**. Carapace length and width. **B**. Length and width of the sternum; sternum landmarks. **C**. Length of legs and pedipalp (legs 3 and 4 not visible in the image). **D**. Shape and representation of the contour of the copulatory bulb. E. Eye landmarks

Linear Morphometric Analysis

Firstly, the mean, the standard deviation and the minimum and maximum values were generated for each linear measurement obtained. To perform the morphometric analysis of linear measurements, seven relative measurements were generated, from the ratio between the length and width of the carapace and sternum and between the length of each of the legs and the pedipalp by the width of the carapace. The ratios were used because they better characterize the proportional morphological variation between different groups and better reflect the adaptation of the specimens to different environments (Lapinski et al., 2015).

Then, the relative variables were subjected to a series of multivariate analyses. To explore and visualize possible patterns of similarity between the specimens, the relative data were submitted to a Principal Coordinate Analysis

(PCoA) calculated from the Gower coefficient of similarity. Finally, to investigate whether there is structuring of the specimens in relation to the biomes, two complementary analyzes were carried out. First, a Canonical Variable Analysis (CVA) was performed to visualize the structuring patterns of the specimens between the biomes, that is, Amazon, Caatinga and Cerrado. This analysis maximizes the variation between the previously defined groups, by comparing the samples classified a priori and calculating the probability of individuals belonging to a different group (Strauss, 2010). Then, a Permutational Multivariate Analysis of Variance (PERMANOVA) was conducted, to test from a non-parametric method, based on permutation tests, if there are significant differences between the analyzed groups (Anderson, 2001). PERMANOVA was based on the Gower similarity index, with 10.000 permutations. P values were corrected for pairwise comparisons using Bonferroni's correction; p values < 0.01 were considered statistically significant. All multivariate analyzes of linear measurements were conducted using PAST (Paleontological Statistics) version 4.03 (Hammer et al., 2001).

Geometric Morphometric Analysis

1 - Geometric morphometric analysis based in outlines

To investigate the variation in the shape of the copulatory bulb (Figure 2D), analyzes were performed using Fourier Elliptic Functions, which describe and characterize the outlines of the analyzed structures in a quantifiable way (Kuhl & Giardina, 2001).

To perform the analyses, initially, the images of the copulatory bulbs were converted into silhouettes, using the Photoshop CC 2018 software. The following analyzes were performed on the RStudio platform (R software v. 4.2).

First, through the R package *Momocs* v. 1.3.0, a series of procedures necessary to perform the Elliptic Fourier Analysis was performed (Bonhomme et al., 2014). For this, the contours of the copulatory bulb images were first extracted and smoothed. Then, from the function *calibrate_harmonicpower_efourier*, a series of harmonics were generated, which are functions resulting from the accumulation of sine and cosine functions, detecting an increasing form of outline details. These harmonics predict the number of contours needed to achieve 95%

to 99% of the shape variation, called Fourier Power. With the number of harmonics defined, the Fourier Elliptics were analyzed using the *eFourier* function, which normalizes all images with respect to rotation, size, and orientation (Bonhomme et al., 2014).

The generated coefficients were submitted to Principal Component Analysis (PCA), in order to visualize the distribution of the copulatory bulb outlines in morphospace (*PCA* function) and characterize their variation, based on the values of the first two Principal Components (*PCcontrib* function). Finally, as a way of visualizing the variation in the shape of the copulatory bulb in relation to the biome and calculating the hit rate in relation to the groups defined a priori, a CVA was performed through the R package MASS (*Ida* function).

2 - Geometric morphometric analysis based in landmarks

To investigate the variation in the shape of the sternum (Figure 2B) and eye arrangements (Figure 2E), which present well-defined geometric structures and allow the insertion of replicable reference points, morphometric analyzes based on landmarks were performed.

First, image libraries were built using the TPSUtil software. Then, the landmaks were inserted, with the help of the TPSDig2 v. 1.31 (Rohlf, 2001). Ten landmarks were defined for the sternum (Figure 2B), and eight landmarks for the ocular arrangement, referring to the central position of each eye (Figure 2E).

The following morphometric and statistical analyzes were performed using MorphoJ v. 1.06 (Klingenbert, 2010). First, information regarding shape was extracted through Generalized Procrustes Analysis (GPA). This analysis removes size, orientation, and position information, keeping only information regarding the shape, ie. the Procrustes coordinates, and standardizes each specimen to a single unit centroid size (Dryden & Mardia, 1998, Zelditch et al., 2004). Then, for each structure, a PCA was performed, based on the covariance matrix of the Procrustes forms, followed by Canonical Variates Analysis (CVA).

The significance of the CVA was evaluated through the values of the Procrustes and Mahalanobis distances, as well as the respective p-values, with 10,000 permutation replicates; p values <0.01 were considered statistically significant.

Finally, to investigate the influence of size on shape (allometric effect), multivariate regression was performed between centroid size (independent variable) and Procrustes coordinates (dependent variable), followed by a permutation test of 10,000 interactions.

RESULTS

Linear Morphometry

The total variation among the specimens for each linear morphometric variable is presented in Table 1 and the variation by biomes is presented in Table S2. In relation to the multivariate analyzes of traditional relative measures, the PCoA, calculated from the similarity coefficient from Gower, resulted in seven axes, of which the first two described 59.8% of the variation (Axis 1: 50.1%, Axis 2: 9.7%; Figure S1) Regarding the CVA, the scatter plot (Figure 3A) also shows the differentiation of the Caatinga specimens, separated from the others and distributed along the left portion of the graph, while the Amazon and Cerrado specimens are superimposed in the right portion of the graph. The differentiation between the groups was confirmed by the general PERMANOVA (F: 11.55, $p < 0.001$). The separation of Caatinga specimens in relation to specimens from other biomes was evidenced by PERMANOVA pairwise, both between Caatinga and Amazon (F: 14.74, $p < 0.001$) and between Caatinga and Cerrado (F: 14.6, $p < 0.001$). There was no significant difference between specimens from Amazon and Cerrado (Table 2A).

Table 1. Mean, standard deviation, and minimum and maximum values for each linear variable measure of *I. pirassununguensis*.

Linear Measurements	Mean (mm)	SD	Min-Max (mm)
Carapace length (CL)	7	0.07	5.53 - 8.2
Carapace width (CW)	6.56	0.08	4.97 - 8
Sternum length (SL)	4.07	0.04	3.10 - 4.8
Sternum width (SW)	3.61	0.05	2.66 - 4.4
Leg length 1 (LL1)	23.34	0.28	17.89 - 27.08
Leg length 2 (LL2)	19.31	0.3	13.92 - 23.13
Leg length 3 (LL3)	16.93	0.28	12.23 - 20.6
Leg length 4 (LL4)	22.88	0.38	16.62 - 28.15
Pedipalp length (PL)	12.33	0.2	9.01 - 15.16

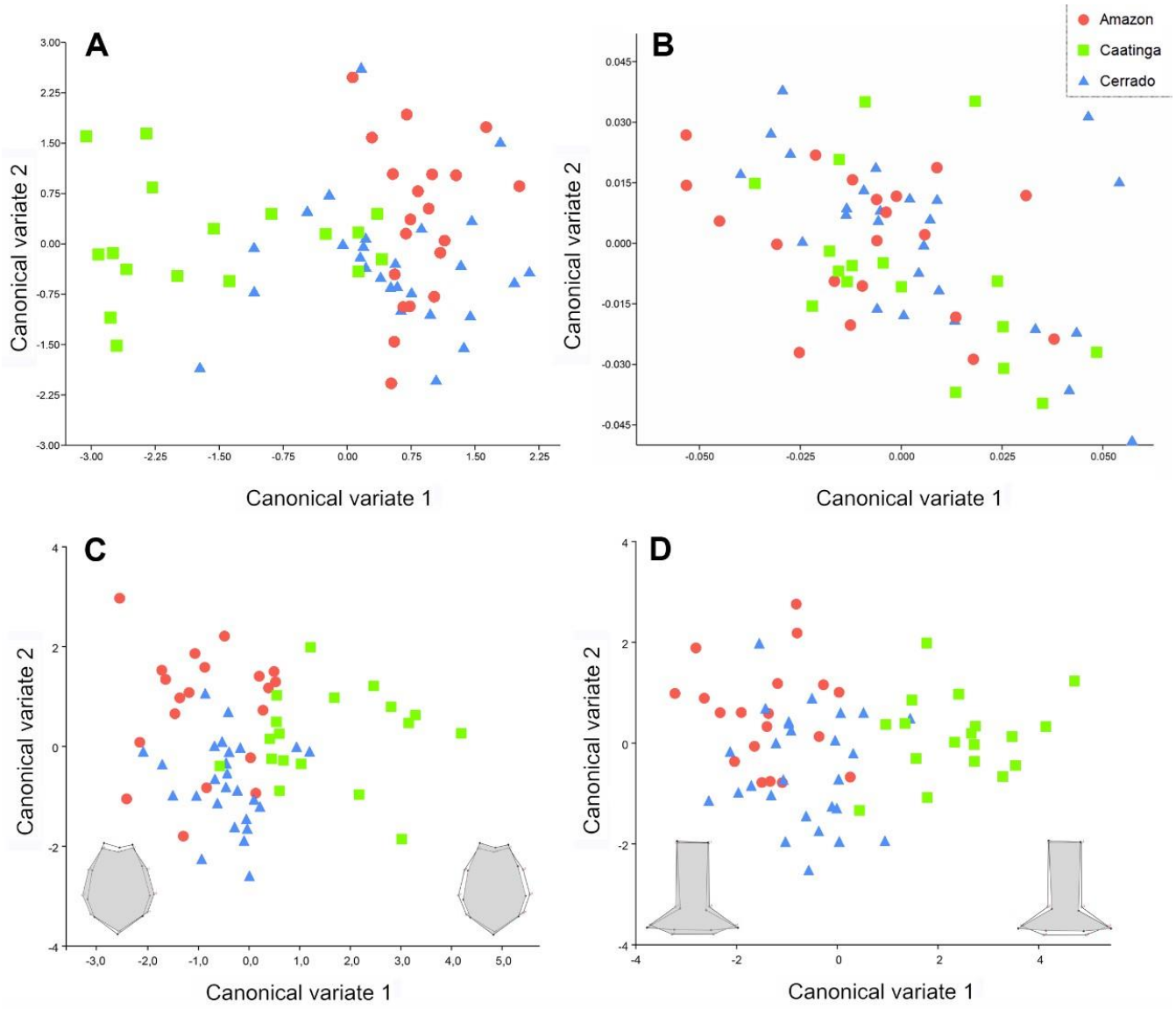

Figure 3. Canonical Variable Analysis (CVA) scatterplots of different morphometric variables of *I. pirassununguensis* in relation to the biome of occurrence. **A**. Linear measurements. **B**. Bulb copulatory. **C**. Sternum (transformation grids at the bottom of the scatterplot). **D**. Eye arrangement (transformation grids at the bottom of the scatterplot). The different biomes are represented by the following symbols and colors: Amazon (red dots), Caatinga (green squares), Cerrado (blue triangles).

Table 2. Statistical results of the Discriminant Analysis in relation to the biomes of occurrence of *I. pirassununguensis*. **A**. Linear measurements (PERMANOVA). **B**. Bulb copulatory (Contingency table). **C**. Sternum (Mahalanobis Distance). **D**. Sternum (Procrustes Distance). **E**. Eye arrangement (Mahalanobis Distance). **F**. Eye arrangement (Procrustes Distance). For **A**, the values on the left of the diagonal represent F values while those on the left represent p values. For **C** and **E**, the Mahalanobis Distance values are on the left of the diagonal and their respective p-values are on the right. The same goes for D and F in relation to the values of Procrustes Distances. For all cases, significant values (p-value < 0.01) were highlighted with an asterisk.

A. Linear measurements (PERMANOVA)			
Biome	Amazon	Caatinga	Cerrado
Amazon	-	0.0003	0.9141
Caatinga	14.74*	-	0.0006
Cerrado	1.166	14.16*	-

B. Bulb copulatory (Contingency table)			
Biome	Amazon	Caatinga	Cerrado
Amazon	65%	10%	25%
Caatinga	0%	78%	22%
Cerrado	11.50%	11.50%	77%

C. Sternum (Mahalanobis Distance)			
Biome	Amazon	Caatinga	Cerrado
Amazon	-	< 0001	0.0135
Caatinga	2.4948*	-	< 0001
Cerrado	1.5567	2.1968*	-

D. Sternum (Procrustes Distance)			
Biome	Amazon	Caatinga	Cerrado
Amazon	-	0.0007	0.5837
Caatinga	0.0293*	-	0.0004
Cerrado	0.0089	0.0298*	-

E. Eye arrangement (Mahalanobis Distance)			
Biome	Amazon	Caatinga	Cerrado
Amazon	-	< 0001	0.0912
Caatinga	3.8638*	-	< 0001
Cerrado	1.3003	3.1691*	-

F. Eye arrangement (Procrustes Distance)			
Biome	Amazon	Caatinga	Cerrado
Amazon	-	0.0009	0.3244
Caatinga	0.0343*	-	0.0049
Cerrado	0.0172	0.0291*	-

Geometric Morphometry

Copulatory Bulb

To perform the Fourier Elliptic Analysis, seven harmonics were needed, which explained 99% of the variation in the dorsal shape of the copulatory bulb. The PCA resulted in 28 PC axes, of which the first five contributed 90.6% of the variation. The first two PCs contributed 75.4% of the total shape variation (PC1: 52.6%, PC2: 22.8%; Figure S2), with the variation in the first Principal Component (PC1) mainly related to tegulum width and the variation in the second Principal Component (PC2) related to mainly with the angulation of the embolus.

In relation to CVA (Figure 3B), the scatter plot indicates that there was not a clear separation of the specimens in relation to the biome since the specimens of the three biomes are mostly overlapping. According to the Contingency Table,

the hit rates for each biome were 65% for the Amazon, 77% for the Caatinga and 77% for the Cerrado (Table 2B).

Sternum

The PCA resulted in 16 PC axes, of which the first five contributed 76.8% of the sternum shape variation. The first two PCs contributed 54.5% of the total shape variation (PC1: 44.4%, PC2: 10.1%; Figure S3), with the variation in the first Principal Component (PC1) mainly related to sternum width and length and the variation in the second Principal Component (PC2) related to the variation in the shape of the anterior portion of the sternum.

According to the CVA scatter plot (Figure 3C), specimens from the Caatinga differ from those from the Amazon and Cerrado, which present more cohesive forms. CV1 explained 70.9% of the variation, which was related to a greater narrowing and elongation of the sternum of individuals from the Caatinga, when compared to the others. When compared with the Amazon and Cerrado groups, the Caatinga specimens present the highest values of Procrustes Distances and Mahalanobis Distances, with significant p values ($p < 0.001$) that evidence the distinction between these groups (Table 2C-D).

Multiple regression showed that despite the allometry effect having a significant permutation value ($p < 0.01$), size contributed only with 8.8% of the shape variation. From the multiple regression scatter plot (Figure 4), it is possible to observe that specimens from the Caatinga tend to be smaller than their conspecifics from the other analyzed biomes.

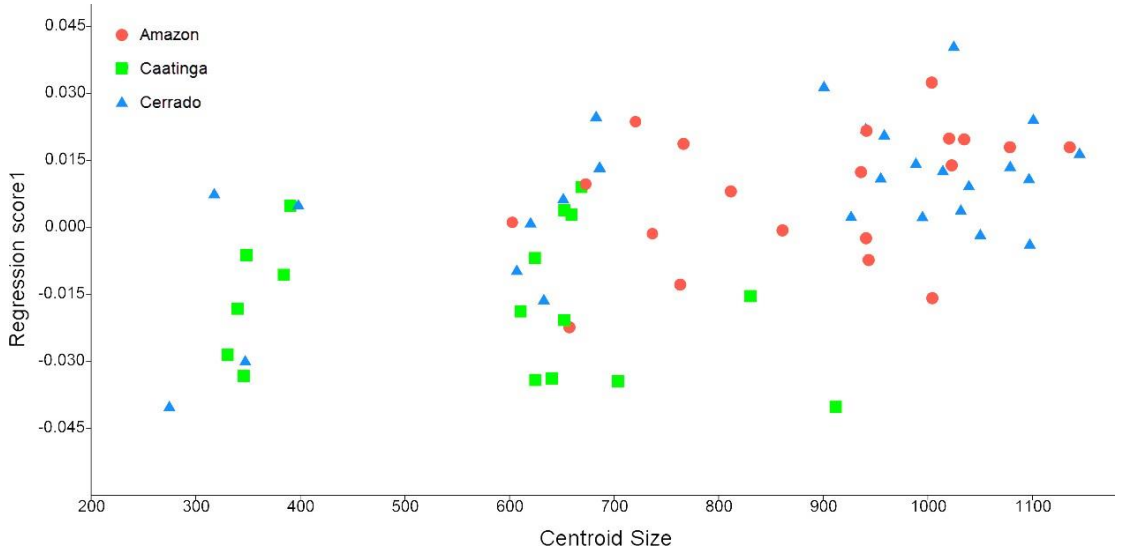

Figure 4. Multivariate regression of sternum shape on sternum centroid size of *I. pirassununguensis*. The different biomes are represented by the following symbols and colors: Amazon (red dots), Caatinga (green squares), Cerrado (blue triangles).

Eye Arrangement

Regarding the shape of the eye arrangement, PCA resulted in 12 PC axes, of which the first five contributed to 80.3% of the shape variation. The first two PCs contributed 51.6% of the total shape variation (PC1: 28.7%, PC2: 22.9%; Figure S4). The first Principal Component (PC1) is mainly related to the length of the eye tubercle and the distance of the eye tubercle in relation to the Anterior Lateral Eyes (ALE). The second Principal Component (PC2) explains part of the variation related to the arrangement of the Anterior Median Eyes (AME) and Posterior Lateral Eyes (PLE).

According to the CVA results (Figure3D), the Caatinga specimens show a separation pattern similar to the sternum when compared to their conspecifics from the Amazon and Cerrado, presenting significant values ($p < 0.001$) for the Mahalanobis and Procrustes Distances (Table 2D-E). CV1 explained 92.1% of the variation, which was related to a greater narrowing of the eye tubercle and a distance between the Anterior Lateral Eyes (ALE) of Caatinga individuals when compared to specimens from the other biomes.

Although multiple regression indicated that 3% of the size variation is related to shape, this analysis did not provide significant support in the

permutation test (p-value: 0.06).

DISCUSSION

This study represents the first morphometric investigation of a species of trapdoor spider in the family Idiopidae. When investigating the intraspecific morphometric variation of males of *I. pirassununguensis*, we found evidence that indicates the existence of morphological differentiation between the specimens in relation to the biomes of occurrence. The results of the analyzes based on the traditional morphometry of linear measurements and the geometric morphometry of the sternum and the eye arrangment were congruent and complementary, indicating that the specimens from the Caatinga are morphologically distinct from their conspecifics from the Amazon and the Cerrado, which did not show significant variation between each other. Regarding the results of the morphogeometric analysis of the copulatory bulb, there was no separation of the specimens in relation to the biomes, which was expected as the main diagnostic characters for the delimitation of the species are related to the shape of the male genitalia (Fonseca-Ferreira et al., 2021).

According to our results, individuals from the Caatinga tend to be smaller when compared to specimens from the Amazon and Cerrado, in addition to having shorter legs and pedipalps, a narrower and elongated sternum, a narrower eye tubercle, and Anterior Lateral Eyes (ALE) furthest from the eye tubercle. This differentiation of Caatinga specimens may be associated with morphological and physiological adaptations related to thermoregulation and water balance of these spiders to the restrictions imposed by the arid environment (Main, 1982; Cloudsley-Thompson, 1983*;* Canals et al., 2015), such as that found in the semi-arid Caatinga, which is characterized by having high average annual temperature, low annual thermal amplitude, low annual precipitation concentrated in a few consecutive months and low relative humidity (Bucher, 1982; Prado, 2003). They may also be related to ecological limitations, associated with the lower availability of food resources, water resources and shelter, common in arid and open environments affected by drought, typical of this biome (Bucher, 1982; Silva et al., 2017).

According to Main (1982) and Cloudsley-Thompson (1983), most spiders found in arid environments show an increase in body size as a way of increasing

the surface-to-volume ratio of the body and, thus, reducing evapotranspiration. Despite this, our results showed the opposite effect, that is, the specimens found in the Caatinga are smaller than their conspecifics from the other biomes. This pattern was also observed in other studies that found similar results. In a study carried out with scorpions from the Caatinga and Atlantic Forest of Northeastern Brazil, Lira et al. (2021) indicated that temperature appears to be a determinant of body size variation, so that increasing environmental temperature had a negative effect on the body size of the species. In an intraspecific context, the authors also suggest that the reduction in the size of the specimens found in the Caatinga may be related to the molting process and the physiological restrictions imposed by it, so that in unfavorable conditions of temperature and humidity, spiders can delay ecdysis (Lira et al., 2021). In a laboratory experiment on the growth rate of *Acheta domesticus* crickets subjected to different hydration states, McCluney & Date (2008) concluded that water stress conditions, such as those found in arid and semi-arid environments, can negatively influence body size of the crickets. Finally, in another study, de Oliveira et al. (2021) analyzed the geographic variation in populations of the lizard species *Gonatodes humeralis* and found populations with smaller body sizes in the Caatinga when compared to Amazonian populations. The authors suggest that this variation can be influenced both by abiotic factors such as temperature, and biotic factors such as availability of food resources and by the interaction between these factors (de Oliveira et al., 2021).

Regarding body elongation, a large study carried out with Gymnophthalmidae lizards, based on morphological and phylogenetic analyses, concluded that body elongation for these lizards was directly related to climatic conditions, so that species that inhabit more arid regions were generally more elongated (Grizante et al., 2012). The authors also argue that habitat structure can also influence body size, as aridity is associated with high temperatures and low rainfall, which can affect resource availability (Grizante et al., 2012). In another study, Ferreira-Sousa et al. (2021) explored the relationship between body elongation and sun exposure in orbicular spiders and observed that sun-exposed spiders developed more elongated bodies than those protected from the sun. They also suggest, based on a heat transfer model, that the elongation of the body of these spiders decreases the risk of high body temperatures (Ferreira-

Sousa et al., 2021). Although the target species of our study is a trapdoor spider, which does not build orb webs, body elongation may be related to heat transfer, since males are wanderers and spend part of their lives outside of burrows looking for females, and occasionally they can be exposed to the sun, since the Caatinga environments are characterized by having open, seasonally dry and deciduous tropical phytophysiognomies.

It is worth noting, however, that part of these morphological variations, mainly associated with arid and semi-arid environments, may also be related to the evolutionary and biogeographic history of the species (Wolff et al., 2022). According to Rix et al. (2017), who consider that the family Idiopidae presents useful lineages to understand speciation in arid zones, the diversification of Idiopids from the subfamily Arbanitinae in the Australian arid zone is the reflection of three independent incursions into these environments during the Miocene. According to the authors, independent lineages evolved phragmotic abdominal morphologies, which may be associated with physiological resistance to desiccation, in addition to similar patterns of reinforced trapdoor burrow construction, indicating a convergent evolution associated with arid environments (Rix et al., 2017). Under an approach focused on Brazilian open biomes, and mainly on the Caatinga, phylogeographic studies of different groups show the genetic structuring associated with the biome along the Dry Diagonal region, which comprises three open biomes biogeographically and climatically related, Caatinga, Cerrado and Chaco (Werneck, 2011). Studies with spiders (Magalhães et al., 2014), lizards (Werneck et al., 2012, Fonseca et al., 2018), amphibians (Thomé et al., 2021), and birds (Moura et al., 2018, Rocha et al., 2020) found similar patterns of diversification and structuring, mainly related to the Pliocene and Pleistocene periods, showing genetic lineages with occurrence restricted to the Caatinga.

The use of different morphometric methods in this work demonstrates the strength of combined analyzes in the quantification of morphological variation and in the identification of morphologically distinct groups. The results found in this study, based on analyzes of linear and geometric structures of specimens of *I. pirassununguensis*, indicate that there is morphological differentiation in terms of size and shape of specimens originating from the Caatinga, when compared to their conspecifics from the Amazon and Cerrado. This pattern of variation and

structuring, based on morphometric evidence, seems to be in line with what was observed for other taxa found in the Caatinga and in other arid environments. These results, associated with an apparently conserved male genitalia and a wide geographic distribution of the species, uncommon for trapdoor spiders, provide subsidies for future investigations, which involve possible adaptive processes associated with the evolution of these spiders in arid environments and the study of possible genetic and biogeographic structuring patterns among *I. pirassununguensis* lineages, especially those associated with semi-arid Caatinga environments.

ACKNOWLEDGEMENTS

We wish to give our thanks to all curators for the loan of specimens. We also thank Ana Lúcia Tourinho, Arthur Galleti Lima, Facundo Labarque, Felipe Garcia, Guilherme H. F. Azevedo, João Carlos Pena, Juliano Zardetto, Leonardo S. Carvalho, Milton Ribeiro, Pedro H. Martins, Rafael P. Indicatti and Tadeu Siqueira for their help and critical suggestions for this work. This study was funded by Fundação de Amparo à Pesquisa do Estado de São Paulo (FAPESP 2018/02842-2 for RFF and FAPESP 2017/11985-9 for JPLG).

REFERENCES

Aglagane, A., Tofilski, A., Er-Rguibi, O., Laghzaoui, E.-M., Kimdil, L., El Mouden, E. H., Fuchs, S., Oleksa, A., Aamiri, A., & Aourir, M. (2022). Geographical variation of honey bee (*Apis mellifera* L. 1758) populations in South-Eastern Morocco: a geometric morphometric analysis. *Insects*, **13** (3), 288. https://doi.org/10.3390/insects13030288

Álvarez-Varas, R., Véliz, D., Vélez-Rubio, G. M., Fallabrino, A., Zárate, P., Heidemeyer, M., Godoy, D. A., & Benítez, H. A. (2019). Identifying genetic lineages through shape: An example in a cosmopolitan marine turtle species using geometric morphometrics. *PLOS ONE*, **14** (10), e0223587. https://doi.org/10.1371/journal.pone.0223587

Anderson, M. J. (2001). A new method for non-parametric multivariate analysis of variance. *Austral Ecology*, **26** (1), 32–46. https://doi.org/10.1046/j.1442-9993.2001.01070.x

Bond, J. E., & Beamer, D. A. (2006). A morphometric analysis of mygalomorph spider carapace shape and its efficacy as a phylogenetic character (Araneae). *Invertebrate Systematics*, **20** (1), 1. https://doi.org/10.1071/is05041

Bond, J. E., & Stockman, A. K. (2008). An integrative method for delimiting cohesion species: finding the population-species interface in a group of californian trapdoor spiders with extreme genetic divergence and geographic structuring. *Systematic Biology*, **57** (4), 628–646. https://doi.org/10.1080/10635150802302443

Bonhomme, V., Picq, S., Gaucherel, C., & Claude, J. (2014). Momocs: Outline Analysis Using R. *Journal of Statistical Software*, **56** (13). https://doi.org/10.18637/jss.v056.i13

Bucher, E. H. (1982). Chaco and Caatinga — South American arid savannas, woodlands and thickets. In *Ecological Studies* (pp. 48–79). Springer Berlin Heidelberg. https://doi.org/10.1007/978-3-642-68786-0_4

Canals, M., Veloso, C., & Solís, R. (2015). Adaptation of the spiders to the environment: the case of some Chilean species. *Frontiers in Physiology*, *6*. https://doi.org/10.3389/fphys.2015.00220

Chown, S. L., & Gaston, K. J. (2010). Body size variation in insects: a macroecological perspective. *Biological Reviews*, **85** (1), 139–169. https://doi.org/10.1111/j.1469-185x.2009.00097.x

Cloudsley-Thompson, J. L. (1983). Desert adaptations in spiders. *Journal of Arid Environments*, **6** (4), 307–317. https://doi.org/10.1016/s0140-1963(18)31410-1

Cordeiro-Estrela, P., Baylac, M., Denys, C., & Marinho-Filho, J. (2006). Interspecific patterns of skull variation between sympatric brazilian vesper mice: geometric morphometrics assessment. *Journal of Mammalogy*, **87** (6), 1270–1279. https://doi.org/10.1644/05-mamm-a-293r3.1

Costa-Schmidt, L. E., & de Araújo, A. M. (2010). Genitalic variation and taxonomic discrimination in the semi-aquatic spider genus *Paratrechalea* (Araneae: Trechaleidae). *Journal of Arachnology*, **38** (2), 242–249. https://doi.org/10.1636/joa_a09-75.1

de Oliveira, F. R., Passos, D. C., & Borges-Nojosa, D. M. (2021). Ecology of the lizard *Gonatodes humeralis* (Sphaerodactylidae) in a coastal area of the Brazilian semiarid: What differs from the Amazonian populations? *Journal of Arid Environments*, **190**, 104506. https://doi.org/10.1016/j.jaridenv.2021.104506

Dippenaar-Schoeman, A. S. (2002) *Baboon and trapdoor spiders of southern Africa: an identification manual*; Pretoria, Agricultural Research Council.

Dryden, I. L.; Mardia K. V. (1998). *Statistical shape analysis*. John Wiley & Sons.

Endler, J. A. (1977). *Geographic variation, speciation, and clines*. Princeton

University Press.

Entling, W., Schmidt-Entling, M. H., Bacher, S., Brandl, R., & Nentwig, W. (2010). Body size-climate relationships of European spiders. *Journal of Biogeography*, **37** (3), 477–485. https://doi.org/10.1111/j.1365-2699.2009.02216.x

Fernández-Montraveta, C., & Marugán-Lobón, J. (2017). Geometric morphometrics reveals sex-differential shape allometry in a spider. *PeerJ*, **5**, e3617. https://doi.org/10.7717/peerj.3617

Ferreira, V., Aguiar, C., Costa, M., & Silva, J. (2011). Morphometric analysis of populations of *Centris aenea* Lepeletier (Hymenoptera: Apidae) from Northeastern Brazil. *Neotropical Entomology*, **40** (1), 97–102. https://doi.org/10.1590/s1519-566x2011000100014

Ferreira-Sousa, L., Rocha, P. N., Motta, P. C., & Gawryszewski, F. M. (2021). Shaped by the Sun: the effect of exposure to sunlight on the evolution of spider bodies. *Biology Letters*, **17** (11). https://doi.org/10.1098/rsbl.2021.0369

Fonseca, E. M., Gehara, M., Werneck, F. P., Lanna, F. M., Colli, G. R., Sites, J. W., Rodrigues, M. T., & Garda, A. A. (2018). Diversification with gene flow and niche divergence in a lizard species along the South American “diagonal of open formations”. *Journal of Biogeography*, **45** (7), 1688–1700. https://doi.org/10.1111/jbi.13356

Fonseca-Ferreira, R., Guadanucci, J. P. L., Yamamoto, F. U., & Brescovit, A. D. (2021). Taxonomic revision of the Neotropical spiders of the genus *Idiops* Perty, 1833 (Araneae, Idiopidae), with description of four new species. *European Journal of Taxonomy*, **780**, 1–71. https://doi.org/10.5852/ejt.2021.780.1581

Gould, S. J., & Johnston, R. F. (1972). Geographic Variation. *Annual Review of Ecology and Systematics*, *3*(1), 457–498. https://doi.org/10.1146/annurev.es.03.110172.002325

Grizante, M. B., Brandt, R., & Kohlsdorf, T. (2012). Evolution of body elongation in gymnophthalmid lizards: relationships with climate. *PLoS ONE*, **7** (11), e49772. https://doi.org/10.1371/journal.pone.0049772

Hammer, Ø.; Harper, D. A.; Ryan, P. D. (2001). PAST: Paleontological statistics software package for education and data analysis. *Palaeontologia electronica*, **4** (1), 9.

Harrison, S. E., Harvey, M. S., Cooper, S. J. B., Austin, A. D., & Rix, M. G. (2017). Across the Indian Ocean: A remarkable example of trans-oceanic dispersal in an austral mygalomorph spider. *PLOS ONE*, **12** (8),

e0180139. https://doi.org/10.1371/journal.pone.0180139

IBGE. (2019). Biomas e sistema costeiro-marinho do Brasil: compatível com a escala 1: 250 000. *Série Relatórios Metodológicos. v. 45*.

Kallal, R. J., Moore, A. J., & Hormiga, G. (2019). The shape of weaver: investigating shape disparity in orb-weaving spiders (Araneae, Araneidae) using geometric morphometrics. *Evolutionary Biology*, **46** (4), 317–331. https://doi.org/10.1007/s11692-019-09482-w

Klingenberg, C. P. (2010). Evolution and development of shape: integrating quantitative approaches. *Nature Reviews Genetics*, **11** (9), 623–635. https://doi.org/10.1038/nrg2829

Klingenberg, C. P. (2010). MorphoJ: an integrated software package for geometric morphometrics. *Molecular Ecology Resources*, **11** (2), 353–357. https://doi.org/10.1111/j.1755-0998.2010.02924.x

Krehenwinkel, H., Graze, M., Rödder, D., Tanaka, K., Baba, Y. G., Muster, C., & Uhl, G. (2016). A phylogeographical survey of a highly dispersive spider reveals eastern Asia as a major glacial refugium for Palaearctic fauna. *Journal of Biogeography*, **43** (8), 1583–1594. https://doi.org/10.1111/jbi.12742

Kuhl, F. P., & Giardina, C. R. (1982). Elliptic Fourier features of a closed contour. *Computer Graphics and Image Processing*, **18** (3), 236–258. https://doi.org/10.1016/0146-664x(82)90034-x

Lapinski, W., Walther, P., & Tschapka, M. (2015). Morphology reflects microhabitat preferences in an assemblage of neotropical wandering spiders. *Zoomorphology*, **134** (2), 219–236. https://doi.org/10.1007/s00435-015-0257-8

Lira, A. F. A., Foerster, S. I. A., Albuquerque, C. M. R., & Moura, G. J. B. (2021). Contrasting patterns at interspecific and intraspecific levels in scorpion body size across a climatic gradient from rainforest to dryland vegetation. *Zoology*, **146**, 125908. https://doi.org/10.1016/j.zool.2021.125908

Magalhaes, I. L. F., Oliveira, U., Santos, F. R., Vidigal, T. H. D. A., Brescovit, A. D., & Santos, A. J. (2014). Strong spatial structure, Pliocene diversification and cryptic diversity in the Neotropical dry forest spider *Sicarius cariri*. *Molecular Ecology*, **23** (21), 5323–5336. https://doi.org/10.1111/mec.12937

Main, B. Y. (1982). Adaptations to arid habitats by mygalomorph spiders. In W. R. Barker & P. J. M. Greenslade, *Evolution of the flora and fauna of arid Australia* (pp. 273-83). Peacock Publications.

Mason, L. D., Wardell-Johnson, G., & Main, B. Y. (2018). The longest-lived spider: mygalomorphs dig deep, and persevere. *Pacific Conservation Biology*, **24** (2), 203. https://doi.org/10.1071/pc18015

Mayr, E. (1970). *Populations, species, and evolution: An abridgment of Animal species and evolution.* Belknap Press of Harvard University Press.

McCluney, K. E., & Date, R. C. (2008). The effects of hydration on growth of the house cricket, *Acheta domesticus*. *Journal of Insect Science*, **8** (32), 1–9. https://doi.org/10.1673/031.008.3201

Moura, C. C. d. M., Araujo, H. F. P. d., Aleixo, A., Wink, M., & Fernandes, A. M. (2018). The role of landscape change and paleoclimatic events in shaping the evolutionary history of the *Polioptilagnat* catchers (Passeriformes, Polioptilidae) with emphasis on species associated with open habitats. *Journal of Avian Biology*, **49** (5), jav—012409. https://doi.org/10.1111/jav.01692

Nattero, J., Piccinali, R. V., Macedo Lopes, C., Hernández, M. L., Abrahan, L., Lobbia, P. A., Rodríguez, C. S., & Carbajal de la Fuente, A. L. (2017). Morphometric variability among the species of the *Sordida* subcomplex (Hemiptera: Reduviidae: Triatominae): evidence for differentiation across the distribution range of *Triatoma sordida*. *Parasites & Vectors*, **10** (1). https://doi.org/10.1186/s13071-017-2350-y

Opatova, V., & Arnedo, M. A. (2014). Spiders on a hot volcanic roof: colonisation pathways and phylogeography of the canary islands endemic trap-door spider *Titanidiops canariensis* (Araneae, Idiopidae). *PLoS ONE*, **9** (12), e115078. https://doi.org/10.1371/journal.pone.0115078

Opatova, V., Hamilton, C. A., Hedin, M., De Oca, L. M., Král, J., & Bond, J. E. (2020). Phylogenetic systematics and evolution of the spider Infraorder Mygalomorphae using genomic scale data. *Systematic Biology*, **69** (4), 671–707. https://doi.org/10.1093/sysbio/syz064

Pérez-Miles, F., & Perafán, C. (2017). Behavior and Biology of Mygalomorphae. In C. Viera, & M. O. Gonzaga (Eds.), *Behaviour and Ecology of Spiders* (pp. 29–54). Springer International Publishing. https://doi.org/10.1007/978-3-319-65717-2_2

Prado, D. E. (2003). As caatingas da América do Sul. *Ecologia e conservação da Caatinga*, *2*, 3-74.

Puzin, C., Leroy, B., & Pétillon, J. (2014). Intra- and inter-specific variation in size and habitus of two sibling spider species (Araneae: Lycosidae): taxonomic and biogeographic insights from sampling across Europe. *Biological Journal of the Linnean Society*, **113** (1), 85–96. https://doi.org/10.1111/bij.12303

Recoder, R. S., Ribeiro, M. C., & Rodrigues, M. T. (2013). Spatial variation in morphometry in *Vanzosaura rubricauda* (Squamata, Gymnophthalmidae) from open habitats of south america and its environmental correlates. *South American Journal of Herpetology*, **8** (3), 186–197. https://doi.org/10.2994/sajhd1200019.1

Regueira, J. C. S., Damasceno, E. M., & Iannuzzi, L. (2020). Shape variation of *Cydianerus latruncularius* (Coleoptera, Curculionidae) across biomes and sexes. *Zoologischer Anzeiger*, **289**, 96–107. https://doi.org/10.1016/j.jcz.2020.10.002

Reyment, R. A. (2010). Morphometrics: An Historical Essay. In A. M. T. Elewa (Ed.), *Morphometrics for Nonmorphometricians* (pp. 9–24). Springer Berlin Heidelberg. https://doi.org/10.1007/978-3-540-95853-6_2

Ríos-Tamayo, D. (2016). Variación intra-específica en machos de *Actinopus* sp. (Mygalomorphae: Actinopodidae) del norte argentino. *Acta Zoológica Lilloana*, **60** (1), 78-88.

Rix, M. G., Cooper, S. J. B., Meusemann, K., Klopfstein, S., Harrison, S. E., Harvey, M. S., & Austin, A. D. (2017). Post-Eocene climate change across continental Australia and the diversification of Australasian spiny trapdoor spiders (Idiopidae: Arbanitinae). *Molecular Phylogenetics and Evolution*, **109**, 302–320. https://doi.org/10.1016/j.ympev.2017.01.008

Rocha, A. V., Cabanne, G. S., Aleixo, A., Silveira, L. F., Tubaro, P., & Caparroz, R. (2020). Pleistocene climatic oscillations associated with landscape heterogeneity of the South American dry diagonal explains the phylogeographic structure of the narrow-billed woodcreeper (*Lepidocolaptes angustirostris*, Dendrocolaptidae). *Journal of Avian Biology*, **51** (9). https://doi.org/10.1111/jav.02537

Rohlf, F. J. 2001. 'tpsDig.' Available online at: http://life.bio.sunysb.edu/morph.

Rull, V., & Carnaval, A. C. (2020). *Neotropical Diversification: Patterns and Processes*. Springer.

Silva, A. C. S. d., Andrade Nunes, L., Batista, W. d. L., & Lhano, M. G. (2018). Morphometric variation among males of *Orphulella punctata* (De Geer, 1773) (Acrididae: Gomphocerinae) from different biomes in Brazil. *Journal of Orthoptera Research*, **27** (2), 163–171. https://doi.org/10.3897/jor.27.21203

Silva, J. M. C. d., Barbosa, L. C. F., Leal, I. R., & Tabarelli, M. (2017). The Caatinga: understanding the challenges. In *Caatinga* (pp. 3–19). Springer International Publishing. https://doi.org/10.1007/978-3-319-68339-3_1

Smith, C. H., Johnson, N. A., Inoue, K., Doyle, R. D., & Randklev, C. R. (2019).

Integrative taxonomy reveals a new species of freshwater mussel, *Potamilus streckersoni* sp. nov. (Bivalvia: Unionidae): implications for conservation and management. *Systematics and Biodiversity*, **17** (4), 331–348. https://doi.org/10.1080/14772000.2019.1607615

Strauss, R. E. (2010). Discriminating Groups of Organisms. In A. M. T. Elewa (Ed.), *Morphometrics for Nonmorphometricians* (pp. 73–91). Springer Berlin Heidelberg. https://doi.org/10.1007/978-3-540-95853-6_4

Struck, T. H., Feder, J. L., Bendiksby, M., Birkeland, S., Cerca, J., Gusarov, V. I., Kistenich, S., Larsson, K.-H., Liow, L. H., Nowak, M. D., Stedje, B., Bachmann, L., & Dimitrov, D. (2018). Finding evolutionary processes hidden in cryptic species. *Trends in Ecology & Evolution*, **33** (3), 153–163. https://doi.org/10.1016/j.tree.2017.11.007

Thomé, M. T. C., Carstens, B. C., Rodrigues, M. T., Alexandrino, J., & Haddad, C. F. B. (2021). Genomic data from the Brazilian sibilator frog reveal contrasting pleistocene dynamics and regionalism in two South American dry biomes. *Journal of Biogeography*, **48** (5), 1112–1123. https://doi.org/10.1111/jbi.14064

Valdez-Mondragón, A., Navarro-Rodríguez, C. I., Solís-Catalán, K. P., Cortez-Roldán, M. R., & Juárez-Sánchez, A. R. (2019). Under an integrative taxonomic approach: the description of a new species of the genus *Loxosceles* (Araneae, Sicariidae) from Mexico City. *ZooKeys*, **892**, 93–133. https://doi.org/10.3897/zookeys.892.39558

Vilaseca, C., Méndez, M. A., Pinto, C. F., Lemic, D., & Benítez, H. A. (2021). Unraveling the morphological variation of *Triatoma infestans* in the peridomestic habitats of Chuquisaca Bolivia: a geometric morphometric approach. *Insects*, **12** (2), 185. https://doi.org/10.3390/insects12020185

Werneck, F. P. (2011). The diversification of eastern South American open vegetation biomes: Historical biogeography and perspectives. *Quaternary Science Reviews*, **30** (13-14), 1630–1648. https://doi.org/10.1016/j.quascirev.2011.03.009

Werneck, F. P., Gamble, T., Colli, G. R., Rodrigues, M. T., & Sites Jr, J. W. (2012). Deep diversification and long-term persistence in the south american 'Dry Diagonal': integrating continent-wide phylogeography and distribution modeling of geckos. *Evolution*, **66** (10), 3014–3034. https://doi.org/10.1111/j.1558-5646.2012.01682.x

Wilson, J. D., Zapata, L. V., Barone, M. L., Cotoras, D. D., Poy, D., & Ramírez, M. J. (2021). Geometric morphometrics reveal sister species in sympatry and a cline in genital morphology in a ghost spider genus. *Zoologica*

Scripta, **50** (4), 485–499. https://doi.org/10.1111/zsc.12478

Wolff, J. O., Wierucka, K., Paterno, G., Coddington, J. A., Hormiga, G., Kelly, M. B. J., Herberstein, M. E., & Ramírez, M. J. (2022). Stabilized morphological evolution of spiders despite mosaic changes in foraging ecology. *Systematic Biology,* syac023. https://doi.org/10.1093/sysbio/syac023

Wong, M. K. L., Woodman, J. D., & Rowell, D. M. (2017). Short-range phenotypic divergence among genetically distinct parapatric populations of an Australian funnel-web spider. *Ecology and Evolution*, **7** (14), 5094–5102. https://doi.org/10.1002/ece3.3084

Zelditch, M., Swiderski, D., Sheets, D. H., & Fink, W. (2004). *Geometric Morphometrics for Biologists*. Academic Press.

Zúñiga-Reinoso, Á., & Benítez, H. A. (2015). The overrated use of the morphological cryptic species concept: An example with Nyctelia darkbeetles (Coleoptera: Tenebrionidae) using geometric morphometrics. *Zoologischer Anzeiger - A Journal of Comparative Zoology*, **255**, 47–53. https://doi.org/10.1016/j.jcz.2015.01.004